

University of Alberta

Photochromic Molecules in the Development of All-Photon Mode Molecular Devices

by

Andrew J. Myles



A thesis submitted to the Faculty of Graduate Studies and Research in partial fulfillment of the requirements for the degree of Doctor of Philosophy

Department of Chemistry

Edmonton, Alberta
Fall 2002



National Library
of Canada

Acquisitions and
Bibliographic Services

395 Wellington Street
Ottawa ON K1A 0N4
Canada

Bibliothèque nationale
du Canada

Acquisitions et
services bibliographiques

395, rue Wellington
Ottawa ON K1A 0N4
Canada

Your file Votre référence

Our file Notre référence

The author has granted a non-exclusive licence allowing the National Library of Canada to reproduce, loan, distribute or sell copies of this thesis in microform, paper or electronic formats.

The author retains ownership of the copyright in this thesis. Neither the thesis nor substantial extracts from it may be printed or otherwise reproduced without the author's permission.

L'auteur a accordé une licence non exclusive permettant à la Bibliothèque nationale du Canada de reproduire, prêter, distribuer ou vendre des copies de cette thèse sous la forme de microfiche/film, de reproduction sur papier ou sur format électronique.

L'auteur conserve la propriété du droit d'auteur qui protège cette thèse. Ni la thèse ni des extraits substantiels de celle-ci ne doivent être imprimés ou autrement reproduits sans son autorisation.

0-612-81246-4

Canada

University of Alberta

Library Release Form

Name of Author: Andrew J. Myles

Title of Thesis: Photochromic Molecules in the Development of All-Photon Mode Molecular Devices

Degree: Doctor of Philosophy

Year this Degree Granted: 2002

Permission is hereby granted to the University of Alberta Library to reproduce single copies of this thesis and to lend or sell such copies for private, scholarly or scientific research purposes only.

The author reserves all other publication and other rights in association with the copyright in the thesis, and except as herein before provided, neither the thesis nor any substantial portion thereof may be printed or otherwise reproduced in any material form whatever without the author's prior written permission.



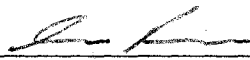
Andrew J. Myles
49 Cortland St.
Charlottetown, PEI
C1E1T4

September 30, 2002

University of Alberta

Faculty of Graduate Studies and Research

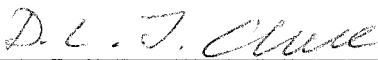
The undersigned certify that they have read, and recommend to the Faculty of Graduate Studies and Research for acceptance, a thesis entitled "Photochromic Molecules in the Development of All-Photon Mode Molecular Devices" submitted by Andrew J. Myles in partial fulfillment of the requirements for the degree of Doctor of Philosophy.



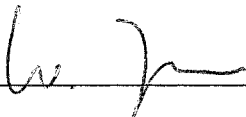
Associate Professor Neil R. Branda




Professor Jeffrey M. Stryker



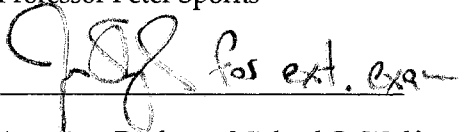
Professor Derrick L. J. Clive



Associate Professor Wolfgang Jäger



Professor Peter Sporns



Associate Professor Michael O. Wolf

9/24/02

To my wife Heather,
whose love and support has guided me
through the most difficult times of my life.

Abstract

Photochromic molecules interconvert between two forms upon irradiation with light of appropriate wavelengths. These molecules have the potential to act as molecular switches, possessing an *on* and an *off* state. A series of photochromic systems is presented as potential components in all-photon mode molecular devices.

1,2-bis(3-thienyl)cyclopentenes are photochromic molecules that interconvert between a colorless open form and a colored closed form upon irradiation with appropriate wavelengths of light. Practical application of these photochromic systems requires them to be in a polymeric rather than a monomeric form. A series of homopolymers of 1,2-bis(3-thienyl)cyclopentene was synthesized using Ring Opening Metathesis Polymerization (ROMP) and characterized both in solution and in the solid-state using gel permeation chromatography, UV-vis spectroscopy, differential scanning calorimetry and thermogravimetric analysis. It was found that the photochromism of the polymers compared to their corresponding monomers was identical in solution. Solid-state photochromism was also observed in all polymers cast as thin films.

Phenoxynaphthacenequinone (PNQ) is a photochromic quinone, interconverting between its *trans*- and *ana*-form, of which the *ana*-form possesses a less negative reduction potential (better electron acceptor). A series of porphyrinic PNQ hybrids was synthesized and characterized as photochromic systems to regulate photo-induced electron transfer (PET)

between the porphyrin and PNQ. Covalent linking of a porphyrin to a PNQ results in the inhibition of photoisomerization. A hybrid in which the porphyrin and PNQ are associated through hydrogen bonds circumvents this problem. Upon photoisomerization of the PNQ between its *trans*- and *ana*-form within this hydrogen-bonded hybrid, the emission of the porphyrin decreases, suggesting an increase in PET between the porphyrin and the *ana*-PNQ. A porphyrinic PNQ copolymer was synthesized using ROMP and UV-vis spectroscopy indicated photoisomerization of the PNQ in solution. Similarly, the emission of the porphyrin decreases upon photoisomerization of the *trans*- to *ana*-form of the PNQ within the copolymer, attributed to an increase in PET between the porphyrin and *ana*-PNQ.

A phenoxynaphthacenequinone 1,2-bis(3-thienyl)cyclopentene hybrid was synthesized and characterized using UV-vis spectroscopy as a potential multi-addressable photochromic molecule. Irradiation of the hybrid with appropriate wavelengths of light allows four different states to be addressed, more specifically the *trans*-open, *trans*-closed, *ana*-open and *ana*-closed forms.

Table of Contents

1	Introduction	1
1.1	Molecular Machines	1
1.2	Light Energy	3
1.3	Photochemistry and Photophysics	4
1.4	Photo-Regulated Molecular Device Components	10
1.5	Photochromic Molecules	12
1.5.1	Photochromic Terminology	14
1.5.2	Desired Characteristics of Photochromic Molecules	17
1.5.3	Common Photochromic Molecules	18
1.5.3.1	Azobenzenes	18
1.5.3.2	Spiropyrans	19
1.5.3.3	Fulgides	20
1.5.3.4	1,2-Bis(3-thienyl)cyclopentene Derivatives	21
1.5.3.5	Phenoxynaphthacenequinones	25
1.6	Preview of Thesis	29
1.6.1	Chapter 2	29
1.6.2	Chapter 3	30
1.6.3	Chapter 4	30
1.6.4	Thesis Statement	31

1.7	References	32
2	Synthesis and Characterization of Photochromic Homopolymers Based on 1,2- Bis(3-thienyl)cyclopentene using Ring Opening Metathesis Polymerization.	36
2.1	1,2-bis(3-thienyl)cyclopentene Derivatives	36
2.1.1	Regulation of Current Using DTE	38
2.1.2	Regulation of Magnetic Interactions Using DTE	39
2.1.3	Regulation of Fluorescence using DTE	40
2.2	Polymeric DTE's	41
2.3	Ring Opening Metathesis Polymerization	44
2.4	Photochromic Homopolymers based on DTE	47
2.4.1	Synthesis of Monomers	48
2.4.2	Synthesis and Characterization of Polymers	50
2.4.2.1	Gel Permeation Chromatography	53
2.4.2.2	Differential Scanning Calorimetry	56
2.4.2.3	Thermogravimetric Analysis	57
2.4.2.4	UV-vis Spectroscopy in Solution	58
2.4.2.5	UV-vis Spectroscopy in the Solid-State	62
2.5	Concluding Remarks and Future Prospects	64
2.6	Experimental	66
2.7	References	80

3	Photo-Regulation of Photo-Induced Electron Transfer within Porphyrinic Phenoxynaphthacenequinone Hybrid Systems	83
3.1	Photo-Induced Electron Transfer (PET)	83
3.2	PET Regulation	86
3.2.1	Chemical Regulation of PET	87
3.2.2	Electrochemical Regulation of PET	89
3.2.3	Photochemical Regulation of PET	90
3.2.4	Phenoxynaphthacenequinones as Photo-Regulated Electron Acceptors	91
3.3	Phenoxynaphthacenequinones (PNQ's)	93
3.3.1	Synthesis	93
3.3.2	UV-vis Absorption Spectroscopy	95
3.3.3	Cyclic Voltammetry	96
3.4	Covalent Porphyrinic Phenoxynaphthacenequinone Hybrid	98
3.4.1	Synthesis	98
3.4.2	UV-vis Absorption Spectroscopy	99
3.4.3	Possible Mechanisms of the Inhibition of Photoisomerization of Hybrid 3.1	104
3.4.3.1	Mechanism A	107
3.4.3.2	Mechanism B	108
3.4.3.3	Mechanism C	108
3.4.3.4	Mechanism D	109
3.4.3.5	Summary	110

3.5	Non-Covalent Porphyrinic Phenoxynaphthacenequinone	110
3.5.1	Synthesis	111
3.5.2	Cyclic Voltammetry	113
3.5.3	Free Energy of PET Calculations	114
3.5.4	Association Measurements of 3.3 with 3.2t and 3.2a	116
3.5.5	UV-vis Absorption Spectroscopy	118
3.5.6	Evaluation of PET using Luminescence Spectroscopy	120
3.5.7	Transient Absorption Spectroscopy	123
3.6	Polymeric Porphyrinic Phenoxynaphthacenequinone Hybrid	129
3.6.1	Synthesis of Monomers	130
3.6.2	Synthesis of Copolymers	131
3.6.3	UV-vis Absorption Spectroscopy	134
3.6.4	Regulation of PET	136
3.7	Concluding Remarks	140
3.8	Experimental	142
3.9	References	157
4	A Multi-Addressable Phenoxynaphthacenequinone-Dithienylethene Hybrid Photochromic System	161
4.1	Introduction	161
4.2	Multi-Addressable Molecular Switches in the Literature	162
4.3	A Phenoxynaphthacenequinone-Dithienylethene Hybrid	166

4.3.1	Synthesis	168
4.3.2	UV-vis Absorption Spectroscopy of Control Molecules	171
4.3.3	UV-vis Absorption Spectroscopy of PNQ-DTE Hybrid 4.5	174
4.4	Summary	180
4.5	Experimental	182
4.6	References	189
5	Conclusion	190
5.1	Chapter 1: Introduction	190
5.2	Chapter 2: Dithienylethenes (DTE)	191
5.3	Chapter 3: Phenoxynaphthacenequinone (PNQ)	194
5.4	Chapter 4: PNQ-DTE Hybrid	197
5.5	Summary	199
5.6	References	200

List of Tables

Chapter 2

Table 2.1	Polymer characterization data	56
Table 2.2	Solution UV-vis absorption data	61

List of Figures

Chapter 1

Figure 1.1	Energy diagram of photoexcitation of a chromophore	5
Figure 1.2	Schematic of intersystem crossing	5
Figure 1.3	Deactivation pathways of the excited state of a molecule	6
Figure 1.4	Schematic of energy transfer	8
Figure 1.5	Schematic of electron transfer	9
Figure 1.6	Photo-regulated molecular shuttle	11
Figure 1.7	Photochromism	13
Figure 1.8	UV-vis spectrum of a photochrome illustrating isobestic points	16
Figure 1.9	Schematic of photostationary state	16
Figure 1.10	Molecular orbitals of 1,2-bis(3-thienyl)cyclopentene derivatives	23
Figure 1.11	Rotation of thiophene rings in DTE	23
Figure 1.12	UV-vis spectrum of DTE	24
Figure 1.13	UV-vis spectrum of PNQ	27
Figure 1.14	Proposed transition state of PNQ	28

Chapter 2

Figure 2.1	UV-vis absorption spectra of DTE illustrating effect elongating the conjugation pathway created upon photocyclization	37
Figure 2.2	Photoregulation of electron flow using DTE	39

Figure 2.3	Photoregulation of magnetic interactions using DTE	40
Figure 2.4	Photoregulation of fluorescence using DTE	41
Figure 2.5	Photochromic copolymers based on DTE	43
Figure 2.6	Schematic of olefin metathesis	45
Figure 2.7	Photochromic homopolymers of DTE synthesized using ROMP	47
Figure 2.8	¹ H NMR spectral changes upon polymerization	52
Figure 2.9	Gel permeation chromatography	53
Figure 2.10	Correlation between T _g and inner space of a polymer matrix	57
Figure 2.11	Thermogravimetric analysis	58
Figure 2.12	UV-vis spectral comparison between monomers and polymers	59-60
Figure 2.13	Solid-state UV-vis absorption spectra	63
 Chapter 3		
Figure 3.1	Photosynthetic reaction center	84
Figure 3.2	PET energy diagram	85
Figure 3.3	Synthetic PET systems	86
Figure 3.4	UV-vis absorption spectra of PNQ	95
Figure 3.5	Cyclic voltammogram of PNQ	7
Figure 3.6	UV-vis spectra of hybrid 3.1 and its constituent chromophores	100
Figure 3.7	Photoisomerization of PNQ in the presence of TTP	102
Figure 3.8	Possible mechanisms for inhibition of photoisomerization of 3.1	106

Figure 3.9	Cyclic voltammetry of PNQ 3.2	114
Figure 3.10	¹ H NMR titration of carboxylate 3.2 with urea 3.3	117
Figure 3.11	Photoisomerization of PNQ 3.2 with porphyrin 3.3	119
Figure 3.12	Inverse Stern-Volmer plot assessing PET regulation	122
Figure 3.13	Transient absorption spectroscopy	124
Figure 3.14	Transient absorption spectrum of PNQ 3.2t	125
Figure 3.15	Transient absorption spectrum of PNQ 3.2t with 0.1 mM <i>N,N</i> -dimethylaniline	127
Figure 3.16	Transient absorption spectrum of PNQ 3.2t with 0.1 M <i>N,N</i> -dimethylaniline	128
Figure 3.17	UV-vis spectra of porphyrinic-PNQ copolymers	135
Figure 3.18	Emission spectral changes of porphyrinic-PNQ copolymers	138
Figure 3.19	Emission regulation using porphyrinic-PNQ copolymer	139
 Chapter 4		
Figure 4.1	UV-vis spectra of control photochromes	172
Figure 4.2	UV-vis spectra of a 1:1 mixture of control photochromes	174
Figure 4.3	UV-vis spectral comparison of 1:1 mixture of control photochromes and PNQ-DTE hybrid 4.5	176
Figure 4.4	UV-vis spectral changes of PNQ-DTE hybrid 4.5 in which three states are accessible	177
Figure 4.5	UV-vis spectral changes of PNQ-DTE hybrid 4.5 in which all four states are accessible	179

Chapter 5

Figure 5.1 Photochromic homopolymers based on DTE

192

List of Schemes

Chapter 1

Scheme 1.1	<i>Cis-trans</i> isomerization of azobenzene	18
Scheme 1.2	Spiropyran photoisomerization	19
Scheme 1.3	Photoisomerization of fulgides	20
Scheme 1.4	Photoisomerization of 1,2-bis(3-thienyl)cyclopentene derivatives	21
Scheme 1.5	Photochromism of phenoxynaphthacenequinone	25
Scheme 1.6	Transient species in PNQ photoisomerization	28

Chapter 2

Scheme 2.1	DTE photoisomerization	36
Scheme 2.2	Ring opening metathesis polymerization (ROMP)	44
Scheme 2.3	Mechanism of ROMP	46
Scheme 2.4	Synthesis of monomers	49
Scheme 2.5	Synthesis of homopolymers	51

Chapter 3

Scheme 3.1	Chemical regulation of PET	88
Scheme 3.2	Electrochemical regulation of PET	89
Scheme 3.3	Photochemical regulation of PET	91

Scheme 3.4	Proposed gated PET system	92
Scheme 3.5	Photoisomerization of phenoxynaphthacenequinone	93
Scheme 3.6	Synthesis of PNQ	94
Scheme 3.7	Synthesis of Zn-porphyrin-PNQ hybrid 3.9 and amido-linked hybrid 3.10	103
Scheme 3.8	Schematic of PET regulation within a hydrogen bonded porphyrinic-PNQ hybrid	111
Scheme 3.9	Synthesis of PNQ 3.2 and porphyrin urea 3.3	112
Scheme 3.10	Ring opening metathesis polymerization	130
Scheme 3.11	Synthesis of PNQ and porphyrin monomers	131
Scheme 3.12	Synthesis of porphyrinic-PNQ copolymers using ROMP	133

Chapter 4

Scheme 4.1	Multi-addressable molecular switch using light and pH	163
Scheme 4.2	Multi-addressable molecular switch based on a bis-dimethyldihydropyrene-metacyclophanediene photochrome	164
Scheme 4.3	Multi-addressable molecular switch based on a DTE-DHA/VHF hybrid	165
Scheme 4.4	Photochromism of DTE and PNQ	167
Scheme 4.5	Schematic of potential multi-addressable photochromic system based on a PNQ-DTE hybrid	168
Scheme 4.6	Synthesis of PNQ-DTE hybrid 4.5	170
Scheme 4.7	Schematic of possible transformation of PNQ-DTE hybrid 4.5	180

Chapter 5

Scheme 5.1	DTE photoisomerization	191
Scheme 5.2	Photoisomerization of PNQ	194
Scheme 5.3	Schematic of PET regulation within a porphyrinic-PNQ hybrid	195
Scheme 5.4	Schematic of possible transformation of PNQ-DTE hybrid 4.5	198

List of Equations

Chapter 3

Equation 3.1	Synthesis of PNQ 3.7a	96
Equation 3.2	Synthesis of porphyrinic-PNQ hybrid 3.1	98
Equation 3.3	Free energy of PET calculation	115

List of Abbreviations

AcOH	acetic acid
arb.	arbitrary
br	broad
calcd	calculated
CIMS	chemical ionization mass spectrometry
D	chemical shift in parts per million downfield from TMS
d	doublet
DMF	dimethylformamide
DMSO	dimethylsulfoxide
DSC	differential scanning calorimetry
DTE	dithienylethene (1,2-bis(3-thienyl)cyclopentene)
ΔG	change in free energy
$\Delta \eta$	change in refractive index
ϵ	molar absorptivity coefficient
e-	electron
E°	potential

EIMS	electron impact mass spectrometry
EPR	electron paramagnetic resonance
ESMS	electrospray mass spectrometry
eT	electron transfer
ET	energy transfer
FTIR	Fourier transform infrared spectroscopy
g	gram
GPC	gel permeation chromatography
h ν	light energy
HOMO	highest occupied molecular orbital
HPLC	high performance liquid chromatography
Hz	hertz
<i>J</i>	coupling constant
K _a	association constant
kcal	kilocalories
LUMO	lowest unoccupied molecular orbital
λ	wavelength

λ_{\max}	longest wavelength at which the largest absorbance is observed in the UV-vis spectrum
m	multiplet
M	molar (moles/L)
MHz	megahertz
M.p.	melting point
m/z	mass to charge ratio
nm	nanometer
NMR	nuclear magnetic resonance
PDI	polydispersity index
PET	photo-induced electron transfer
PNQ	phenoxynaphthacenequinone
ppm	parts per million
ROMP	ring opening metathesis polymerization
s	singlet
S_1	first singlet excited state
SOMO	singly occupied molecular orbital
t	triplet

T ₁	first triplet excited state
T _g	glass transition temperature
TAS	transient absorption spectroscopy
TGA	thermogravimetric analysis
THF	tetrahydrofuran
TMS	tetramethylsilane
TTP	5,10,15,20-tetratolylporphyrin
UV	ultraviolet
V	volt
vis	visible

Photochromic Molecules in the Development of All-Photon Mode Molecular Devices

Chapter 1 – Introduction

1.1 – Molecular Machines

Making machines out of molecules: it sounds like science fiction to some, however for others, such as our research group, this is an active pursuit. A machine is defined as an apparatus using or applying mechanical power, having several parts each with a definite function and together performing certain kinds of work.¹ Similarly, a molecular machine is made up of several molecular components, each performing a specific task key in the operation of the whole system.

Molecular machines were first seriously contemplated by physicist Richard Feynman during his 1959 American Physical Society lecture titled “There is Plenty of Room at the Bottom”.² However, the concept is by no means novel, as plants and animals are examples of molecular machines, with a multitude of parts simultaneously functioning to keep them alive. Molecules in chloroplasts convert sunlight into chemical energy. Enzymes are groups of molecules that function to regulate numerous cellular processes, such as DNA replication and

protein synthesis.³ Ion channels are regulated through molecular activation, a phenomenon significant in transduction of nerve impulse pathways.⁴

Since Feynman's famous lecture, advances in probe microscopies, supramolecular chemistry and photo-induced electron transfer mechanisms have provided important tools key in the development of molecular machines and devices. In a world run by economics, the most significant push for molecular machines is the realization by the electronics industry that the "top-down" approach has intrinsic limitations in the development of microelectronics. Mechanically engineered devices have a finite size limit, whereas engineering a device at the molecular level has the potential of being orders of magnitude smaller than that limit.⁵ This has led the industry to consider the use of molecular electronics, which offer advantages in efficiency and size. Industry interest also provides funding for scientists who not only find the applications interesting, but are truly driven by the academic challenge of making functional machines from such small components.

Every machine is made up of individual components. Simple components key to the development of molecular devices include rotors, shuttles and switches that operate at the molecular level. Each one must be controlled by an external stimulus, such as chemical

reagents, electrons or photons. Chemical reagents produce waste upon their consumption; removal of these byproducts is difficult, especially in a device whose size is on the molecular scale. Electrons or photons are more desirable as stimuli as they can be introduced controllably and without build up of byproducts. It is predicted that photons will do for the 21st century what electrons have done for the 20th century due to light's fast and efficient nature.⁶ For this reason, my research has focused on all-photon mode molecular devices.

1.2 – Light Energy

Light is electromagnetic radiation in the visible, near ultraviolet and near infrared spectral range. There are two common models for understanding light energy: the wave model and the particle model.⁷ In the wave model, the electromagnetic radiation is described by a wavelength (λ), a frequency (ν) and a velocity (c). The c term is a constant (2.998×10^8 m/s, the speed of light), and all three terms are related by the equation:

$$\lambda\nu = c$$

The frequency of the wave decreases with increasing wavelength and vice versa, making these two terms inversely proportional. Light travelling in one direction has an oscillating electric field at a right angle to its direction of propagation.⁸ This is accompanied by an oscillating magnetic field at right angles to both the electric field and the direction of the light beam. The electric field associated with light can interact with charged particles, such as electrons in molecules. This interaction can result in the molecules absorbing the light energy by

promoting an electron to an excited state. The energy corresponding to the wavelength of light absorbed is equal to the energy gap between the ground state and excited state of the molecule.

In the particle or quantum model of light, the light beam is composed of quanta of energy called photons. Each photon has a specific energy (E) determined by the frequency (ν) of the electromagnetic radiation and Planck's constant (h) in the equation:

$$E = h\nu$$

A photon is commonly represented by the term $h\nu$. In this equation, the frequency and energy are directly proportional. The frequency and wavelength are inversely proportional, therefore as the wavelength of light increases, the energy of that light decreases.

1.3 – Photochemistry and Photophysics

Light energy can be absorbed by a molecule, termed a chromophore, to generate an electronically excited state of that molecule, represented in Figure 1.1.

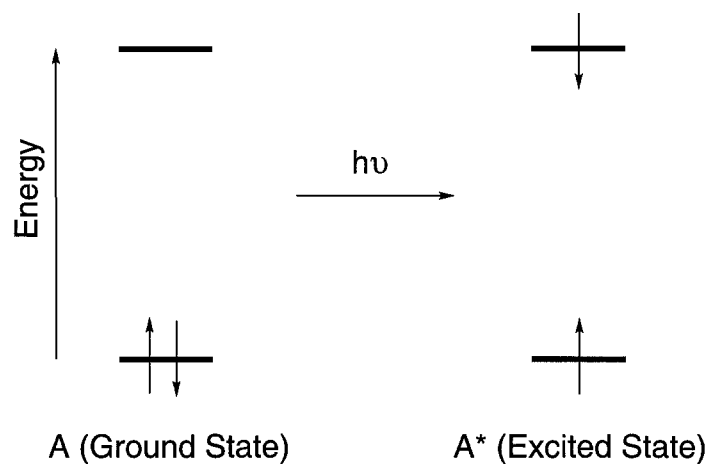


Figure 1.1. Energy diagram of photoexcitation of ground state to excited state of a chromophore (A).

This excited state is a new chemical species, as it possesses unique chemical and physical properties. Photochemistry involves the chemical reactivity of excited state molecules; photophysics involves the physical properties and processes of excited states.

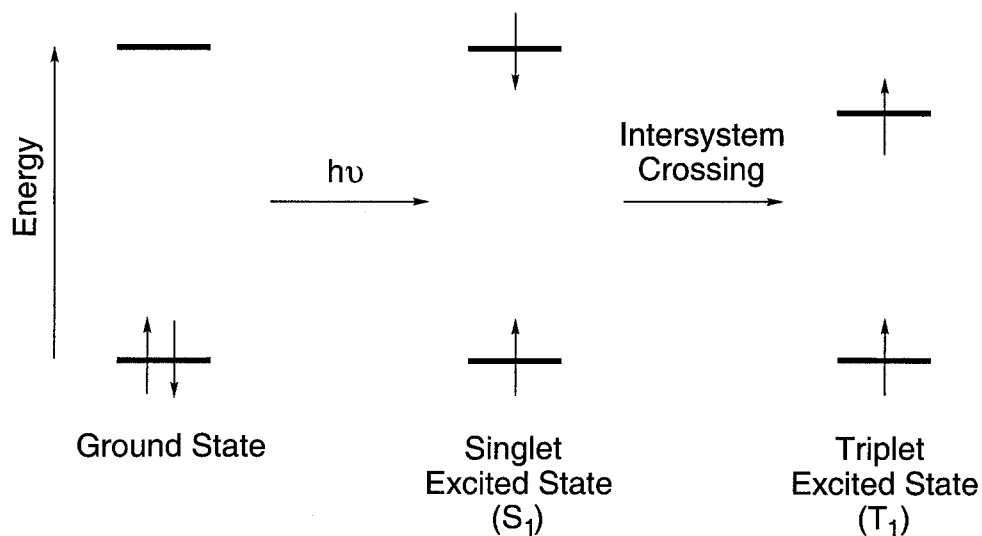


Figure 1.2. Schematic of intersystem crossing between the first singlet excited state (S₁) and the lower energy first triplet excited state (T₁).

As illustrated in Figure 1.2, once a chromophore absorbs energy, it immediately forms an excited state in which the ground state electron and the excited-state electron are of opposite spins. This state is known as the first singlet excited state (S_1). In some cases, this singlet excited state can undergo intersystem crossing, which involves a spin flip of the excited electron. This transition forms the first triplet excited-state (T_1), which is longer lived than the singlet excited state as it must undergo another spin flip of the excited electron before returning to the ground state.

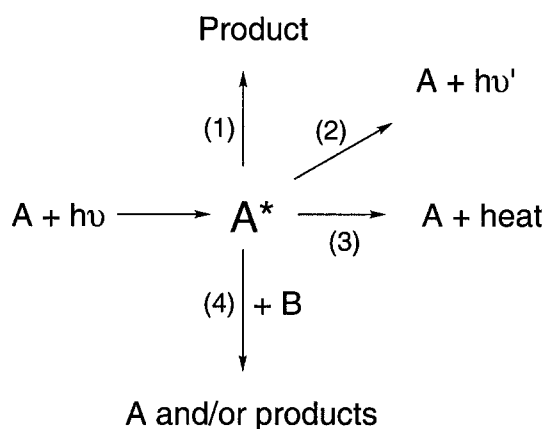


Figure 1.3. Deactivation pathways of the excited state of a molecule. Pathways: (1) unimolecular reactions; (2) radiative decay; (3) non-radiative decay; and (4) bimolecular reactions.

An excited state can return to a ground state through various mechanisms, such as decay pathways, unimolecular photoreactions and bimolecular photoreactions. These mechanisms are represented schematically in Figure 1.3. Decay pathways involve the collapse

of the excited state to the ground state with the release of energy. There are two types of decay from the excited state: radiative and non-radiative. Radiative decay involves emission of light (pathway 2 in Figure 1.3), and the most common radiative decay is fluorescence. Non-radiative decay involves deactivation of the excited state via vibrational relaxation, in which the energy is dissipated thermally (pathway 3 in Figure 1.3).

Unimolecular reactions can also occur with excited state molecule (pathway 1 in Figure 1.3), including photodecomposition, photoionization and photoisomerization reactions. Reversible photoisomerization reactions involves the interconversion of a molecule between two isomers. This phenomenon will be discussed later in this introduction and represents an important phenomenon in regulation of molecular devices.

Bimolecular reactions involve the interaction of the excited state chromophore with another ground state molecule (pathway 4 in Figure 1.3). These include chemical reactivity, energy transfer and electron transfer reactions. Photochemical reactions can occur where light provides the energy to overcome the activation energy barrier necessary for the reaction between two starting materials to produce products. Energy transfer involves the energy released from the decay of an excited state chromophore (A^*) being absorbed by another chromophore (B) to produce its excited state (B^*) (Figure 1.4). The resulting excited state can then decay either by a radiative or non-radiative pathway, both resulting in the compound's ground state.

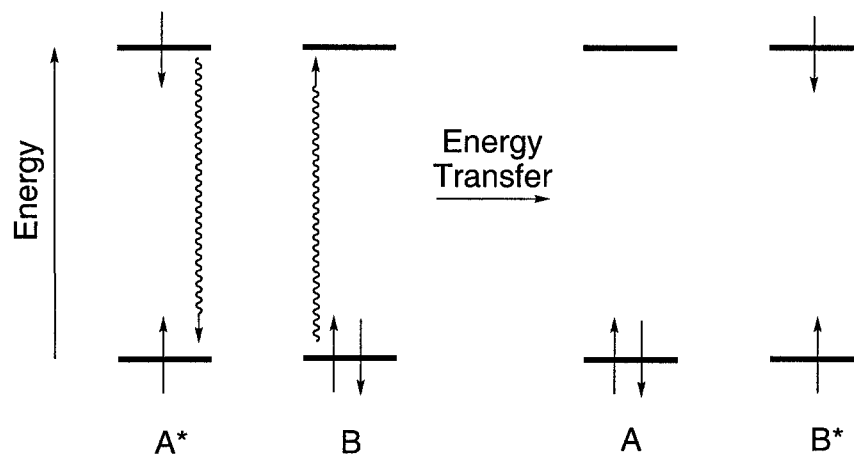


Figure 1.4. Schematic of energy transfer between the excited state of chromophore A (A^*) and the ground state of chromophore B, yielding the excited state of chromophore B (B^*).

A diagram of electron transfer is illustrated in Figure 1.5. Formation of the excited state of a chromophore (A^*) is followed by the transfer of an electron from the excited state to an electron acceptor (pathway 1 in Figure 1.5), or from an electron donor to the excited state chromophore (pathway 2 in Figure 1.5). This transfer results in the radical cation of the donor species and the radical anion of the acceptor species in both cases, referred to as the charge separated state. Charge recombination, also termed back electron transfer, results in both compounds' ground state. The net result is that the energy absorbed by the chromophore (A) is used in these electron transfer processes.

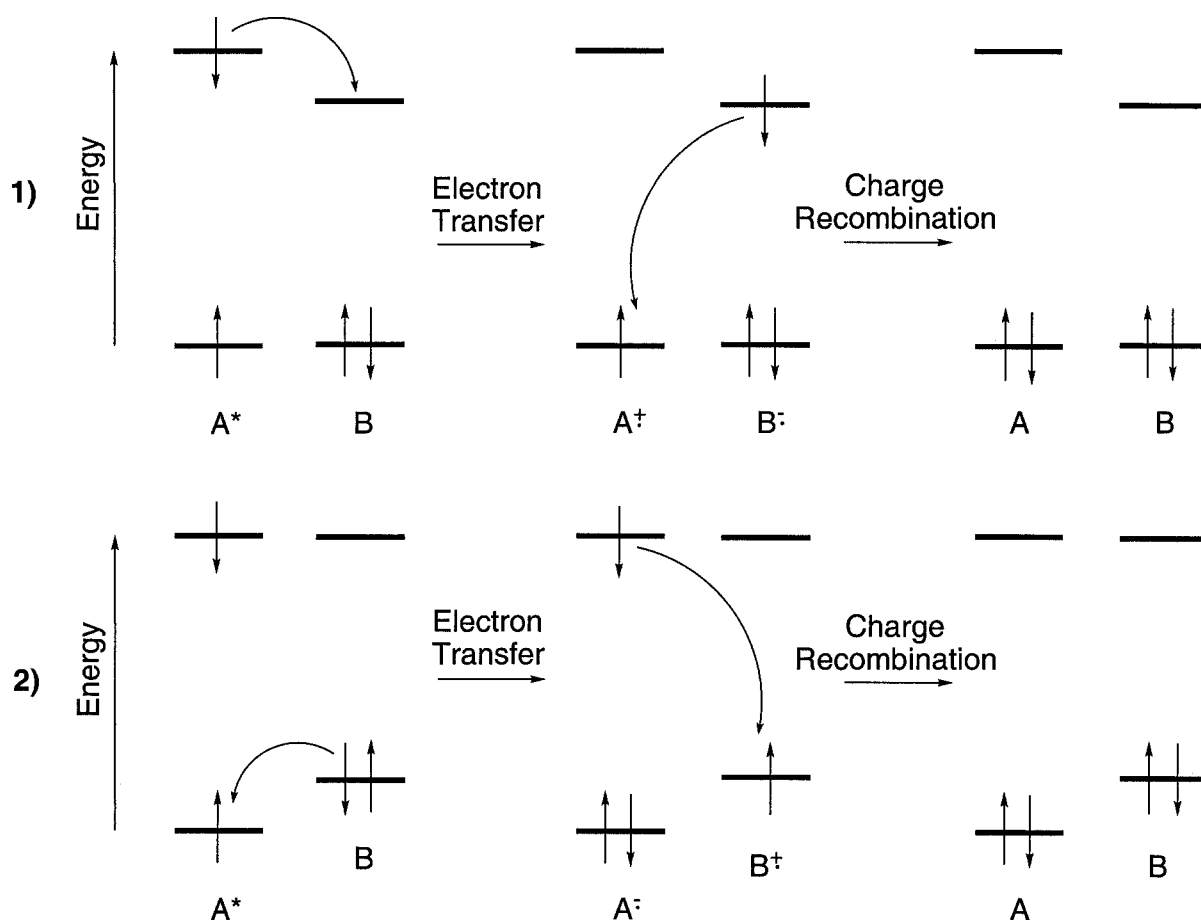


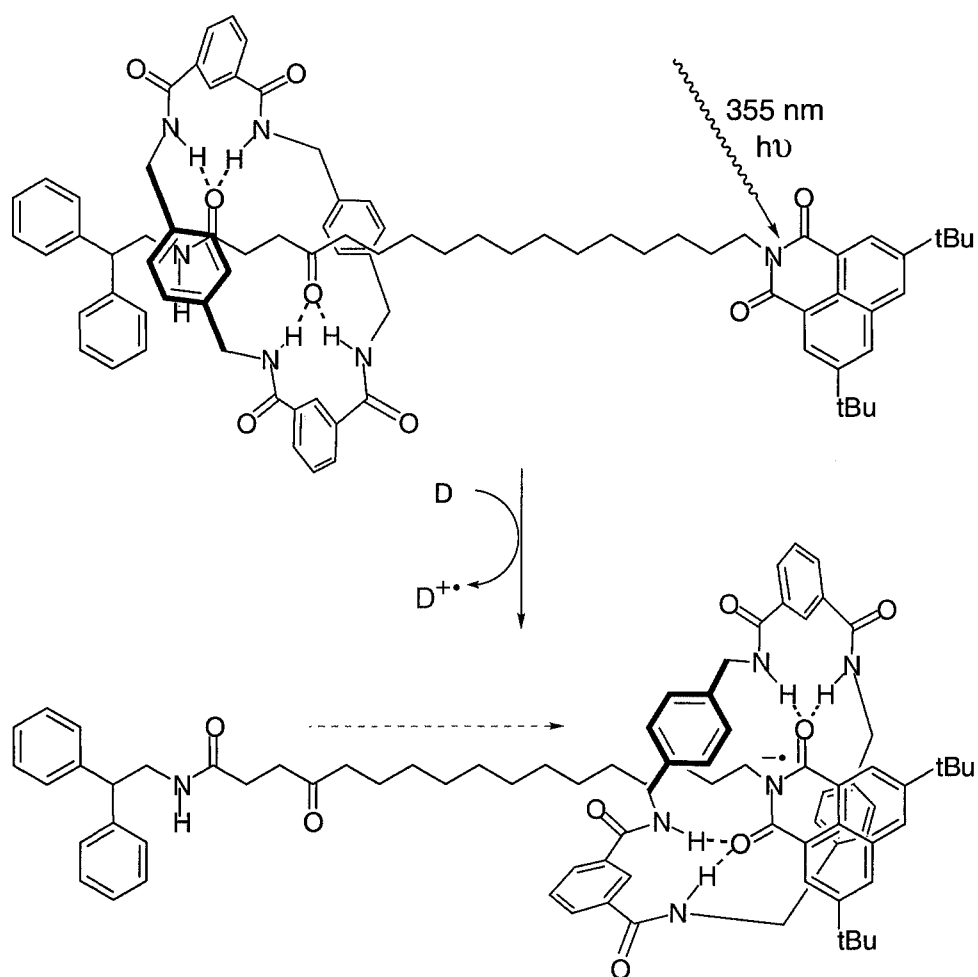
Figure 1.5. Schematic of an electron transfer decay pathway between the excited state of a chromophore (A^*) to another species (B). 1) the excited state (A^*) is the electron donor transferring an electron to an acceptor species (B); 2) the excited state (A^*) is the electron acceptor, accepting an electron from a donor species (B). In both cases, charge recombination of the radical anion/cation pair generates the ground state of both compounds.

Photoinduced Electron Transfer (PET) is one of the key steps in the conversion of light energy to chemical energy, and is used in photosynthetic plants and bacteria to do so. This also is an important theme of this thesis and will be discussed in more detail in Chapter 2.

1.4 – Photo-Regulated Molecular Device Components

As discussed in the previous section, light energy excitation can produce several different effects depending on the chromophore's excited state and environment. The challenge in the development of components for photo-regulated molecular devices is to engineer molecules to respond in a controlled manner to light energy, therefore favoring a particular pathway. For example, Leigh and Wurpel have reported a photo-regulated molecular shuttle in which a rotaxane with a tetra-amide wheel surrounds a hydrocarbon axle with a naphthylimide stopper (Figure 1.6).⁹

The ketone and amide carbonyls on the left-hand side of the hydrocarbon chain can form hydrogen bonds with the tetra-amide wheel in the ground state. Upon photoexcitation of the naphthylimide in the presence of an electron donor, the radical anion of the naphthylimide is formed via electron transfer. The tetra-amide wheel preferentially forms hydrogen bonds with the radical anion, resulting in the wheel sliding to the right along the axle. Upon charge recombination, the ground states are regenerated, and the tetra-amide wheel slides back to hydrogen bond with the ketone and amide on the other end of the hydrocarbon axle.



Leigh and Wurpel, Science 2001

Figure 1.6. Photo-regulated molecular shuttle. Upon irradiation of the naphthylimide in the presence of an electron donor, an electron transfer produces its radical anion. The cyclic tetraamide is shuttled down the hydrocarbon chain, forming a hydrogen bonded complex with the radical anion of the naphthylimide. Upon charge recombination with the radical cation of the electron donor, the cyclic tetraamide dissociates and shuttles back to its original position at the other end of the hydrocarbon chain.

In this example, light energy is used as the stimulus to control the position of a molecular shuttle, however one state is unstable and therefore returns to its original state. A desirable characteristic of such a system is to have two stable states (0 and 1) accessible by irradiation with light, therefore constituting a molecular switch. In such a system, not only is there controlled molecular movement, but information can be stored and/or transferred by differentiating between the two states. The next section discusses a common approach in this pursuit.

1.5 – Photochromic Molecules

An important class of molecules in the development of all-photon mode molecular devices are photochromic molecules, defined as molecules that reversibly change color upon irradiation with appropriate wavelengths of light.¹⁰ Upon irradiation of form **A** of the photochromic molecule, a photoisomerization reaction takes place resulting in form **B** (Figure 1.7). Form **B** can revert to form **A** thermally, in the case of *T*-type photochromic molecules, or photochemically by irradiation with another wavelength of light, termed *P*-type photochromic molecules. The two forms differ not only in their structure but also in their corresponding absorption spectra, signifying the change in color.

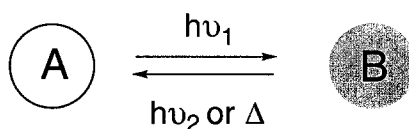


Figure 1.7. Photochromism

This phenomenon is most commonly exploited in photochromic ophthalmic lenses in which the lenses darken in high intensity light and lighten in low intensity light. The change in structure is often accompanied not only by a color change, but also in other physical properties such as refractive index, optical rotation, luminescence, conjugation and electronics. Exploiting these accompanying changes is the focus of current photochromic research and shows promise in applications such as optical waveguides for fiber optics¹¹, actinometry¹², and especially in molecular information storage systems.¹³

Pre-compact disk memory media were based primarily on inorganic materials and utilized magneto-optical (MO) technology as the foundation for optical recording.¹⁴ They were erasable because the change in the physical property at the storage location (the magnetic alignment of molecules based on their Curie-point temperatures) was reversible. The development of compact disk (CD) technology and the use of organic dyes such as cyanine, phthalocyanine or aza dyes as the memory medium and reflected laser light as the readout source introduced the more appealing use of optical data storage. The harnessing of laser light to read the information provided high resolution and high speed data processing, but the user gave up the convenience of erasability. The CD media available at this time consisted of write-

once read-only memory (WORM) and, as a consequence, multiple writing and erasing events could not be performed on them.

Only recently has an erasable CD-R (compact disk-recordable) medium become commercially available. This heat-mode medium operates by detecting differences in reflectance based on phase change (PC) effects between crystalline and amorphous states of polycarbonate substrates containing inorganic alloys of silver, indium, germanium, tellurium and antimony.¹⁵ They are termed heat-mode memories because the applied laser converts focused light energy to heat energy on the recording medium. This raises the temperature at the storage site above the melting temperature to initiate the phase change. This process is effective, but the high cost of these inorganic materials prohibits widespread commercial applications. A viable alternative is the implementation of economic organic based photochromes as the memory medium.

Some important terms that are used in describing photochromism must be defined before continuing.

1.5.1 – Photochromic Terminology: Isobestic Points and the Photostationary State¹⁶

The two forms of the photochrome possess different UV-vis absorption spectra, giving rise to the change in color between them. Upon irradiation of form A at $h\nu_1$, the absorption of

form **B** increases in intensity, as illustrated in Figure 1.8. The maximum absorbing wavelength (λ_{max}) is the longest wavelength that results in the highest absorbance, and changes upon photoisomerization between form **A** and **B**. An intermediate spectrum is shown, which is formed after an intermediate irradiation time. The wavelength at which all the spectra intersect is called the isobestic point, the presence of which confirms a one-step photoisomerization between two forms. If no isobestic point is present, there exists another step in the photoisomerization reaction between **A** and **B**.

In Figure 1.8, it is illustrated that form **A** and **B** absorbs at $h\nu_1$. The result of this is that a photochemical equilibrium is set up upon irradiation of form **A** with $h\nu_1$ between the two forms. Upon photoisomerization of form **A** to **B**, form **B** is excited and can undergo photoisomerization back to **A**. The ratio of form **B** to form **A** at this equilibrium is termed the photostationary state, and is usually represented as a percent value associated with the wavelength of irradiation (Figure 1.9). Form **A** has no absorption at $h\nu_2$, at which form **B** is irradiated. This results in complete conversion of the photostationary state back to form **A**.

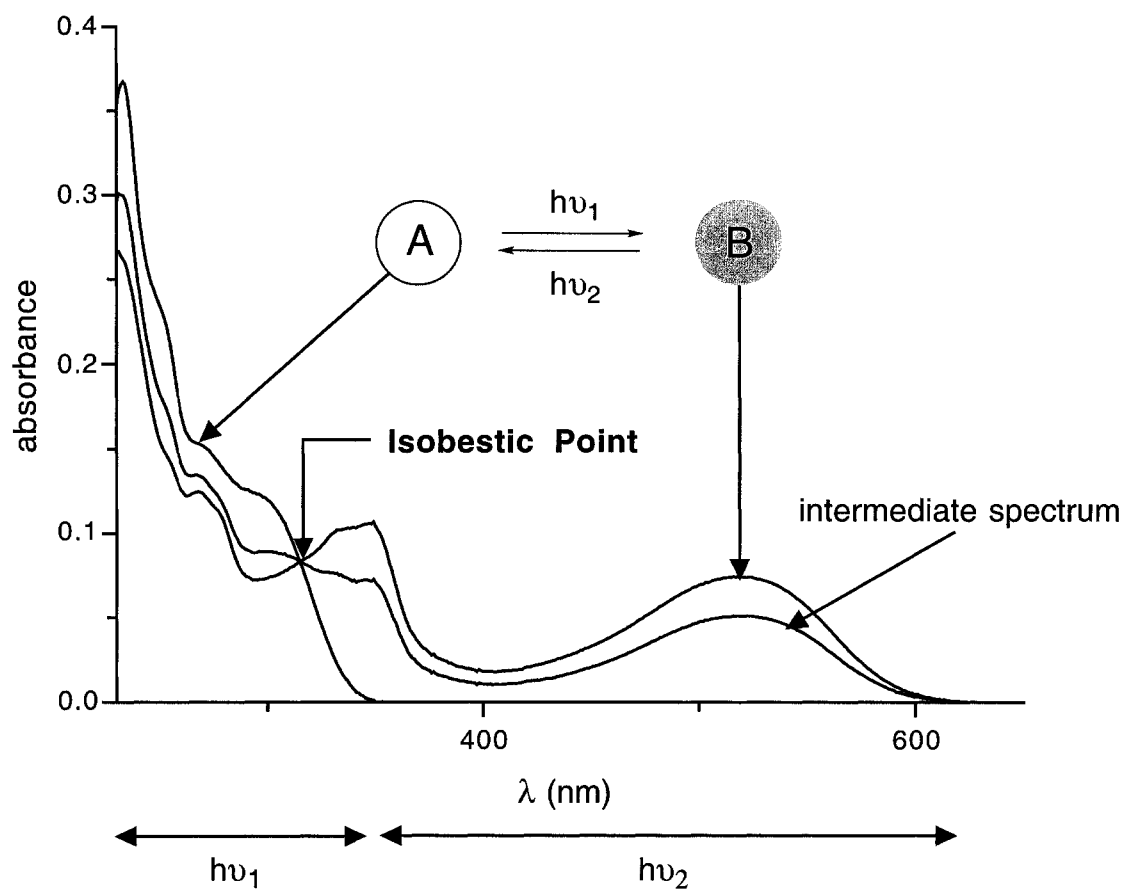


Figure 1.8. A representative UV-vis absorption spectrum of photochromism of **A** and **B**, illustrating the isobestic point, the point at which all spectra intersect.

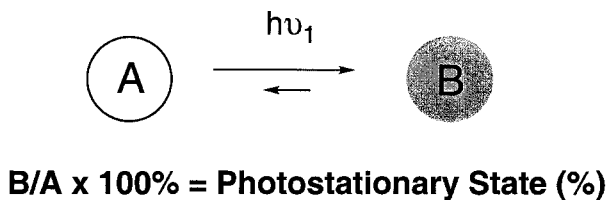


Figure 1.9. Schematic of photostationary state resulting from the photochemical equilibrium between form **B** and **A** at $h\nu_1$.

1.5.2 – Desired Characteristic of Photochromic Molecules

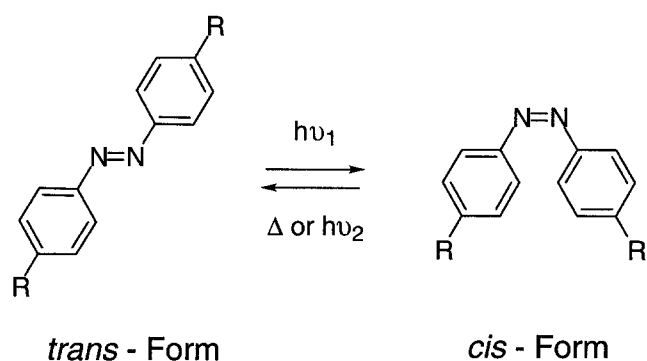
In choosing a photochrome for an application, it is important that it possesses certain desired characteristics. The photochrome must have a high fatigue resistance, meaning the two forms can interconvert numerous times without degradation. Independently addressable absorptions is also preferred to ensure maximum conversion of one form to the other. Reversibility is an important issue to address, as thermal or photochemical reversibility is desired depending on the application of interest. Photochromic ophthalmic lenses, for example, will darken on exposure to high intensity light; upon entering a dark room, it is desirable for them to lighten again. Since there is little light, it is desirable to use a thermally reversible photochromic molecule (*T*-type) in the lenses.

For applications using photochromic molecules as switches, such as waveguides and molecular information storage systems, it is desirable to have definite *on/off* states that are completely controlled. Supposing each form represents *on* or *off*, it is important to the application that it remains *on* or *off* until the appropriate stimulus is applied. For these applications, it is important to use a thermally irreversible photochromic molecule (*P*-type) so that each form remains in its appropriate state until irradiation with the appropriate wavelength of light.

My interest in photochromic molecules lies in their ability to act as photochemical molecular switches, therefore the research presented in this thesis is focused on *P*-type photochromism, in which the photochromic system has definite, stable *on/off* states interconvertible by irradiation with light of specific wavelengths. A survey of some common photochromes is presented, with specific emphasis on the most promising systems for the development of molecular switches.

1.5.3 – Common Photochromic Molecules

1.5.3.1 - Azobenzenes

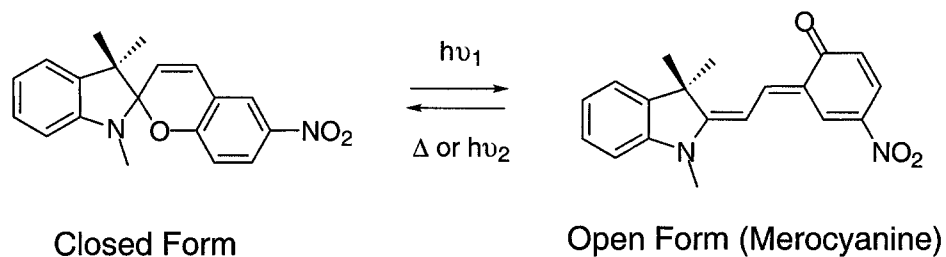


Scheme 1.1. *Cis-trans* isomerization of azobenzene

Azobenzenes undergo a *trans* to *cis* isomerization of the N=N double bond upon irradiation with an appropriate wavelength of light (Scheme 1.1), usually in the UV region of the spectrum. The *cis* form can revert to the *trans* form either photochemically, by irradiation

with another wavelength of light, or thermally. Exploiting this photochrome most often lies in the difference in orientation between the pendant 'R' groups upon photoisomerization. By appending groups on each end of the molecule, photoisomerization can trigger a tweezer effect, bringing the two groups closer together. This has been exploited in biological systems in which photoisomerization of the azobenzene chromophore changes the conformation of a pendant protein.¹⁷ The main set-back of this photochromic molecule is its thermal reversibility and the significant overlap of each form's absorptions, making it ineffective as a molecular switch.

1.5.3.2 - Spiropyrans

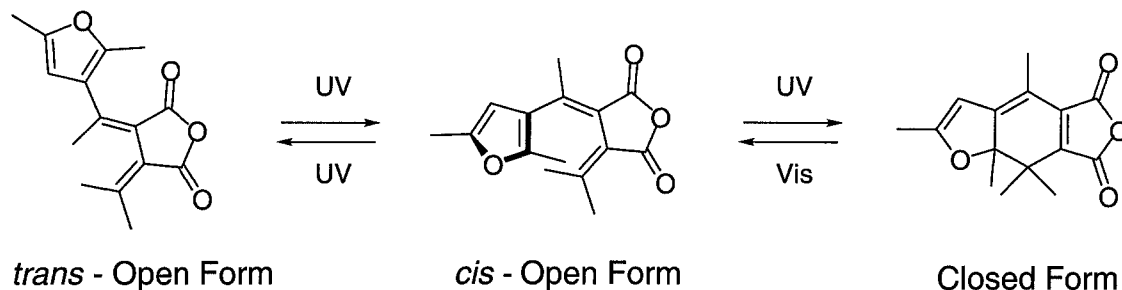


Scheme 1.2. Spiropyran photoisomerization

Photoisomerization of spiropyrans involves a reversible photochemical ring-opening/ring-closing reaction between the colorless spiro form and the colored merocyanine form (Scheme 1.2). More papers have been published on spiropyrans than on any other

photochromic molecule.¹⁸ Despite these photochromic molecules possessing low fatigue resistance due to photooxidation reactions relative to others, they have had much success in the development of photochromic ophthalmic lenses. Its thermal reversibility at ambient temperature hinders it from being applied as an optical molecular switch.

1.5.3.3 - Fulgides

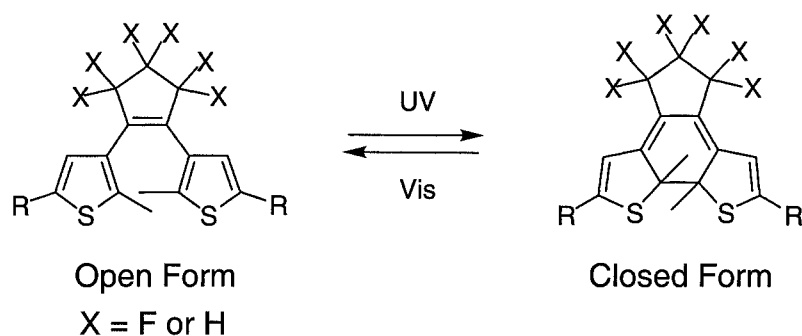


Scheme 1.3. Photoisomerization of fulgides

Photoisomerization of fulgides involve photoinduced conrotatory electrocyclic ring-closing/ring opening-reactions between the colorless open and colored closed forms (Scheme 1.3). Due to the nature of the electrocyclic reaction, the photochromism is thermally irreversible, making them attractive candidates for applications in optical information storage and as molecular switches. Fulgides have also been exploited in regulation of fluorescence, optical rotation, non-linear optical properties, liquid crystalline properties, and biological

activities.¹⁸ The efficiency of this photochrome is limited due to the competing *cis-trans* isomerization that is competing with the ring-closing reaction upon irradiation with UV light.

1.5.3.4 - 1, 2 Bis(3-thienyl)cyclopentene derivatives



Scheme 1.4. Photoisomerization of 1,2-bis(3-thienyl)cyclopentene derivatives

Similar to the fulgides, 1,2-bis(3-thienyl)cyclopentene derivatives, or dithienylethenes (DTE's), undergo a photoinduced electrocyclic ring-opening/ring-closing reaction between their colorless ring-open and colored ring-closed forms (Scheme 1.4).¹⁹ This class of photochromic molecule is popular in the literature due to its impressive fatigue resistance and thermal irreversibility properties. DTE's not only possess higher fatigue resistance than the fulgides, their synthesis of the photochromic backbone is much shorter.

In terms of fatigue resistance, DTE's have been reported to undergo 10,000 switching cycles before significant degradation. The thermal irreversibility stems from the disallowed thermal disrotatory electrocyclic ring-opening of the closed form. Disrotatory ring closing is allowed; however, the methyl groups on the 2-position of the thiophene heterocycles sterically inhibit this process. The open form of DTE undergoes a photochemical conrotatory electrocyclic reaction. Upon irradiation of the open-form with UV light, an electron is promoted to an excited state, forming the excited state HOMO, allowing the 6 π electron conrotatory electrocyclic ring closing according to Woodward-Hoffman rules (Figure 1.10).

The open form of DTE photochromes can exist in a parallel or anti-parallel conformation with respect to the thiophene rings (Figure 1.11). In order for the photocyclization to proceed, the thiophene rings must be in the anti-parallel conformation to allow for efficient overlap of the appropriate p-orbitals.

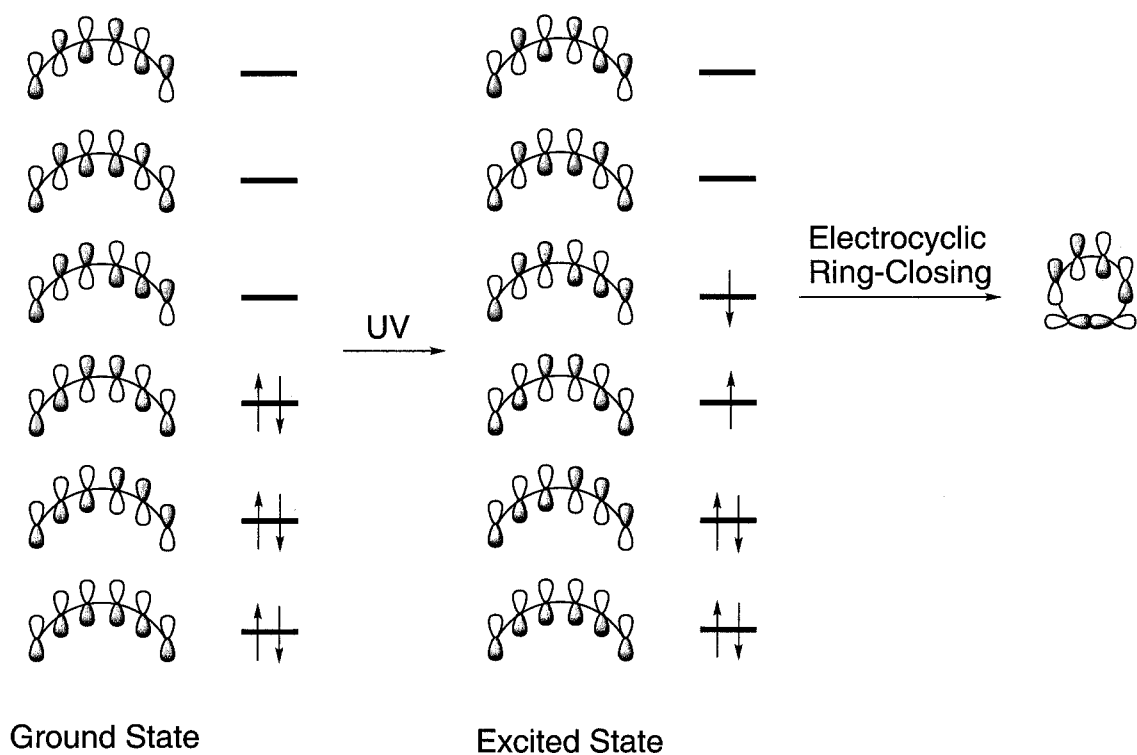


Figure 1.10. Molecular orbital representation of the electrocyclic ring closing reaction of the hexatriene system in 1,2-bis(3-thienyl)cyclopentene derivatives.

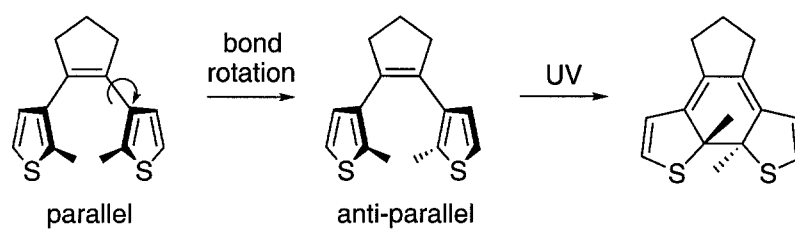


Figure 1.11. Rotation of the thiophene rings to produce the photochromic anti-parallel conformation of DTE.

A linear conjugation pathway between the two 5-positions of the thiophene heterocycles is created upon cyclization of the DTE photochrome (R groups in Scheme 1.4). Extending the π system in the closed form results in a red shift of the absorbance compared to the open-form, giving the closed form its color. This can be monitored by UV/Vis spectroscopy (Figure 1.12).

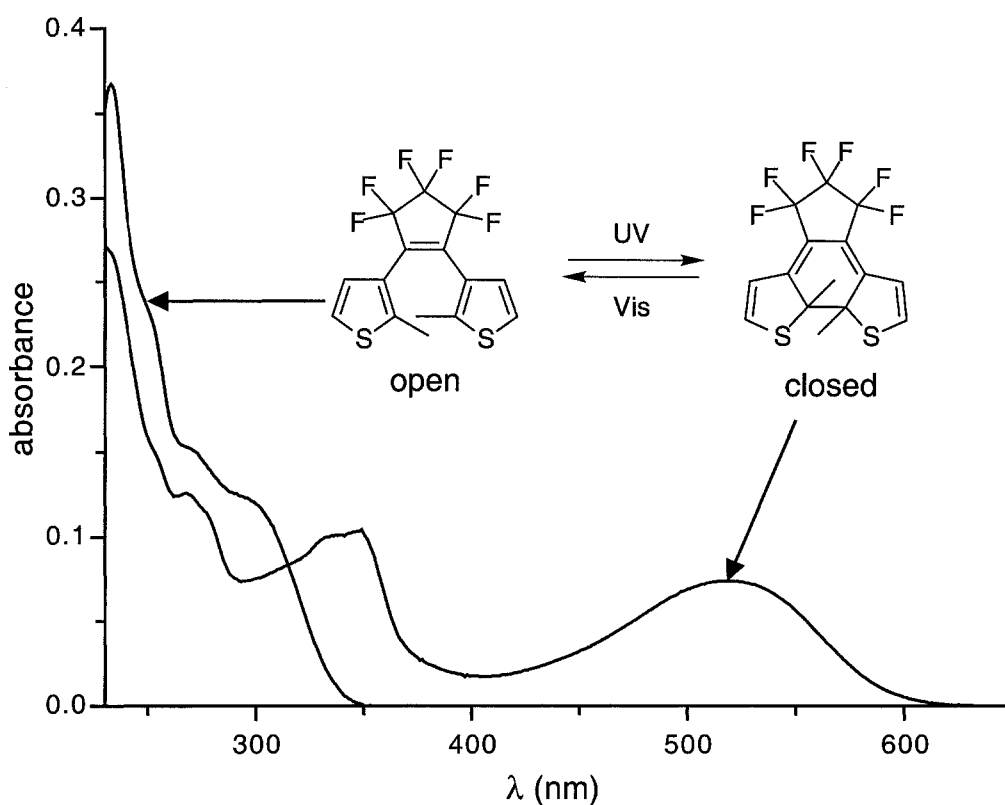
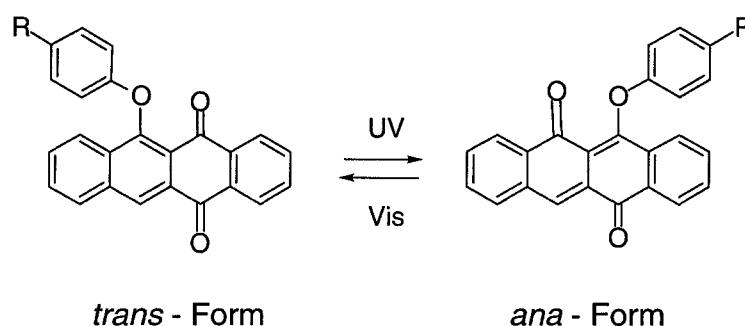


Figure 1.12. UV-vis spectrum of open and closed-forms of a DTE photochrome. The spectrum of the closed-form was obtained by irradiation of 2×10^{-5} M CH_2Cl_2 solutions of the open-form with 313 nm (UV) light for 30 seconds. The spectrum of the open-form was regenerated by irradiation of the closed-form with broad band light > 434 nm for 60 seconds.

DTE's have been studied in which the cyclopentene ring connecting the two thiophene rings is substituted with hydrogens or fluorines ($X = H$ or F in Scheme 1.4). Perfluorinated 1,2-bis(3-thienyl)cyclopentene derivatives are common in the literature and have precedent for being more robust than their hydrogenated counterparts,²⁰ however this phenomenon has never been rigorously studied.

Switching between the two forms of 1,2-bis(3-thienyl)cyclopentene derivatives has been found to be accompanied by changes in physical properties other than absorbance¹, such as luminescence,²¹ refractive index,²² electronic conduction,²³ pKa,²⁴ viscosity,²⁵ and optical rotation.²⁶ Applications using this photochrome come from exploiting these accompanying physical changes and offer promise in actinometry, rewritable optical data storage, waveguides, holography and molecular transistors. This photochromic molecule is the subject of Chapter 2 of this thesis.

1.5.3.5 – Phenoxyanthracenequinones



Scheme 1.5. Photochromism of phenoxyanthracenequinone

Phenoxynaphthacenequinones (PNQ's) are photochromic molecules that undergo a reversible photoisomerization between their yellow *trans*- and orange *ana*-forms upon irradiation with UV and visible light (Scheme 1.5).²⁷ This phenomenon has been the subject of several studies since its discovery by Gerasimenko and Poteleshenko in 1971²⁸ due to the PNQ's thermal irreversibility²⁹ and high fatigue resistance.³⁰

The photochromism of PNQ is most conveniently monitored by UV-vis spectroscopy (Figure 1.13). Upon irradiation of the *trans*-form ($\lambda_{\text{max}} = \sim 400$ nm) with UV light (365 nm), two absorbances at $\lambda_{\text{max}} \sim 450$ and ~ 480 nm appear, corresponding to the absorption of the *ana*-form. Upon irradiation with visible light (> 434 nm), the original spectrum is obtained illustrating the reversibility of the photochemical transformation. The λ_{max} and the molar absorption coefficients (ϵ) of both forms are little affected by substituents on the phenoxy group as their electronic effects are buffered by the oxygen atom between the naphthacene and phenyl rings.³¹ The photostationary state achieved upon UV irradiation, however, varies as the substituents vary, usually ranging between 70 – 90% of the *ana*-form.

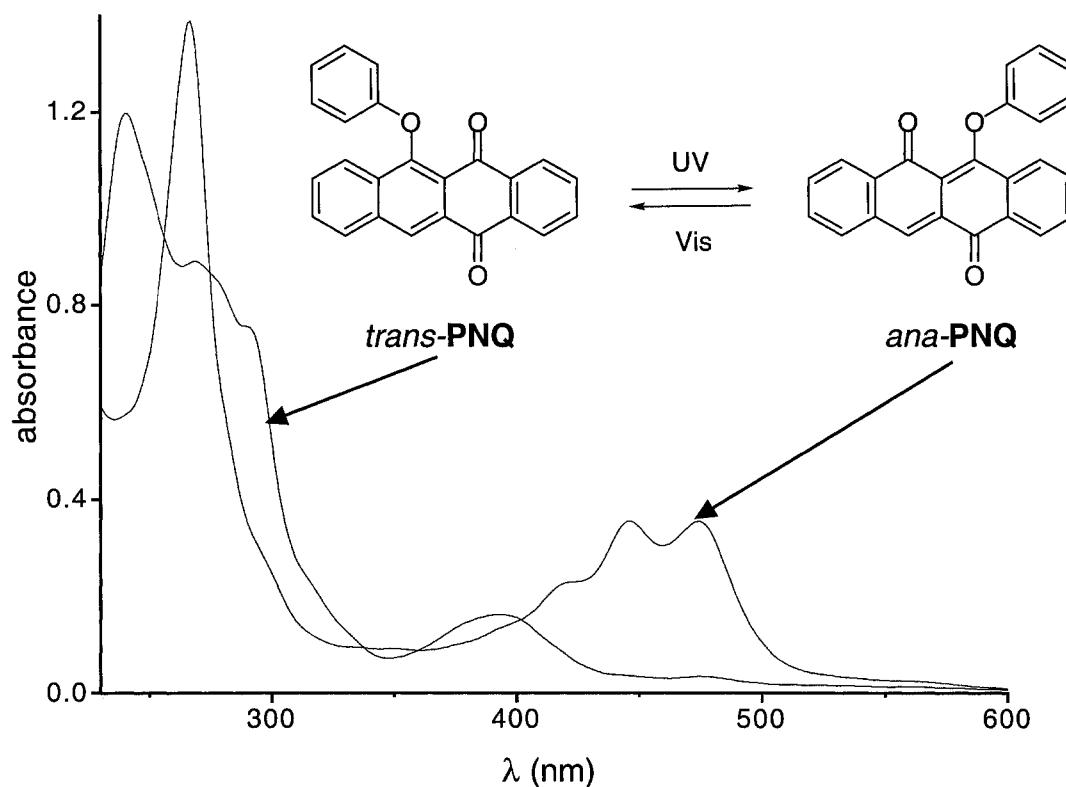


Figure 1.13. UV-vis absorption spectral changes upon photoisomerization of PNQ. The spectrum of the *ana*-form was obtained by irradiation of a 2.5×10^{-5} M CH_2Cl_2 solution of *trans*-PNQ with 365 nm light for 50 seconds. The original spectrum of *trans*-PNQ is regenerated upon irradiation of the *ana*-form with broad band light > 434 nm for 60 seconds.

The mechanism of photoisomerization has been proposed to go through a spirocyclic zwitterionic transition state as illustrated in Figure 1.14.^{31,32} This mechanism lacks experimental confirmation, however, EPR studies have shown no evidence of a radical present, suggesting heterolytic C–O cleavage.³²

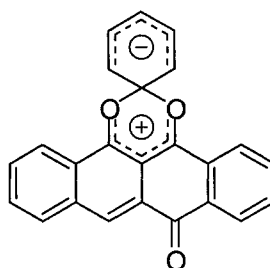


Figure 1.14. Proposed transition state of PNQ photoisomerization

Transient absorption spectroscopy has been performed on PNQ in order to probe the transient species involved in its photochromism.³³ It was found that the photoisomerization reaction of the *trans*- to *ana*-PNQ is an adiabatic photoreaction proceeding via the triplet state. Photoexcitation of the *trans*-form directly results in its singlet excited state (*trans* S₁). Intersystem crossing results in its triplet state (*trans* T₁), which then undergoes the isomerization to the *ana*-form triplet state (*ana* T₁). Thermal decay of this excited state results in the *ana*-form ground state. This transition is represented in scheme 1.6.



Scheme 1.6. Transient species involved in PNQ photoisomerization.

Relative to the other photochromic molecules discussed, very little has been reported on PNQ's; reviews and books written on photochromism have no mention of it despite its ideal photochromic properties. In the literature, PNQ photochromes have been investigated in solution, polymers, Langmuir Blodgett films and self-assembled monolayers; however, only a

couple of examples exist in the literature where the changes in properties other than absorbance are exploited.³⁴ These involve reversible transduction of current between two electrodes separated by a layer of PNQ; upon photoisomerization, the current can be turned *on* or *off*. This suggests a change in electronic properties between the two forms, however no systematic physical characterization of such a change existed in the literature before my work with PNQ. The PNQ photochrome is the subject of Chapter 3 of this thesis.

1.6 - Preview of Thesis

Due to the impressive features of 1,2-bis(3-thienyl)cyclopentene derivatives and phenoxynaphthacenequinones, my research has focussed on these two photochromic molecules as components in molecular devices.

1.6.1 – Chapter 2

Chapter 2 focuses on the DTE class of photochromic molecules. Practical handling of these photochromes, in applications such as molecular information storage, requires them to be in a polymeric rather than a monomeric form. I sought to explore a novel polymerization method to generate DTE polymers that is compatible with a maximum number of pendant functional groups. It is also important that polymerization does not affect its photochromism;

photoisomerization must still be allowed in the solid-state to be useful in molecular device applications. A series of DTE homopolymers were prepared and characterized using Ring Opening Metathesis Polymerization (ROMP) and their photochromic properties in solution and the solid-state were investigated.

1.6.2 – Chapter 3

Chapter 3 focuses on exploiting PNQ's photochromism. Photosynthetic plants and bacteria use quinones as electron acceptors in photoinduced electron transfer (PET) reactions; this involves photoexcitation of a porphyrin chromophore followed by electron transfer to a quinone to generate a charge separated state. Charge separation is one of the key step in conversion of light energy into chemical energy. I sought to explore changing the electron accepting ability of the quinone moiety by using a photochromic PNQ, therefore regulating PET.

1.6.3 – Chapter 4

Chapter 4 focuses on combining the two photochromes of interest into a multi-addressable photochromic molecule; a system in which four states can be accessed results in more information stored per molecule. A hybrid PNQ-DTE photochrome was synthesized and

characterized in order to investigate this phenomenon. By tailoring the irradiation wavelength, four different states can be accessed within the same molecule.

1.6.4 – Thesis Statement

The main theme of this thesis is the exploitation of photochromic compounds in all-photon mode molecular devices. Investigations in such areas are important in making more efficient devices powered and controlled by light energy. In the conclusion of this thesis, I will present some future directions for this research as I see it, as well as the area of all-photon-mode molecular devices.

1.7 – References

1. Pearsall, J.; Trumble, B. Eds. *The Oxford English Reference Dictionary*, 2nd Edition, Oxford University Press: New York, 1996.
2. Balzani, V.; Credi, A.; Raymo, F. M.; Stoddart, J. F. *Angew. Chem. Int. Ed.* **2000**, *39*, 3348-3391.
3. Voet, D.; Voet, J. G. *Biochemistry*, 2nd Ed., John Wiley and Sons, Inc.: New York, 1995, Chapt. 29-31.
4. Alberts, B.; Bray, D.; Lewis, J.; Raff, M.; Roberts, K.; Watson, J. D. *Molecular Biology of the Cell*, 3rd Ed., Garland Publishing, Inc.: New York, 1994, pp. 536-542.
5. “Molecular-Level Machines and Logic Gates”: A. Credi, Ph.D. thesis, Università di Bologna, **1998** (available at <http://www.ciam.uinbo.it/photochem.html>)
6. Feringa, B. L., Ed. *Molecular Switches*, Wiley-VCH: Weinheim, 2001; pp. 63-106.
7. (a) Balzani, V.; Scandola, F., Eds. *Supramolecular Photochemistry*, Ellis Horwood: London, 1991; pp. 25-50. (b) Kavarnos, G. J. *Fundamentals of Photoinduced Electron Transfer*, VCH: New York, 1993.
8. Sharma, A.; Schulman, S. G. *Introduction to Fluorescence Spectroscopy*, John Wiley and Sons, Inc.: New York, 1999, pp. 1-26.
9. Brouwer, A. M.; Frochot, C.; Gatti, F. G.; Leigh, D. A.; Mottier, L.; Paolucci, F.; Roffia, S.; Wurpel, G. W. H. *Science*, **2001**, *291*, 2124-2128.
10. Bouas-Laurent, H.; Durr, H. *Pure Appl. Chem.* **2001**, *73*, 639-665.

11. Okamoto, K. *Fundamentals of Optical Waveguides*, Academic: San Diego, 2000.
12. (a) Ern, J.; Bens, A. T.; Martin, H. D.; Kudlova, K.; Trommsdorff, H. P.; Krysch, C. J. *Phys. Chem. A* **2002**, *106*, 1654-1660. (b) Willett, K. L.; Hites, R. A. *J. Chem. Ed.* **2000**, *77*, 900-902. (c) Uhlmann, E.; Gauglitz, G. *J. Photochem. Photobiol. A* **1996**, *98*, 45-49.
13. Myles, A. J.; Branda, N. R. *Adv. Funct. Mater.* **2002**, *12*, 167-173.
14. This article describes the physical limits to high-density magnetic recording; White, R. L. *J. Magn. Magn. Mater.* **2000**, *209*, 1.
15. Gonzalez-Hernandez, J.; Chao, B. S.; Strand, D.; Ovshinsky, S. R.; Pawlik, D.; Gasiorowski, P. *Appl. Phys. Commun.* **1992**, *11*, 557.
16. For a good overview of photochromic molecules, terminology in the area, and representative examples, see: Crano, J. C.; Guglielmetti, R. J., Eds. *Organic Photochromic and Thermochromic Compounds*, Vol. 1, Plenum Press: New York, 1999.
17. Feringa, B. L., Ed. *Molecular Switches*, Wiley-VCH: Weinheim, 2001; pp. 399-419.
18. Crano, J. C.; Guglielmetti, R. J., Eds. *Organic Photochromic and Thermochromic Compounds*, Vol. 1, Plenum Press: New York, 1999; pp. 11-84.
19. Feringa, B. L., Ed. *Molecular Switches*, Wiley-VCH: Weinheim, 2001; pp. 37-62.
20. Peters, A.; Branda, N. R. *Adv. Mater. Opt. Electron.* **2000**, *10*, 245-249.
21. (a) Norsten, T. B.; Branda, N. R. *J. Am. Chem. Soc.* **2001**, *123*, 1784-1785. (b) Norsten, T. B.; Branda, N. R. *Adv. Mater.* **2001**, *13*, 347-349. (c) Fernandez-Acebes, A.; Lehn, J.-M. *Chem. Eur. J.* **1999**, *5*, 3285-3292. (d) Tsivgoulis, G. M.; Lehn, J.-M. *Chem. Eur. J.* **1996**, *2*, 1399-1406.

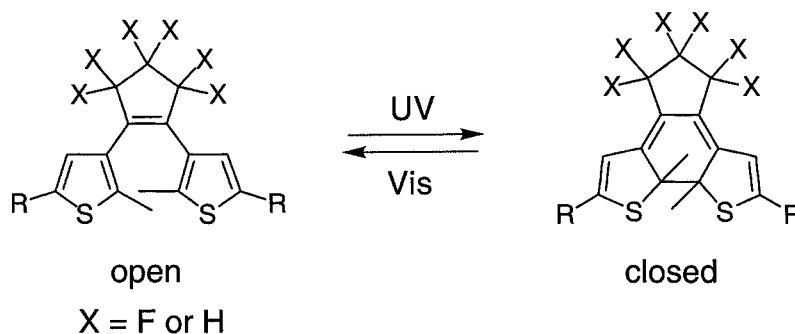
22. Kawai, T.; Fukuda, N.; Groschl, D.; Kobatake, S.; Irie, M. *Jpn. J. Appl. Phys.* **1999**, *38*, L1194-L1196. (b) Biteau, J.; Chaput, F.; Lahlil, K.; Boilot, J.-P.; Tsivgoulis, G. M.; Lehn, J.-M.; Darracq, B.; Marois, C.; Levy, Y. *Chem. Mater.* **1998**, *10*, 1945-1950. (c) Kim, E.; Choi, Y.-K.; Lee, M.-H. *Macromolecules* **1999**, *32*, 4855-4860.
23. Tsujioka, T.; Hamada, Y.; Shibata, K. *Appl. Phys. Lett.* **2001**, *78*, 2282-2284. (b) Kawai, T.; Kunitake, T.; Irie, M. *Chem. Lett.* **1999**, 905-906.
24. Kawai, S. H.; Gilat, S. L.; Lehn, J.-M. *Eur. J. Org. Chem.* **1999**, 2359-2366.
25. Lucas, L. N.; van Esch, J.; Kellogg, R. M.; Feringa, B. L. *Chem. Commun.* **2001**, 759-760.
26. Murguly, E.; Norsten, T. B.; Branda, N. R. *Angew. Chem., Int. Ed.* **2001**, *40*, 1752.
27. Fang, Z.; Wang, S.; Yang, Z.; Chen, B.; Li, F.; Wang, J.; Xu, S.; Jiang, Z.; Fang, T. *J. Photochem. Photobiol., A* **1995**, *88*, 23.
28. Gerasimenko, Y. E.; Poteleshenko, N. T. *Zh. Org. Khim.* **1971**, 2413.
29. Zelichenok, A.; Buchholz, F.; Fischer, E.; Ratner, J.; Krongauz, V. *J. Photochem. Photobiol. A: Chem.* **1993**, *76*, 135-141.
30. Buchholz, F.; Zelichenok, A.; Krongauz, V. *Macromolecules* **1993**, *26*, 906-910.
31. Yokoyama, Y.; Fukui, S.; Yokoyama, Y. *Chem. Lett.* **1996**, 355-356.
32. Gritsan, N. P.; Klimenko, L. S. *J. Photochem. Photobiol. A: Chem.* **1993**, *70*, 103-117.
33. Malkin, J.; Zelichenok, A.; Krongauz, V.; Dvornikov, A. S.; Rentzepis, P. M. *J. Am. Chem. Soc.* **1994**, *116*, 1101-1105.

34. a) Oreshkin, A. I.; Panov, V. I.; Vasilev, S. I.; Koroteev, N. I.; Magnitskii, S. A. *JETP Lett.* **1998**, *68*, 521-526. b) Doron, A.; Katz, E.; Portnoy, M.; Willner, I. *Angew. Chem. Int. Ed. Engl.* **1996**, *35*, 1535-1537.

Chapter 2 – Synthesis and Characterization of Photochromic Homopolymers Based on 1,2-Bis(3-thienyl)cyclopentene using Ring Opening Metathesis Polymerization

1,2-Bis(3-thienyl)cyclopentene derivatives are viewed as the most promising photochromes, showing potential in applications such as molecular information storage, chemical actinometry, optical waveguides and optical switches. This chapter concentrates on the development of 1,2-bis(3-thienyl)cyclopentene polymers to facilitate their incorporation into functional molecular devices. An introduction to 1,2-bis(3-thienyl)cyclopentene derivatives was presented in Chapter 1. In this chapter, key points concerning 1,2-bis(3-thienyl)cyclopentenones will first be presented, followed by our approach to polymerizing them, and finally a detailed characterization of the resulting polymers.

2.1 - 1,2-Bis(3-thienyl)cyclopentene Derivatives



Scheme 2.1

Photochromic compounds based on 1,2-bis(3-thienyl)cyclopentene derivatives, also called dithienylethenes (DTE), undergo reversible photocyclization between their colorless ring-open and colored ring-closed forms when irradiated with appropriate wavelengths of light (Scheme 2.1).¹ 1,2-Bis(3-thienyl)cyclopentene derivatives not only exhibit excellent photochromic properties, as described in the introduction, the color of the closed forms can be tuned by tailoring the electronic distribution in the conjugated pathway created upon cyclization. This is most conveniently accomplished by changing the pendant functional groups on the thiophene heterocycles, represented by 'R' in Scheme 2.1. Appending groups that extend the linear conjugation pathway of the closed form results in red-shifting of its absorbance (Figure 2.1).

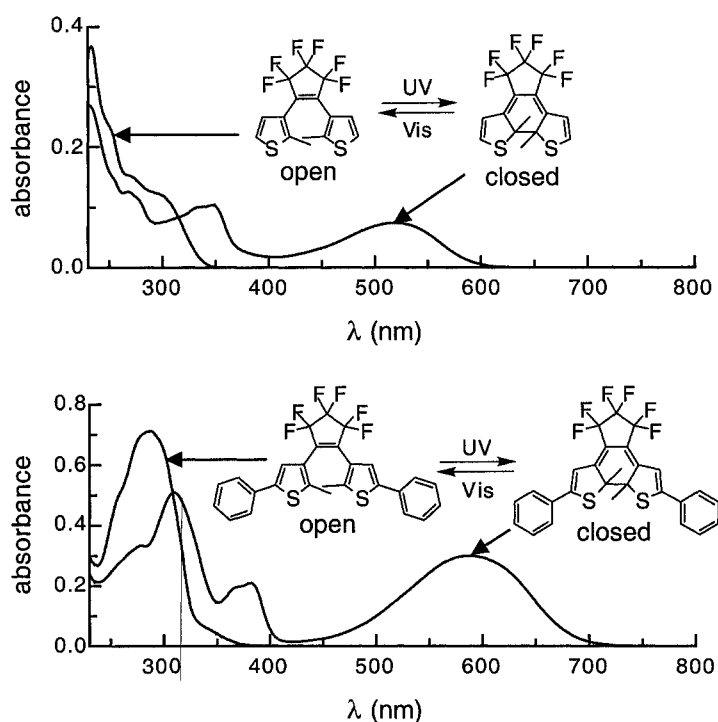


Figure 2.1. Extending the linear conjugation pathway created upon cyclization results in a red-shift in the λ_{\max} of the closed form of DTE. Photoisomerization from the open to closed form was performed by irradiation with 313 nm light for 30 seconds of 2×10^{-5} M CH_2Cl_2 solutions. Irradiation with light > 434 nm regenerated the original spectrum.

As mentioned in the introduction, this structural change is also accompanied by changes in physical properties other than absorbance. Examples of changing physical properties other than absorbance are presented in the following examples.

2.1.1 – Regulation of Current Using DTE's

Figure 2.2 represents an example in which the change in linear conjugation pathway upon photoisomerization of DTE results in a change in electron flow between the two pendant pyridinium moieties.² The open form shows no electrochemical process between 0.6 and -0.6 V. Upon photoisomerization to the closed form, a clear, reversible and monoelectronic reduction wave is observed at -0.23 V. In the open form, there is no linear conjugation pathway between the two pyridinium moieties, therefore each one will be reduced independently and at high potential. In the closed form, the two pyridinium moieties are linearly conjugated, therefore upon reduction, the radical produced can be stabilized between the two pyridiniums. This gain in stability of the closed form radical anion results in a less negative reduction potential, translating into a molecule which can accept an electron easier in one form than the other. Potential applications of such systems include photo-transistors where the molecules act as a photochemical gate between two electrodes.

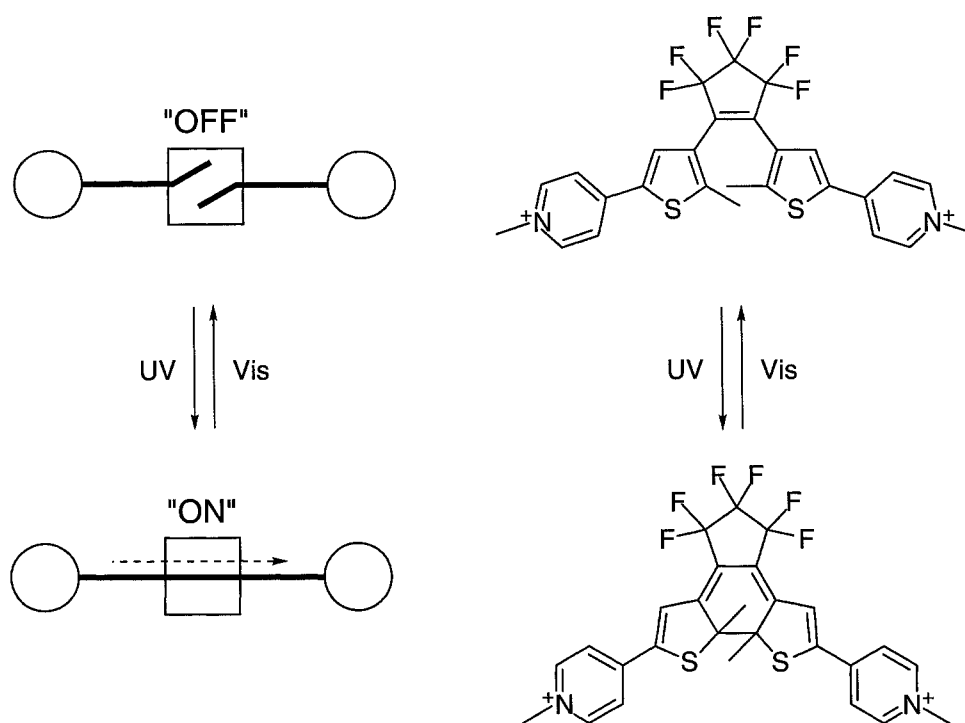


Figure 2.2. Photoregulation of electron flow with a DTE derivative

2.1.2 – Regulation of Magnetic Interactions Using DTE

The magnetic interaction between two nitronyl nitroxide radicals can be regulated by photoisomerization of the DTE derivative illustrated in Figure 2.3.³ Upon ring closing, the two nitronyl nitroxide radicals can communicate through the linear conjugation pathway created upon photocyclization. The result of this communication is the alignment of the electronic spins of the two radical species. The net effect of this alignment is the creation of a net magnetization. By switching between the two forms of DTE, the magnetism of the molecule can be reversibly controlled.

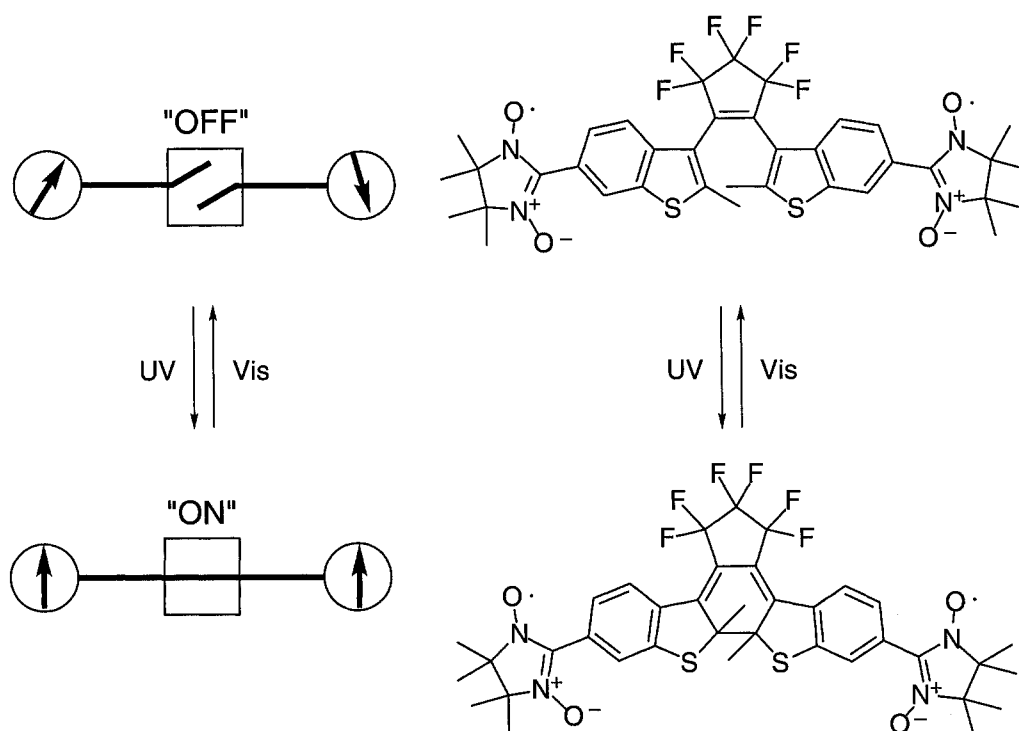


Figure 2.3. Photoregulation of intramolecular magnetic interaction

2.1.3 – Regulation of Fluorescence Using DTE

A diporphyrinic DTE derivative was studied to investigate the effect of photoisomerization on the fluorescence properties of the porphyrins (Figure 2.4).⁴ The porphyrins' fluorescence is maintained in the open-form, however upon photoisomerization to the closed-form, the porphyrins' fluorescence decreases in intensity. Irradiation with visible light results in the original fluorescence, confirming the reversibility of this effect. The decrease in fluorescence of the closed form is proposed to be due to an energy transfer pathway between the porphyrins and the closed form DTE, however no direct evidence of this decay pathway has yet been reported.

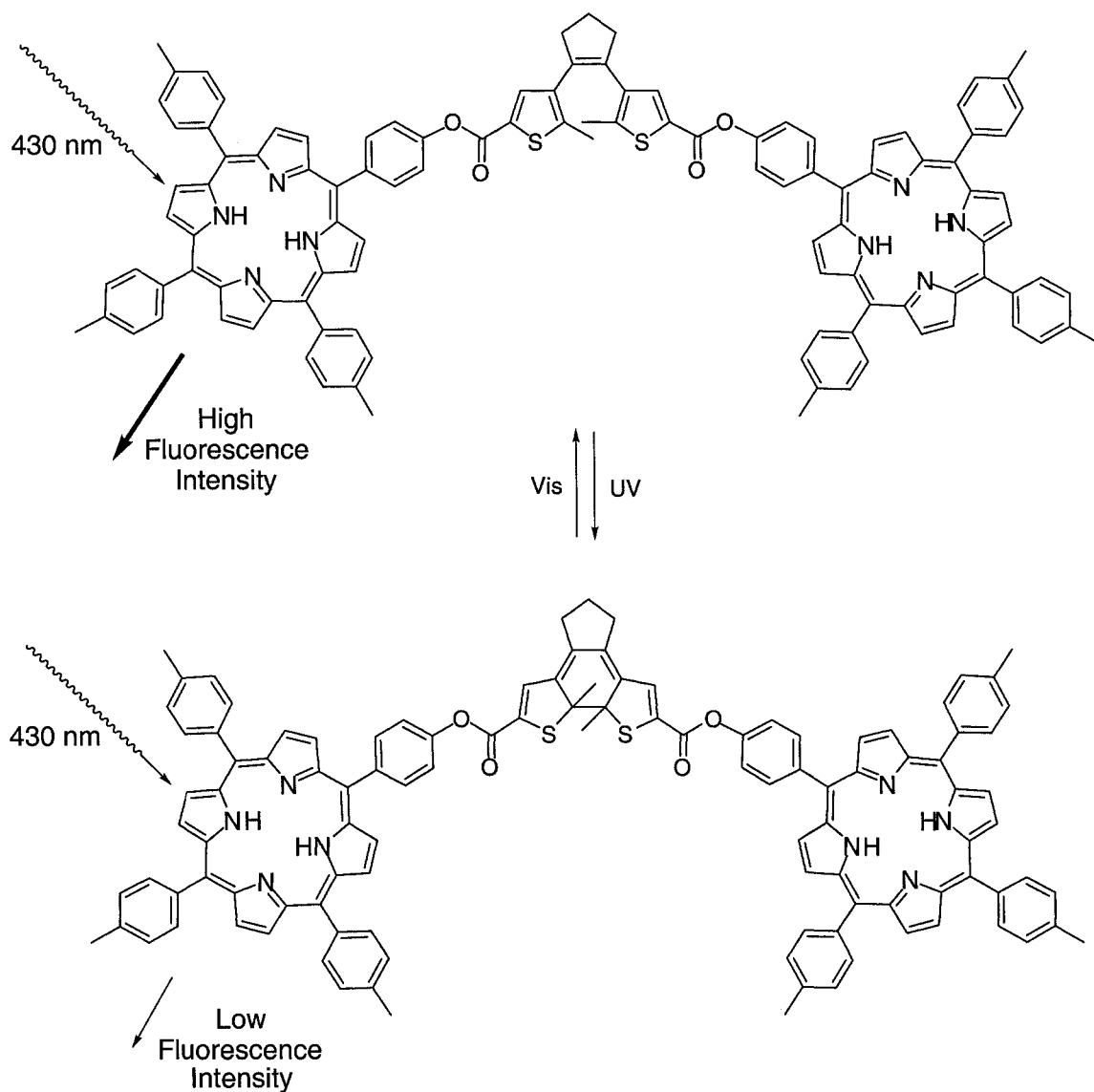


Figure 2.4. Photoregulation of fluorescence.

2.2 - Polymeric DTE's

Despite the breadth of the potential applications of photochromic DTE's as functional materials, the published studies, with a few exceptions,^{6e,j} have focused on evaluating the utility

of monomeric photochromic systems in solution. Practical application of this technology requires the photochromic compounds to be in the form of a film, sheet or bead, which dictates the use of a polymeric rather than a monomeric form.⁵ Photochromic polymers have the potential advantage of having a high photochrome concentration without problems of crystallization, phase separation or the formation of concentration gradients.^{6c}

Several examples of photochromic polymers have been reported, using 1,2-bis(3-thienyl)cyclopentene⁶ and other photochromic derivatives.⁷ The most common method for the introduction of DTE photochromes into polymer matrices, such as polystyrene and polymethacrylate, is by doping them. This involves trapping single molecules within the polymer matrix. Polymers doped with 1,2-bis(3-thienyl)cyclopentene derivatives show efficient photochromism, however the low concentration of photochrome in the polymer matrix make them inefficient for application.

Several copolymers (polymers containing two different repeating units)⁸ of DTE have been reported, as illustrated in Figure 2.5. Polymer **A**^{6b} is a polymethacrylate copolymer and polymer **B**^{6c} is a polystyrene copolymer. Both of these polymers show efficient photochromism in the solid state, however polymer **A** only contains 0.34% DTE and **B** only contains 2% DTE, with respect to the total mass of the polymer. Also, both rely on radical polymerization techniques limiting the choices of pendant functionality on the photochrome. Polymer **C**^{6j} is synthesized using sol-gel techniques where the DTE photochrome is covalently linked to a silica matrix. This polymer contains a higher concentration of DTE (~ 40%), and shows significant refractive index changes upon photoirradiation ($\Delta\eta = 0.04$). The problem with polymer **C** is the technique used in its synthesis. The sol-gel process requires several steps followed by a slow,

intense heating process, making it incompatible with a wide range of pendant functionality necessary in successfully exploiting this photochrome.

It is desirable to develop photochromic polymers that are not only easily synthesized, but have a high concentration of the photochrome in the polymer, as it will result in amplification of the desired effect. For example, homopolymers (polymers containing one repeating unit)⁸ are more desirable in applications such as information storage systems due to the increased density of photochromic compound per unit area or volume. Other problems to overcome in the area of photochromic polymers are poor solubility, making it difficult to cast the polymers as thin films, and poor photochromic activity of the polymer relative to the monomers.

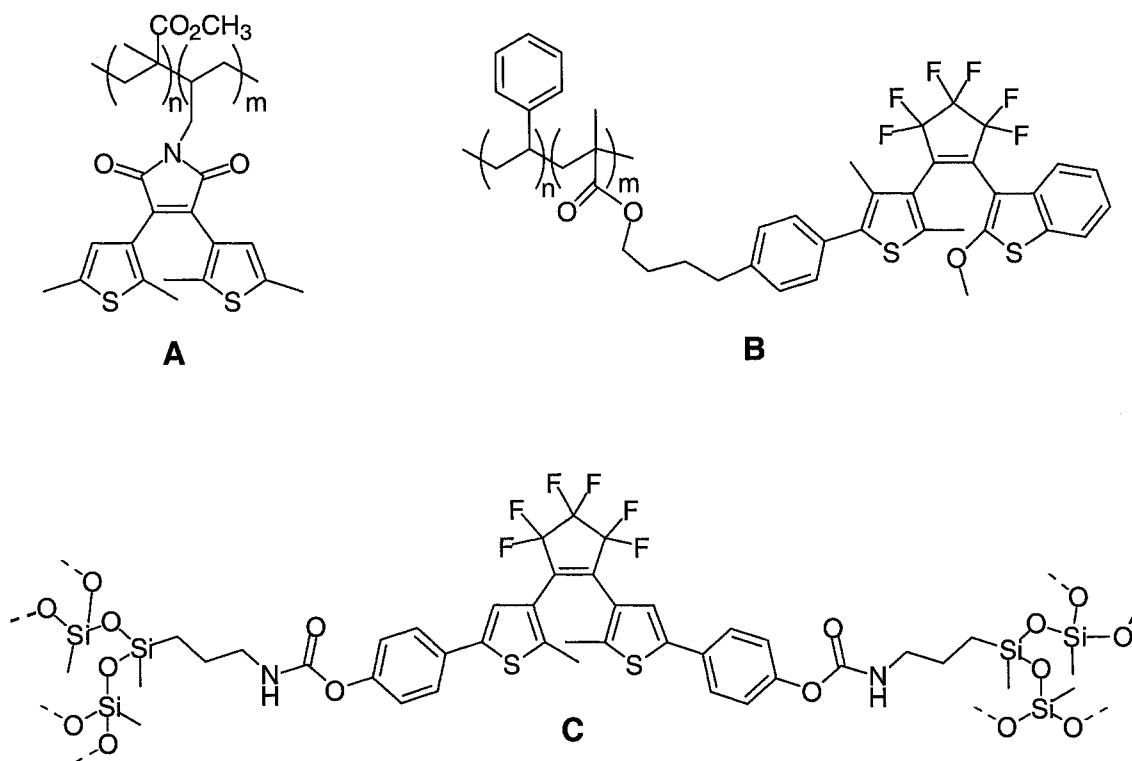
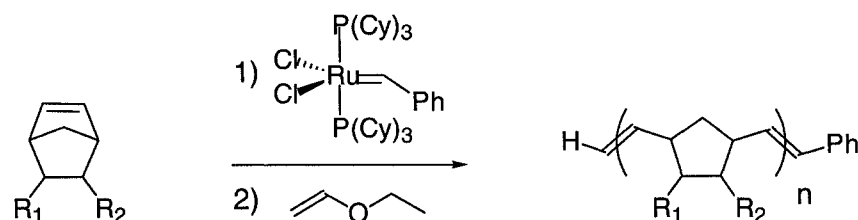


Figure 2.5. Photochromic copolymers based on DTE's A, B and C.

In terms of fully exploiting the DTE photochromes in the solid state, it is also important to develop a mild polymerization method so as not to limit the pool of functional groups available as pendant groups on the photochrome. Ring Opening Metathesis Polymerization (ROMP) involves the living polymerization of strained bicyclic olefins.⁹ This technique has gained much popularity due to its very mild reaction conditions, tolerance of a wide range of functional groups, and control over the polymer chain length, which results in polymers with low polydispersities (Scheme 2.2). By exploiting these features of ROMP, the first mild and controllable method for synthesizing photochromic polymers is reported herein.



Scheme 2.2

2.3 - Ring Opening Metathesis Polymerization (ROMP)

Olefin metathesis reactions are defined by a metallo-carbene insertion into a double bond, as illustrated in Figure 2.6.¹⁰ Historically, olefin metathesis reactions have relied on harsh reaction conditions and therefore remained uncommon in organic synthesis.¹¹ However, over the past two decades, the advent of new efficient catalysts displaying high specificity, mild reaction conditions and functional group compatibility has completely changed this scenario. ROMP involves metathesis of cyclic olefins, where upon ring opening, the propagating metallo-carbene species is attached to the metathesized olefin by a tether. As long as the ring-opening reaction is favored over the ring closing reaction, a polymer is formed.

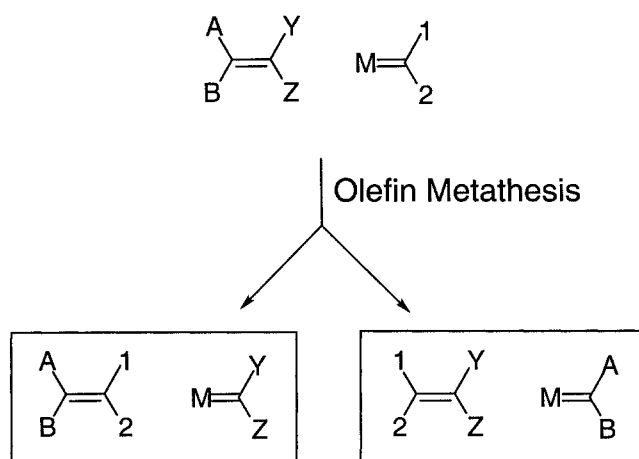
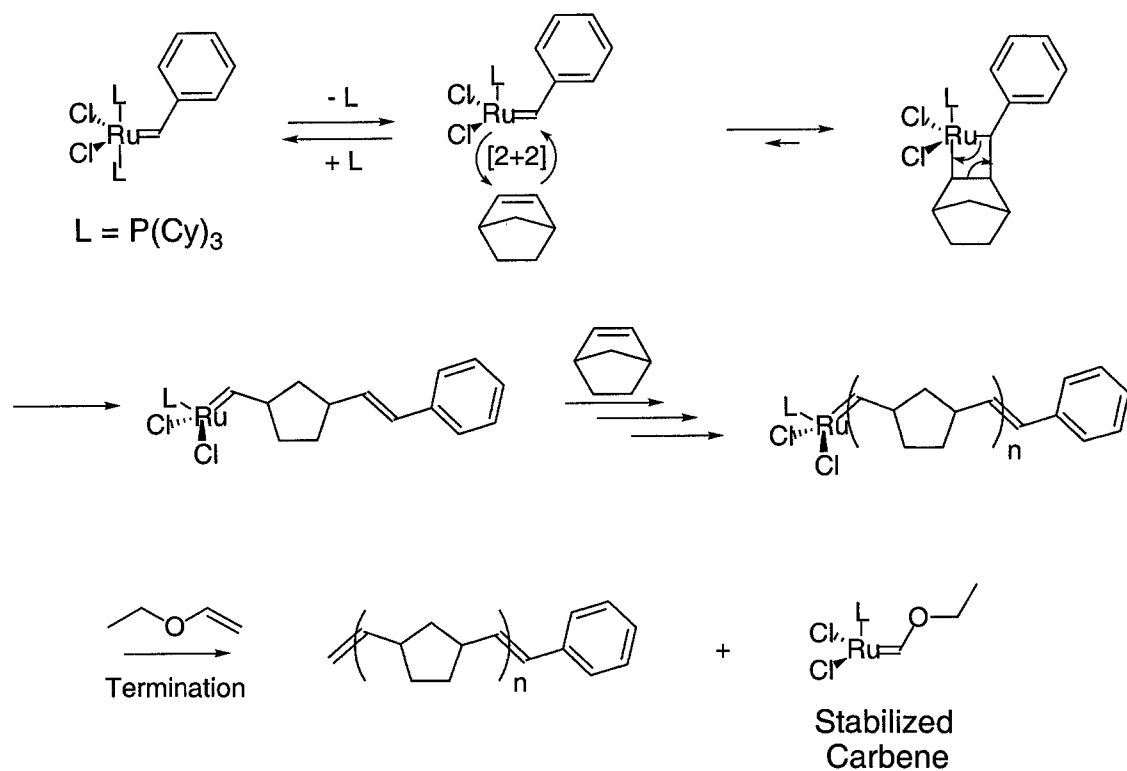


Figure 2.6. Schematic of olefin metathesis

The ruthenium based metathesis catalysts, developed primarily by Grubbs, have shown the most promise in terms of ROMP catalysts, as they are tolerant to several functional groups, more robust to air and protic media, and produce polymers with low polydispersities due to its living nature.¹² Living polymerizations involve the catalyst reacting with a monomer producing another catalytically active species, where one end is the catalyst and the other the growing part of the polymer, that can only react with another monomer. This propagating species does not undergo chain transfer or termination. Once 100% conversion is complete, a chain termination reagent must be added in order to deactivate the propagating species. This ensures stepwise growth of the polymer chain, which is crucial for molecular weight control.

Scheme 2.3 shows the ROMP mechanism of norbornene polymerization using bis(tricyclohexylphosphine)benzylidene ruthenium(IV)dichloride (Grubbs' catalyst), the most common ROMP catalyst. Dissociation of the phosphine ligand affords the initiator species, which subsequently undergoes a [2+2] cycloaddition reaction with norbornene, affording the four membered ruthenium heterocyclic intermediate. A [2+2] cycloreversion of this ring favors

breaking of the strained sigma bond of the bicyclic norbornene, therefore affording the ring-opened norbornene bound to the active ruthenium catalyst. This active species can then react with another norbornene monomer and the process repeats until there is no norbornene left in solution. At this point, the catalyst is still active. Termination is achieved by addition of excess ethyl vinyl ether, which similarly undergoes a [2+2] cycloaddition/cycloreversion reaction with the catalyst to afford the terminated polymer chain and the ruthenium species bound to a stabilized carbene, in which the carbon attached to the metal is bound to an oxygen. A lone pair on the oxygen can donate electrons to the carbene, therefore stabilizing the carbene making it unreactive in metathesis reactions.¹³



Scheme 2.3

2.4 - Photochromic Homopolymers Based on DTE

Our strategy in developing photochromic homopolymers of 1,2-bis(3-thienyl)cyclopentenes using ROMP involves tethering a strained bicyclic olefin to a DTE photochrome followed by polymerization with Grubbs' catalyst. Six polymers were synthesized, as illustrated in Figure 2.7. The polymer chain lengths are represented by the values "n", which are given as absolute values. The polymers are not monodispersed and therefore this value is meant to represent the approximate chain length as determined by Gel Permeation Chromatography (GPC) and the catalyst to substrate stoichiometry.

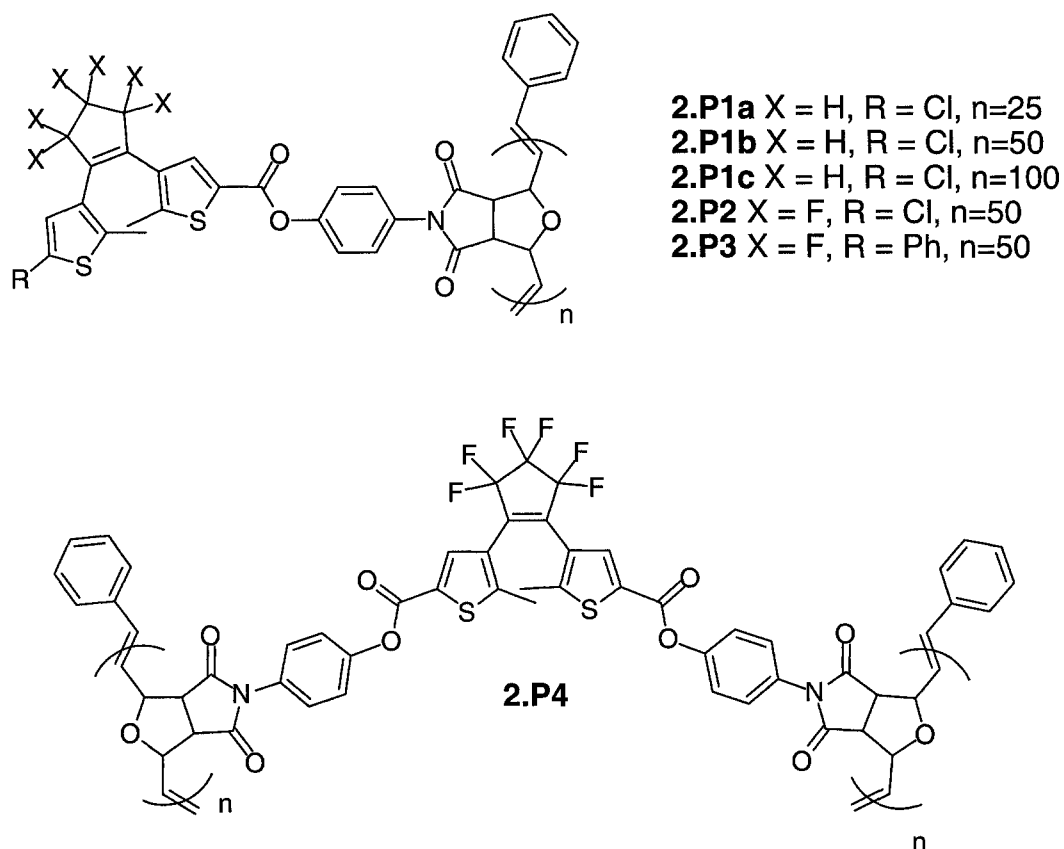


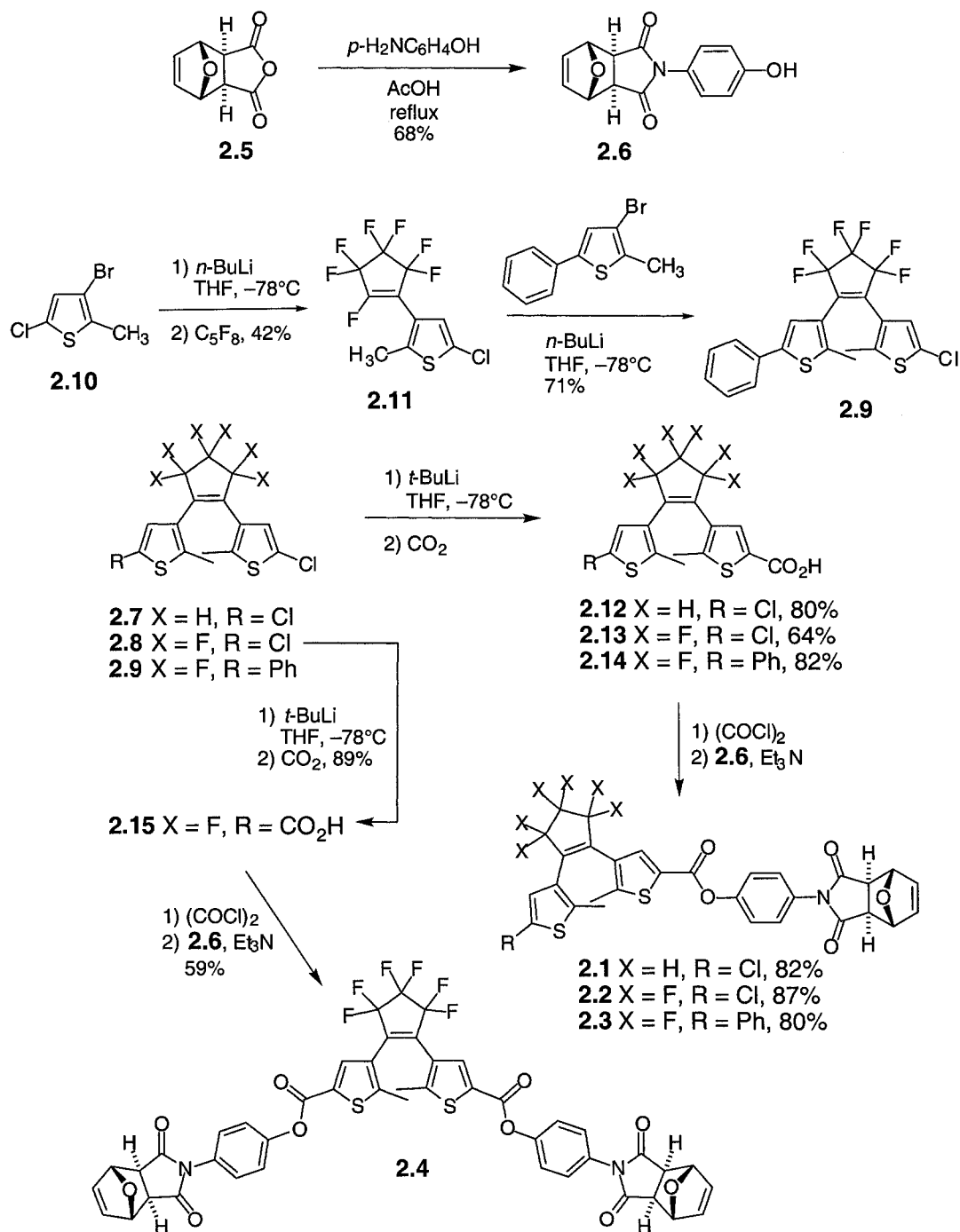
Figure 2.7. Photochromic homopolymers synthesized using ROMP

The **2.P1** polymers (a-c) are all synthesized from a common monomer, differing only in their chain lengths. **2.P2** is identical to **2.P1b** apart from the cyclopentene ring being perfluorinated, which has precedent for being more robust. Perfluorination of the cyclopentene also results in the color of the polymer changing from red to purple, resulting from the red shift in the λ_{max} . **2.P3** has a phenyl group appended to the thiophene heterocycle in place of the chlorine. Upon photocyclization of the photochrome, the molecule has a longer linear conjugation pathway than **2.P2** resulting in a larger λ_{max} and change of color from purple to blue. **2.P4** is a cross-linked polymer synthesized to increase to robustness of the polymer as a whole and to assess the effect of cross-linking on the photochromism. The synthesis and characterization of these photochromic polymers are described in the following sections.

2.4.1 - Synthesis of Monomers.

All of the requisite monomers (**2.1–2.4**) rely on the presence of the 7-oxanorbornene moiety **3.6** in order to facilitate the ROMP process and generate the polymers **2.P1–2.P4** (Scheme 3.4). Oxanorbornene **2.6** can be readily prepared in good yield by condensing the known 7-oxa-bicyclo[2.2.1]hept-5-ene-2,3-dicarboxylic anhydride **2.5**¹⁴ with *p*-aminophenol. The direct precursors to monomers **2.1–2.3** are the photochromic carboxylic acids **2.12–2.14** which can be prepared from dichlorides **2.7**¹⁵ and **2.8**¹⁶ and monochloride **2.9**. This monochloride is prepared by treating 3-bromo-5-chloro-2-methylthiophene **2.10**¹⁷ with *n*-butyl lithium followed by quenching with commercially available octafluorocyclopentene. The synthesis of the photochromic backbone in **2.9** is completed by reacting the lithium salt of 3-bromo-5-phenyl-2-methylthiophene¹⁸ with compound **2.11**. When dichloride **2.8** is treated with an excess of *t*-butyl lithium and quenched with carbon dioxide the diacid **2.15** is the

product. All four photochromic carboxylic acids **2.12**–**2.15** can be coupled to oxanorbornene **2.6** through their respective acid chlorides.

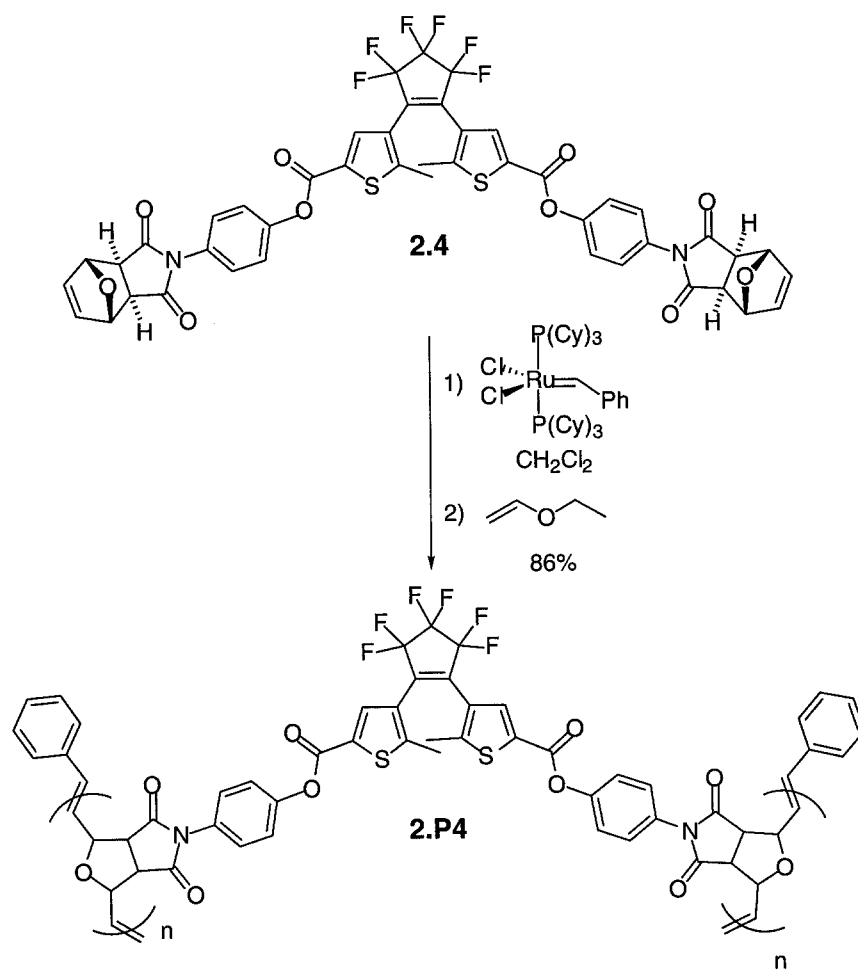
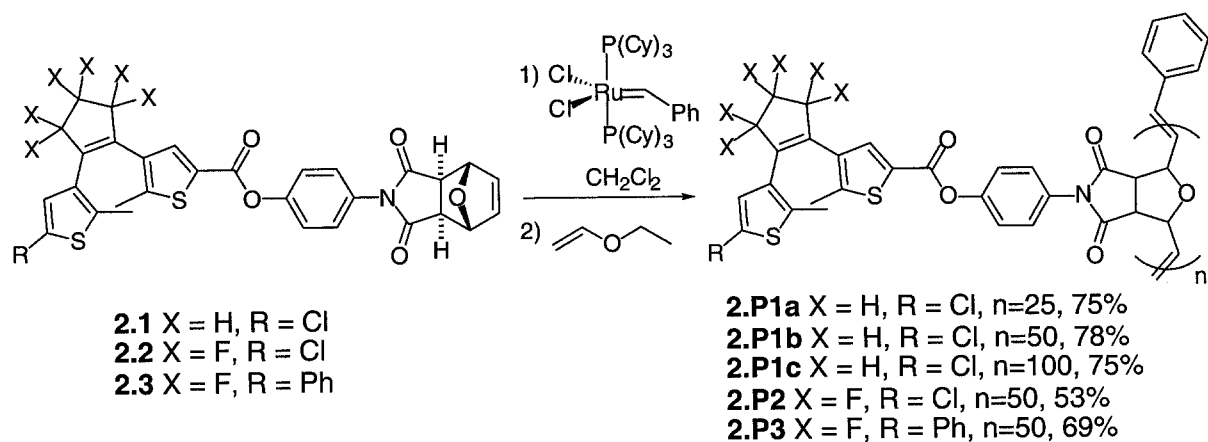


Scheme 2.4. Synthesis of monomers **2.1** - **2.4**.

2.4.2 - Synthesis and Characterization of Polymers

Monomers **2.1–2.4** were subjected to the ROMP conditions shown in Scheme 2.5. In a typical polymerization procedure, a CH_2Cl_2 solution of commercially available bis(tricyclohexylphosphine)benzylidene ruthenium(IV)dichloride (Grubbs' catalyst) is cannulated into a vigorously stirred CH_2Cl_2 solution of appropriate monomer under anhydrous conditions. The resulting homogeneous solution is stirred for 16 hours at room temperature, after which time it is treated with excess ethyl vinyl ether to terminate the living polymerization reaction. All polymers can be conveniently isolated in high purity by precipitating them out of their CH_2Cl_2 solutions by adding excess diethyl ether and collecting them by filtration. Because the fluorinated polymers **2.P2** and **2.P3** are partially soluble in ether the isolated yields were decreased using this particular isolation procedure.

The ^1H NMR spectra of all polymers **2.P1–2.P4** show broadened peaks compared to those of the monomers, characteristic of polymers. The important characteristic of the spectrum is the absence of the peak for the vinylic protons of the strained olefin monomer and presence of a new peak corresponding to the polymer back-bone olefin protons (see Figure 2.8 for a representative example). All other peaks in the ^1H NMR spectrum of the polymers overlap with the corresponding peaks of their respective monomer.



Scheme 2.5

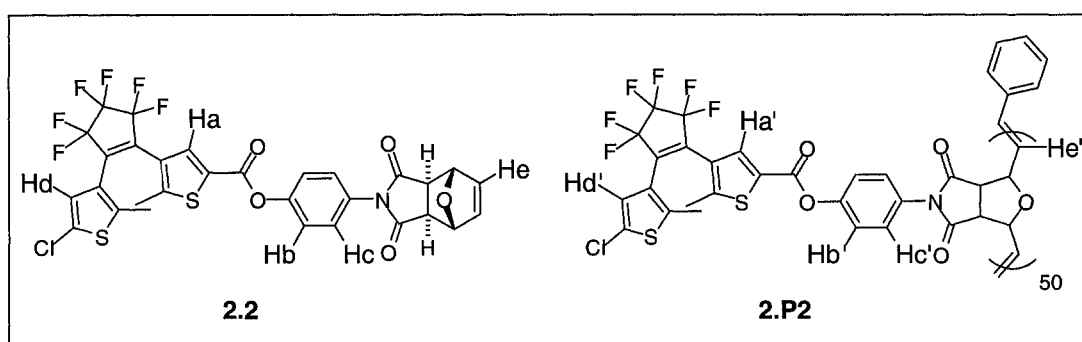
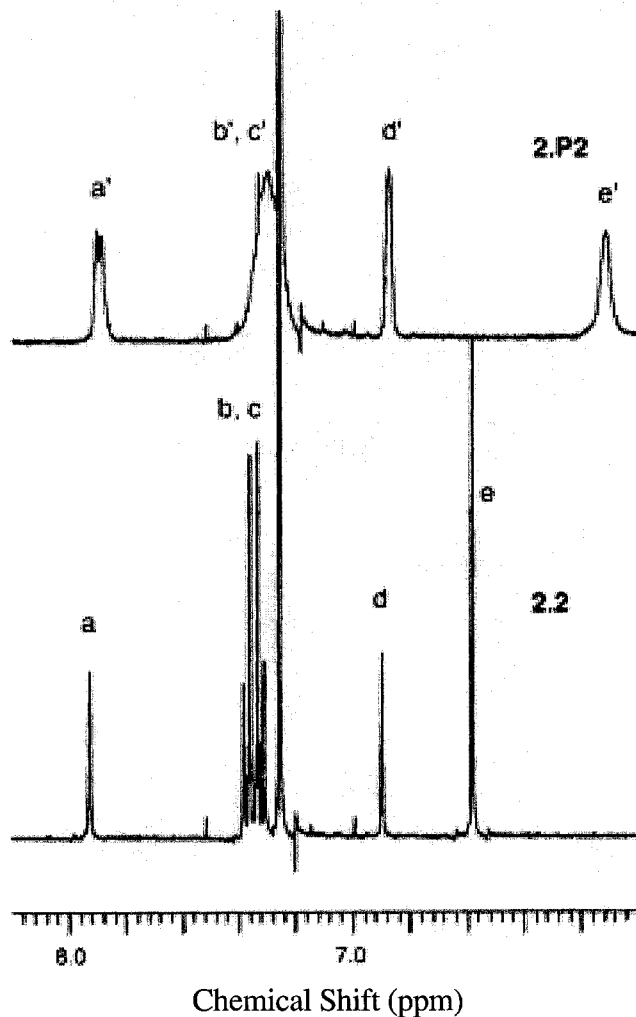


Figure 2.8. ¹H NMR spectra of **2.2** and **2.P** in CDCl₃: Polymerization of **2.2** is characterized by the disappearance of the strained olefin proton peak of **2.2** at 6.6 ppm and the appearance of the new olefinic proton peak of **2.P2** at 6.1 ppm.

2.4.2.1 - Gel Permeation Chromatography

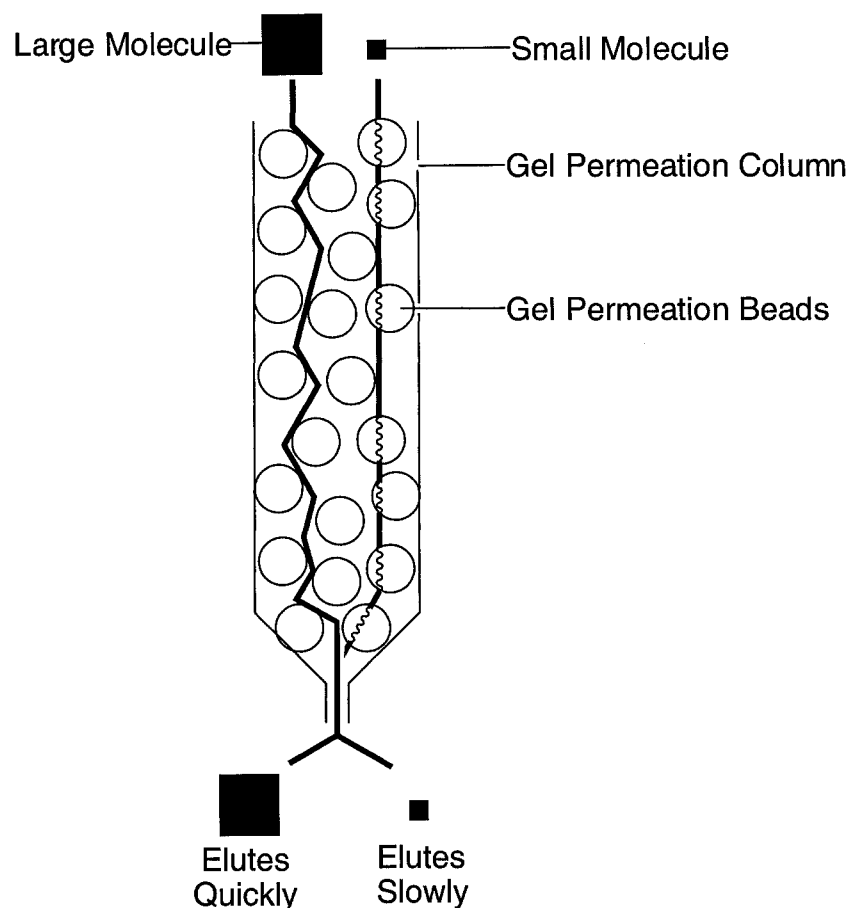


Figure 2.9. Gel permeation chromatography schematic. Larger molecules travel around the gel beads whereas small molecules pass through them, resulting the large molecules eluting more quickly.

Polymer chain lengths were determined using gel permeation chromatography (GPC).¹⁹ Figure 2.9 shows a schematic of a GPC column and illustrates how molecules of different sizes travel through the column at different rates. The GPC column is packed with microporous gel particles that can accommodate small molecules but not large ones. This results in the large

molecules passing around the beads whereas small molecules pass through them. Passing through the beads is much slower than going around them, therefore large molecules travel through the column much faster than small molecules. The column is calibrated with polystyrene polymers of different, known molecular weights or chain lengths. Their elution times are then related to their molecular weights, providing a direct relationship between them.

From GPC analysis, the number average molar mass (M_n) and mass average molar mass (M_w) can be obtained. M_n is the average chain length of the polymer chains, as defined by the following equation:

$$M_n = (\sum N_i M_i) / (\sum N_i)$$

The variable N_i is the number of molecules with M_i particle size. M_w is the average molecular weight of the polymers, as defined by the following equation:

$$M_w = (\sum N_i M_i^2) / (\sum N_i M_i)$$

This differs from M_n in that the polymers with a higher molecular weight contribute more to M_w , resulting in a larger number, due to the exponential in the numerator of its defining equation. The ratio M_w/M_n is an indication of the range of polymer chain lengths, and is termed the polydispersity index (PDI). If there is only one polymer chain length (polymer with one molecular weight), M_w and M_n will be equal and the PDI will be 1. Practically, a PDI under 1.5 is viewed as a low polydispersed polymer chain length distribution.

The chain length of the non-fluorinated polymer can be tailored and, in the present case, three different polymers **2.1a–c** made from the same monomer are described. This is achieved by simply varying the relative molar amounts of monomer **2.1** and the ROMP catalyst. By using catalyst stoichiometries of 1, 2 and 4 mole %, the 100-mer (**2.P1c**), the 50-mer (**2.P1b**) and the 25-mer (**2.P1a**) can all be isolated, respectively. GPC showed that the relative ratio of

the number average molecular weights (M_n) was approximately 4:2:1 respectively as expected (Table 2.1).

The only polymers made from the fluorinated monomers **2.2** and **2.3** are the 50-mers, which are prepared using 2 mole % catalyst stoichiometry. All of these polymers showed narrow polydispersity indices (Table 2.1), confirming the synthesis of well-ordered polymers. When the symmetrical monomer **2.4** is polymerized using 2 mole % catalyst stoichiometry per oxanorbornene unit, the cross-linked polymer **2.P4** is produced. Due to the cross-linked nature of this polymer, GPC data is uninformative.

It is worth noting the difference in the polydispersity indices between polymers **2.P1a-c** and **2.P2/2.P3**. The large difference between them is due to a different GPC set-up in the determination of their corresponding M_n and M_w 's. Polymers **2.P1a-c** were run using only one column, whereas polymers **2.P2** and **2.P3** were run using two columns in succession. This results in a polymers **2.P2** and **2.P3** seeming as if they possess a more narrow PDI when this may not be the case. In order to confirm this hypothesis, polymers **2.P1a-c** should be run on the same set-up as were **2.P2** and **2.P3**. Absolute molecular weights for polymers of this size are often determined by MALDI mass spectrometry, however several attempts using several different polymers proved to be futile.

Table 2.1. Polymer characterization data of polymers **2.P1-2.P4**.

Polymer	Monomer (equivalents) ^a	% Yield	M _w	M _n	PDI (M _w /M _n)	T _g (°C)
2.P1a	2.1 (25)	76	11917	7920	1.50	-51
2.P1b	2.1 (50)	78	24577	16771	1.47	-36
2.P1c	2.1 (100)	75	43820	28007	1.56	-42
2.P2	2.2 (50)	53	26150	22869	1.14	-55
2.P3	2.3 (50)	69	25382	21447	1.18	-43
2.P4	2.4 (50)	86	–	–	–	-50

^aRelative to the molar equivalents of catalyst.

2.4.2.2 – Differential Scanning Calorimetry

The glass transition temperatures (T_g) is the temperature at which the polymer changes from a glass to a rubber, or amorphous phase. T_g 's for all polymers were measured using differential scanning calorimetry (DSC) and are included in Table 2.1. Low T_g 's correspond to a higher inner volume within the polymer matrix at ambient temperature (Figure 3.10). Photochromic polymers **2.P1-2.P4** all show low T_g 's (between -36 and -55°C), which is especially alluring in these photochromic polymers as it provides space for rotational freedom of the photochromes at ambient temperature, facilitating photocyclization.^{6c}

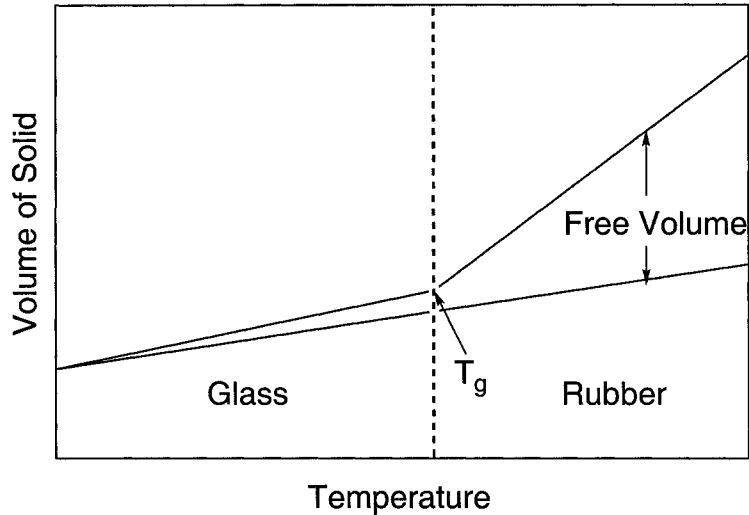


Figure 2.10. Correlation diagram between T_g and free inner space of a polymer matrix.

2.4.2.3 – Thermogravimetric Analysis

Thermogravimetric analysis (TGA) involves heating a sample and monitoring the mass loss as a function of temperature and serves as a measure of a polymers stability. TGA of all polymers was performed. The results indicate mass loss starting at 340°C for all polymers. These results cannot be extrapolated to infer stability at high temperatures as other chemistry could be occurring which results in no mass loss. A representative example is given in Figure 2.11.

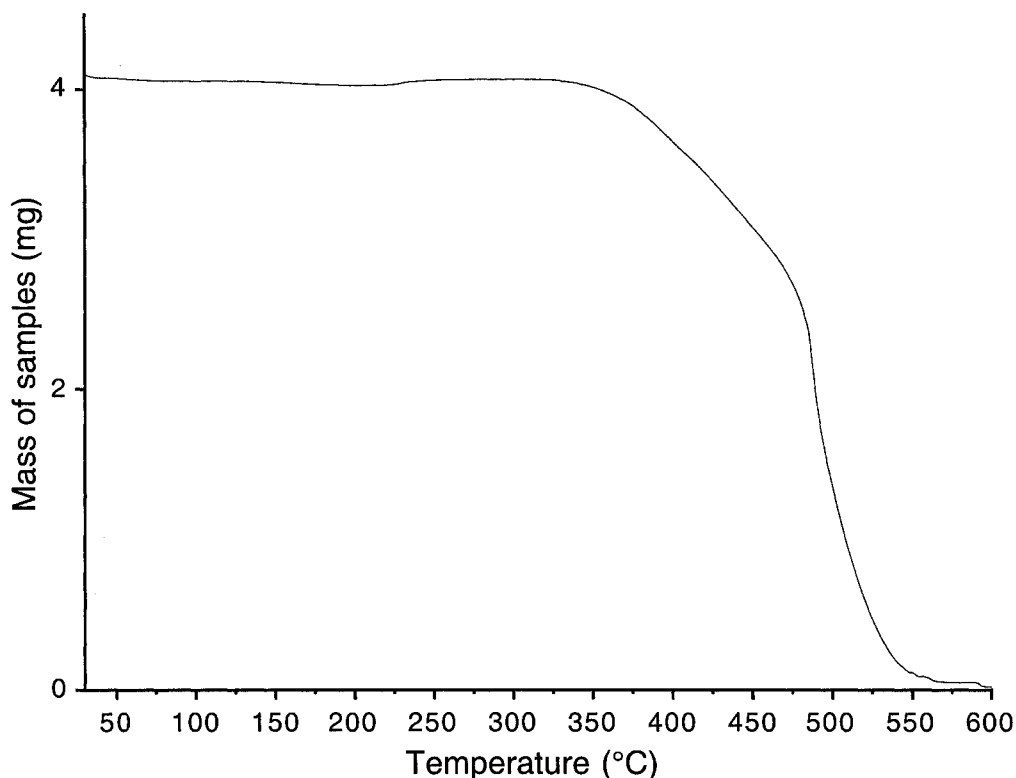


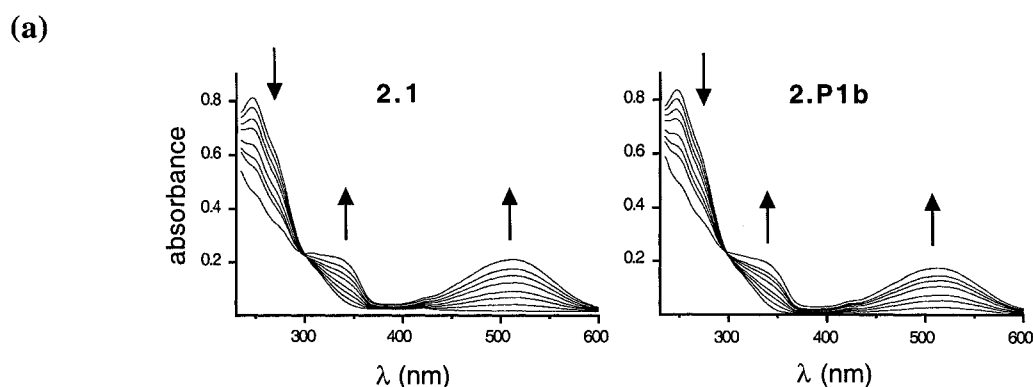
Figure 2.11. Thermogravimetric analysis of polymer **2.P2**. Upon heating the sample, the mass loss is monitored. Significant mass loss occurs at temperatures above 340°C. Polymers **2.P1b-2.P4** all show a similar trend.

2.4.2.4 - UV-vis Spectroscopy in Solution

All polymers were compared to their corresponding monomers by performing UV-vis spectroscopy in THF solutions at identical concentrations with respect to the photochromic unit. **2.P1a-c** and **2.1**, **2.P2** and **2.2**, and **2.P3** and **2.3** all showed similar absorption and photochromic behavior in their polymeric and monomeric form, as well as their open and closed forms (Figure 2.12 and Table 2.2). Upon irradiation of the photochromic solutions with UV light (254 nm), an increase in absorption at longer wavelength is observed with clear isobestic

points, indicating a clean transformation from the open to closed form of the photochrome. Upon irradiation with broad-band visible light using a cutoff filter to eliminate light of wavelengths less than 434 nm, the original absorption spectrum is obtained, confirming the reversibility of the electrocyclic reaction.

Cross-linked polymer **2.P4** however behaved differently than did its monomeric precursor **2.4**. The absorption spectra of the open forms of **2.P4** and **2.4** overlap, however upon ring closing with 254 nm light the absorption of the closed form of **2.P4** is only 25% as intense that for **2.4**. We attribute this decrease in photoisomerization to the decrease in rotational freedom about the bond between the thiophene and cyclopentene rings, which is essential in order to orient the orbitals for the electrocyclic ring closing reaction, due to the rigidification of each side of the photochrome in the polymer backbone. The overall tensile strength of the polymer may increase, however the photochromic behavior decreases due to cross-linking.



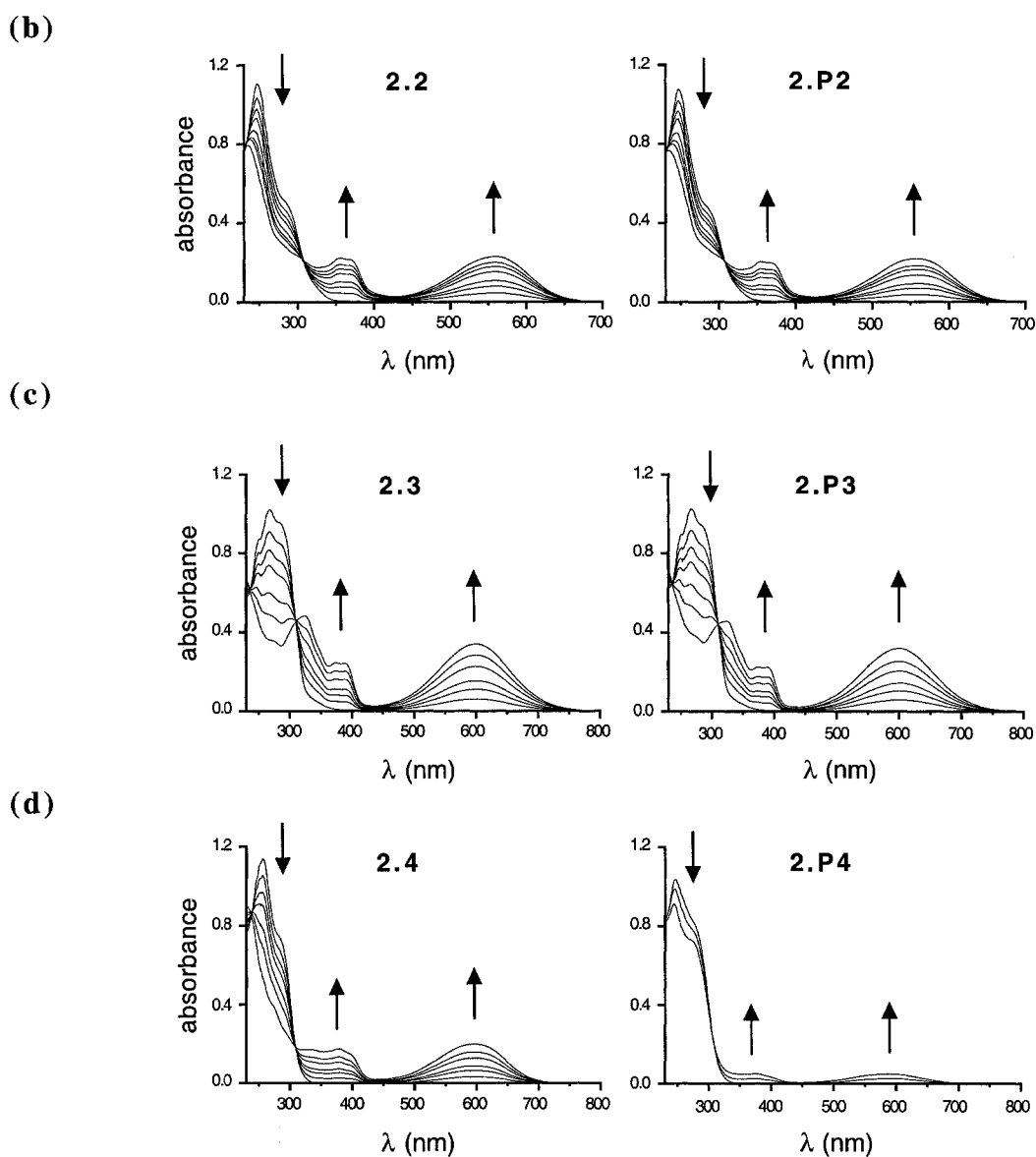


Figure 2.12. Changes in the UV-vis absorption spectra of monomers **2.1b–2.4** compared to their corresponding polymers **2.P1b–2.P4** in solution (THF at 3×10^{-5} M) when irradiated with 254-nm light. (a) **2.1b** and **2.P1b** irradiation periods: 0, 2, 4, 6, 10, 15, 20, and 40 seconds. (b) **2.2** and **2.P2** irradiation periods: 0, 2, 4, 6, 10, 15, 20, and 40 seconds. (c) **2.3** and **2.P3** irradiation periods: 0, 2, 4, 6, 10, 15 and 30 seconds. (d) **2.4** irradiation periods: 0, 2, 4, 6, 10, 15, and 30 seconds. **2.P4** irradiation periods: 0, 10 and 60 seconds. Upon irradiation of all solutions with broad band light > 434 nm the original spectra were obtained.

Table 2.2 tabulates the UV-vis absorption data presented in Figure 2.12. The maximum absorbing wavelength (λ_{\max}) is the longest wavelength that results in the highest absorbance. The molar absorptivity values (ϵ) are calculated from a derivation of Beer-Lambert Law, expressed by the equation:

$$\epsilon = A/(cl)$$

where A is absorbance, c is the concentration of the solution, and l is the path length through the cell containing the solution. This value is commonly used as a reference value for a specific molecule as it is concentration independent.

Table 2.2. Solution UV-vis absorption data for monomers **2.1b–2.4** and their corresponding polymers **2.P1b–2.P4** in solution (THF at 3×10^{-5} M).

compound	$\lambda_{\max} / \text{nm}$ ($\epsilon \times 10^{-4} \text{ Lmol}^{-1}\text{cm}^{-1}$)		color of the ring-closed form
	ring-open form	ring-closed form ^a	
2.1b	246 (2.70)	512 (0.703)	red
2.P1b	247 (2.79)	512 (0.587)	red
2.2	247 (3.69)	558 (0.760)	purple
2.P2	247 (3.58)	557 (0.727)	purple
2.3	267 (3.40)	600 (1.13)	blue
2.P3	267 (3.42)	599 (1.06)	blue
2.4	256 (3.80)	596 (0.660)	blue
2.P4	244 (3.41)	587 (0.164)	blue

^a Obtained by irradiating (254 nm) THF solutions of the ring-open forms for 30 seconds for all monomers and polymers **2.P1b–P3**, and 60 seconds for cross-linked polymer **2.P4**.

The values tabulated in Table 2.2 clearly indicated that the photochromic behavior of the polymers relative to the monomers is similar, except for the case of cross-linked polymer **2.P4**, as previously explained. Similar λ_{max} and ϵ values are obtained for each of the polymers **2.P1-2.P3** compared to their corresponding monomers **2.1-2.3**. These successful results led us to the next step of our investigation of these photochromic polymers: do these polymers possess solid-state photochromism?

2.4.2.5 – UV-Vis Spectroscopy in the Solid-State

Spin coating CHCl_3 solutions of the polymers onto quartz substrates resulted in thin films of approximately 250 nm thickness, as measured by an Alpha Step 100 profilometer. Similar to the solution UV-vis studies, photocoloration of the films with 254 nm light substantiates solid-state photochromism; clean photochemical transformation is confirmed by the presence of clear isobestic points (Figure 2.13). The resulting solid-state UV-vis spectrum of each film shows similar absorbances to the corresponding spectrum in solution. The photostationary state of films **2.P1-2.P3** is attained after 3 minutes of irradiation at 254 nm, whereas that of **2.P4** is attained after 4 minutes. Upon broad band irradiation above 434 nm for 1 minute, the ring-closed form of the polymer films are decolorized resulting in the original UV-vis spectrum, confirming the reversibility of the photocyclization in the solid-state.

Akin to its photochromic behavior in solution, polymer film **2.P4** shows a smaller change in absorbance upon 254 nm irradiation than its non-cross-linked counterparts **2.P1-**

2.P3. We again attribute this to the decrease in rotational freedom of the open-form of the photochrome within the cross-linked polymer.

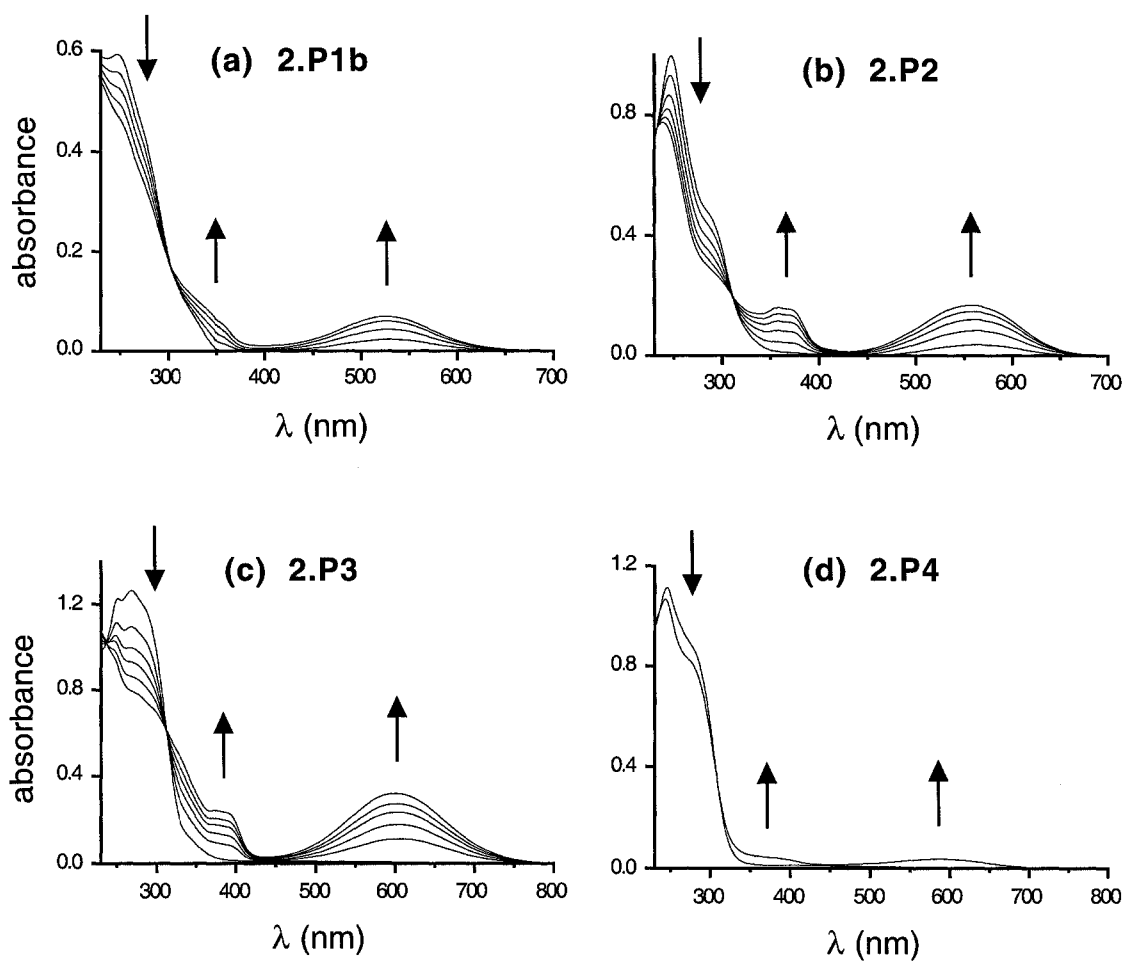


Figure 2.13. Solid-State UV-vis of polymers **2.P1b-2.P4**. Irradiation of polymers films of ~250 nm thickness cast on quartz substrates with 254 nm light resulted in solid-state photochromism. (a) **2.P1b**, (b) **2.P2**, and (c) **2.P3** irradiation times: 0, 10, 30, 60, 100, and 180 seconds. (d) **2.P4** irradiation times: 0 and 240 seconds.

2.5 – Concluding Remarks and Future Prospects

As alluded to in the introduction, changing the pendant functionality on the thiophene ring from a chloro to a phenyl group, in **2.P2** and **2.P3** respectively, results in a red shift in the absorbance of the corresponding closed form of the photochrome. This is attributed to the longer linear conjugation pathway created upon cyclization of the **2.P3** photochrome compared to that of **2.P2**. This effect can be seen by the blue color of **2.P3** compared to the purple color of **2.P2**. This phenomenon is effectively exploited in these polymers in solution and solid-state which allows for the development of polymers whose color can be predetermined by choosing the appropriate pendant functionality.

I have successfully demonstrated that ROMP provides a mild, versatile and well controlled method to generate photochromic polymers of 1,2-bis(3-thienyl)cyclopentene derivatives. The homopolymers synthesized are soluble, have low polydispersities, are easily cast as thin films and retain their photochromic properties in the solid-state. The next challenge is to use this technology to exploit DTE's changes in properties other than absorbance.

Due to literature precedent for the use of DTE polymers in the photochemical regulation of refractive index, I decided to investigate these polymers with this objective. A collaboration was formed with Dr. Christopher Barrett at McGill University and the refractive indices of both forms of the photochromic polymer **2.P1b** were measured using ellipsometry. Preliminary data suggested a significant refractive index change between the two forms ($\Delta\eta = 0.03$), which is comparable to refractive index changes found in other DTE polymers ($\Delta\eta = 0.04$).^{6j} The measurements, however, were performed using a wavelength at which the closed form of DTE

in **2.P1b** absorbs, therefore the measurements must be repeated with a wavelength outside the absorption range of both forms of the photochrome to ensure accuracy. Progress in this area will be reported in due course.

2.6 - Experimental Section

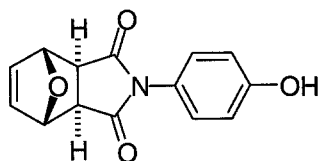
General: All solvents for synthesis were purchases from Caledon Laboratories Limited. THF and diethyl ether were distilled over sodium/benzophenone, hexane was distilled over potassium/benzophenone, and CH₂Cl₂ was distilled over calcium hydride before use. All other solvents were used as received. Solvents for NMR analysis were purchased from Cambridge Isotope Laboratories and used as received. Column chromatography was performed using silica gel 60 (230-400 mesh) from Silicycle Inc.. Bis(tricyclohexylphosphine)benzylidene ruthenium(IV)dichloride (Grubbs' catalyst) was purchased from Strem Chemical Company and was stored and weighed in a glove box under a nitrogen atmosphere. All other reagents and starting materials were purchased from Aldrich. 7-Oxa-bicyclo[2.2.1]hept-5-ene-2,3-dicarboxylic anhydride (**2.5**),¹⁴ 3-bromo-5-chloro-2-methylthiophene (**2.10**),¹⁷ 3-bromo-2-methyl-5-phenylthiophene,¹⁸ and the photochromic dichlorides **2.7**¹⁵ and **2.8**¹⁶ were prepared as described in the literature. The CO₂ source was dry ice, which was put in a 100 mL round bottom flask fitted with a hose adapter. A Nalgene hose was fitted on top of the round bottom flask on one end and a drying tube (CaCl₂) on the other. A second Nalgene tube was fitted on the other end of the drying tube which was fitted with a needle adapter and needle. This way, the CO₂ travels through the drying tube and out the end of the needle into the reaction mixture.

GPC samples were prepared by dissolving ~5 mg of polymer in 1 mL of distilled THF, of which 100 ul was injected into the apparatus. GPC analyses (calibrated by polystyrene) were

performed using THF as the eluent using a Waters 515 HPLC pump and 2410 Refractive Index or a 486 Tunable Absorbance Detector at a flow rate of 1.0 mL/min through a 7.8×300 mm column running at 30 °C. ^1H NMR characterizations were performed on a Varian Inova-300 or Bruker AMX 400 instrument. ^{13}C NMR characterizations were performed on a Bruker 300 or Bruker AMX 400 instrument. Chemical shifts (δ) are reported in parts per million relative to tetramethylsilane using the residual solvent peak as a reference standard. Coupling constants (J) are reported in Hertz. The number of ^{13}C NMR resonances of several compounds do not equal the number of different carbons in the molecule. This is especially true for the compounds containing perfluorinated cyclopentene rings. This is due to the two and three bond ^{19}F - ^{13}C coupling, which causes splitting of the signal making it indistinguishable from the baseline noise. This problem may be circumvented by performing ^{19}F -decoupled ^{13}C NMR experiments. Also, consecutive quaternary carbons show very weak signals due to longer relaxation times and poor NOE's to ^1H atoms. This problem may be circumvented by increasing the concentration of the sample and by increasing the acquisition time.²⁰

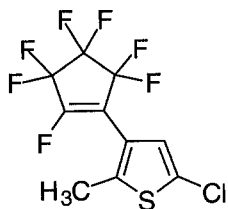
FT-IR measurements were performed using a Nicolet Magna-IR 750 or a Nexus 670 instrument and values are reported in cm^{-1} . UV-vis measurements were performed using a Pharmacia Biotech Ultraspec 3000 or a Varian Cary 300 Bio spectrophotometer. UV irradiation was performed using a hand-held UV lamp operating at $420 \mu\text{W}/\text{cm}^2$ for 254 nm. Irradiation with visible light was performed using the light of a 150-W tungsten source that was passed through a 434 nm (> 434 nm) cutoff filter to eliminate higher energy light.

Differential Scanning Calorimetry (DSC) was performed using a Seiko Instruments Inc. EXSTAR 6000 and DSC 6200 instrument. Thermogravimetric analysis was performed using a Shimadzu TGA-50 Thermogravimetric Analyzer. Solid-state UV-vis spectra were obtained from polymer films spin-coated onto quartz plates from CHCl_3 solutions (3 mg of polymer in 0.5 mL CHCl_3). The polymer films were between 160 and 270 nm thick as measured using a Tencor Instruments Alpha Step 100 profilimeter.

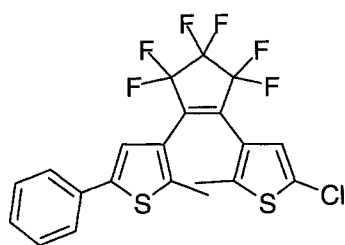


Synthesis of *exo*-N-(*p*-hydroxyphenyl)-3,6-epoxy-4-cyclohexene-1,2-dicarboximide (2.6).

A mixture of 7-oxa-bicyclo[2.2.1]hept-5-ene-2,3-dicarboxylic anhydride (**2.5**)¹⁴ (2.0 g, 12 mmol), *p*-aminophenol (1.31 g, 12 mmol) and glacial acetic acid (3 mL) were heated at reflux for 10 min after which time a precipitate formed. The heating source was removed and the reaction mixture was allowed to cool to room temperature. The precipitate was collected by vacuum filtration, washed with water and dried *in vacuo* to afford 2.10 g (68%) of **2.6** as a white solid. Mp = 188–189 °C. ¹H NMR (300 MHz, DMSO-*d*₆) δ 9.71 (s, 1H), 6.95 (d, *J* = 9 Hz, 2H), 6.83 (d, *J* = 9 Hz, 2H), 6.58 (s, 2H), 5.21 (s, 2H), 3.02 (s, 2H). ¹³C NMR (75.49 MHz, DMSO-*d*₆) δ 175.95, 157.27, 136.53, 127.98, 123.19, 115.38, 80.66, 47.20; FTIR 3334, 3143, 3102, 3076, 3049, 3029, 2973, 1775, 1697, 1612, 1594, 1516, 1448, 1402, 1273, 1223, 1191, 1162, 1149, 1015, 915, 875, 855, 846, 809; MS (EI): *m/z* = 257 [M]⁺, 189 [M-C₄H₄O]⁺.

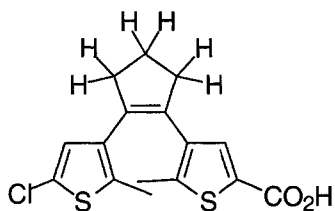


Synthesis of cyclopentene 2.11. A vigorously stirred solution of 3-bromo-5-chloro-2-methylthiophene (**2.10**)¹⁷ (1.0 g, 4.7 mmol) in Et₂O (20 mL) cooled to $-78\text{ }^{\circ}\text{C}$ was treated with *n*-butyllithium (1.88 mL of 2.5 M solution in hexanes, 4.7 mmol) dropwise under argon. This solution was added through a canula to a solution of octafluorocyclopentene (1.2 ml, 9.5 mmol) in 1:1 THF:Et₂O (10 mL) also cooled to $-78\text{ }^{\circ}\text{C}$. The reaction mixture was stirred at this temperature for 1 h, the cooling bath was removed and the mixture was allowed to warm to room temperature where it was stirred for a total of 16 h. The solvent was removed in vacuo and the residue mixture was partitioned between CH₂Cl₂ and H₂O. The organic layer was separated, washed with water and then brine, dried over Na₂SO₄, filtered and evaporated in vacuo. Purification by column chromatography through silica (hexanes) afforded 0.63 g (42%) of the product as a colorless oil. ¹H NMR (400 MHz, CDCl₃) δ 6.91 (s, 1H), 2.39 (d, $J_{\text{HF}} = 3$ Hz, 3H). ¹³C NMR (125 MHz, CDCl₃) δ (7 of 10 signals were observed) 152.78, 149.81, 142.36, 128.24, 125.48, 118.99, 14.47 (d, $J_{\text{CF}} = 6$ Hz). FTIR (KBr-cast) 3110, 2972, 2931, 2869, 1703, 1469, 1390, 1358, 1331, 1282, 1205, 1157, 1121, 1040, 996, 973. MS (EI): $m/z = 324$ [M]⁺, 305 [M-F]⁺, 289 [M-Cl]⁺.

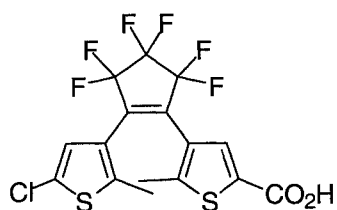


Synthesis of photochromic chloride 2.9. A vigorously stirred solution of 3-bromo-2-methyl-5-phenylthiophene¹⁸ (837 mg, 3.3 mmol) in a mixture of hexanes (20 mL) and THF (5 mL) cooled to $-78\text{ }^{\circ}\text{C}$ was treated with *n*-butyllithium (1.32 mL of a 2.5 M solution in hexanes, 3.3 mmol) dropwise under argon. After stirring at this temperature for 10 min, a solution of cyclopentene **2.11** (1.06 g, 3.3 mmol) in hexanes (10 mL) was added through a canula. The reaction mixture was stirred at $-78\text{ }^{\circ}\text{C}$ for 1 h, the cooling bath was removed and the mixture allowed to warm to room temperature where it was stirred for 16 h. The solvent was removed in vacuo and the residue was partitioned between CH_2Cl_2 and H_2O . The organic layer was separated, washed with water ($2 \times 30\text{ mL}$) and then brine (30 mL), dried over Na_2SO_4 , filtered and evaporated in vacuo. Purification by column chromatography through silica (hexanes) afforded 1.11 g (71%) of the product as a viscous yellow oil. ^1H NMR (400 MHz, CDCl_3) δ 7.54 (d, $J = 7\text{ Hz}$, 2H), 7.39 (t, $J = 8\text{ Hz}$, 2H), 7.31 (t, $J = 8\text{ Hz}$, 1H), 7.24 (s, 1H), 6.93 (s, 1H), 1.97 (s, 3H), 1.88 (s, 3H). ^{13}C NMR (125 MHz, CDCl_3) δ (14 of 19 signals were observed) 142.46, 141.25, 140.47, 133.19, 129.01, 127.99, 127.75, 125.59, 125.51, 125.46, 123.35, 122.18, 14.52, 14.35. FTIR (KBr-cast) 3060, 3026, 2957, 2922, 2853, 1462, 1441, 1335, 1275, 1194, 1136, 1118, 1060, 1004, 982, 898, 888, 755, 742, 690. MS (CI): $m/z = 479$ $[\text{M}+\text{H}]^+$.

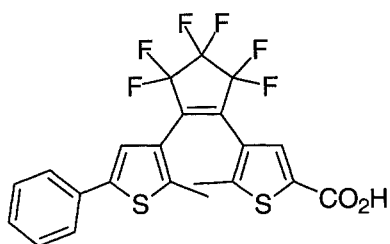
Synthesis of carboxylic acids 2.12–2.14. A solution of the appropriate dichloride **2.7–2.9** in dry THF or Et₂O cooled to –78 °C was treated with *tert*-butyllithium (1.7 M solution in hexane) dropwise under argon. After stirring for 10–15 min, excess dry CO₂ was bubbled through the solution. The reaction mixture was removed from the cooling bath, allowed to warm to room temperature, quenched with 5% HCl and extracted three times with dichloromethane. The combined organic layers were dried over Na₂SO₄, filtered and evaporated *in vacuo*. The products were purified by column chromatography through silica (2–5% CH₃OH/CH₂Cl₂).



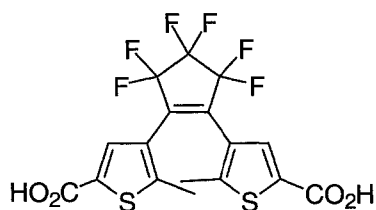
(2.12) Dichloride **2.7**¹⁵ (385 mg, 1.17 mmol) and *tert*-butyllithium (0.7 mL, 1.17 mmol) in THF (50 mL) afforded 318 mg (80%) of acid **2.12** a pale yellow solid after purification. Mp = 175–176 °C. ¹H NMR (400 MHz, CDCl₃) δ 7.59 (s, 1H), 6.56 (s, 1H), 2.79–2.73 (m, 4H), 2.05 (quintet, *J* = 8 Hz, 2H), 1.99 (s, 3H), 1.84 (s, 3H). ¹³C NMR (125 MHz, CDCl₃) δ 167.15, 144.78, 137.12, 136.00, 135.17, 134.63, 134.05, 134.00, 133.26, 126.55, 125.48, 38.49, 38.42, 22.80, 14.94, 14.14. FTIR (KBr-cast) 3428, 2959, 2924, 2841, 1669, 1552, 1448, 1310, 1269, 1159, 1000, 993, 731. MS (CI): *m/z* = 339 [M+H]⁺.



(2.13) Dichloride **2.8**¹⁶ (1.01 g, 2.3 mmol) and *tert*-butyllithium (1.36 mL, 2.3 mmol) in Et₂O (100 mL) afforded 660 mg (64%) of acid **2.13** as a white solid after purification. ¹H NMR (400 MHz, CDCl₃) δ 7.83 (s, 1H), 6.85 (s, 1H), 2.02 (s, 3H), 1.83 (s, 3H).



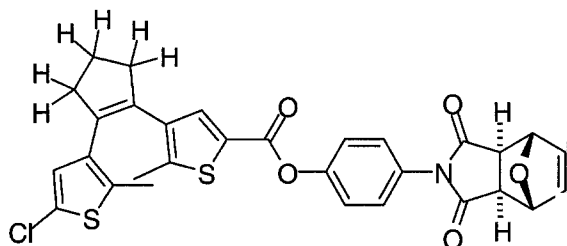
(2.14) Chloride **2.9** (1.11 g, 2.34 mmol) and *tert*-butyllithium (1.38 mL, 2.34 mmol) in Et₂O (50 mL) afforded 900 mg (82%) of acid **2.14** as a white solid after purification. Mp = 189–191 °C. ¹H NMR (400 MHz, CDCl₃) δ 7.89 (s, 1H), 7.53 (d, *J* = 7 Hz, 2H), 7.39 (t, *J* = 8 Hz, 2H), 7.31 (t, *J* = 8 Hz, 1H), 7.24 (s, 1H), 2.02 (s, 3H), 1.94 (s, 3H). ¹³C NMR (125 MHz, CDCl₃) δ (15 of 20 signals were observed) 166.03, 150.40, 142.79, 141.27, 134.88, 133.08, 130.51, 129.04, 128.08, 126.28, 125.62, 125.29, 122.03, 15.04, 14.52. FTIR (KBr-cast) 3414, 3028, 2924, 2855, 1678, 1545, 1462, 1274. MS (CI): *m/z* = 489.5 [M+H]⁺.



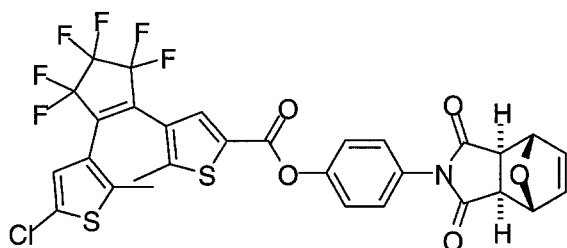
Synthesis of dicarboxylic acid 2.15. A solution of dichloride **2.8**¹⁶ (646 mg, 1.48 mmol) in Et₂O (70 mL) cooled to $-78\text{ }^{\circ}\text{C}$ was treated dropwise with *tert*-butyllithium (1.74 mL of 1.7 M solution in hexane, 2.96 mmol) under argon. After stirring for 15 min, excess dry CO₂ was bubbled through the solution. The cooling bath was removed and mixture was allowed to warm to room temperature. The precipitated dicarboxylate was dissolved in H₂O (10 mL) and acidified with conc. HCl (2 mL). The precipitate formed upon acidification was collected by vacuum filtration, washed with H₂O and dried in vacuo to afford 600 mg (89%) of the product as a white solid. Mp = 227–229 °C. ¹H NMR (400 MHz, CD₃OD) δ 8.67 (s, 2H), 2.93 (s, 6H). ¹³C NMR (125 MHz, CD₃OD) δ (6 of 9 signals were observed) 164.05, 150.46, 134.56, 133.97, 126.52, 14.91. FTIR (KBr-cast): 3073, 2983, 2918, 2857, 1676, 1547, 1465, 1336, 1262, 1193, 1120, 1038, 982, 896, 758, 667. MS (EI): m/z = 456 [M]⁺, 438 [M-H₂O]⁺.

Synthesis of photochromic monomers 2.1–2.4. A vigorously stirred solution of the appropriate carboxylic acid **12–15** and DMF (5 drops) in CH₂Cl₂ cooled to 0 °C was treated dropwise with a solution of oxalyl chloride in CH₂Cl₂ under argon over 10 min. After stirring at room temperature for 2 h (15 was allowed to stir for 16 hours), the reaction mixture was concentrated to dryness in vacuo. The residue was dissolved in CH₂Cl₂ (25 mL/mmol carboxylic acid) and added dropwise over 10 min to a solution of *exo-N*-(*p*-hydroxyphenyl)-

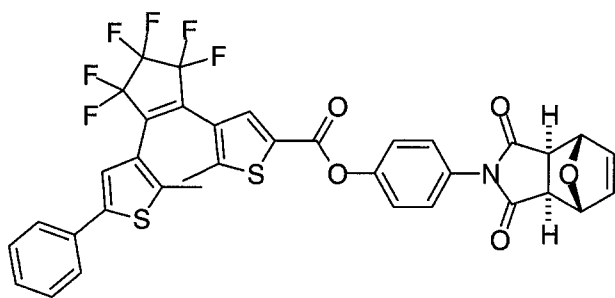
3,6-epoxy-4-cyclohexene-1,2-dicarboximide (**2.6**) and triethylamine in acetone cooled to 0 °C. The reaction mixture was stirred overnight under argon then the solvent was removed in vacuo. The products were purified by column chromatography through silica.



(**2.1**) Carboxylic acid **2.12** (136 mg, 0.4 mmol), oxalyl chloride (254 mg, 2.0 mmol), dicarboximide **2.6** (154 mg, 0.6 mmol) and triethylamine (0.5 mL) afforded 188 mg (82%) of monomer **2.1** as a pale yellow solid after purification by column chromatography through silica (2% CH₃OH/CHCl₃). Mp = 94–95 °C. ¹H NMR (300 MHz, CDCl₃) δ 7.67 (s, 1H), 7.36–7.27 (m, 4H), 6.56 (s, 3H), 5.39–5.37 (m, 2H), 3.00 (s, 2H), 2.82–2.71 (m, 4H), 2.12–1.99 (m, 5H), 1.87 (s, 3H). ¹³C NMR (75.49 MHz, CDCl₃) δ 175.22, 159.95, 150.56, 144.60, 137.19, 136.78, 136.02, 135.33, 134.75, 134.14, 133.36, 129.16, 128.03, 127.62, 126.66, 125.59, 122.38, 81.51, 47.59, 38.61, 38.52, 22.89, 14.98, 14.30. FTIR (KBr-cast) 3050, 2951, 2843, 1778, 1713, 1508, 1202. ESMS (+ive): *m/z* = 600.0 [M+Na]⁺, 532 [M-Cl]⁺. Anal. Calcd for C₃₀H₂₄ClNO₅S₂: C, 62.33; H, 4.18; N, 2.42. Found: C, 61.95; H, 4.16; N, 2.45.

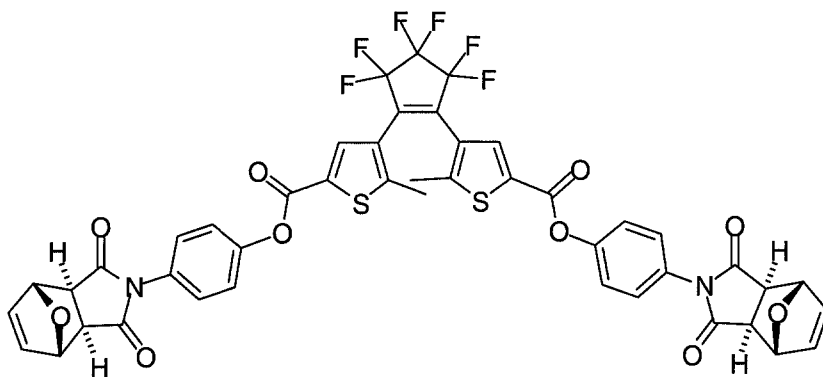


(**2.2**) Carboxylic acid **2.13** (254 mg, 0.57 mmol), oxalyl chloride (361 mg, 2.8 mmol), dicarboximide **2.6** (221 mg, 0.86 mmol) and triethylamine (0.5 mL) afforded 358 mg (87%) of monomer **2.2** as a pale yellow solid after purification by column chromatography through silica (CHCl_3). Mp = 141.5–142.5 °C. ^1H NMR (300 MHz, CDCl_3) δ 7.91 (s, 1H), 7.37-7.29 (m, 4H), 6.88 (s, 1H), 6.57-6.56 (m, 2H), 5.39-5.38 (m, 2H), 3.01 (s, 2H), 2.04 (s, 3H), 1.88 (s, 3H). ^{13}C NMR (75.49 MHz, CDCl_3) δ (18 of 24 signals were observed) 175.20, 159.12, 150.19, 140.64, 136.79, 134.56, 130.66, 129.50, 128.40, 127.74, 126.02, 125.48, 123.91, 122.25, 81.52, 47.59, 15.08, 14.52. FTIR (KBr-cast) 3015, 1714, 1508, 1272, 1189. ESMS (+ive): $m/z = 703.1$ $[\text{M}+\text{NH}_4]^+$. Anal. Calcd for $\text{C}_{29}\text{H}_{18}\text{ClF}_6\text{NO}_5\text{S}_2$: C, 51.68; H, 2.69; N, 2.08. Found: C, 51.66; H, 2.69; N, 1.97.



(**2.3**) Carboxylic acid **2.14** (252 mg, 0.52 mmol), oxalyl chloride (330 mg, 2.60 mmol), dicarboximide **2.6** (200 mg, 0.78 mmol) and triethylamine (0.5 mL) afforded 300 mg (80%) of

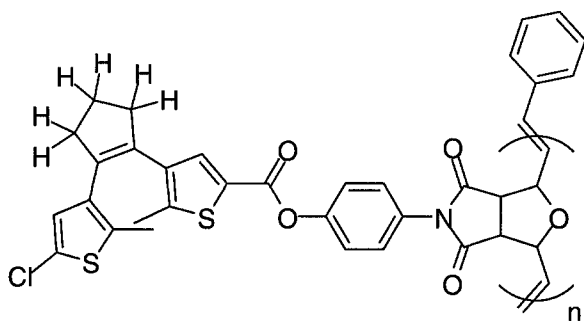
monomer **2.3** as a pale blue solid after purification by column chromatography through silica (2% CH₃OH/CHCl₃). Mp = 149–151 °C. ¹H NMR (400 MHz, CDCl₃) δ 7.98 (s, 1H), 7.41 (d, *J* = 7 Hz, 2H), 7.42–7.29 (m, 7H), 7.26 (s, 1H), 6.58 (s, 2H), 5.41 (s, 2H), 3.03 (s, 2H), 2.04 (s, 3H), 1.98 (s, 3H). ¹³C NMR (125 MHz, CDCl₃) δ (24 of 28 signals were observed) 206.93, 175.14, 159.15, 150.11, 142.80, 141.30, 136.72, 134.67, 133.10, 130.35, 129.37, 129.04, 128.08, 127.67, 126.29, 125.64, 125.31, 122.22, 122.06, 81.45, 47.53, 30.91, 15.04, 14.64. FTIR (KBr-cast) 3064, 3017, 2914, 2849, 1719, 1715, 1508, 1452, 1387, 1275, 1185. Anal. Calcd for C₃₆H₂₃F₆NO₅S₂: C, 59.42; H, 3.19; N, 1.92. Found: C, 59.24; H, 3.25; N, 1.90.



(**2.4**). Dicarboxylic acid **2.15** (100 mg, 0.22 mmol), oxalyl chloride (280 mg, 2.2 mmol), dicarboximide **2.6** (170 mg, 0.66 mmol) and triethylamine (0.5 mL) afforded 120 mg (59%) of monomer **2.4** as a pale yellow solid after purification by column chromatography through silica (5% MeOH/CHCl₃) followed by recrystallization from CH₂Cl₂/hexanes. Mp = 150–152 °C. ¹H NMR (400 MHz, CDCl₃) δ 7.95 (s, 2H), 7.38 (d, *J* = 9 Hz, 4H), 7.33 (d, *J* = 9 Hz, 4H), 6.58 (s, 4H), 5.41 (s, 4H), 3.03 (s, 4H), 2.06 (s, 6H). ¹³C NMR (125 MHz, CDCl₃) δ (13 of 17 signals were observed) 175.15, 159.01, 150.08, 149.98, 136.72, 134.37, 130.84, 127.70,

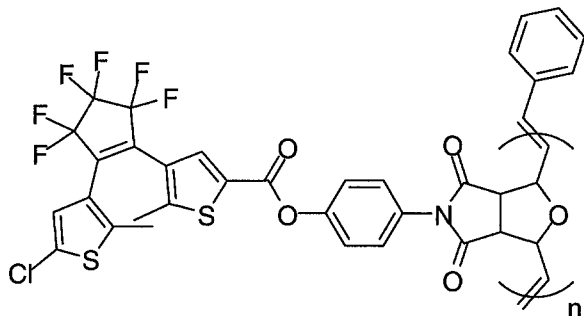
125.72, 122.21, 81.45, 47.53, 15.15. FTIR (KBr-cast) 3097, 3007, 2924, 1724, 1717, 1710, 1510, 1400, 1276, 1179. Anal. Calcd for $C_{45}H_{28}F_6N_2O_{10}S_2$: C, 57.82; H, 3.02; N, 3.00. Found: C, 58.01; H, 2.99; N, 2.99.

Polymerization of monomers 2.1–2.4. A solution of the appropriate monomer **2.1–2.4** dissolved in dry deoxygenated CH_2Cl_2 was added through a canula into a CH_2Cl_2 solution of bis(tricyclohexylphosphine)benzylidene ruthenium(IV)dichloride. The final monomer concentrations were 0.1 M. After stirring at room temperature for 14 h, excess ethyl vinyl ether was added and the resulting solutions were stirred while exposed to the atmosphere for 30 min. The polymers were precipitated in high purity by pouring the reaction solutions into cold Et_2O and collected by vacuum filtration. The success of each polymerization reaction was assessed by 1H NMR spectroscopy. Typically, in the 1H NMR spectrum of the monomer, the peak corresponding to the methine proton of the bicyclic olefin comes at 6.56 ppm. After the polymerization reactions, the peak at 6.56 ppm disappears and a new peak for the olefin protons appears at 6.10 ppm. See text table for GPC characterization.

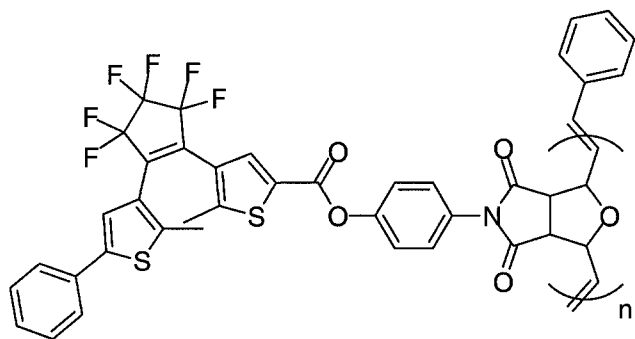


(**2.P1**) Monomer **2.1** was polymerized with 0.04, 0.02 and 0.01 molar equiv. of bis(tricyclohexylphosphine)benzylidene ruthenium(IV)dichloride to afford polymers **2.P1a**

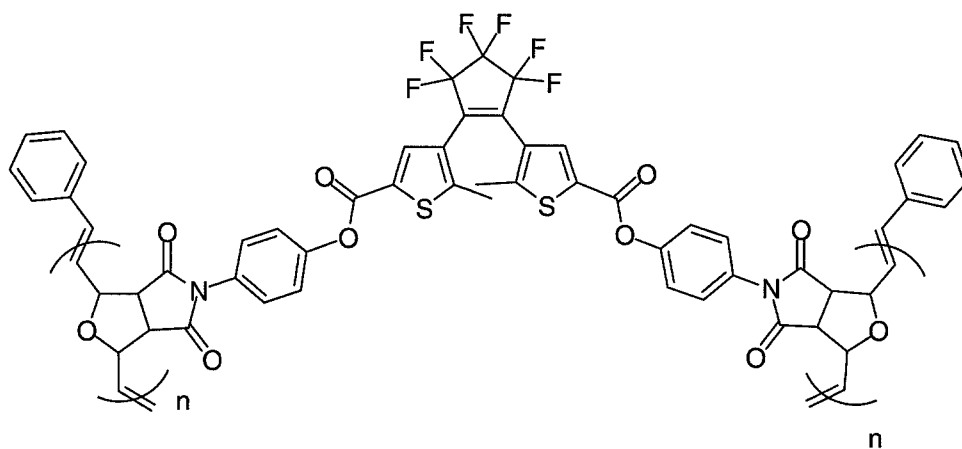
(75% yield), **2.P1b** (78% yield) and **2.P1c** (75% yield), respectively. A typical ^1H NMR spectrum is as follows (400 MHz, CDCl_3): δ 7.6 (br s), 7.3 (br s), 6.6 (br s), 6.1 (br s), 5.9-5.7 (m), 5.2-5.0 (m), 4.7-4.5 (m), 3.4 (br s), 2.7 (br s), 2.1-1.9 (m), 1.8 (br s).



(**2.P2**) Monomer **2.2** (37.5 mg, 55 μmol) was polymerized with bis(tricyclohexylphosphine)benzylidene ruthenium(IV)dichloride (1.8 mg, 2.2 μmol , 0.04 molar equiv.). The isolation procedure was identical to that for **2.P1** except that the precipitation procedure was carried out twice, first with Et_2O and then with CH_3OH to afford polymer **2.P2** in 53% yield. ^1H NMR (400 MHz, CDCl_3) δ 7.9 (br s), 7.3 (br s), 6.9 (br s), 6.1 (br s), 5.8 (br d), 5.2 (br s), 4.6 (br d), 3.4 (br s), 2.1-1.9 (m), 1.8 (br s).



(**2.P3**) Monomer **2.3** (110 mg, 180 μ mol) was polymerized with bis(tricyclohexylphosphine)benzylidene ruthenium(IV)dichloride (5.85 mg, 7.1 μ mol, 0.04 molar equiv.) to afford polymer **2.P3** in 69% yield. $^1\text{H NMR}$ (400 MHz, CDCl_3) δ 7.9 (br s), 7.5 (br s), 7.4-7.2 (m), 6.1 (br s), 5.8 (br d), 5.2 (br s), 4.6 (br d), 3.4 (br s), 2.0-1.8 (m).



(**2.P4**) Monomer **2.4** (58.4 mg, 62.5 μ mol) was polymerized with bis(tricyclohexylphosphine)benzylidene ruthenium(IV)dichloride (2.1 mg, 2.5 μ mol, 0.04 molar equiv.) to afford polymer **2.P4** in 86% yield. $^1\text{H NMR}$ (400 MHz, CDCl_3) δ 8.1-6.8 (br m), 6.4-5.6 (br m), 5.4-4.3 (br m), 3.8-3.0 (br m), 2.8-1.7 (br m).

2.7 – References

1. Feringa, B. L., Ed. *Molecular Switches*, Wiley-VCH: Weinheim, 2001; pp. 37-62.
2. Gilat, S. L.; Kawai, S. H.; Lehn, J.-M. *Chem. Eur. J.* **1995**, *1*, 275-284.
3. Matsuda, K.; Irie, M. *J. Am. Chem. Soc.* **2000**, *122*, 7195-7201.
4. Norsten, T. B.; Branda, N. R. *J. Am. Chem. Soc.* **2001**, *123*, 1784-1785.
5. Crano, J. C., Gugliemetti, R. J., Eds. *Organic Photochromic and Thermochromic Compounds*; Plenum Press: New York, NY, 1999; Vol. 2, pp. 9-63.
6. (a) Bobrovsky, A. Y.; Boiko, N. I.; Shibaev, V. P.; Kalik, M. A.; Krayushkin, M. M. *J. Mater. Chem.* **2001**, *11*, 2004-2007. (b) Tian, H.; Tu, H.-Y. *Adv. Mater.* **2000**, *12*, 1597-1599. (c) Kwon, D.-H.; Shin, H.-W.; Kim, E.; Boo, D. W.; Kim, Y.-R. *Chem. Phys. Lett.* **2000**, *328*, 234-243. (d) Irie, S.; Irie, M. *Bull. Chem. Soc. Jpn.* **2000**, *73*, 2385-2388. (e) Nakashima, H.; Irie, M. *Polym. J.* **1998**, *30*, 985-989. (f) Uchida, K.; Takata, A.; Nakamura, S.; Irie, M. *Chem. Lett.* **2002**, 476-477. (g) Stellacci, F.; Bertarelli, C.; Toscano, F.; Gallazzi, M. C.; Zotti, G.; Zerbi, G. *Adv. Mater.* **1999**, *11*, 292. (h) Munakata, M.; Wu, L. P.; Kuroda-Sowa, T.; Maekawa, M.; Suenaga, Y.; Furuichi, K. *J. Am. Chem. Soc.* **1996**, *118*, 3305. (i) Matsuda, K.; Takayama, K.; Irie, M. *Chem. Commun.* **2001**, 363. (j) Biteau, J.; Chaput, F.; Lahlil, K.; Boilot, J.-P.; Tsivgoulis, G. M.; Lehn, J.-M.; Darracq, B.; Marois, C.; Levy, Y. *Chem. Mater.* **1998**, *10*, 1945-1950.
7. (a) Alonso, M.; Reboto, V.; Guiscardo, L.; Mate, V.; Rodriguez-Cabello, J. C. *Macromolecules* **2001**, *34*, 8072-8077. Marsella, M. J.; Wang, Z.-Q.; Mitchell, R. H. *Org. Lett.* **2000**, *2*, 2979-2982. (b) Hattori, H.; Uryu, T. *J. Polym. Sci.* **1999**, *37*, 3513-3529. (c) Gu, J.; Liang, B.; Liu, L.; Tian, Y.; Chen, Y.; Lu, B.; Lu, Z. *Thin Solid Films* **1998**, 427-430. (d) Levesque, I.; Leclerc, M. *Macromolecules* **1997**, *30*, 4347-4352. (e) Warshawsky, A.; Kahana, N.; Buchholtz, F.; Zelichenok, A.; Ratner, J.; Krongauz, V.

- Ind. Eng. Chem. Res.* **1995**, *34*, 2825-2832. (f) Buchholtz, F.; Zelichenok, A.; Krongauz, V. *Macromolecules* **1993**, *26*, 906-910. (g) Kumar, S. G.; Neckers, D. C. *Chem. Rev.* **1989**, *89*, 1915-1925.
8. Odian, G. *Principles of Polymerization* 3rd Ed. John Wiley and Sons, Inc.: New York. 1991, pp. 40-186.
9. (a) Grubbs, R. H.; Tumas, W. *Science* **1989**, *243*, 907-915. (b) Sanford, M. S.; Love, J. A.; Grubbs, R. H. *J. Am. Chem. Soc.* **2001**, *123*, 6543-6554.
10. Ivin, K. J.; Mol, J. C.; *Olefin Metathesis and Metathesis Polymerization*, Academic Press: San Diego, 1997.
11. Pariya, C.; Jayaprakash, K. N.; Sarkar, A. *Coord. Chem. Rev.* **1998**, *168*, 1-48.
12. (a) Schwab, P.; Grubbs, R. H.; Ziller, J. W. *J. Am. Chem. Soc.* **1996**, *118*, 100. (b) Trnka, T. M.; Grubbs, R. H. *Acc. Chem. Res.* **2001**, *34*, 18.
13. Carey, F. A.; Sundberg, R. J. *Advanced Organic Synthesis*, 2nd Ed., Part B, Plenum Press: New York, 1983, pp. 424-429.
14. Bolm, C; Dinter, C. L.; Seger, A.; Höcker, H.; Brozio, J. *J. Org. Chem.* **1999**, *64*, 5730-5731.
15. Lucas, L. N.; van Esch, J.; Kellogg, R. M.; Feringa, B. L. *Chem. Commun.* **1998**, 2313-2314.
16. Lucas, L. N.; van Esch, J.; Kellogg, R. M.; Feringa, B. L. *Tetrahedron Lett.* **1999**, 1775-1778.
17. Tsivgoulis, G. M.; Lehn, J.-M. *Chem. Eur. J.* **1996**, *2*, 1399-1406.
18. Irie, M.; Lifka, T.; Kobatake, S.; Kato, N. *J. Am. Chem. Soc.* **2000**, *122*, 4871-4876.
19. Campbell, D.; Pethrick, R. A.; White, J. R. *Polymer Characterization*, 2nd Ed., Stanley Thornes: Cheltenham, UK, 1989, pp. 15-50.

20. Kalinowski, H.-O.; Berger, S.; Braun, S. *Carbon-13 NMR Spectroscopy* John Wiley and Sons Ltd.: New York, 1984.

Chapter 3 – Photo-Regulation of Photo-Induced Electron Transfer within Porphyrinic Phenoxynaphthacenequinone Hybrid Systems.

3.1 – Photo-Induced Electron Transfer (PET)

Photo-induced electron transfer (PET) involves an electron transfer from a donor to an acceptor species upon photoexcitation of either one.¹ This phenomenon is one of the key steps in the conversion of light energy to chemical/electrical energy. The most common example of PET is found in plants and purple bacteria, in which photosynthesis provides the organisms' energy. Figure 3.1 shows the photosynthetic reaction center in a purple bacterium, *Rhodobacter sphaeroides*.² Photoexcitation of porphyrin molecules D_M and D_L results in the generation of their excited states, which can then transfer an electron down a cascade of porphyrins (B_A and Φ_A) to quinone electron acceptors (Q_A and Q_B). The net result is a charge-separated state, in which the radical cation of the porphyrin D_L and the radical anion of Q_B are formed. This sets up an electrochemical potential across a membrane driving redox reactions, resulting in reduction of carbon dioxide to carbohydrates and the oxidation of H_2O to O_2 .

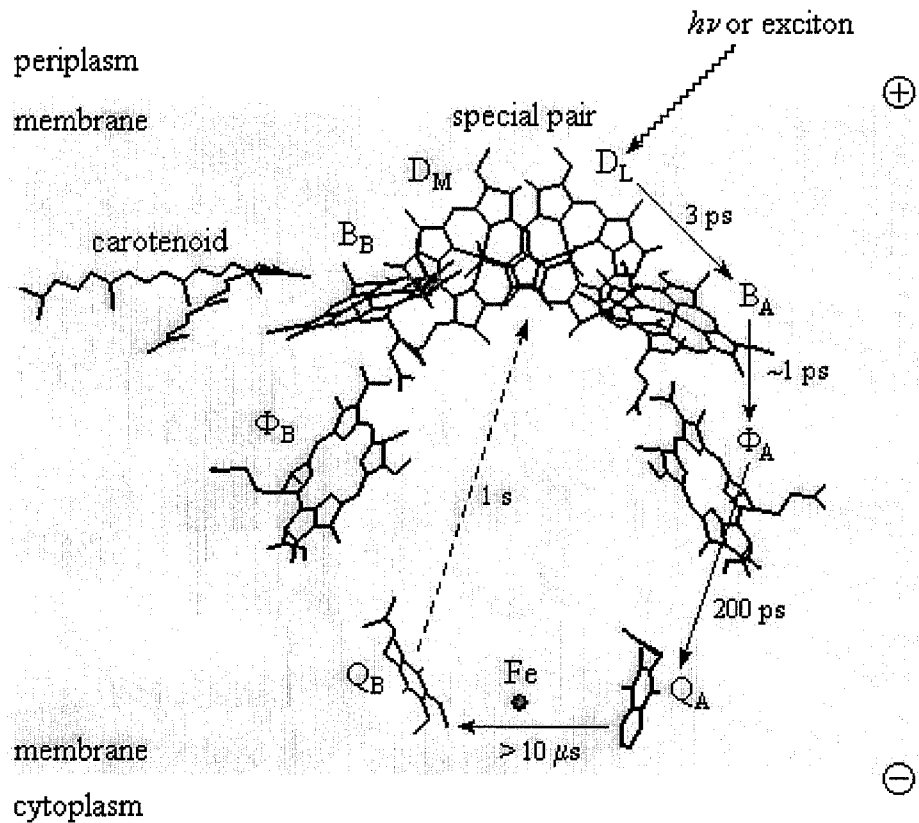


Figure 3.1. Photosynthetic reaction center of purple bacterium *Rhodospirillum rubrum*.²

Figure 3.2 represents a simplified energy diagram of PET between a photo-induced electron donor (D) and an electron acceptor (A). Photoexcitation of the donor species (D) results in its excited state (D*), which can then undergo electron transfer to the acceptor species (A). This creates the charge separated state discussed above in photosynthesis. Charge recombination regenerates the ground states of the donor and acceptor species. This process is competing with other decay pathways such as thermal decay and luminescence. The

more favorable the electron transfer step is, the more electrical/chemical energy can be isolated from the system.

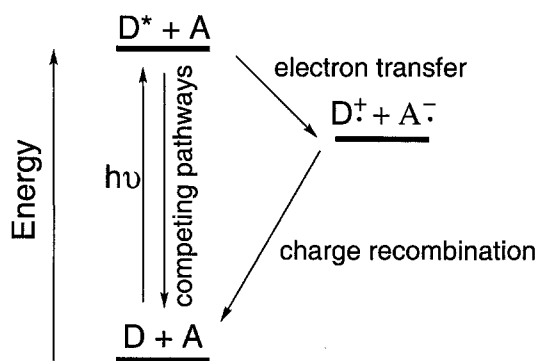


Figure 3.2. PET energy diagram

Synthetic chemists have reported dozens of examples of photosynthetic mimics, in which porphyrins and quinones in covalent or non-covalent arrays to allow for PET upon photoexcitation of the porphyrin.^{1,3} Figure 3.3 shows two examples of synthetic PET systems, one covalent⁴ and one non-covalent.⁵ Sakata and coworkers developed the first example in which a porphyrin and quinone are separated by a decalin linker, allowing through-space electron transfer between the porphyrin and quinone. The second example, developed by Hunter and coworkers, illustrates a complex system that assembles via well-defined molecular recognition elements. The assembly of the porphyrin and quinone by the cyclic tetra-amide allows PET between the porphyrin and quinone. The ability to effectively mimic this process will allow for the development of efficient photovoltaics and other photonic devices in which the main power source is light energy.⁶

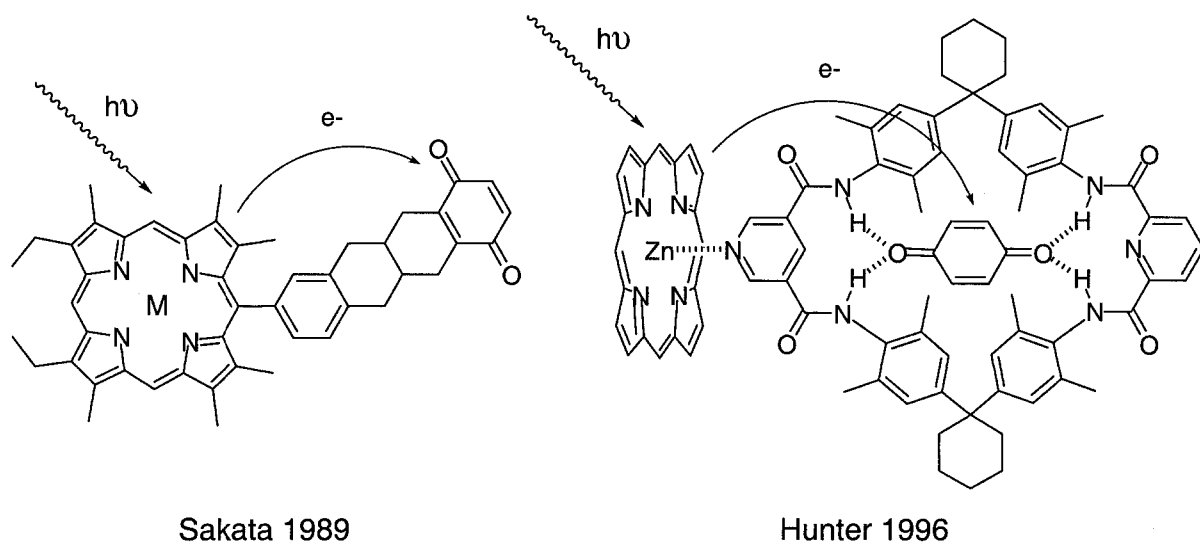


Figure 3.3. Synthetic PET systems

3.2 - PET Regulation

My interest in PET concerns controlling the generation of the charge separated state by reversibly allowing/disallowing the PET process. Switchable PET systems have potential applications in efficient and fast-responding photonic devices,⁷ using the “ON/OFF” properties of the system to store and/or transfer information in a non-destructive manner. For example, turning PET on or off may function as photo-regulated transistor, in which a current can be turned on or off by applying a specific stimulus.

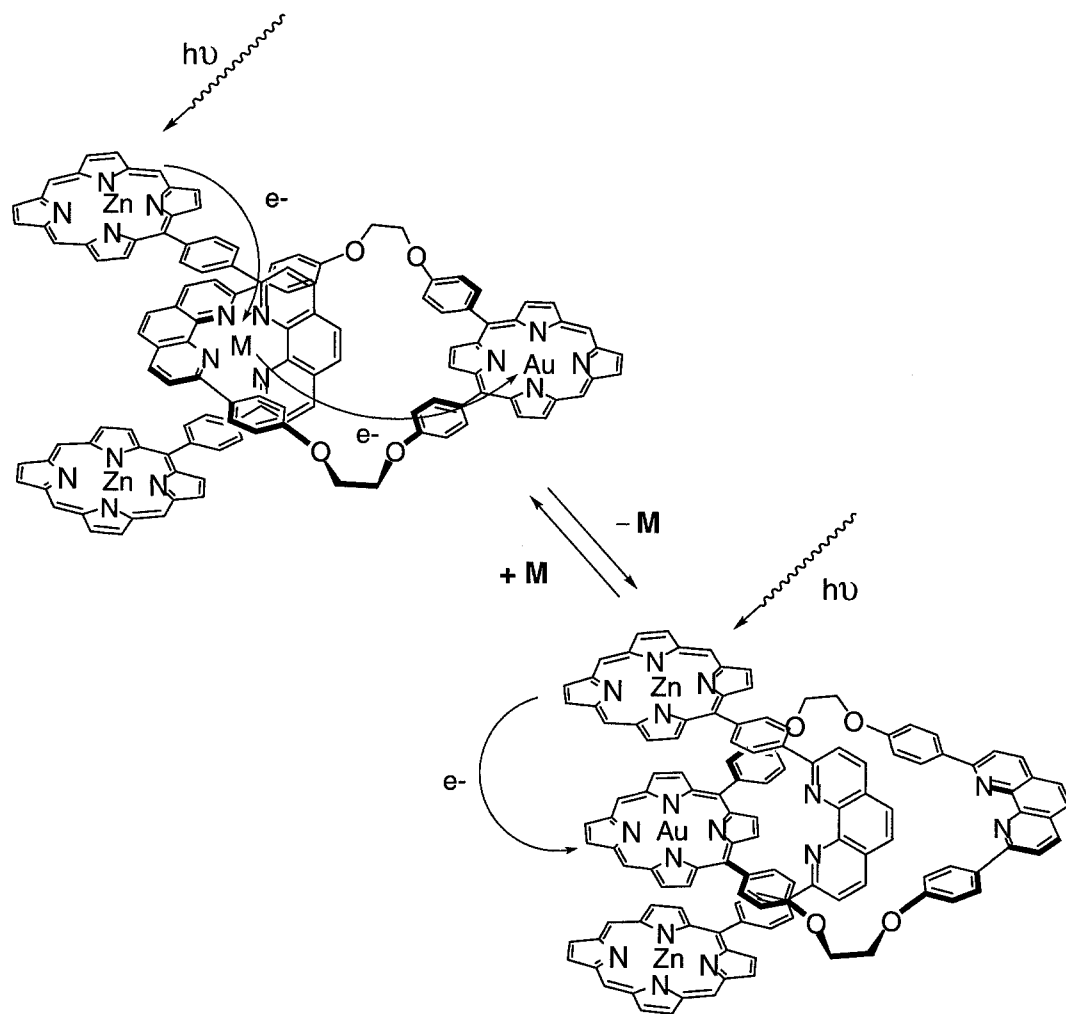
There are three possible mechanisms for regulating PET. By varying the oxidation potential (electron donating ability) of the electron donor species, the electron transfer step

will change accordingly. Similarly, altering the reduction potential (electron accepting ability) of the acceptor species results in a change in PET. Altering the conjugation pathway or through space orientation between the donor and acceptor species offers another method of PET regulation. If the PET step proceeds via a through bond mechanism, breaking the conjugation pathway between the donor and acceptor will disrupt the electron transfer step. If the PET proceeds via a through space mechanism, pulling the donor and acceptor further away from each other will hinder the electron transfer step. Several examples of PET regulation have been reported,^{8,9} most of which use the method of changing the communication between the donor and acceptor species. The following sections give examples of how PET can be regulated using chemical reagents, electrons and photons.

3.2.1 – Chemical Regulation of PET

Sauvage and coworkers describe a very elegant PET regulation system using a porphyrinic terpyridine rotaxane.^{8a} In this case, the mechanism of PET is changed, however the net charge separated formation remains similar. Addition or removal of a metal results in a change of orientation between the Zn and Au porphyrins (Scheme 3.1). When the metal is chelated in the terpyridine units, the Zn and Au porphyrins are far apart, therefore the PET proceeds through the metal center. Upon removal of the metal, the Zn and Au porphyrins can form a sandwich complex, allowing direct PET from the Zn porphyrin to the Au porphyrin.

Despite this example being academically interesting, this system shows little promise in terms of applications due to the similar net effect of PET.

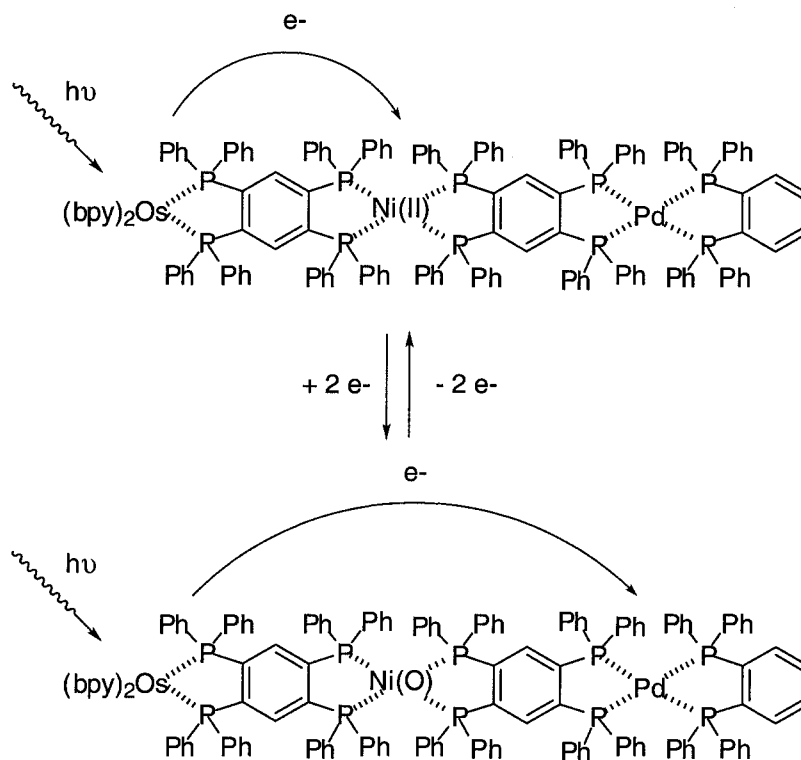


Sauvage 2000

Scheme 3.1

3.2.2 – Electrochemical Regulation of PET

In terms of device applications, using chemical reagents as the regulatory stimulus is not realistic due to accumulation of by-products, which are not easily removed.¹⁰ More practical is the use of electrons or photons. An electric current or a beam of light can easily be switched on or off, without accumulation of byproducts as long as the substrate is stable to the applied stimulus.



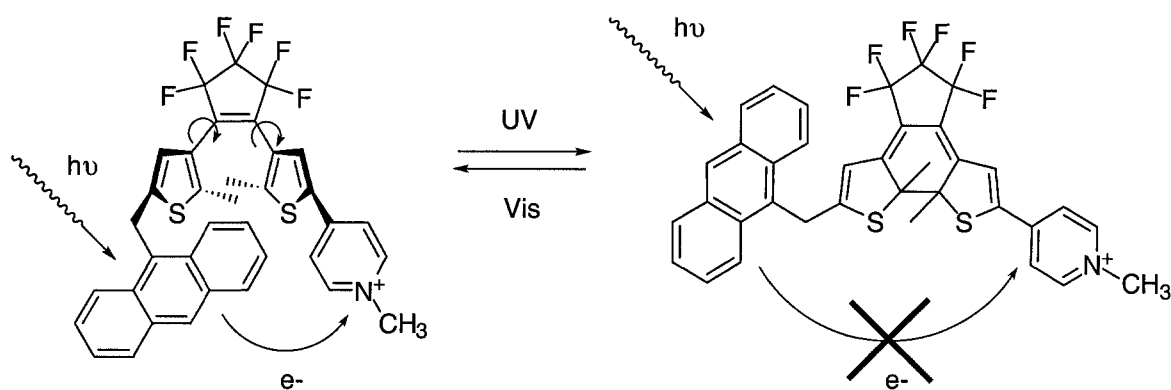
Fox 1998

Scheme 3.2

Fox and coworkers have reported a gated PET system which relies on redox chemistry of a Ni bridge between an Os terpyridine complex and a Pd phosphine complex (Scheme 3.2).^{8b} The oxidation/reduction of the nickel disallows/allows electron transfer, respectively, to the Pd complex from the photoexcited Os terpyridine. In the Ni(II) complex, photoexcitation of the Os terpyridine is followed by an electron transfer to the Ni(II) complex. The reduction potential Ni(II) center is less negative (an electron can be accepted into a lower energy orbital) than that of the Pd center, therefore electron transfer to the Pd center from the Ni(II) center is energetically disallowed. Upon reduction of the Ni(II) to Ni(0), the reduction potential of the Ni(0) center is more negative than that of the Pd center. Therefore upon photoexcitation of the Os terpyridine, electron transfer to the Ni(0) center is followed by another electron transfer to the Pd center.

3.2.3 – Photochemical Regulation of PET

As the theme of my research is the development of all-photon mode molecular devices using photochromic molecules, I set out to develop a switchable PET system that relies on the practical and efficient properties of light energy as the regulatory stimulus.⁹ As discussed in the introduction, photochromic molecules are ideal candidates for photonic molecular switching components as they interconvert between two stable states using light energy and each state possesses different physical properties.



Port 2000

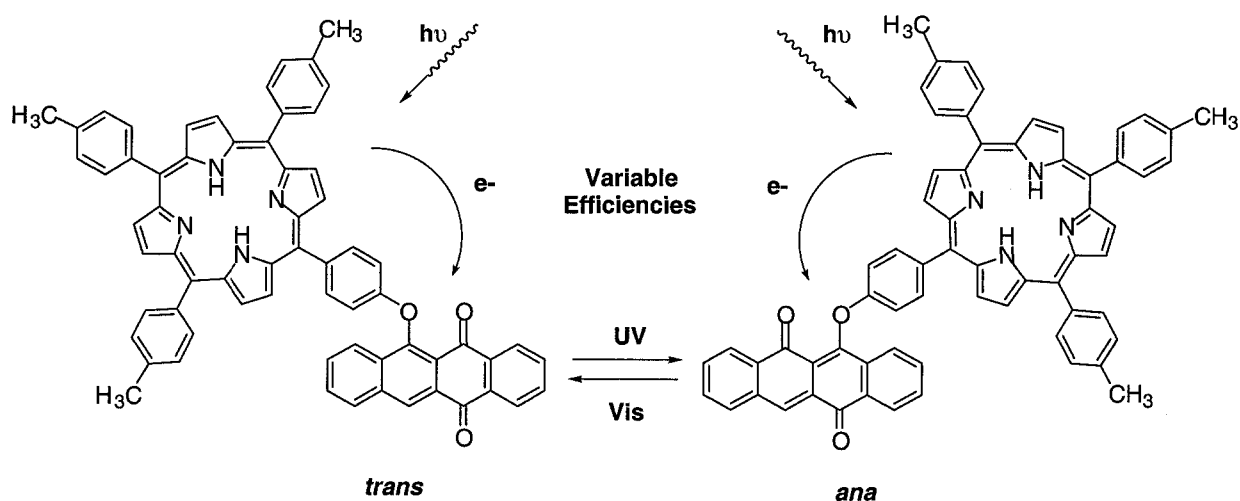
Scheme 3.3

Port and coworkers have demonstrated photoregulated PET between an anthracene electron donor and a pyridinium electron acceptor linked via a photochromic dithienylethene backbone (Scheme 3.3).^{9a} In the open form of the DTE photochrome, free bond rotation of the thiophene rings allows close, through-space interaction between the anthracene and pyridinium, providing a means for PET. Photocyclization rigidifies the backbone disallowing through space communication between the donor and acceptor, therefore shutting down PET.

3.2.4 – Phenoxynaphthacenequinones as Photo-Regulated Electron Acceptors

All of the previous examples showing the regulation of PET by means of a chemical reagent, electrons and photons do so by modifying the linker between the donor and acceptor. My strategy to regulate PET involves reversibly changing the reduction potential of the acceptor species by joining a porphyrinic photoinduced electron donor with a photochromic phenoxynaphthacenequinone electron acceptor (Scheme 3.4). By exploiting the expected

difference in reduction potentials between the *trans*- and *ana*-forms of the photochrome, a photocontrolled PET system can be realized. Not only is this hybrid one of few examples of photocontrolled PET, it represents the first example of photoregulation of PET in a porphyrin-quinone system by reversibly changing the electronic properties of the electron acceptor.

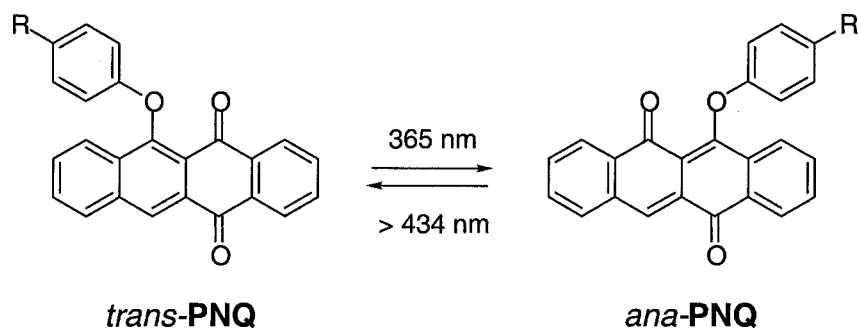


Scheme 3.4. Proposed Gated PET System

This chapter focuses on my investigation of this porphyrinic phenoxynaphthacenequinone hybrid. I will first give the preliminary data that led us to investigate phenoxynaphthacenequinones as photoregulated electron acceptors. This will be followed by the syntheses and studies of three hybrid systems and then a conclusion on what the future holds for these systems.

3.3 – Phenoxynaphthacenequinones (PNQ's)

As mentioned in the introduction, phenoxynaphthacenequinones (PNQ) are photochromic molecules that undergo a reversible photoisomerization between their yellow *trans*- and orange *ana*-forms upon irradiation with UV and visible light (Scheme 3.5).¹¹ PNQ possess desirable characteristics for applications as photo-regulated molecular switches due to their impressive fatigue resistance and thermal irreversibility.

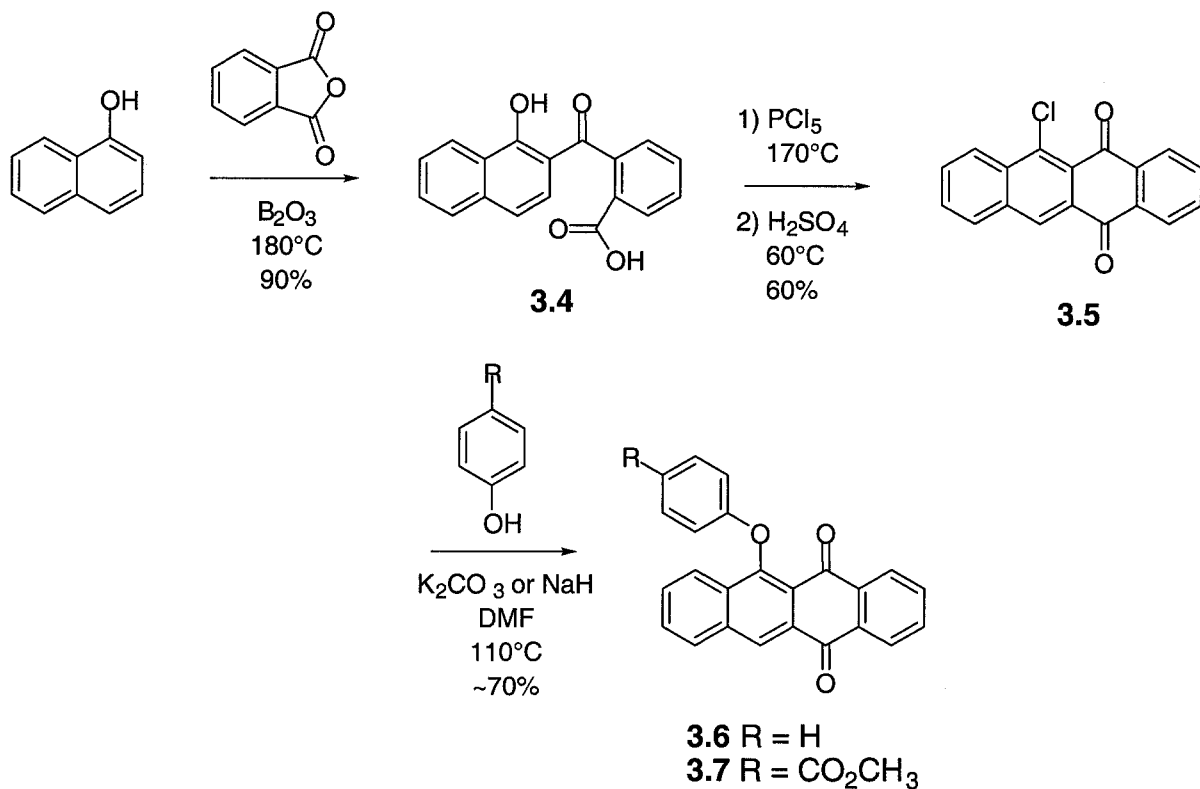


Scheme 3.5. Photoisomerization of Phenoxynaphthacenequinone

3.3.1 – Synthesis

Synthesis of a PNQ derivative is very straightforward from readily available starting materials (Scheme 3.6). Condensation of 1-naphthol with phthalic anhydride using boron oxide as a Lewis acid is accomplished by melting the mixture at 180°C to afford keto-acid **3.4** in good yield.¹² Formation of the acid chloride followed by ring closing is realized by melting the keto-acid **3.4** in PCl_5 at 170°C, which also chlorinates the quinone formed upon ring

closing. Heating this intermediate in concentrated H_2SO_4 at 60°C followed by pouring it onto ice affords chloronaphthacenequinone **3.5** in good yield over two steps.¹² All of the preceding steps can be performed on a multigram scale. PNQ derivatives are easily obtained from the chloronaphthacenequinone **3.5** via addition of the appropriate phenol under basic conditions. Two derivatives of PNQ's are defined in Scheme 4: the unsubstituted PNQ **3.6**¹³ and the carboxymethyl derivative **3.7**. These two derivatives will be used as controls throughout this chapter.



Scheme 3.6

3.3.2 – UV-vis Absorption Spectroscopy

UV-vis spectroscopy is a convenient technique to monitor the photoisomerization reaction between the *trans*- and *ana*-forms of PNQ and will be used throughout this chapter for this purpose. Figure 3.4 shows the UV-vis spectrum of the *trans*- and *ana*-forms of PNQ **3.6** (**3.6t** and **3.6a** respectively). Photoisomerization from **3.6t** to **3.6a** is performed by irradiation 365 nm light and is characterized by the appearance of two new absorption peaks at ~ 450 and ~ 480 nm. The original spectrum corresponding to **3.6t** is regenerated by broad band irradiation > 434 nm. This trend will be seen throughout this chapter.

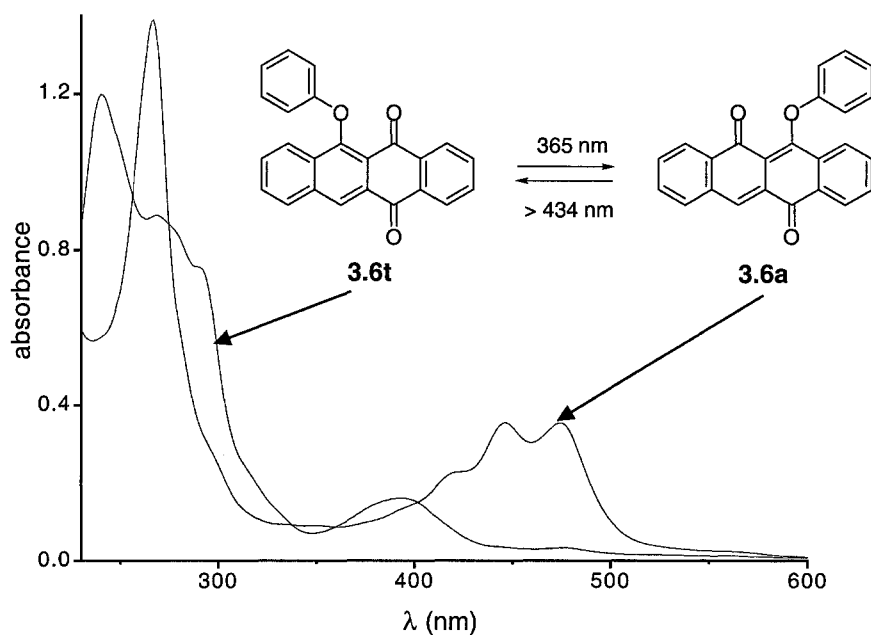
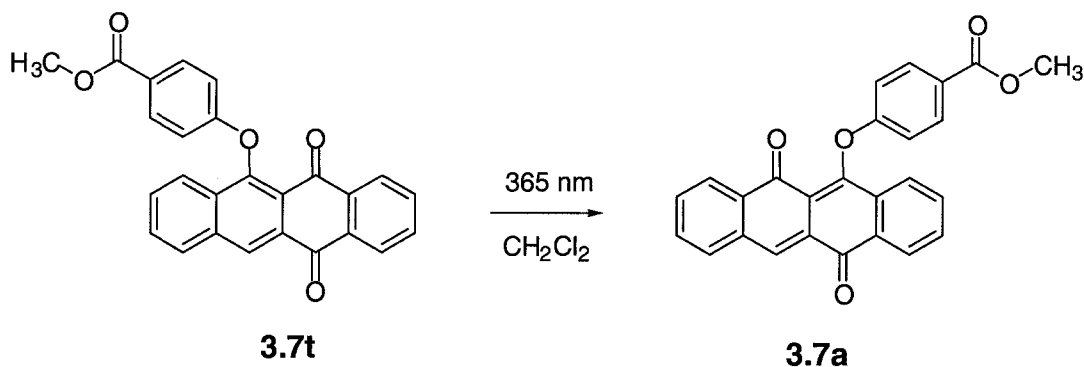


Figure 3.4. UV-vis absorption change upon photoisomerization of PNQ **3.6**. The spectrum of the **3.6a** was obtained by irradiation of a 2.5×10^{-5} M CH_2Cl_2 solution of **3.6t** with 365 nm light for 50 seconds. The original spectrum of **3.6t** is regenerated upon irradiation of the **3.6a** with broad band light > 434 nm for 60 seconds.

3.3.3 – Cyclic Voltammetry

Our hypothesis of photoregulating PET relies on having a change in electron accepting ability between the *trans*- and *ana*-forms of PNQ. Photoisomerization between the *trans*- and *ana*-forms of PNQ in a monolayer has shown reversible vectorial electron transfer between an electrode and gold substrate, suggesting a change in electronic properties between the two forms.¹⁴ Cyclic voltammetry experiments using PNQ **3.7** were performed to quantify this difference. The *ana*-form of **3.7** (**3.7a**) was synthesized by irradiation of a CH₂Cl₂ solution of *trans*-**3.7** (**3.7t**) with 365 nm light followed by purification by HPLC (Equation 3.1).



Equation 3.1. Synthesis of **3.7a** from **3.7t**.

Cyclic voltammograms were obtained for 10⁻³ M CH₂Cl₂ solutions of both isomers with 0.1 M tetrabutylammonium hexafluorophosphate as the electrolyte (Figure 3.5). A glassy carbon working electrode, silver wire reference electrode, and platinum counter electrode were used. The voltammogram of **3.7t** shows a reversible reduction peak centered at -1.14 V.

Another reversible reduction peak was observed at more negative potential however this peak is not shown in Figure 2.4. Repeating this experiment with **3.7a**, two reversible reduction peaks are observed centered at -0.69 V and -1.19 V. When assessing the ability for a molecule to accept an electron, the least negative reduction must be considered. The less negative the reduction potential, the easier it is for the molecule to accept an electron. The resulting voltammograms show a negative reduction potential of -1.1 V for **3.7t** and -0.7 V for **3.7a** (Figure 3.5). These results clearly show that the *ana*-isomer should act as a better electron acceptor than the *trans*-isomer of PNQ. These results suggest the possibility that PET can be regulated by photoisomerization of a PNQ electron acceptor.

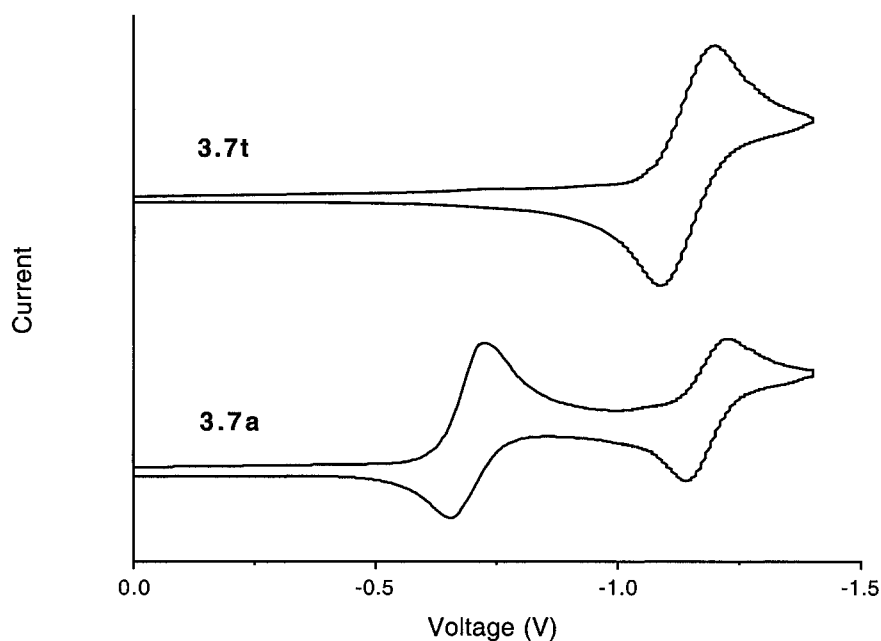
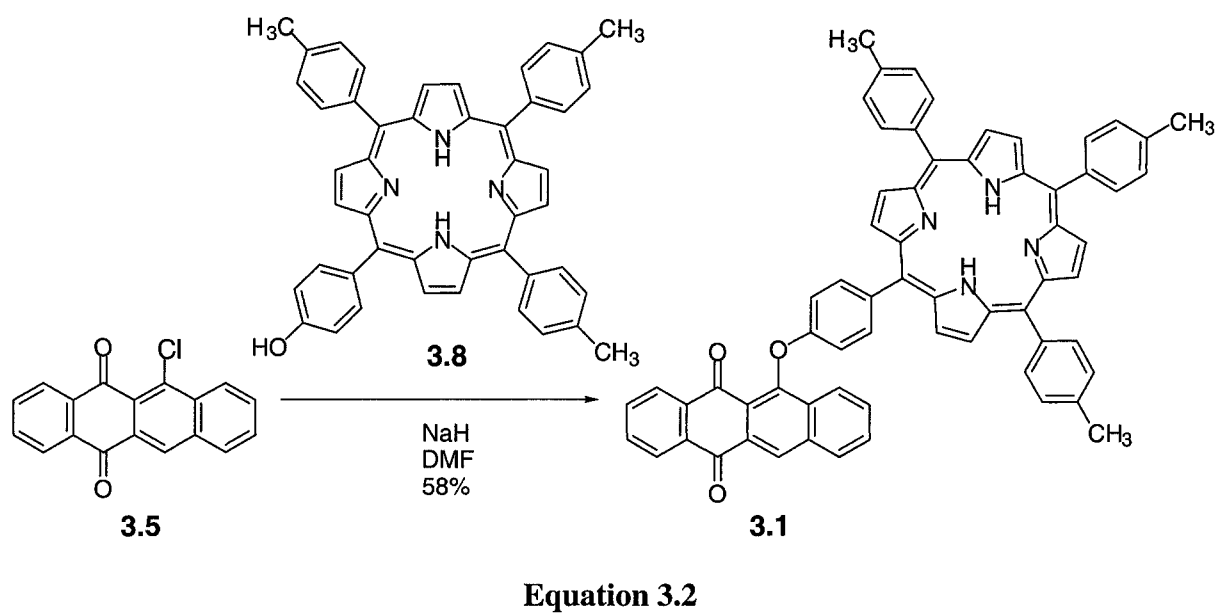


Figure 3.5. Cyclic voltammogram of **3.7t** (top) and **3.7a** (bottom) using 10^{-3} M CH_2Cl_2 solutions of both isomers with 0.1 M tetrabutylammonium hexafluorophosphate as the electrolyte. A glassy carbon working electrode, silver wire reference electrode, and platinum counter electrode were used.

3.4 - Covalent Porphyrinic Phenoxynaphthacenequinone Hybrid¹⁵

3.4.1 – Synthesis

The porphyrinic phenoxynaphthacenequinone **3.1** is conveniently prepared in one step in moderate yield from chloronaphthacenequinone **3.5** and known mono-phenoxy porphyrin **3.8**,¹⁶ using sodium hydride as the base in anhydrous dimethylformamide (Equation 3.2). The resulting ¹H NMR spectrum shows the peaks of each component integrating to the expected relative values. Electrospray mass spectrometry of the product shows the mass peak plus H⁺ at 929.3.



3.4.2 – UV-vis Absorption Spectroscopy

The UV-vis absorption spectrum of **3.1** is essentially equivalent to the sum of the absorption spectra of the molecule's components, **3.6t** and 5,10,15,20-tetratolylporphyrin (**TTP**, shown in the inset in Figure 3.6) indicating there is little change in the ground state of either chromophore upon covalent linking (Figure 3.6). This suggests negligible electronic communication between the two chromophores, allowing each one to be addressed independently. This is important because the desired effect of PET regulation requires each chromophore to be independently addressable, rather than act as one new chromophore.

The excited state behaviour of **3.1**, however, differs significantly from that of its constituents. When **3.1** was irradiated with light of wavelengths varying from 240 to 280 nm and from 350 to 380 nm, which normally cause the photoisomerization of the *trans*- to *ana*-form of PNQ, there was no observable change in the absorption spectrum. Specifically, the disappearance of the absorbances corresponding to *trans*-**3.1** at the expense of the absorbances corresponding to the *ana*-**3.1**, characteristic of the isomerization of the phenoxynaphthacenequinone chromophore, was absent even after prolonged exposure to high intensity light at several wavelengths within these ranges. Hunter and Irie have both previously reported a similar porphyrin-induced inhibition of the photoisomerization of the azobenzene and dithienylethene chromophores respectively.^{17,18} Similarly, upon irradiation of

the porphyrinic photochrome at various wavelengths, no photoisomerization could be detected by UV-vis absorption.

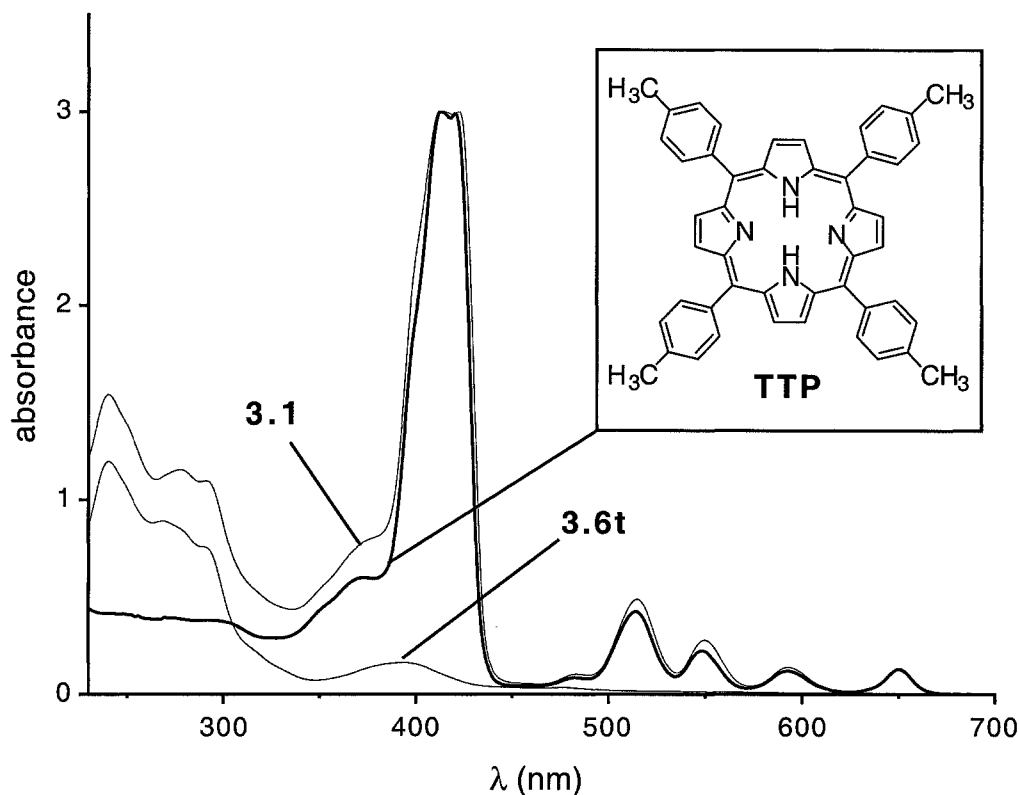


Figure 3.6. UV-vis spectra of **3.1** compared to its constituent chromophores **3.6t** and tetratolylporphyrin (**TTP**), shown in the inset. Spectra were run using 2.5×10^{-5} M CH_2Cl_2 solutions of each chromophore.

In order to evaluate the intermolecular effect of a porphyrin chromophore on the photoisomerization of PNQ, a control study was performed using PNQ **3.6** and **TTP**. Irradiation of an equimolar mixture of **3.6t**, and **TTP** at 254 nm or 365 nm resulted in the rapid disappearance of the absorbances corresponding to the **3.6t** at $\lambda_{\text{max}} = 240$ and 292 nm and

the appearance of the absorbances corresponding to **3.6a** at $\lambda_{\text{max}} = 267$ and 476 nm (Figure 3.7). This result clearly indicates that the mere presence of porphyrin in solution has no effect on preventing the photochemical isomerization of the phenoxynaphthacenequinone, which suggests an intramolecular quenching process of the porphyrin on the photoisomerization of PNQ.

In order to study this intramolecular quenching process, the studies described above were repeated in several different solvents such as toluene, THF, DMSO and acetonitrile, however no photoisomerization was observed, ruling out solvent effects as a possible quenching mechanism. Two other covalently linked porphyrinic PNQ's were also synthesized. The effect of changing the porphyrinic chromophore was assessed by synthesizing metalloporphyrinic PNQ **3.9** (Scheme 3.7), in which the free-base porphyrin is replaced by a Zn porphyrin. Treatment of hybrid **3.1** with zinc acetate afforded Zn hybrid **3.9** in good yield. Changing the through bond communication pathway between the porphyrin and PNQ was investigated with amido-hybrid **3.10** (Scheme 3.7). Hydrolysis of methyl ester **3.7** with NaOH afforded carboxylic acid **3.8** in good yield. Conversion of **3.8** to its acid chloride using SOCl_2 followed by coupling of aminoporphyrin **3.11**¹⁹ afforded amido linked porphyrinic PNQ hybrid **3.10**, albeit in low yield.

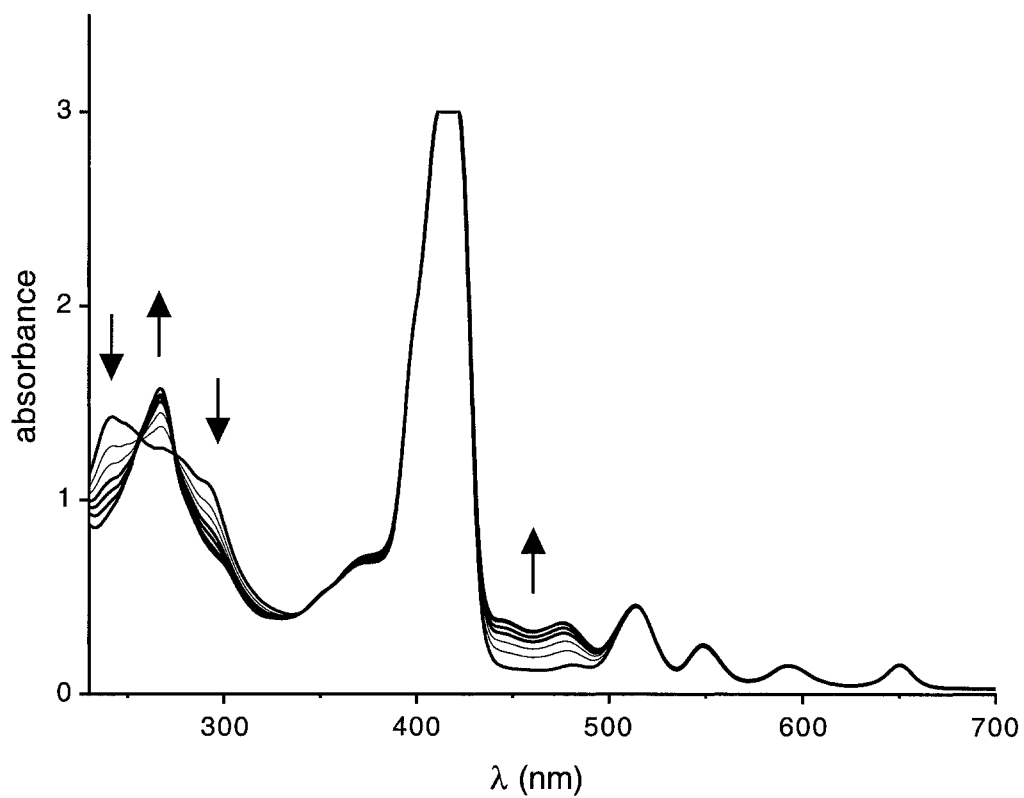
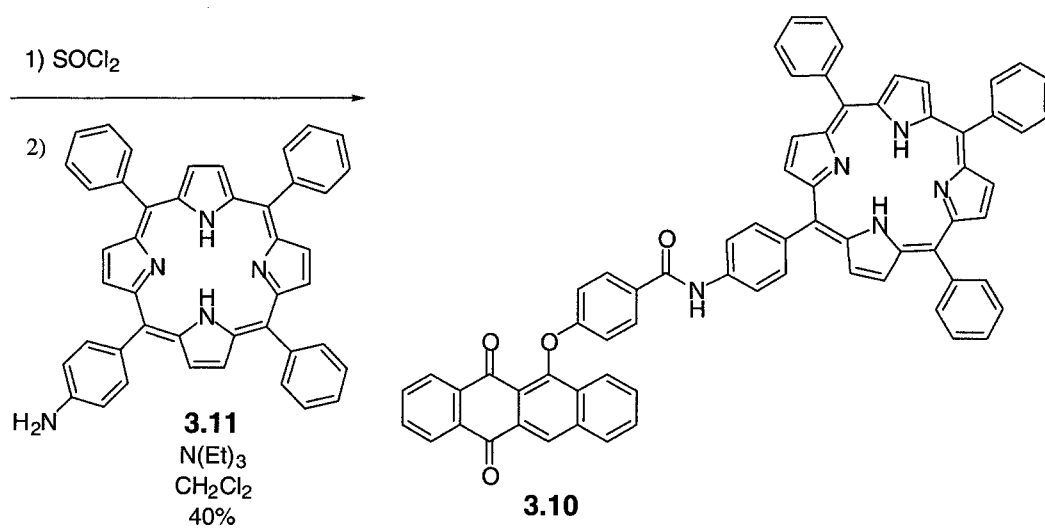
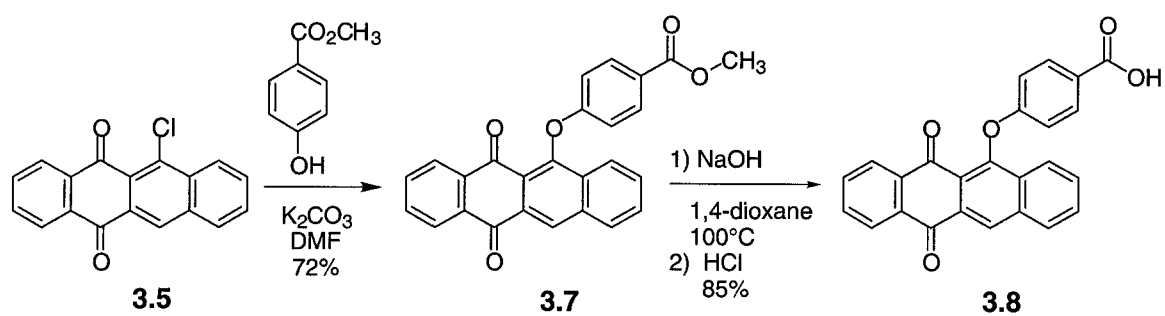
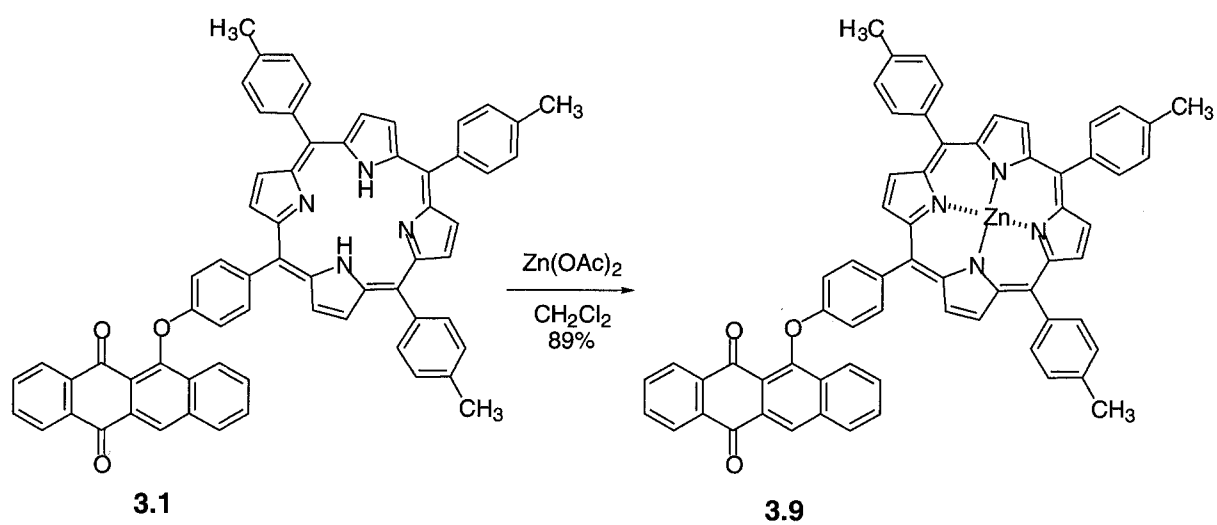


Figure 3.7. Photoisomerization of **3.6t** to **3.6a** in the presence of **TTP** upon irradiation with 365 nm light. Spectra were run using 2.5×10^{-5} M CH_2Cl_2 solutions of both chromophores. Irradiation times are 0, 10, 20, 30, 40, 60, and 180 seconds.



Scheme 3.7

UV-vis absorption studies were performed on both of the new hybrids **3.9** and **3.10**. Similar to the studies performed using hybrid **3.1**, upon irradiation of CH₂Cl₂ solutions of both **3.9** and **3.10** at wavelengths throughout the UV spectral region, no change in absorption is observed. The fact that amido-linked hybrid **3.10** shows no photoisomerization suggests a through space quenching mechanism, as conjugation through the amide linkage is minimal.

3.4.3 – Possible mechanisms of the Inhibition of Photoisomerization of Hybrid 3.1

The previous studies illustrate that the two chromophores must be intimately associated in order to shut down the photoisomerization process. Clearly, there exists a pathway for the decay of the excited state of the phenoxynaphthacenequinone component in **3.1** that is faster than the photochemical isomerization reaction, and this decay involves the pendant porphyrin chromophore. A detailed discussion of the possible mechanisms for this inhibition of photoisomerization follows.

Upon irradiation of phenoxynaphthacenequinone, the chromophore absorbs light energy and promotes an electron to the excited state. This electron can participate in several possible pathways to return to a ground state, such as thermal relaxation, fluorescence, electron transfer, energy transfer and chemical reactivity otherwise known as photoisomerization. Upon irradiation of the covalent hybrid **3.1**, no photoisomerization is observed. This means another pathway is favored over photoisomerization due to the presence

of the porphyrin chromophore. The mechanism for this inhibition is not certain, however the possibilities are listed in Figure 3.8. The figure represents the simplified ground and excited state electron configurations of each chromophore.

Upon irradiation of the hybrid **3.1** at 365 nm, both the porphyrin and the phenoxynaphthacenequinone chromophores absorb, therefore both excited states must be considered. The relative orbital energy levels (HOMO and LUMO) of each of the chromophores were estimated using cyclic voltammetric data. The reduction potential of *trans*-PNQ **3.6t** is approximately -1.1 V whereas the reduction potential of the **TTP** is more negative than -2 V. Therefore the LUMO of the PNQ lies at a lower energy than that of the porphyrin. The oxidation potential of the porphyrin is approximately 0.9 V whereas that of the PNQ is more positive than 2 V. Therefore the HOMO of PNQ lies at a lower energy than that of the porphyrin. This allows us to set up a qualitative Jablonski diagram in order to assess the possible photoisomerization quenching mechanisms involved in hybrid **3.1** (Figure 3.8).

The following is a discussion of each of the possible quenching pathways A, B, C and D, represented in Figure 3.8.

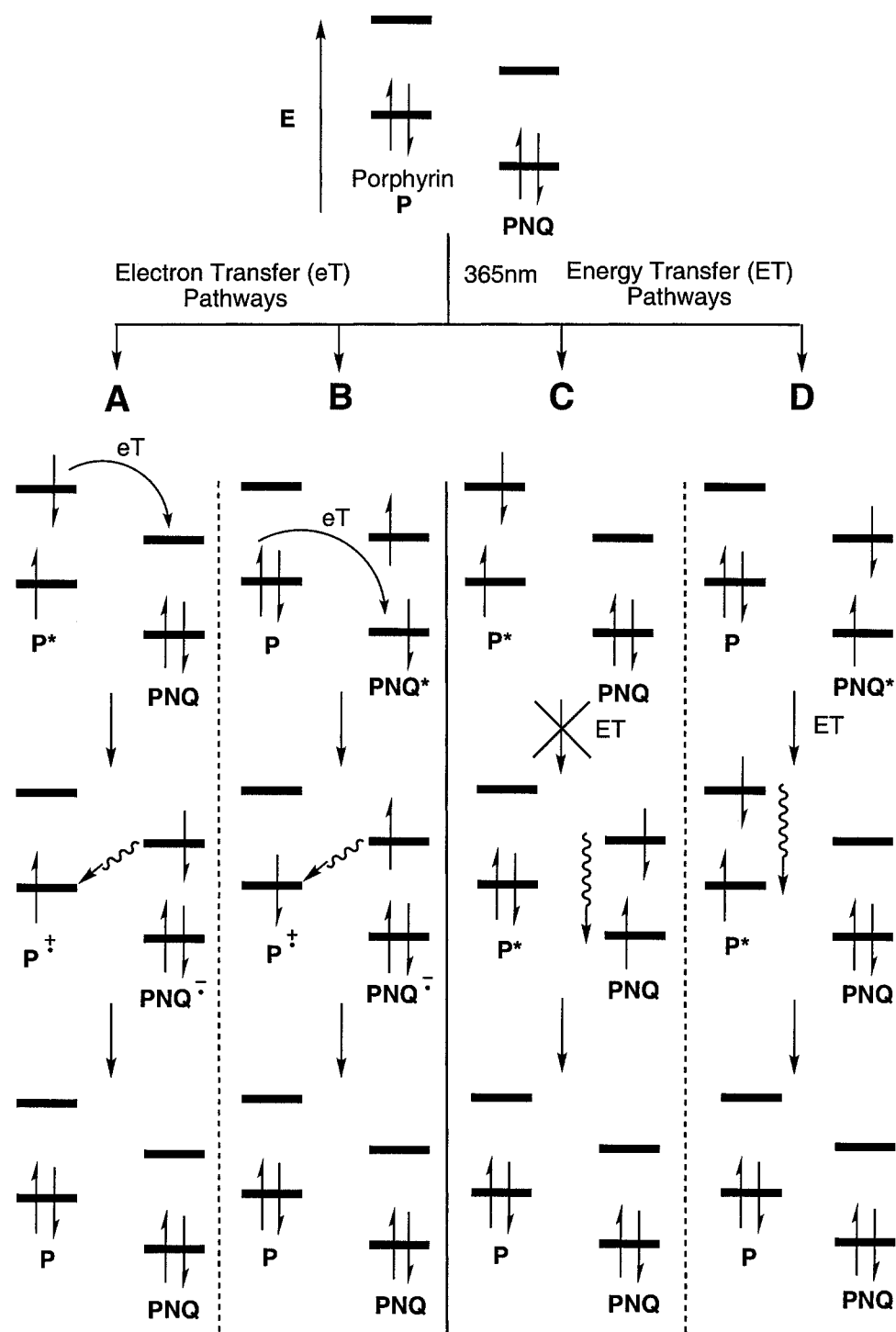


Figure 3.8. Possible mechanisms for the quenching of photoisomerization of 3.1 (See Text)

3.4.3.1 - Mechanism A

Upon excitation of the porphyrin chromophore, electron transfer from its excited state to the LUMO of the PNQ is energetically favorable, therefore is a viable pathway. Since electron transfer is dependent on the distance between the donor and acceptor species, it makes sense that quenching by this pathway would not occur in the dilute solution of PNQ and TTP. This is supported by the fact that PNQ photoisomerizes in the presence of TTP, as illustrated in the control study performed in section 3.4.2 (Figure 3.7). The intimacy of the porphyrin to the PNQ in the covalent hybrid could allow for efficient electron transfer between the two chromophores. Porphyrin-quinone hybrids are the most common natural and synthetic photosynthetic electron donor/acceptor pairs, further justifying this possibility. The goal of this project is to regulate PET between the porphyrin and PNQ, therefore it is desirable to have PET between the two chromophores. However, the phenomenon of PET that I want to exploit in this hybrid may be shutting down the photoisomerization of the PNQ photochrome.

The electron transfer creates the radical anion of the PNQ and the radical cation of the porphyrin. This charge separated state would thermally recombine to generate the original ground states of each chromophore. The overall result of this new pathway is that the PNQ chromophore is being converted to its radical anion, which may not undergo photoisomerization, at least not when irradiated with UV light. Studies on the photochromism of the radical anion of PNQ must be studied to confirm this.

3.4.3.2 - Mechanism B

Upon excitation of the PNQ chromophore, electron transfer from the ground state of the porphyrin to the lower orbital of the PNQ excited state occurs. Another way to visualize this transfer is that the hole in the excited PNQ is transferred to the porphyrin ground state. This transfer is also energetically favorable and results in the same charge separated state created in **Mechanism A**. In this case, the electron is promoted to generate the excited state of PNQ necessary for photoisomerization, however this excited state is quenched by rapid electron transfer generating the radical anion. Upon thermal recombination of the charge separated state, the ground state of each chromophore is regenerated. The light energy, in this case as well as in **Mechanism A**, is consumed by electron transfer rather than by photoisomerization.

3.4.3.3 - Mechanism C

Upon excitation of the porphyrin chromophore, the excited state can decay by releasing its energy in the form of a photon. This phenomenon is the basis of luminescence spectroscopy. If the PNQ absorbs light at the wavelength at which the porphyrin luminesces, the result will be a transfer of excited state energy from the porphyrin to the PNQ. If this occurs, it is expected to see some photoisomerization of the PNQ upon irradiation of the porphyrin. By comparing the UV-vis spectrum of the PNQ with the luminescence spectrum of

the porphyrin, there is no overlap between the absorption and emission bands, technically termed a zero integral overlap. This suggests that this energy transfer pathway is unlikely.

3.4.3.4 - Mechanism D

The same type of energy transfer can occur from the PNQ to the porphyrin. The excited state of the PNQ could relax emitting photon energy corresponding to a certain wavelength. If the porphyrin absorbs this energy and this process is faster than photoisomerization, the result would be a complete quenching of the PNQ excited state. A small fluorescence of the PNQ is observed within the absorption range of the porphyrin chromophore, therefore this pathway remains a possibility.

To test this mechanism, the fluorescence spectra of the porphyrin alone and the porphyrin-PNQ hybrid must be compared. If the fluorescence of the porphyrin chromophore in the hybrid is more intense than that of the porphyrin alone, energy transfer from the PNQ is occurring. Since there is so much variation in porphyrin's fluorescence intensity depending on its appended functionality, a control porphyrin would have to be used which was isoelectronic with the porphyrin contained in the hybrid. These studies prove to be much more than I was able to complete.

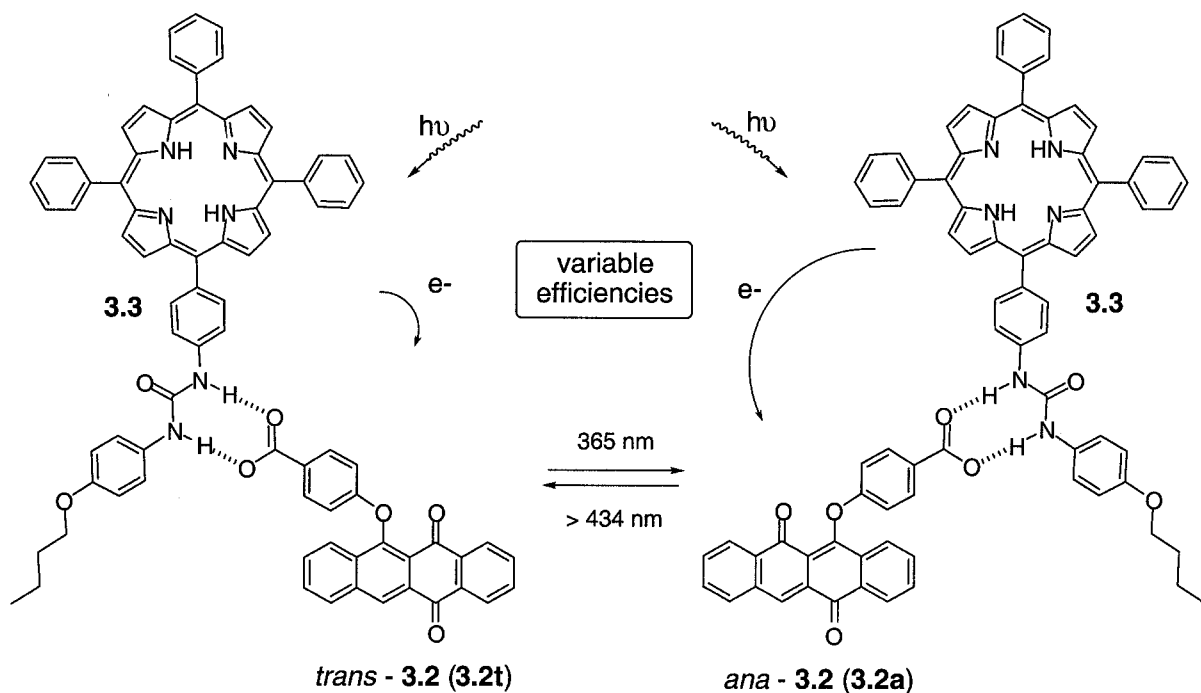
3.4.3.5 – Summary

The quenching of the photoisomerization within the covalently linked porphyrinic PNQ **3.1** could be due to **Mechanism A, B, D**, a combination of two, or all three. Transient absorption spectroscopy experiments (see section 3.5.7) must be performed to understand the excited state behaviour of these chromophores.; however, due to absorption overlap of the PNQ and porphyrin transients, the information obtained from such experiments may prove to be inconclusive. Having discussed this issue with several physical chemists and physicists, we decided to close the books on this covalent PNQ-porphyrin hybrid.

3.5 - Non-Covalent Porphyrinic Phenoxynaphthacenequinone²⁰

The observed inhibition of photoisomerization of hybrid **3.1** is due to the intimacy between the porphyrin and PNQ chromophore. To circumvent this problem, I resolved to synthesize a dynamic two-component system in which the association of the porphyrin **3.3** and the phenoxynaphthacenequinone **3.2** relies on hydrogen bonding, as illustrated in Scheme 3.8. Our design takes advantage of strong hydrogen bonding between a carboxylate acceptor and a urea donor. These molecular recognition elements were chosen to ensure that the supramolecular structures are retained even at the low concentrations required to conveniently evaluate electron transfer processes using luminescence spectroscopy without having to add excessive quantities of the quenching component. The ON/OFF nature of the hydrogen

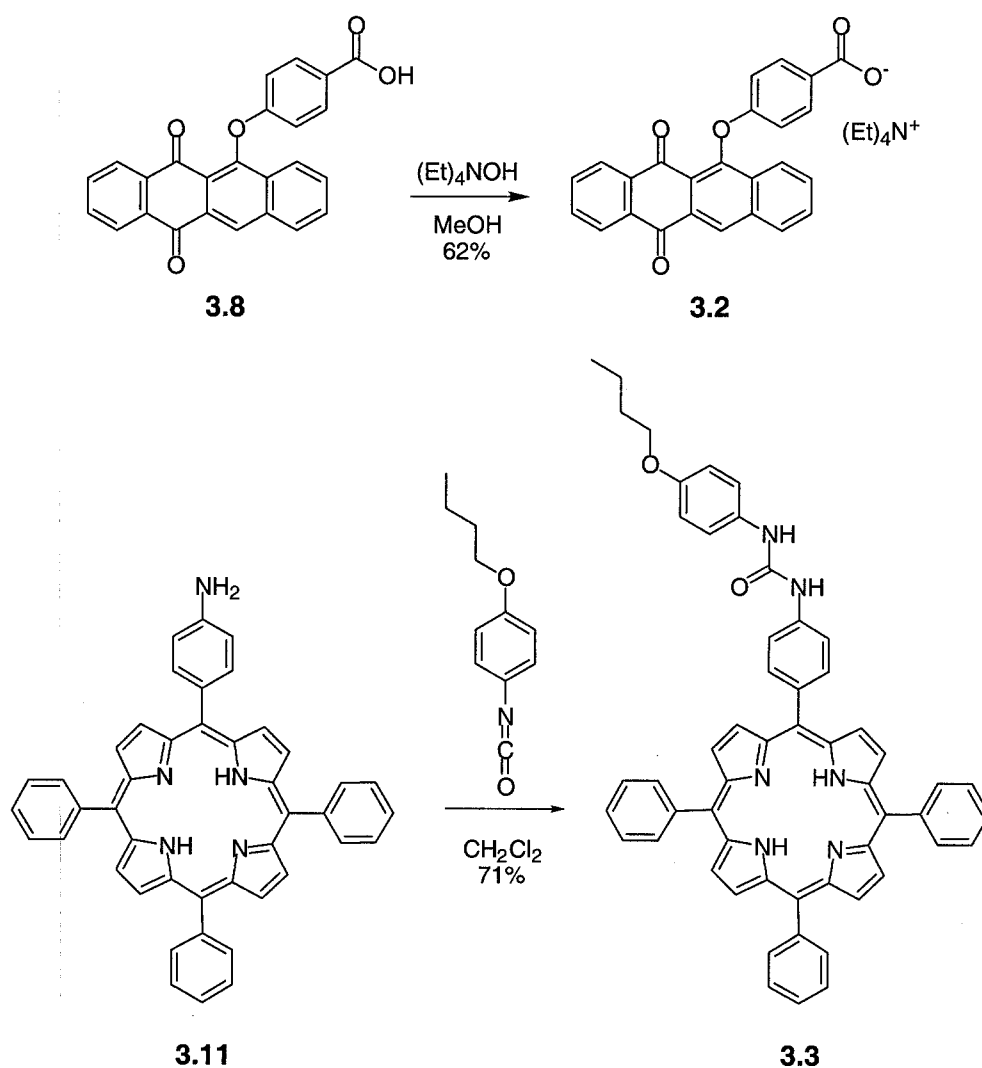
bonded system will allow the two chromophores to be sufficiently far apart to allow photoisomerization of the PNQ photochrome while allowing sufficient association for PET to occur.



3.5.1 - Synthesis

The synthesis of each of the components **3.2** and **3.3** is very straightforward (Scheme 3.9). Hydrolysis of the PNQ methyl ester **3.7** afforded carboxylic acid **3.8** in good yield. Acid **3.8** was subsequently deprotonated with tetraethyl ammonium hydroxide to generate the tetraethylammonium carboxylate **3.2** in moderate yield. The tetraethylammonium counterion

was used to promote the solubility of the carboxylate in non-polar solvents. Carboxylate **3.2** is soluble in CH_2Cl_2 , whereas the acid precursor **3.8** is only sparingly soluble in this solvent. The ^1H NMR spectrum indicated the appropriate PNQ peaks, integrating accordingly with the ethyl peaks of the ammonium counterion. Due to the hygroscopic nature of this compound, I was unable to acquire an accurate elemental analysis for **3.2**.



Scheme 3.9

Amino porphyrin **3.11**¹⁹ was treated with 4-butoxyphenyl isocyanate to yield porphyrin urea **3.3**. The 4-butoxy substituent was used to increase the urea's solubility in non-polar solvents and to simplify analysis by ¹H NMR spectroscopic methods. The product's structure is characterized not only by mass spectrometry, but the ¹H NMR spectrum shows the appearance of two new broad singlet peaks at δ 6.9 and δ 6.6, corresponding to the urea's two N-H protons.

3.5.2 – Cyclic Voltammetry

Electrochemical studies were performed using the tetraethylammonium carboxylate PNQ **3.2**. When a CH₂Cl₂ solution of *trans*-**3.2** (**3t.2t**) was irradiated at 365 nm, the peak corresponding to the reduction of the *trans*-isomer was replaced by two new peaks representing the reduction of the *ana*-**3.2** (**3.2a**) (Figure 3.9). The peak for the reduction of **3.2t** never fully disappears in the cyclic voltammogram and ¹H NMR spectroscopy reveals the photostationary state generated with 365 nm light is made up of a 4:1 **3.2a**:**3.2t** mixture. The solution can be irradiated with light greater than 434 nm to reform **3.2t** and regenerate the original voltammogram. These experiments confirm that photoisomerization of PNQ **3.2** results in a change in its electron accepting ability, more specifically the **3.2a** is a better electron acceptor than **3.2t**. This change in reduction potential is also reversible, a key factor in device applications.

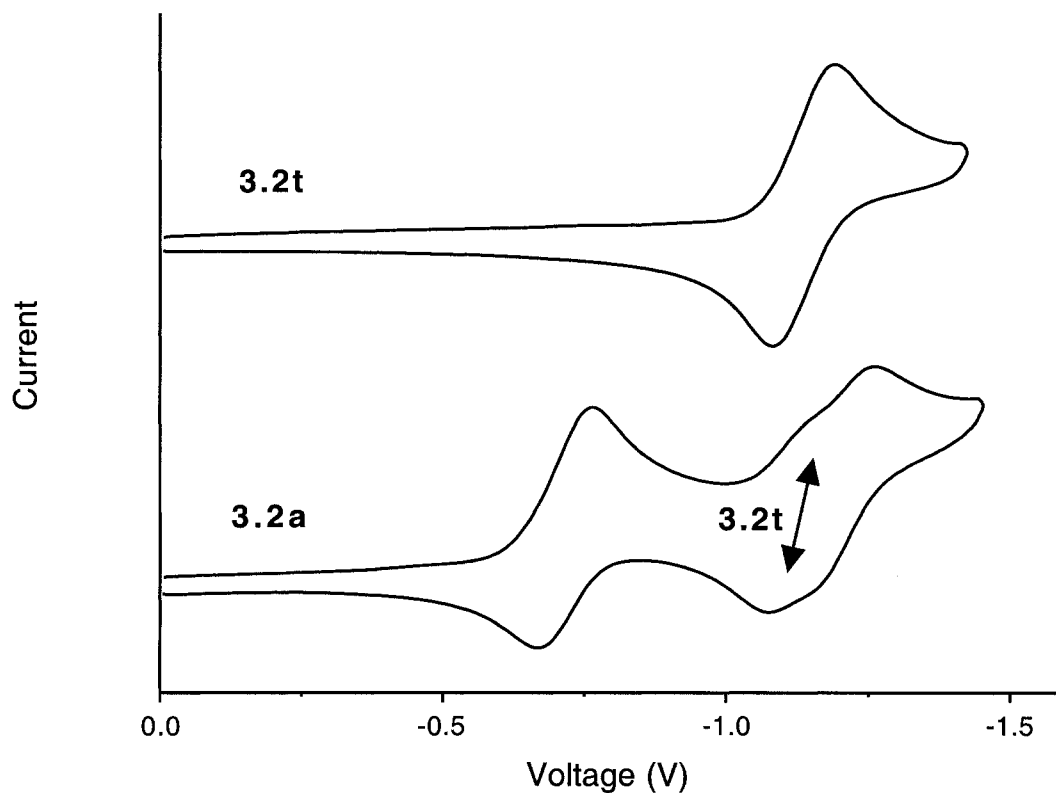
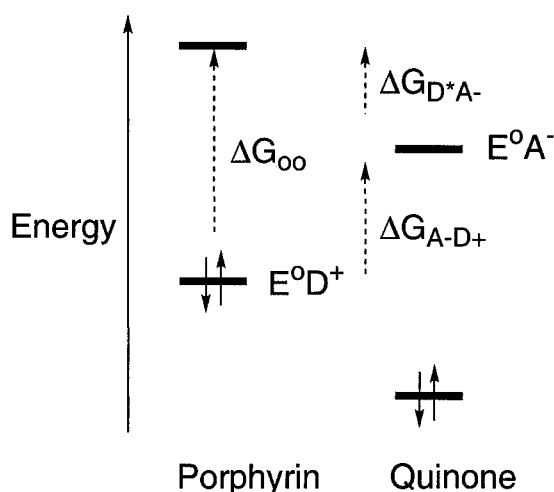


Figure 3.9. Cyclic voltammograms of 10^{-4} M CH_2Cl_2 solutions of **3.2t** (top) and the photostationary state of **3.2a+3.2t** generated with 365 nm light (bottom). Residual **3.2t** is highlighted in the bottom trace.

3.5.3 – Free Energy of PET Calculations

To relate the change in reduction potential to difference in efficiency in PET, the changes in free energies of PET were calculated using the Rehm equation (Equation 3.3).²¹



$$E = hc/\lambda$$

$$= [(6.626 \times 10^{-34} \text{ J s})(2.9979 \times 10^8 \text{ m/s})] / 0.000000560 \text{ m} = 3.55 \times 10^{-19} \text{ J}$$

$$\Delta G_{oo} = E N_A = (3.55 \times 10^{-19} \text{ J}) (6.022 \times 10^{23} / \text{mol})$$

$$= 2.14 \times 10^5 \text{ J/mol} = 214 \text{ kJ/mol}$$

$$= 51.1 \text{ kcal/mol}$$

$$wp = \{332[(zD^+) (zA^-)]\} / (d_{cc} E_s)$$

$$= \{332[(1) (-1)]\} / [(12.252) (9.08)]$$

$$= -2.98$$

Rehm Equation:

$$\Delta G_{PET} = 23.06 [E^\circ (D^+/D) - E^\circ (A/A^-)] - wp - \Delta G_{oo}$$

ΔG 3.3:3.2t

$$= 23.06 [E^\circ (D^+/D) - E^\circ (A/A^-)] - wp - \Delta G_{oo}$$

$$= 23.06 [(0.902) - (-1.145)] - (-2.98) - (51.1)$$

$$= -0.916 \text{ kcal/mol}$$

ΔG 3.3:3.2a

$$= 23.06 [E^\circ (D^+/D) - E^\circ (A/A^-)] - wp - \Delta G_{oo}$$

$$= 23.06 [(0.902) - (-0.723)] - (-2.98) - (51.1)$$

$$= -10.6 \text{ kcal/mol}$$

E = energy in kcal/mol of the light used, in this case wavelength $\lambda = 560 \text{ nm}$

h = Planck constant

c = speed of light

ΔG_{oo} = the change in free energy of the electron donor upon excitation with light

wp = electrostatic component which allows for a more accurate approximation of ΔG of electron transfer

zD^+ = charge on electron donor after electron transfer

zA^- = charge on electron acceptor after electron transfer

d_{cc} = center to center distance between the electron donor and electron acceptor, approximated using molecular modeling

program Macromodel 6.5, Schrodinger, Inc. E_s = dielectric constant of the solvent used, in this case dichloromethane (CH_2Cl_2)

Equation 3.3. Free Energy of PET between 3.3 and 3.2t and 3.2a.

The negative values of the free energies for photoinduced electron transfer calculated for **3.3:3.2t** ($-0.94 \text{ kcal mol}^{-1}$) and **3.3:3.2a** ($-10.67 \text{ kcal mol}^{-1}$) indicate that both reactions are thermodynamically favorable with that for the **3.2a** being significantly more exergonic.

3.5.4 – Association Measurements of 3.3 with 3.2t and 3.2a

The association of **3.3** with both **3.2t** and **3.2a** must be measured to ensure a similar concentration of complex if they are to be compared. The free energies of association for both **3.2t** and **3.2a** with **3.3** were measured by ^1H NMR titration experiments (Figure 3.10). The two N-H protons on the urea become more electropositive upon hydrogen bonding to the carboxylate, as electron density is pulled away from them to form the hydrogen bond. This will result in a downfield shift of the protons' resonances. The significant downfield shift ($\Delta\delta$ greater than δ 5) observed for the urea N-H protons of **3.3** (1.09 mM in CD_2Cl_2) as it is treated with aliquots of a solution of either **3.2t** or the photostationary state of 4:1 **3.2a:3.2t** (6.54 mM in the same solvent) clearly indicate effective hydrogen bonding. For these experiments, solutions of the **3.2a** were prepared by irradiating the **3.2t** at 365 nm until its photostationary state was reached, at which time the mixture contained 80% **3.2a** (4:1 **3.2a:3.2t**). Data from all titrations correlate well with calculated curves using 1:1 binding models²² and give values for the free energy of association of $-6.15 \pm 0.12 \text{ kcal mol}^{-1}$ for **3.2t** and $-5.15 \text{ kcal mol}^{-1}$ for the photostationary state at 365 nm, 80% **3.2a**.

The value measured for the **3.2a** greatly depends on the relative amount of this isomer present in solution, and when the titration experiments were repeated with solutions containing less of **3.2a**, more negative free energy values were obtained ($-5.60 \text{ kcal.mol}^{-1}$ at 78% **3.2a**, and $-5.99 \text{ kcal.mol}^{-1}$ at 74% **3.2a**). These observations indicate that the association of **3.2t** is slightly greater than that of **3.2a**. This must be considered upon analysis of the data when assessing the efficiency of PET between the two forms.

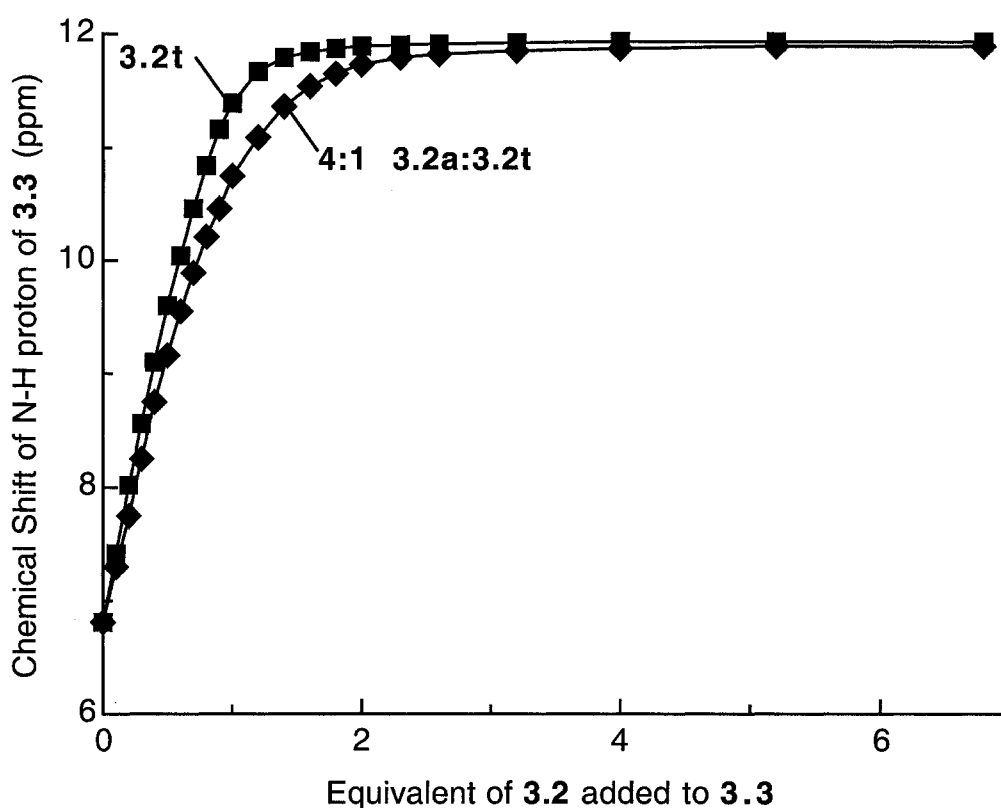


Figure 3.10. ^1H NMR Titration curves of **3.3** with **3.2t** (■) and 4:1 **3.2a:3.2t**(◆). Titrations were performed using **3.3** (1.09 mM in CD_2Cl_2) as it was treated with aliquots of a solution of either **3.2t** or the photostationary state of 4:1 **3.2a:3.2t** (6.54 mM in the same solvent). The urea N-H proton at δ 6.6 of **3.3** was monitored as it shifted downfield upon hydrogen bonding to the carboxylate of **3.2**.

3.5.5 – UV-vis Absorption Spectroscopy

Photophysical studies show that the absorption spectrum in the UV-Vis region for the hydrogen bonded complex **3.3:3.2t** is essentially the sum of the absorption spectra of its components, indicating the two chromophores can be addressed independently. The low energy absorptions of the porphyrin allow for the porphyrin to be selectively irradiated at a region of the spectrum where photochrome **3.2t** and **3.2a** are transparent. This is particularly important in all photon-mode molecular device applications to ensure control over the process, in this case PET. Otherwise, irradiation to create the charge separated state would also result in photoisomerization of the photochrome, which in turn affects the creation of the charge-separated state; the information obtained from such a system is therefore unreliable.

Upon irradiation of **3.3:3.2t** at 365 nm, **3.2t** cleanly, but not completely, photoisomerizes to **3.2a** as shown by the appearance of a new absorption at 480 nm (Figure 3.11). This trend mimics the changes that occur when phenoxynaphthacenequinone **3.2t** is irradiated alone. Irradiation of **3.2a** at wavelengths greater than 434 nm results in the original absorption spectrum, confirming the reversible photoisomerization of the phenoxynaphthacenequinone in the presence of porphyrin. This result also confirms that the dynamic association between the two chromophores allows for efficient photoisomerization of PNQ.

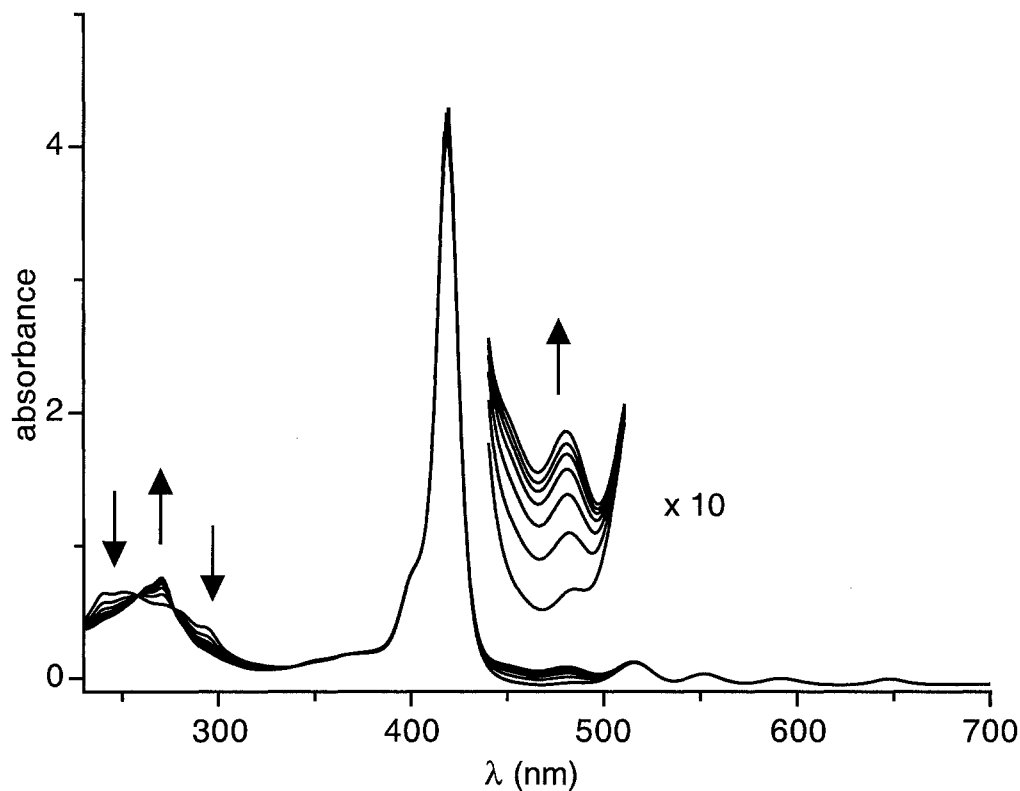


Figure 3.11. Changes in the UV-Vis absorption spectra of a CH_2Cl_2 solution of **3.3:3.2t** (1×10^{-5} M) upon irradiation with 365 nm light. Irradiation periods are 0, 10, 20, 30, 40, 80 and 120 seconds.

The photoisomerization of the PNQ within this porphyrinic array allows my original hypothesis to be put to the test: can switching between the *trans*- and *ana*-forms of the PNQ photochrome regulate PET between the porphyrin and PNQ?

3.5.6 – Evaluation of PET using Luminescence Spectroscopy

PET was evaluated using luminescence spectroscopy. Upon photo-excitation of the porphyrin **3.3** alone at 560 nm, the excited state relaxes back to the ground state in a radiative process by emitting light at 650 nm. Once the porphyrin is coupled to an electron acceptor, the excited state can decay via an electron transfer reaction, causing a decrease in its emission at 650 nm; the energy that was formerly given off as light is now going towards electron transfer. This phenomenon is known as luminescence quenching. Therefore, if there is a difference in PET between **3.3** and the two forms of the photochrome **3.2t** and **3.2a**, there should be a change in emission between the two hybrid systems.

This change in emission is graphed using an inverse Stern Volmer plot (Figure 3.12). This involves titrating aliquots of the quencher (PNQ) into a solution of the chromophore (porphyrin) of which the emission is being monitored. The x-axis is the total concentration of quencher added; the y-axis is the normalized emission of the chromophore, calculated by dividing the observed emission intensity after addition of the quencher by the initial emission intensity with no quencher present.

Before observing the effects of **3.2t** and **3.2a** on the emission of **3.3**, control titrations were performed. Titrating CH₂Cl₂ solutions of porphyrin urea **3.3** with tetrabutylammonium 4-methylbenzoate dissolved in the same solvent assessed the effect of hydrogen bonding on the emission spectrum of the porphyrin. Hydrogen bonding afforded an increase in the emission intensity and a slight bathochromic shift (4 nm). Because this system is hydrogen bonded, this emission curve represents the chromophore of interest, not **3.3** alone, and should be treated as the baseline for all subsequent titrations. Analogous titrations of **3.3** with equimolar solutions of tetrabutylammonium 4-methylbenzoate and the PNQ methyl ester of **3.7t** or **3.7a** show a similar trend. We attribute the small decrease in porphyrin emission upon the addition of the esters of **3.7t** and **3.7a** to diffusionally controlled quenching. The addition of **3.2t** resulted in an even greater extent of quenching due to its forming a hydrogen-bonded complex with **3.3**. The most dramatic decrease in the emission intensity was observed when **3.2a** (photostationary state containing 80% **3.2a**) was titrated into **3.3**. In this case, the quenching process more than compensates for the hydrogen bond-induced increase in emission. Even though hydrogen bonding results in an increase in the porphyrin's emission, quenching with **3.2a** is efficient enough to bring its emission down below that of the porphyrin alone. We attribute this quenching to more favorable electron transfer from **3.3** to **3.2a**. These results are consistent with our hypothesis and clearly indicate that photocontrolled PET can be achieved by photoisomerization of phenoxynaphthacenequinone from the *trans*- to the *ana*-form.

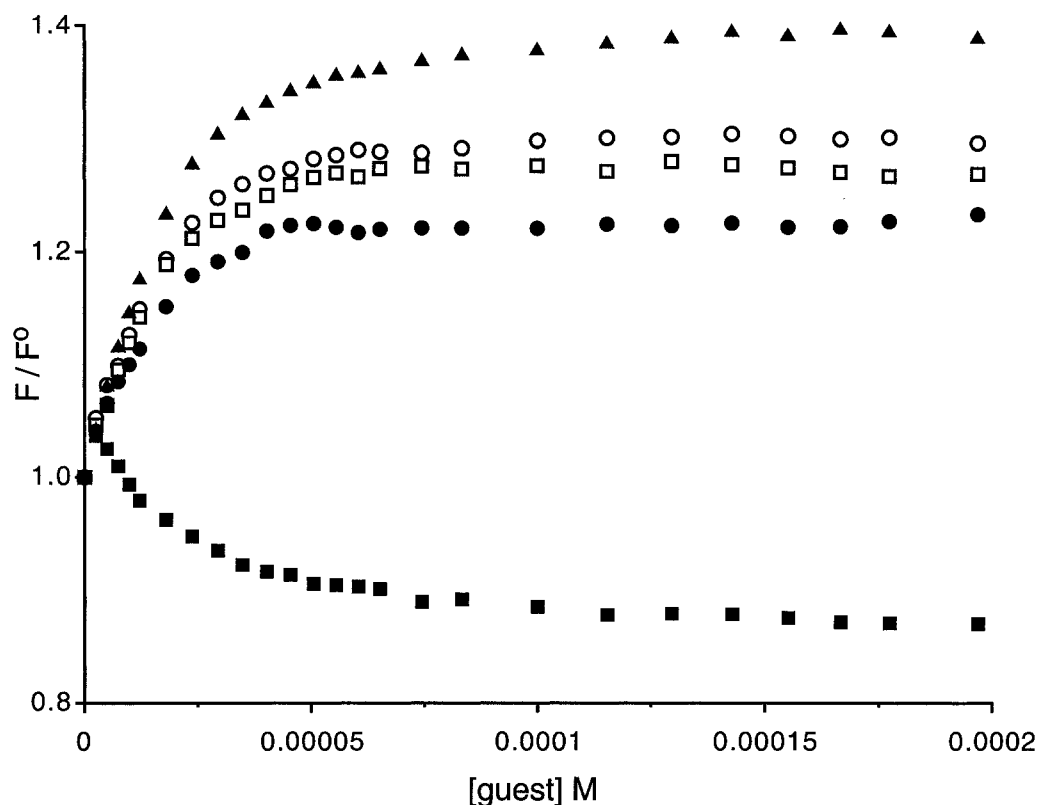


Figure 3.12. Inverse Stern-Volmer quenching of CH_2Cl_2 solutions (1×10^{-5} M) of **3.3** ($\lambda_{\text{excit}} = 560$ nm, $\lambda_{\text{em}} = 652$ nm) when treated with tetrabutylammonium 4-methylbenzoate (\blacktriangle), **3.2t** (\bullet), **3.2a** (\blacksquare), methyl ester **3.7t** + tetrabutylammonium 4-methylbenzoate (\circ) and methyl ester **3.7a** + tetrabutylammonium 4-methylbenzoate (\square).

Energy transfer is not a likely cause of the quenching as there are zero overlap integrals between the absorption and emission spectra of the acceptor and donor, and the calculations of the free energy for electron transfer argues our hypothesis. In order to confirm that PET from **3.3** to **3.2a** is the cause of the decrease in emission intensity of **3.3**, direct observation of the **3.3** radical cation and/or **3.2a** radical anion is necessary. EPR experiments have been used in the past in order to detect radical cations/anions of electron transfer

systems,²³ however the charge separated state of the **3.3:3.2a** system is expected to be extremely short lived making it impossible to detect the radical anion/cation pair using EPR. Recent advances in transient absorption spectroscopy allow for extremely short-lived transients to be monitored down to the femtosecond timescale. A collaboration was set up with Dr. Frances Cozens at Dalhousie University, where I visited for nine days to perform transient absorption spectroscopy experiments to detect the radical cation/anion pair of the **3.3:3.2a** system.

3.5.7 – Transient Absorption Spectroscopy

Transient Absorption Spectroscopy (TAS) involves irradiation of a sample with a short-lived laser pulse followed by a UV-vis absorption measurement (Figure 3.13). Because the transient species formed upon irradiation is short lived, the absorption measurements are performed one wavelength at a time; sequentially plotting the absorbance at each wavelength results in a UV-vis spectrum of the transient species. Disappearance of the transient absorption can also be measured over time to determine lifetimes and kinetics of decay of the transient species. The radical cation of **3.3** and the radical anion of **3.2a** will each have a distinct absorption spectrum; therefore if irradiation of **3.3** at 560 nm causes electron transfer to **3.2a**, transient absorption spectroscopy should detect the absorption of the radical cation of **3.3** and/or the radical anion of **3.2a**. The charge recombination of the charge separated state

formed upon PET is expected to be very fast (picosecond/femtosecond timescale), therefore femtosecond transient absorption spectroscopy will be needed for these experiments.

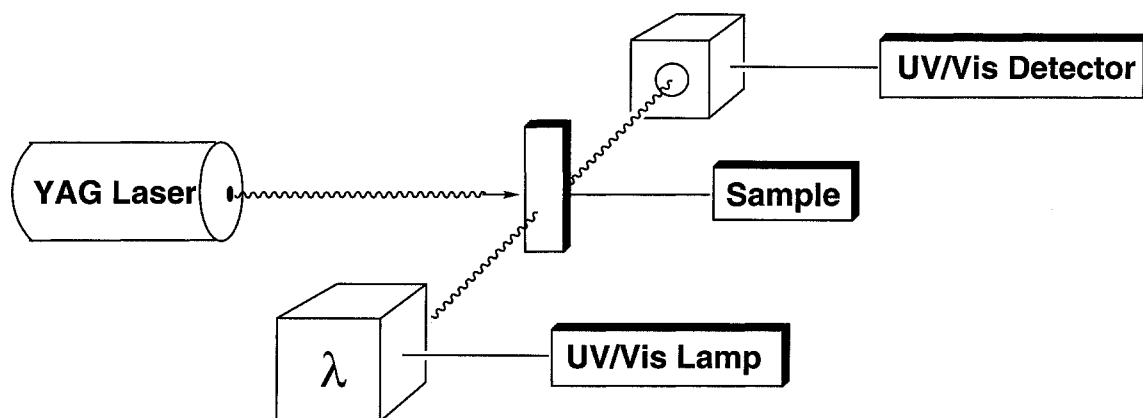


Figure 3.13. Schematic diagram of transient absorption spectroscopy apparatus. Pulse irradiation of a samples with a laser source produces the transient, of which the absorbance is monitored by UV-vis spectroscopy.

The first step in our experiments was to characterize the radical anion of **3.2a** using nanosecond TAS. Repeating the work of Rentzepis and coworkers,²⁴ the transient absorption spectra of PNQ photoisomerization were performed on **3.2t**. The sequence of excited transformations upon irradiation of the *trans*-form is as follows:



Due to the timescale at which I was working, upon photoexcitation of the *trans*-form, the first triplet state of the *ana*-form was detected, the other states being too short lived.

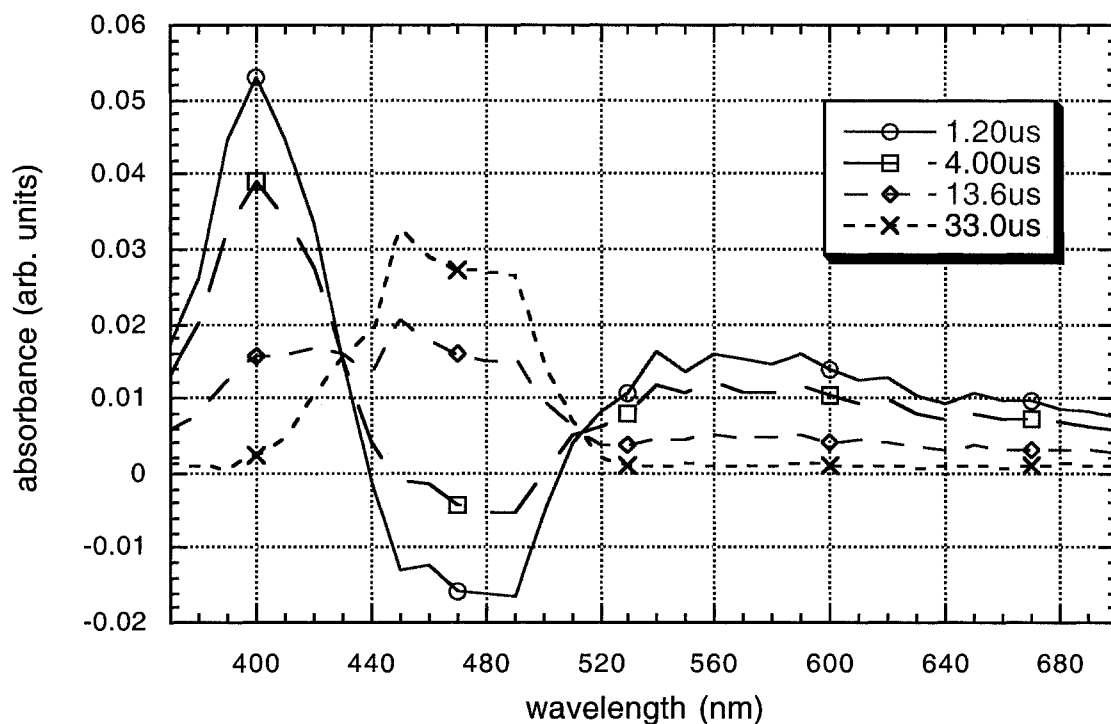


Figure 3.14. Transient absorption spectra of **3.2t** after irradiation with 355 nm. Upon irradiation of **3.2t**, the absorption of the triplet state of **3.2a** is observed; its decay is accompanied by the growth of the absorbances corresponding **3.2a** ground state. Spectra were performed on 1×10^{-4} M 2:1 acetonitrile:water solutions of **3.2t** purged with nitrogen gas.

Upon irradiation of **3.2t** at 355 nm, the triplet state of **3.2a** is detected with an absorption at 400 nm (Figure 3.14). The decay of **3.2a** triplet absorbance is accompanied by an increase in absorbance at 450 and 480 nm, corresponding to the ground state **3.2a** absorption. These observations agree with the results reported by Rentzepis. Our approach to characterizing the radical anion of **3.2a** involved addition of an electron donor, *N,N*-dimethylaniline, to a solution of **3.2t**. Photoexcitation of **3.2t** produces the triplet form of **3.2a**,

which has a lifetime long enough to accept an electron from the electron donor into its low energy SOMO (singly occupied molecular orbital). In this way, the radical anion of **3.2a** is formed and the transient absorption spectrum can be measured.

The experiment was carried out in 2:1 acetonitrile:water under a nitrogen atmosphere with a concentration of **3.2t** of 10^{-4} M. *N,N*-Dimethylaniline, a well-known electron donor, was used at varying concentrations. Transient absorption spectra of **3.2t** with various concentrations *N,N*-dimethylaniline (Figure 3.15 and Figure 3.16) were compared to those taken in the absence of *N,N*-dimethylaniline (Figure 3.14). Figure 3.15 shows the transient spectrum of **3.2t** in the presence of 1×10^{-4} M *N,N*-dimethylaniline. The decay of **3.2a** triplet state is much faster in the presence of the electron donor (3.2 microseconds compared to 33.0 microseconds). This decay is accompanied by an increase in absorbance at 480 nm. Increasing the concentration of *N,N*-dimethylaniline to 0.1 M results in even faster decay of the triplet state absorption of **3.2a**, so fast that is not observed on the nanosecond timescale. This is accompanied by a faster increase in absorption at 480 nm. From this data, I have concluded that the radical anion of **3.2a** has a characteristic absorption with a λ_{max} at 480 nm.

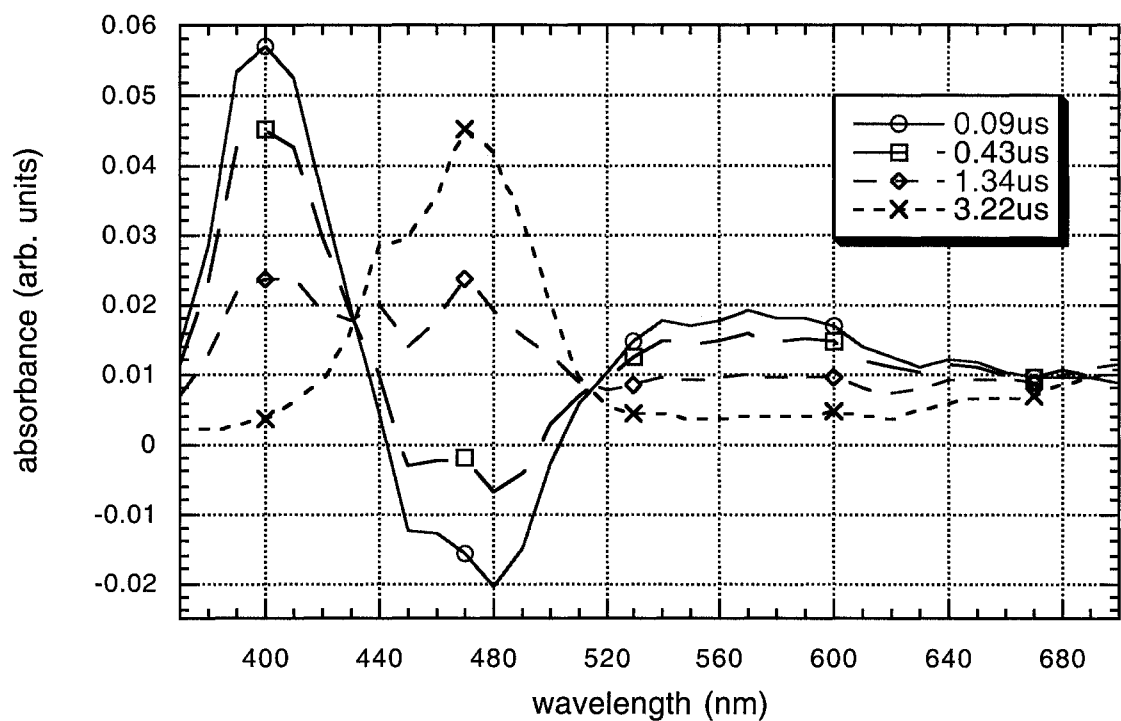


Figure 3.15. Transient absorption spectra of **3.2t** + 0.1 mM *N,N*-dimethylaniline after irradiation at 355 nm. Spectra were performed on 1×10^{-4} M 2:1 acetonitrile:water solutions of **3.2t** purged with nitrogen gas.

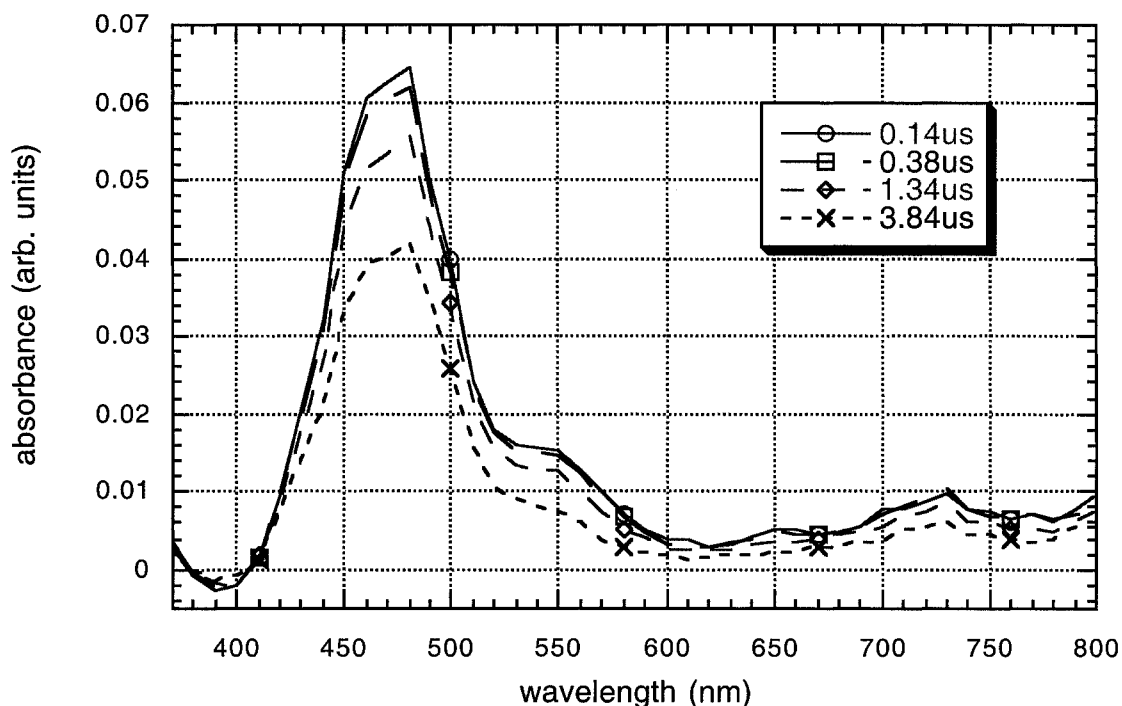


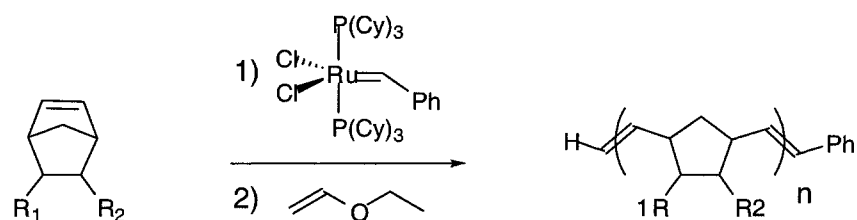
Figure 3.16. Transient absorption spectra of **3.2t** + 0.1 M *N,N*-dimethylaniline after irradiation at 355 nm. Spectra were performed on 1×10^{-4} M 2:1 acetonitrile:water solutions of **3.2t** purged with nitrogen gas.

The next task is to characterize the radical cation of **3.3**, therefore we attempted to photoionize **3.3** with 355 nm light in different solvents. As time was running short at this point, no transient spectrum was obtained of **3.3** radical cation. Since then, no new information has come to light regarding this system. The next step in our studies will be characterization of each of the radical cation of **3.3** and the radical anion of **3.2a** using spectrophotoelectrochemistry, which involves the electrochemical oxidation or reduction,

respectively, of each of the species followed by UV-vis spectroscopy measurement of the resulting oxidized/reduced species. This will confirm the absorption of the **3.2a** radical anion, as observed using transient absorption spectroscopy, and characterize the absorption of **3.3** radical cation. Once these species are characterized, femtosecond transient absorption spectroscopy will be performed in order to detect the radical cation/anion pair in a solution of irradiated hybrid system **3.3:3.2a**.

3.6 - Polymeric Porphyrinic Phenoxynaphthacenequinone Hybrids

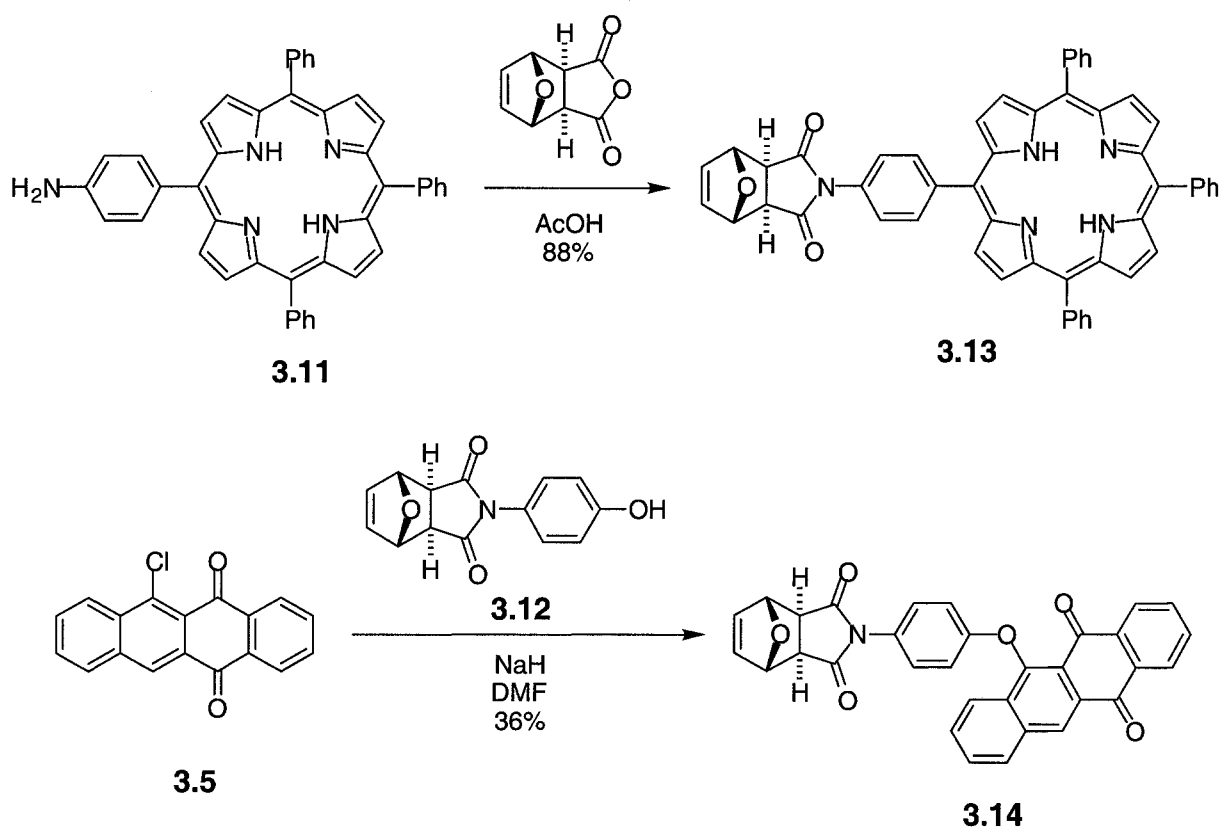
As was discussed in detail in Chapter 2, application of photochromic systems in molecular photonic devices will require the systems to be in a polymeric rather than monomeric form. This concept led me to investigate the PET regulation of porphyrinic phenoxynaphthacenequinone copolymers. From my work on photochromic polymers of dithienylethenes in Chapter 2, Ring Opening Metathesis Polymerization (ROMP) was chosen as the ideal polymerization method due to its mild reaction conditions, functional group compatibility and control over polymer chain length. ROMP involves the living polymerization of strained bicyclic olefins by ring opening the strained double bond using bis(tricyclohexylphosphine)benzylidene ruthenium(IV)dichloride catalyst (Grubbs' catalyst) (Scheme 3.10).



Scheme 3.10

3.6.1 – Synthesis on Monomers

In order to link PNQ's and porphyrins within a copolymer using ROMP, the strained bicyclic olefin derivatives of both a PNQ and a porphyrin must be synthesized. The strained bicyclic olefin porphyrin derivative **3.13** was synthesized in good yield in one step by simply stirring the aminoporphyrin **3.11**¹⁹ and oxonorbornene anhydride²⁵ in acetic acid at room temperature (Scheme 3.11). The ¹H NMR spectrum of the resulting porphyrin showed the disappearance of the amino protons of the starting material as well as the characteristic peaks for the appended strained bicyclic olefin unit. The strained bicyclic olefin PNQ derivative **2.14** was synthesized in low yield from chloronaphthacenequinone **3.5** and phenoxy-imido-oxonorbornene **3.12** using sodium hydride as the base in anhydrous DMF at 110°C (Scheme 3.11). This monomer is also identified by presence of the characteristic oxonorbornene peaks in the ¹H NMR spectrum. Both monomers were also characterized by elemental analysis.



Scheme 3.11

3.6.2 – Synthesis of Copolymers

From monomers **3.13** and **3.14**, three copolymers were synthesized with a 4:1 (**3.P1**), 1:1 (**3.P2**), and 1:4 (**3.P3**) ratio of porphyrin **3.13** to PNQ monomer **3.14** respectively (Scheme 3.12). ROMP was carried out by cannulation of a CH_2Cl_2 solution of Grubb's catalyst into a CH_2Cl_2 solution of the appropriate mixture of monomers described above, with a total concentration of monomer of 0.2 M. The catalyst to monomer stoichiometry in all cases was

2% to yield polymers with total chains lengths of 50 monomer units. Termination was carried out by addition of excess ethyl vinyl ether and the polymers were precipitated out by addition of diethyl ether. This type of polymer is technically termed a random copolymer, in which the order of repeating units is random, as long as the rate of polymerization of both monomers is identical.

The resulting copolymers were all soluble in chloroform and dichloromethane, but were insoluble all other solvents available in our lab (tetrahydrofuran, acetonitrile, dimethylsulfoxide, dimethylformamide, dichloroethane, toluene, carbon tetrachloride, dimethoxyethane). GPC analysis has not yet been performed on these copolymers, therefore polymer chain lengths cannot be reported with confidence. The catalyst to substrate stoichiometry suggests a 50 mer is formed in all cases, and therefore this is assumed in scheme 3.12. Also, the relative values of m and n in scheme 3.12 are assigned from the relative amount of each monomer added to the polymerization reaction should not be read as absolute values.

porphyrin:PNQ. The intensity of the broadened peaks are high in the regions corresponding to the PNQ subunits in **3.P3**, as it contains a 4:1 mixture of PNQ:porphyrin. The ^1H NMR spectrum of **3.P2** shows intermediate intensities of the broadened peaks relative to **3.P1** and **3.P3**. These results, along with the high yield of polymerization, suggest that each polymer contains the expected concentration of porphyrin and PNQ subunit.

3.6.3 – UV-vis Absorption Spectroscopy

UV-vis absorption experiments were performed to assess the photochromism of the PNQ unit within the porphyrinic PNQ copolymer. A CH_2Cl_2 solution of each copolymer was prepared in which the concentration of porphyrin subunit is 10^{-5} M. Upon irradiation of each of the solutions with 365 nm light, an increase in absorbance at 450 and 480 nm corresponding to the *ana*-form of PNQ was observed (Figure 3.17). Irradiation with broad band light > 434 nm results in the original spectrum, confirming the reversibility of this photoisomerization reaction. Isobestic points at 258 and 276 nm indicate clean photoisomerization between the *trans*- and *ana*-forms.

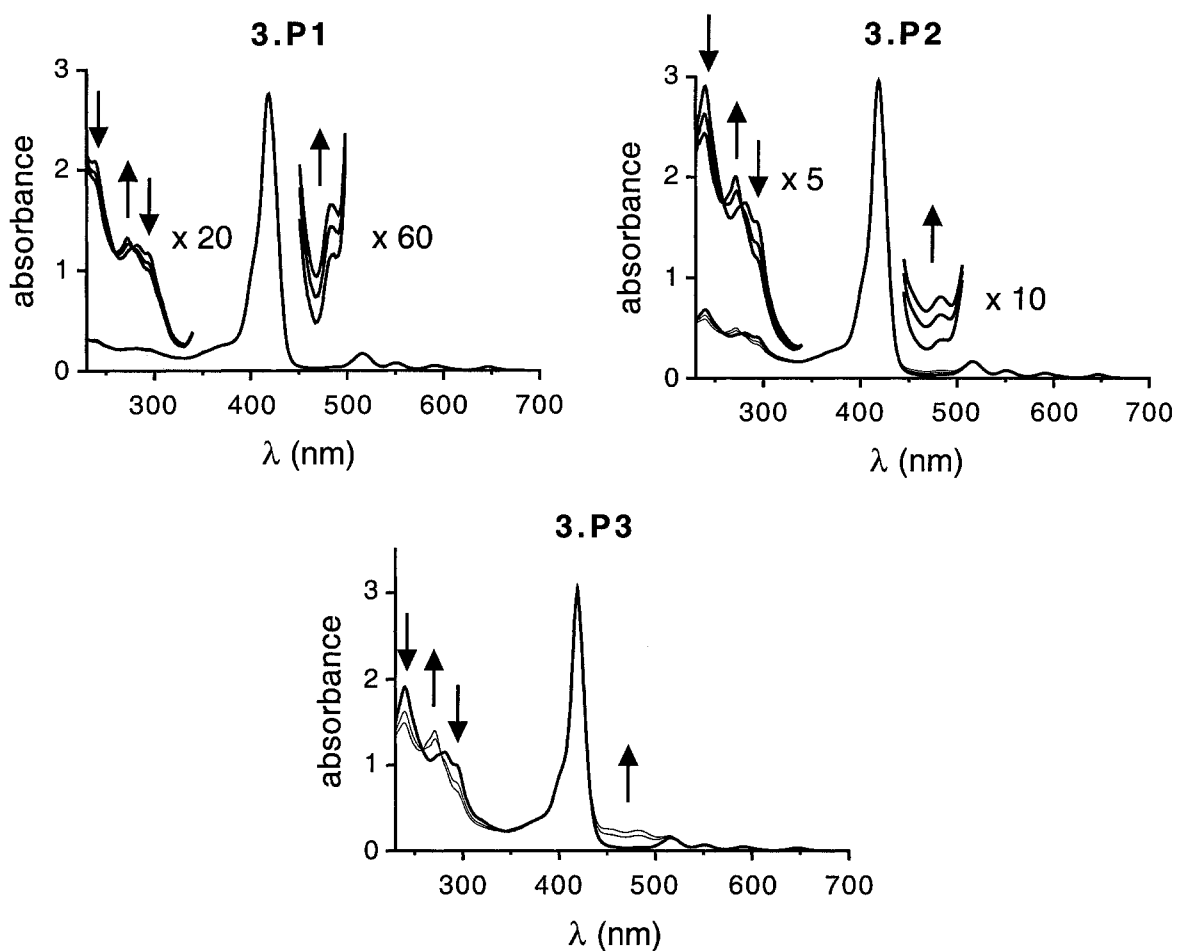


Figure 3.17. UV-vis spectra of copolymers **3.P1-3.P3**. All spectra were performed using 10^{-5} M CH_2Cl_2 solutions with respect to the porphyrin unit. Irradiation times in all graphs: 0, 60, and 120 seconds.

The photoisomerization of the PNQ subunit within the porphyrinic PNQ copolymer is surprising as the two components are linked via a covalent network, albeit a very long one. As illustrated earlier in this chapter, covalent porphyrinic PNQ's **3.1**, **3.9**, and **3.10** showed no photoisomerization. This suggests that the two chromophores are sufficiently removed from each other within the copolymer matrix that the porphyrin does not inhibit the

photoisomerization reaction of PNQ. The relative intensities of the absorbances corresponding to each of the subunits in the copolymer match the relative concentrations of each subunit within the copolymer. The absorbance increase at 450 and 480 nm is very small in **3.P1**, larger in **3.P2**, and largest in **3.P3**. This provides further evidence that the copolymers contain the expected ratios of subunits.

3.6.4 – Regulation of PET

The goal of this project is to develop a polymeric material in which PET can be regulated with light. UV-vis studies show that the chromophores are far enough apart to allow photoisomerization of the PNQ photochrome. Luminescence spectroscopy will tell us whether the chromophores are close enough to allow PET between the two chromophores. It was found in the hydrogen bonded system, using PNQ carboxylate **3.2** and porphyrin urea **3.3**, that the emission intensity of the porphyrin decreased upon photoisomerization of the *trans*-form to the *ana*-form, attributed to the more efficient PET between the porphyrin and the *ana*-form of PNQ. Similarly, PET regulation of copolymers **3.P1-3.P3** was evaluated by monitoring the emission intensity of the porphyrin upon photoisomerization of the PNQ subunit from its *trans*- to *ana*-form.

The same solutions and irradiation times were used for the emission studies of the copolymers as were used for the UV-vis absorption studies. Upon irradiation of each copolymer at 365 nm, the emission of the porphyrin at 650 nm decreases, suggesting an increase in PET between the porphyrin and the *ana*-form of the PNQ subunit within all three copolymers.

Upon irradiation with broad band light > 434 nm, the original emission spectrum is obtained, confirming the reversibility of this effect. As the concentration of the PNQ units increases in the copolymers, a more dramatic change in the emission spectrum is observed. This follows the trend of increased quencher present results in more emission quenching, as expected.

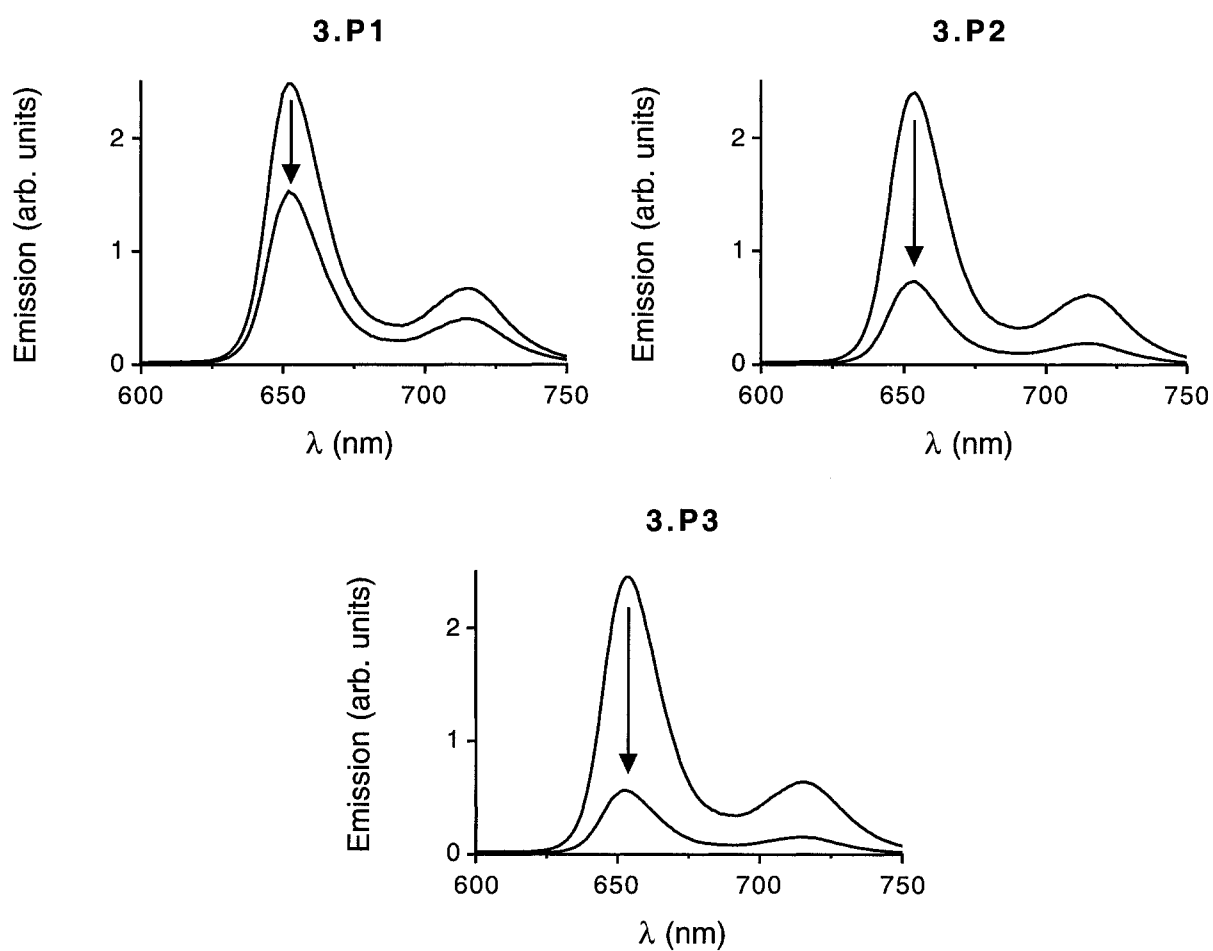


Figure 3.18. Emission spectral changes upon irradiation of the *trans*-PNQ units in polymers **3.P1**, **3.P2**, and **3.P3** with 365 nm light for 120 seconds. All spectra were performed using 10^{-5} M CH_2Cl_2 solutions with respect to the porphyrin unit. Excitation of the porphyrin unit is accomplished using 560 nm light.

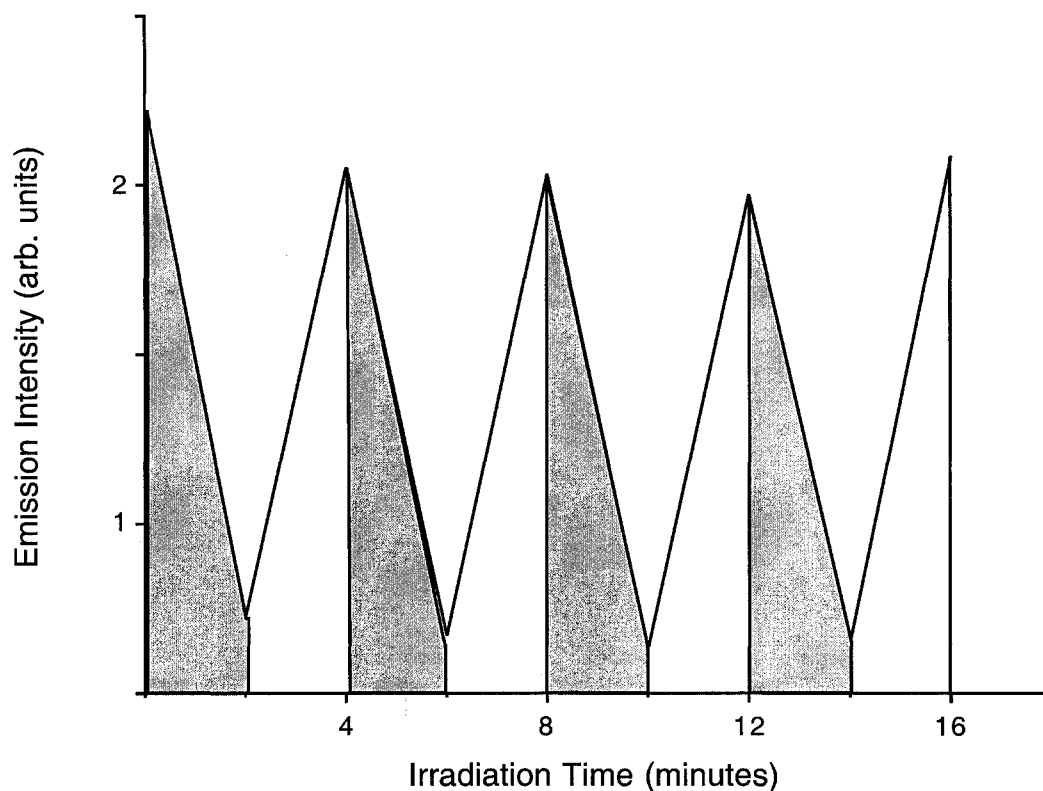


Figure 3.19. Toggling between the *trans*- and *ana*-forms of the PNQ unit results in reversible change in the emission of the porphyrin unit in copolymer **3.P2**. Cycling is shown with 365 nm (shaded area) and > 434 nm light. The experiment is performed using 10^{-5} M CH_2Cl_2 solutions with respect to the porphyrin unit. Excitation of the porphyrin unit is accomplished using 560 nm light. Thus, irradiation with 365 nm for 2 minutes results in a decrease in emission intensity, and subsequent irradiation with > 434 nm results in an increase in emission intensity.

Figure 3.19 shows a cycling experiment in which the emission of the **3.P2** solution is monitored upon alternate irradiation with 365 nm and > 434 nm light. The emission of the porphyrin chromophore is effectively regulated by toggling between the *trans*- and *ana*-form of the PNQ subunit, attributed to the change in PET between the porphyrin and each form of

the PNQ photochrome. This is an example of a photochromic copolymer that achieves photo-regulation of PET.

3.7 - Concluding Remarks

Photoisomerization between the *trans*- and *ana*-form of PNQ results in a change in the electronic properties of the photochrome. Cyclic voltammetry indicates that the *ana*-form is a better electron acceptor than the *trans*-form. Three porphyrinic PNQ hybrid systems have been presented, all in the pursuit of photo-regulating PET between the porphyrin and PNQ by toggling between the poor *trans*-form electron acceptor and the better *ana*-form electron acceptor. The original covalent hybrid **3.1** showed an inhibition of photoisomerization, attributed to the intimacy between the porphyrin and PNQ. The possible mechanisms of this inhibition were presented, however no conclusive studies have been performed to date.

The inhibition of photoisomerization of covalent hybrid **3.1** is circumvented by using a dynamic, non-covalent hybrid **3.2:3.3**, in which strong hydrogen bonds join the porphyrin and the PNQ units. In this system, photoisomerization occurs and photo-regulation of PET is proven by monitoring the emission properties of the porphyrin chromophore. Upon photoisomerization of the PNQ from the *trans*- to *ana*-form, the emission of the hydrogen

bonded porphyrin chromophore decreases, which is attributed to the increase in PET between the porphyrin and the *ana*-PNQ.

The third hybrid system presented was a porphyrinic PNQ copolymer synthesized using ROMP. Solution studies on this copolymer indicate photoisomerization is allowed, even though the two chromophores are associated within a covalent network. Upon photoisomerization from the *trans*- to *ana*-form, the emission of the porphyrin decreases, again attributed to the increase in PET between the porphyrin and the *ana*-form of PNQ. This process is reversible, therefore allowing the reversible regulation of PET via photoisomerization of the PNQ photochrome.

The work presented in the chapter illustrates the usefulness of phenoxynaphthacenequinone as a photo-regulated molecular switch for potential applications in all-photon mode molecular devices. Several projects involving the change in electronics between the two forms, as well as other ways to exploit this well behaved photochrome, are currently underway.

3.8 – Experimental

General: All solvents for synthesis were purchases from Caledon Laboratories Limited. THF and diethyl ether were distilled over sodium/benzophenone, hexane was distilled over potassium/benzophenone, and CH₂Cl₂ was distilled over calcium hydride before use. All other solvents were used as received. Solvents for NMR analysis were purchased from Cambridge Isotope Laboratories and used as received. Column chromatography was performed using silica gel 60 (230-400 mesh) from Silicycle Inc. Bis(tricyclohexylphosphine)benzylidene ruthenium(IV)dichloride (Grubbs's catalyst) was purchased from Strem Chemical Company and was stored and weighed in a glove box under a nitrogen atmosphere. All other reagents and starting materials were purchased from Aldrich. 7-Oxa-bicyclo[2.2.1]hept-5-ene-2,3-dicarboxylic anhydride,²⁵ hydroxy-keto-acid **3.4**,^{1 2} chloronaphthacenequinone **3.5**,¹² phenoxynaphthacenequinone **3.6**,¹³ hydroxyporphyrin **3.8**,¹⁶ and amino porphyrin **3.11**¹⁹ were prepared as described in the literature.

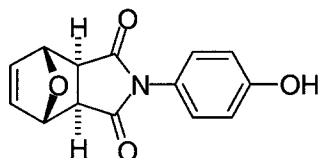
¹H NMR characterizations were performed on a Varian Inova-300 or Bruker AMX 400 instrument. ¹³C NMR characterizations were performed on a Bruker 300 or Bruker AMX 400 instrument. Chemical shifts (δ) are reported in parts per million relative to tetramethylsilane using the residual solvent peak as a reference standard. Coupling constants (J) are reported in Hertz. The number of ¹³C NMR resonances of several compounds do not equal the number of different carbons in the molecule. This is especially true for the porphyrinic compounds.

Porphyrins contain several consecutive quaternary carbons, which show very weak signals due to longer relaxation times and poor NOE's to ^1H atoms. This problem may be circumvented by increasing the concentration of the sample and by increasing the acquisition time.²⁶

FT-IR measurements were performed using a Nicolet Magna-IR 750 or a Nexus 670 instrument and values are reported in cm^{-1} . UV-vis measurements were performed using a Pharmacia Biotech Ultraspec 3000 or a Varian Cary 300 Bio spectrophotometer. UV irradiation was performed using a hand-held UV lamp operating at $420 \mu\text{W}/\text{cm}^2$ for 254 nm and $350 \mu\text{W}/\text{cm}^2$ for 365 nm irradiation. Irradiation with visible light was performed using the light of a 150-W tungsten source that was passed through a 434 nm cutoff filter to eliminate higher energy light. Fluorescence measurements were performed using a PTI C60 photon counting spectrofluorometer. Cyclic voltametry measurements were performed in CH_2Cl_2 using a PINE bipotentiostat, a glassy carbon working electrode, a platinum counter electrode and a silver reference electrode, and tetrabutyl ammonium hexafluorophosphate as the electrolyte. All cyclic voltamograms were referenced to the ferrocenium redox couple.

The photostationary state of **3.2a** (*ana-3.2*) was determined by ^1H NMR spectroscopy. A 6.54 mM solution of **3.2t** (*trans-3.2*) in CD_2Cl_2 was transferred to a quartz NMR tube and irradiated with 365 nm light for 20 minutes. The doublet at δ 6.8, corresponding to the *ortho*-phenoxy protons of **3.2t**, decreases which is accompanied by an increase in a doublet at δ 6.9, corresponding to the *ortho*-phenoxy protons of **3.2a**. After the 20 minutes of irradiation, no

further change in the ^1H NMR spectrum is observed. Integration of both doublets gives a 4:1 ratio of the **3.2a** doublet to the **3.2t** doublet. This translates into a photostationary state of **3.2** upon irradiation with 365 nm light of 80% **3.2a**.

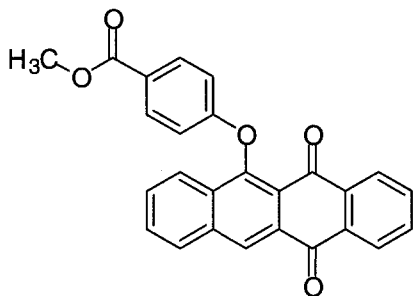


Synthesis of *exo*-N-(*p*-hydroxyphenyl)-3,6-epoxy-4-cyclohexene-1,2-dicarboximide (3.12**).**

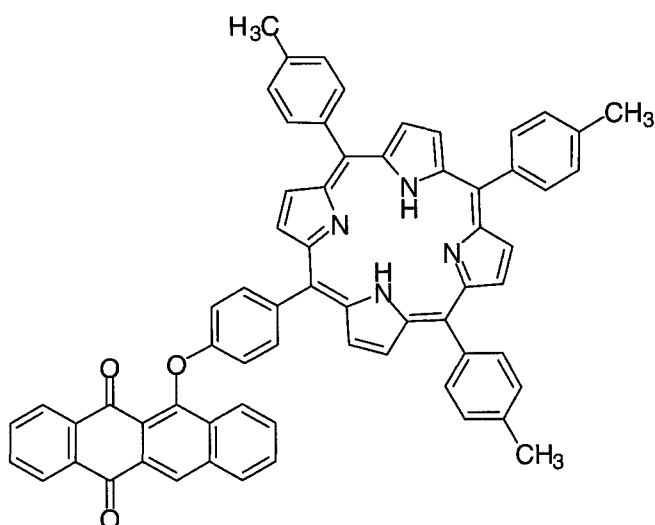
A mixture of 7-oxa-bicyclo[2.2.1]hept-5-ene-2,3-dicarboxylic anhydride (2.0 g, 12 mmol), *p*-aminophenol (1.31 g, 12 mmol) and glacial acetic acid (3 mL) were heated at reflux for 10 min after which time a precipitate formed. The heating source was removed and the reaction mixture was allowed to cool to room temperature. The precipitate was collected by vacuum filtration, washed with water and dried *in vacuo* to afford 2.10 g (68%) of **6** as a white solid. Mp = 188–189 °C. ^1H NMR (300 MHz, DMSO- d_6) δ 9.71 (s, 1H), 6.95 (d, $J = 9$ Hz, 2H), 6.83 (d, $J = 9$ Hz, 2H), 6.58 (s, 2H), 5.21 (s, 2H), 3.02 (s, 2H). ^{13}C NMR (75.49 MHz, DMSO- d_6) δ 175.95, 157.27, 136.53, 127.98, 123.19, 115.38, 80.66, 47.20; FTIR 3334, 3143, 3102, 3076, 3049, 3029, 2973, 1775, 1697, 1612, 1594, 1516, 1448, 1402, 1273, 1223, 1191, 1162, 1149, 1015, 915, 875, 855, 846, 809; MS (EI): $m/z = 257$ $[\text{M}]^+$, 189 $[\text{M}-\text{C}_4\text{H}_4\text{O}]^+$.

General synthesis of PNQ's **3.1, **3.7**, **3.14**.** A mixture of a specific phenoxy compound (1.4 eq.) and K_2CO_3 or NaH (1.4 eq.) in dry DMF was treated with chloronaphthacenequinone **3.5** (1 eq.) and heated at 110°C for 16 h. The heat source was removed, the reaction mixture was

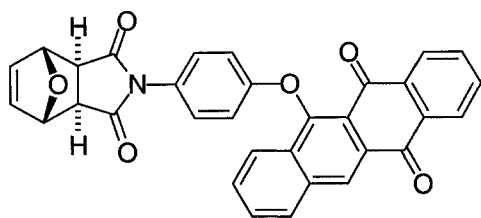
poured onto ice water and the crude product was collected by vacuum filtration. Purification by column chromatography through silica affords the pure product.



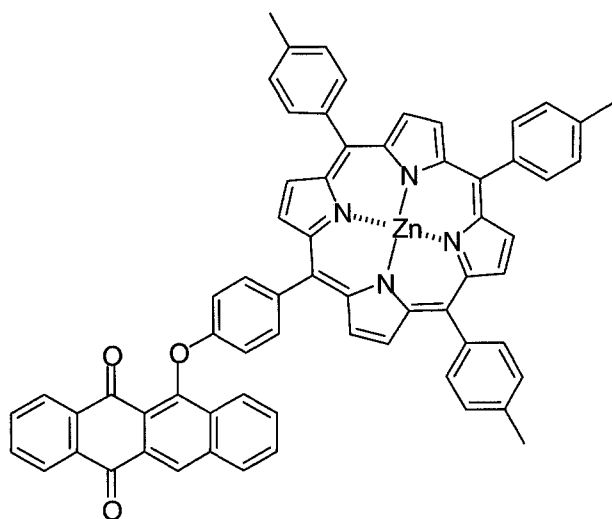
Methyl Ester 3.7. A mixture of methyl 4-hydroxybenzoate (152 mg, 1.0 mmol) and K_2CO_3 (124 mg, 0.9 mmol) in dry DMF (3 mL) was treated with chloronaphthacenequinone **3.5** (200 mg, 0.68 mmol). Purification by column chromatography through silica ($CHCl_3$) afforded 200 mg (72%) of ester **3.7** as an orange solid. Mp = 257-258 °C. 1H NMR(300 MHz, $CDCl_3$) δ 8.89 (s, 1H), 8.36-8.33 (m, 1H), 8.21-8.17 (m, 1H), 8.16 (d, $J = 9.0$ Hz, 2H), 7.97 (d, $J=9.0$ Hz, 2H), 7.79-7.63 (m, 4H), 6.90 (d, $J=9.0$ Hz, 2H), 3.85 (s, 1H). ^{13}C NMR ($CDCl_3$) δ (23 of 24 signals were observed) 182.72, 181.16, 166.61, 162.72, 151.53, 136.15, 135.34, 134.48, 133.92, 133.56, 131.96, 131.26, 130.73, 130.49, 130.38, 130.23, 127.69, 127.19, 124.62, 124.23, 120.83, 114.83, 51.99. FTIR (KBr-cast) 3067, 2950, 1715, 1676, 1652, 1615, 1604, 1583, 1505, 1433, 1398, 1367, 1345, 1275, 1235, 1165, 1108, 1050, 1032, 1012, 986, 920, 850, 767, 754, 717, 703, 585. EIMS (m/z): 408 (M+), 377 (M-OCH₃).



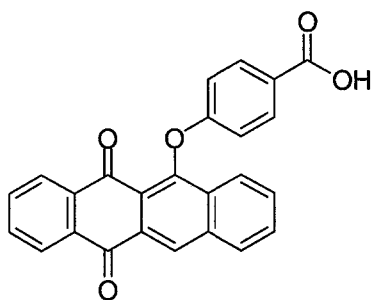
Porphyrin-PNQ Hybrid 3.1. A mixture of hydroxy-porphyrin **3.8** (205 mg, .0.305 mmol) and NaH (15 mg, 0.305 mmol) in dry DMF (5 mL) was treated with chloronaphthacenequinone **3.5** (64 mg, 0.218 mmol). Purification by column chromatography through silica (1:1 CH₂Cl₂:Hexanes) afforded 117 mg (58%) of the product as an purple solid. Mp = >300 °C. ¹H NMR (400 MHz, CD₂Cl₂) δ 8.95 (s, 1H), 8.92-8.85 (m, 8H), 8.60-8.56 (m, 1H), 8.41-8.36 (m, 2H), 8.28-8.25 (m, 1H), 8.12 (d, *J* = 8.4 Hz, 2H), 8.08 (d, *J* = 7.6 Hz, 6H), 7.90-7.83 (m, 4H), 7.57 (d, *J* = 7.6 Hz, 6H), 7.29 (d, *J* = 8.4 Hz, 2H), 2.70 (s, 9H), -2.88 (s, 2H). ¹³C NMR (125.70 MHz, CD₂Cl₂) δ (30 of 43 signals were observed) 183.12, 181.67, 159.56, 152.84, 139.54, 137.96, 136.71, 136.31, 136.15, 136.06, 134.90, 134.87, 134.19, 134.05, 132.16, 131.36, 130.86, 130.68, 130.54, 127.87, 127.83, 127.63, 127.36, 125.35, 121.67, 120.61, 119.77, 113.95, 95.20, 21.63. FTIR (KBr-cast) 3317, 3022, 2920, 1676, 1616, 1596, 1582, 1561, 1502, 1472, 1429, 1397, 1364, 1344, 1304, 1272, 1232, 1214, 1182, 1170, 1107, 1051, 1023, 984, 966, 919, 879, 837, 800, 753, 732, 716, 665. ESMS (+ive): *m/z* = 929.3 [M+H]⁺. Anal. Calcd for C₆₅H₄₄N₄O₃: C, 84.03; H, 4.77; N, 6.03. Found: C, 83.72; H, 4.77; N, 6.30.



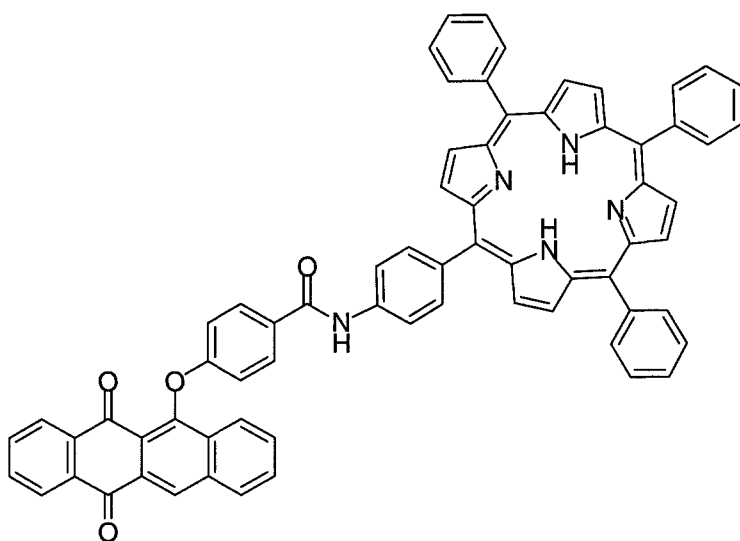
Oxonorbornene PNQ 3.14. A mixture of phenoxy-oxonorbornene **3.12** (933 mg, 3.63 mmol) and NaH (87 mg, 3.63 mmol) in dry DMF (3 mL) was treated with chloronaphthacenequinone **3.5** (690 mg, 2.36 mmol). Purification by column chromatography through silica (3% methanol/ CHCl_3) afforded 432 mg (36%) of pure product as a yellow solid. Mp = 265-267°C. ^1H NMR (400 MHz, CDCl_3) δ 8.89 (s, 1H), 8.36-8.34 (m, 1H), 8.25-8.14 (m, 3H), 7.80-7.73 (m, 3H), 7.70-7.66 (m, 1H), 7.20 (d, $J = 9.2$ Hz, 2H), 6.96 (d, $J = 9.2$ Hz, 2H), 6.55 (s, 2H), 5.37 (s, 2H), 2.98 (s, 2H). ^{13}C NMR (125.70 MHz, CDCl_3) δ (24 of 26 signals were observed) 180.92, 175.42, 158.83, 136.67, 136.00, 135.31, 134.42, 133.75, 133.43, 131.38, 130.64, 130.32, 130.24, 130.13, 127.87, 127.70, 127.50, 127.06, 125.66, 124.86, 120.88, 115.51, 81.37, 47.40. FTIR (KBr-cast) 3060, 3013, 2957, 2926, 2849, 1706, 1672, 1577, 1495, 1426, 1392, 1340, 1275, 1236, 1215, 1185, 1167, 1047, 1016, 986, 939, 917, 878, 805, 754, 715, 641. Anal. Calcd for $\text{C}_{32}\text{H}_{19}\text{NO}_6$: C, 74.85; H, 3.73; N, 2.73. Found: C, 74.51; H, 3.66; N, 2.99.



Zn-porphyrin-PNQ 3.9. To a CH_2Cl_2 solution (9 mL) of porphyrin-PNQ **3.1** (77 mg, 0.083 mmol) was added a methanolic solution (1 mL) of $\text{Zn}(\text{OAc})_2$ (18 mg, 0.083 mmol). The mixture was heated at reflux for 1 h, after which the solvents were removed *in vacuo*. The crude solid was triturated with methanol (5 mL) the precipitate was vacuum filtered to afford 88 mg (89%) of pure product as a purple solid. Mp = >300 °C. ^1H NMR (400 MHz, CD_2Cl_2) δ 8.99-8.91 (m, 8H), 8.77 (s, 1H), 8.57-8.55 (m, 1H), 8.34 (d, $J=7.2$ Hz, 1H), 8.23-8.19 (m, 2H), 8.10-8.06 (m, 8H), 7.87-7.77 (m, 4H), 7.57 (d, $J=7.6$ Hz, 6H), 7.25 (d, $J=8.4$ Hz, 2H), 2.70 (s, 9H). ^{13}C NMR (125.70 MHz, CDCl_3) δ (27 of 43 signals were observed) 182.83, 181.27, 152.66, 150.29, 139.87, 137.03, 136.65, 136.12, 135.50, 134.41, 133.67, 133.41, 131.90, 131.76, 130.66, 130.45, 130.32, 130.20, 130.07, 127.58, 127.26, 127.04, 125.10, 121.08, 121.00, 113.28, 21.50. FTIR (KBr-cast) 3116, 3030, 2918, 2849, 1668, 1495, 1426, 1404, 1336, 1305, 1271, 1232, 1206, 1167, 1107, 999, 982, 922, 840, 801, 745, 715. Anal. Calcd for $\text{C}_{65}\text{H}_{42}\text{N}_4\text{O}_3\text{Zn}$: C, 78.66; H, 4.26; N, 5.64. Found: C, 79.01; H, 4.18; N, 5.49.

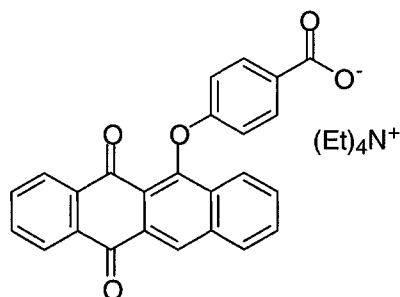


Carboxylic Acid 3.8. A solution of methyl ester **3.7** (108 mg, 0.26 mmol) in 1,4-dioxane (5 mL) was treated with 10% aqueous NaOH (3 mL) and heated at reflux for 1 h. The heat source was removed, the reaction mixture was allowed to cool to room temperature, after which it was acidified with concentrated HCl. The product was collected by filtration, washed with cold CHCl_3 (1 mL) and dried *in vacuo* to afford 81 mg (78%) of the product as a orange solid. $\text{Mp} = >300\text{ }^\circ\text{C}$. $^1\text{H NMR}$ (300 MHz, $\text{DMSO-}d_6$) δ 8.93 (s, 1H), 8.44 (d, $J=9.0\text{Hz}$, 1H), 8.28-8.25 (m, 1H), 8.11-8.06 (m, 2H), 7.92-7.76 (m, 6H), 6.99 (d, $J=9.0\text{Hz}$, 2H). $^{13}\text{C NMR}$ (75.47 MHz, $\text{DMSO-}d_6$) δ (23 of 23 signals were observed) 182.02, 180.53, 166.75, 162.01, 150.25, 135.66, 134.82, 134.68, 134.19, 133.11, 131.50, 130.72, 130.59, 130.52, 130.46, 130.19, 127.07, 126.89, 126.60, 124.49, 123.64, 120.91, 114.90. FTIR (KBr-cast) 3600-2600 (br, OH), 3067, 1671, 1615, 1605, 1594, 1581, 1504, 1457, 1429, 1389, 1348, 1321, 1281, 1246, 1168, 1114, 1066, 1050, 1039, 1027, 1015, 985, 944, 917, 910, 853, 816, 802, 782, 755, 716, 650, 586. ESMS (-ive): $m/z = 393.0$ (M-H).



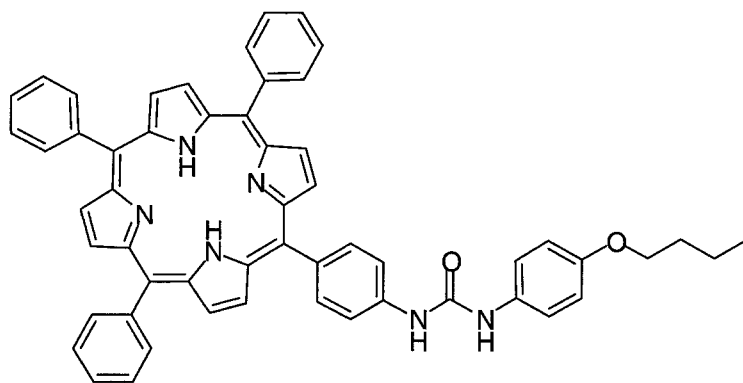
Amido-Porphyrinic-PNQ 3.10. A SOCl_2 solution (1 mL) of carboxylic acid **3.8** (20 mg, 0.051 mmol) was heated at reflux for 1 h. The heating source was removed and the mixture was allowed to cool to room temperature over 30 min. The solvent was removed *in vacuo* and the crude acid chloride mixture was redissolved in anhydrous CH_2Cl_2 (2 mL) under an Ar atmosphere. To this stirred solution was added triethyl amine (10 mg, 0.1 mmol) followed by amino porphyrin **3.11**. After 10 min stirring at room temperature, the solvent was removed *in vacuo*. Purification by column chromatography through silica (CHCl_3) afforded 20 mg (40%) of pure product as a purple solid. Mp = >300 °C. ^1H NMR (400 MHz, CDCl_3) δ 8.94 (s, 1H), 8.89-8.84 (m, 8H), 8.39-8.37 (m, 1H), 8.28-8.18 (m, 13H), 8.09 (s, 1H), 8.15 (dd, $J=8.8$ Hz, $J=2.4$ Hz, 6H), 7.83-7.72 (m, 17H), 7.08 (d, $J=9.2$ Hz, 2H), -2.78 (s, 2H). ^{13}C NMR (125.70 MHz, CDCl_3) δ (24 of 46 signals were observed) 142.49, 138.59, 138.09, 136.46, 135.51, 134.86, 134.79, 134.26, 133.84, 132.80, 131.57, 130.81, 130.73, 130.58, 129.65, 128.02, 128.08, 127.51, 126.98, 124.89, 122.96, 120.45, 118.64, 115.64, . FTIR (KBr-cast) 3319,

3103, 3052, 3026, 2896, 1676, 1598, 1495, 1443, 1400, 1344, 1314, 1280, 1228, 1172, 1068, 1047, 982, 969, 917, 857, 800, 758, 719, 697. ESMS (+ive): $m/z = 1006.3 [M+H]^+$.



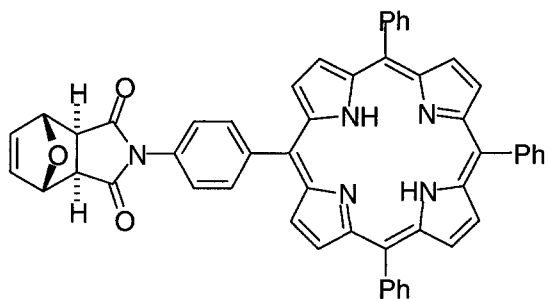
Tetraethyl ammonium carboxylate 3.2. A solution of the carboxylic acid **3.8** (39.4 mg, 0.1 mmol) in methanol (1.0 mL) was treated with a 0.1M methanolic solution of tetraethylammonium hydroxide (1ml) and was stirred at room temperature for 16 h. The solvent was evaporated *in vacuo*, redissolved in a minimal amount of methanol, and precipitated by adding diethyl ether. The product was collected by filtration and dried *in vacuo* to afford 33 mg (62%) of tetraethylammonium carboxylate salt **3.2** as a pale yellow solid. Mp = 232-233°C. ¹H NMR (300 MHz, CD₂Cl₂) δ 8.86 (s, 1H), 8.34-8.31 (m, 1H), 8.24-8.16 (m, 3H), 7.90 (d, $J = 9.0$ Hz, 2H), 7.80-7.72 (m, 3H), 7.66 (t, $J = 7.2$ Hz, 1H), 6.76 (d, $J = 9.0$ Hz, 2H), 3.28 (q, $J = 7.2$ Hz, 8H), 1.28 (t, $J = 7.2$ Hz, 12H). ¹³C NMR (75.47 MHz, DMSO-*d*₆) δ (23 of 25 signals were observed) 181.65, 181.12, 179.91, 166.93, 158.30, 150.98, 135.68, 135.13, 134.48, 134.12, 133.49, 132.60, 130.23, 130.10, 129.88, 129.73, 126.37, 126.01, 123.58, 120.63, 112.53, 50.86, 6.53. FTIR (KBr-cast) 3080, 2924, 1733, 1674, 1596, 1581, 1561, 1493, 1431, 1396, 1362, 1344, 1276, 1265, 1235, 1163, 1077, 1049, 1002, 984,

915, 786, 752, 715, 702. ESMS (-ive): 916 ($M^+ + N(Et)_4 + M^-$), 809 ($M^+ + Na + M^-$), 393 (M^-), 273 ($M - C_6H_4CO_2$).



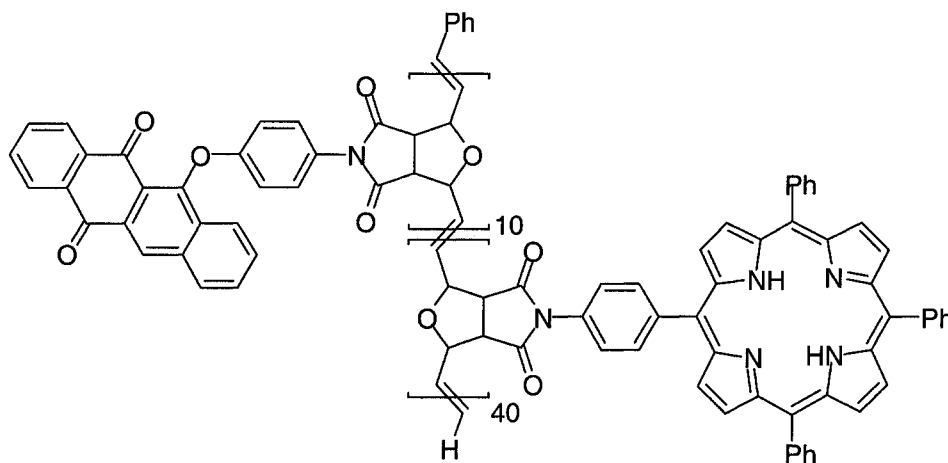
Porphyrin urea 3.3. A solution of 5-(4-aminophenyl)10,15,20-(triphenyl)porphyrin **3.11** (40 mg, 0.06 mmol) in CH_2Cl_2 (4 mL) under argon was treated with 4-butoxyphenylisocyanate (20 mg, 0.1 mmol). After heating at reflux for 2 h, the heating source was removed, the reaction mixture was allowed to cool to room temperature and the reaction mixture was concentrated to dryness *in vacuo*. Purification by column chromatography through silica (1% $CH_3OH/CHCl_3$) followed by recrystallization from CH_2Cl_2 /Hexanes afforded 37 mg (71%) of pure product as a purple solid. Mp = >300 °C. 1H NMR (300 MHz, CD_2Cl_2) δ 8.92-8.85 (m, 8H), 8.23-8.20 (m, 6H), 8.15 (d, $J = 9.0$ Hz, 2H), 7.81-7.74 (m, 11H), 7.40 (d, $J = 9.0$ Hz, 2H), 6.97 (d, $J = 9.0$ Hz, 2H), 6.89 (s, 1H), 6.56 (s, 1H), 4.00 (t, $J = 6.0$ Hz, 2H), 1.78 (p, $J = 6.0$ Hz, 2H), 1.62-1.47 (m, 2H), 0.99 (t, $J = 6.0$ Hz, 3H), -3.56 (s, 2H). ^{13}C NMR (75.47 MHz, CD_2Cl_2) δ (22 of 32 signals were observed) 157.30, 153.92, 142.46, 138.92, 137.34, 135.55, 134.91, 131.44, 130.74, 128.10, 127.12, 127.08, 125.00, 120.58, 120.53, 120.23, 118.43, 115.59, 68.48, 31.73, 19.61, 14.00. FTIR (KBr-cast) 3318, 3056, 2957, 2929, 2870, 1651, 1596, 1546, 1509, 1472,

1441, 1401, 1350, 1312, 1291, 1230, 1180, 1112, 1072, 1032, 1002, 980, 966, 828, 800, 731, 701. ESMS (+ive): 821 (M+H). Anal. Calcd for C₅₅H₄₄N₆O₂: C, 80.46; H, 5.40; N, 10.24. Found: C, 80.51; H, 5.43; N, 10.12.

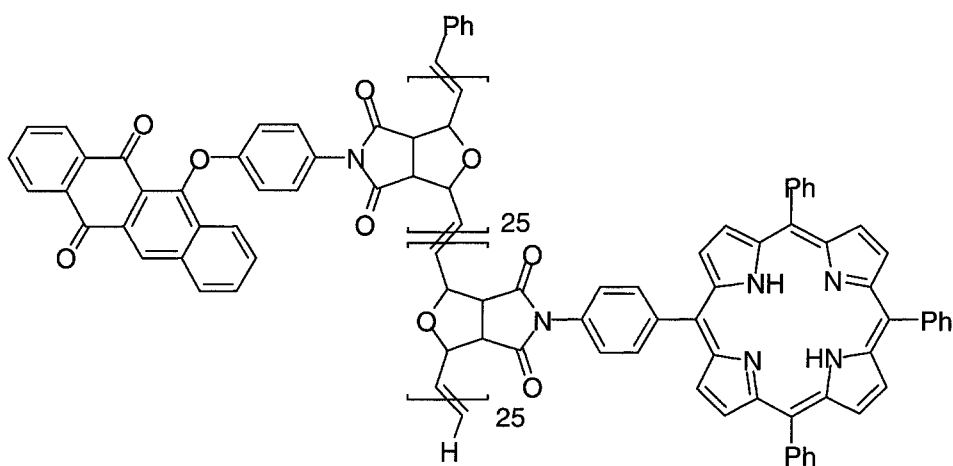


Oxonorbornene porphyrin 3.13. A mixture of amino porphyrin **3.11** (742 mg, 1.18 mmol) and 7-oxa-bicyclo[2.2.1]hept-5-ene-2,3-dicarboxylic anhydride (196 mg, 1.18 mmol) was stirred in glacial acetic acid (20 mL) at room temperature for 24 h. The mixture was poured into water and extracted with CH₂Cl₂ (3 × 75 mL). The organic layers were combined and the solvent was removed *in vacuo*. Purification by column chromatography using silica (CHCl₃) afforded 804 mg (88%) of pure product as a purple solid. Mp = >300 °C. ¹H NMR (400 MHz, CDCl₃) δ 8.90-8.86 (m, 8H), 8.33 (d, *J*=8.4 Hz, 2H), 8.22 (d, *J*=8.0 Hz, 6H), 7.80-7.71 (m, 11H), 6.65 (s, 2H), 5.55 (s, 2H), 3.16 (s, 2H), -2.78 (s, 2H). ¹³C NMR (125.70 MHz, CDCl₃) δ (15 of 27 signals were observed) 175.57, 142.60, 142.10, 136.83, 135.05, 134.56, 131.41, 127.75, 126.71, 124.52, 120.40, 120.29, 118.50, 81.62, 47.72. FTIR (KBr-cast) 3319, 3103, 3077, 3060, 3021, 2918, 2844, 1715, 1594, 1512, 1469, 1443, 1379, 1348, 1271, 1228, 1193, 1154, 1081, 1008, 960, 939, 913, 870, 797, 736, 702. Anal. Calcd for C₅₂H₃₅N₅O₃: C, 80.29; H, 4.54; N, 9.00. Found: C, 80.50; H, 4.55; N, 8.89.

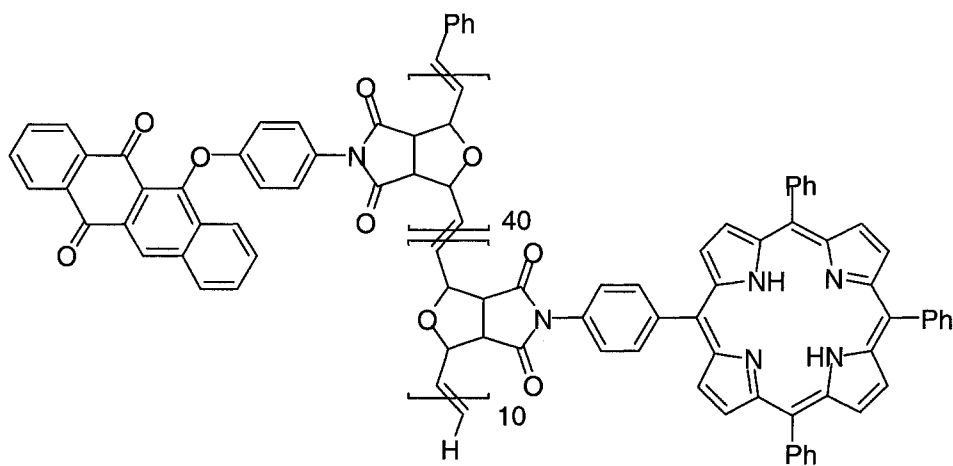
Synthesis of polymers 3.P1-3.P3. A CH_2Cl_2 solution of bis(tricyclohexylphosphine)benzylidene ruthenium(IV)dichloride was added through a canula into a solution of monomers **3.13** and **3.14** dissolved in dry deoxygenated CH_2Cl_2 . The final monomer concentrations were 0.2 M. After stirring at room temperature for 4 h, excess ethyl vinyl ether was added and the resulting solutions were stirred while exposed to the atmosphere for 30 min. The polymers were precipitated in high purity by pouring the reaction solutions into cold Et_2O and collected by vacuum filtration. The success of each polymerization reaction was assessed by ^1H NMR spectroscopy. Typically, in the ^1H NMR spectrum of the monomer shows broadened peaks corresponding to each subunit.



(3.P1) 4:1 porphyrin monomer **3.13** (121 mg, 0.16 mmol) to PNQ monomer **3.14** (20 mg, 0.039 mmol) were copolymerized with 0.02 molar equiv. of bis(tricyclohexylphosphine)benzylidene ruthenium(IV)dichloride to afford 120 mg (85%) of polymer **3.P1** as a purple solid. ^1H NMR (400 MHz, CDCl_3): δ 9.0-8.4 (br s), 8.4-7.9 (br s), 7.8-7.2 (br s), 6.4-5.6 (br s), 5.0-4.0 (br s), 3.5-2.5 (br s), -2.6- -3.4 (br s).



(3.P2) 1:1 porphyrin monomer **3.13** (61 mg, 0.078 mmol) and PNQ monomer **3.14** (40 mg, 0.078 mmol) were copolymerized with 0.02 molar equiv. of bis(tricyclohexylphosphine)benzylidene ruthenium(IV)dichloride to afford 75 mg (75%) of polymer **3.P2** as a purple solid. ^1H NMR (400 MHz, CDCl_3): δ 9.0-8.4 (br m), 8.4-7.9 (br s), 7.8-7.0 (br m), 6.9-6.4 (br s), 6.4-5.6 (br s), 5.0-4.0 (br s), 3.8-2.4 (br s), -2.6- -3.4 (br s).



(3.P3) 1:4 porphyrin monomer **3.13** (23 mg, 0.029 mmol) and PNQ monomer **3.14** (60 mg, 0.12 mmol) were copolymerized with 0.02 molar equiv. of

bis(tricyclohexylphosphine)benzylidene ruthenium(IV)dichloride to afford 60 mg (72%) of polymer **3.P3** as a purple solid. ^1H NMR (400 MHz, CDCl_3): δ 8.9-8.4 (br m), 8.3-6.6 (br m), 6.3-5.8 (br s), 5.4-5.0 (br s), 4.8-4.4 (br s), 3.6-3.0 (br s), -2.6- -3.4 (br s).

3.9 – References

1. (a) Kavarnos, G. J. *Fundamentals of Photoinduced Electron Transfer* VCH: New York, 1993. (b) Ward, M. D. *Chem. Soc. Rev.* **1997**, 26, 365-375.
2. (a) Feher, G.; Allen, J. P.; Okamura, M. Y.; Rees, D. C. *Nature* **1989**, 339, 111-116. (b) Chang, C.-H.; El-Kabbani, O.; Tiede, D.; Norris, J.; Schiffer, M. *Biochemistry* **1991**, 30, 5352-5360. (c) Jordanides, X. J.; Scholes, G. D.; Fleming, G. R. *J. Phys. Chem. B* **2001**, 105, 1652-1669.
3. Gust, D.; Moore, T. A. *Topics in Current Chemistry* **1991**, 159, 103-152.
4. Sakata, Y.; Nakashima, S.; Goto, T.; Tatemitsu, H.; Misumi, S.; Asahi, T.; Hagihara, M.; Nishikawa, S.; Okada, T.; Mataga, N. *J. Am. Chem. Soc.* **1989**, 111, 8979.
5. Hunter, C. A.; Shannon, R. J. *Chem. Commun.* **1996**, 1361-1362.
6. (a) Connolly, J., Ed. *Photochemical Conversion and Storage of Solar Energy*, Academic Press: New York, 1981. (b) Sienicki, K., Ed. *Molecular Electronics and Molecular Electronics Devices*, CRC Press: Boca Raton, 1993, Vol. 1.
7. (a) Balzani, V.; Scandola, F. *Supramolecular Photochemistry*; Ellis Horwood: New York, **1991**; Chapter 12, pp 355-394. (b) Lehn, J.-M.; *Supramolecular Chemistry*; VCH: Weinheim, **1995**; Chapter 8, pp 89-138. (c) Feringa, B. L., Ed. *Molecular Switches*, Wiley-VCH: Weinheim, 2001; pp. 1-35.
8. (a) Linke, M.; Chambron, J.-C.; Heitz, V.; Sauvage, J.-P.; Encinas, S.; Barigelletti, F.; Flamigni, L. *J. Am. Chem. Soc.* **2000**, 122, 11834-11844. (b) Zahavy, E.; Fox, M. A.

- Chem. Eur. J.* **1998**, *4*, 1647-1652. (c) Gosztola, D.; Niemczyk, M. P.; Wasielewski, M. R. *J. Am. Chem. Soc.* **1998**, *120*, 5118-5119. (d) Harada, A.; Yamaguchi, H.; Okamoto, K.; Fukushima, H.; Shiotsuki, K.; Kamachi, M. *Photochem. Photobiol.* **1999**, *70*, 298-302. (e) Hatzidimitriou, A.; Gourdon, A.; Devillers, J.; Launay, J.-P.; Mena, E.; Amouyal, E. *Inorg. Chem.* **1996**, *35*, 2212-2219.
9. (a) Endtner, J. M.; Effenberger, F.; Hartschuh, A.; Port, H. *J. Am. Chem. Soc.* **2000**, *122*, 3037-3046. (b) Daub, J.; Beck, M.; Knorr, A.; Spreitzer, H. *Pure & Appl. Chem.* **1996**, *68*, 1399-1404. (c) Fernandez-Acebes, A.; Lehn, J.-M. *Chem. Eur. J.* **1999**, *5*, 3285-3292. (d) Tsuchiya, S. *J. Am. Chem. Soc.* **1999**, *121*, 48-53. (e) Tsivgoulis, G. M.; Lehn, J.-M. *Chem. Eur. J.* **1996**, *2*, 1399-1406. (f) Huck, N. P. M.; Feringa, B. L. *J. Chem. Soc. Chem. Commun.* **1995**, 1095. (g) Archut, A.; Azzelini, G. C.; Balzani, V.; De Cola, L.; Vogtle, F. *J. Am. Chem. Soc.* **1998**, *120*, 12187-12191. (h) Ranjit, K. T.; Marx-Tibbon, S.; Ben-Dov, I.; Willner, B.; Willner, I. *Isr. J. Chem.* **1996**, *36*, 407-419.
10. Balzani, V.; Credi, A.; Raymo, F. M.; Stoddart, J. F. *Angew. Chem. Int Ed.* **2000**, *39*, 3348-3391.
11. Fang, Z.; Wang, S.; Yang, Z.; Chen, B.; Li, F.; Wang, J.; Xu, S.; Jiang, Z.; Fang, T. *J. Photochem. Photobiol., A* **1995**, *88*, 23.
12. Buchholtz, F.; Zelichenok, A.; Krongauz, V. *Macromolecules* **1993**, *26*, 906-910.
13. Fang, Z.; Wang, S.; Yang, Z.; Chen, B.; Li, F.; Wang, J.; Xu, S.; Jiang, Z.; Fang, T. *J. Photochem. Photobiol., A* **1995**, *88*, 23-30.

14. Doron, A.; Portnoy, M.; Lion-Dagan, M.; Katz, E.; Willner, I. *J. Am. Chem. Soc.* **1996**, *118*, 8937-8944.
15. Myles, A. J.; Branda, N. R. *Tetrahedron Lett.* **2000**, *41*, 3785-3788.
16. Etemad-Moghadam, G.; Ding, L.; Tadj, F; Meunier, B. *Tetrahedron*, **1989**, *45*, 2641.
17. Hunter, C. A.; Sarson, L. D. *Tetrahedron Letters*, **1996**, *37*, 699.
18. Osuka, A.; Fujikane, D.; Shinmori, H.; Kobatake, S.; Irie, M. *J. Org. Chem.*, **2001**, *66*, 3913-3923.
19. Flores, V; Nguyen, C. K.; Sindelar, C. A.; Vasquez, L. D.; Shachter, A. M. *Tetrahedron Lett.*, **1996**, *37*, 8633.
20. Myles, A. J.; Branda, N. R. *J. Am. Chem. Soc.* **2001**, *123*, 177-178.
21. (a) Kavarnos, G. J. *Fundamentals of Photoinduced Electron Transfer* VCH: New York, **1993**. (b) Rehm, D.; Weller, A. *Isr. J. Chem.* **1970**, *8*, 259-271.
22. The ¹H NMR titration data was analyzed using Christopher A. Hunter's 1:1 complexation model program (Krebs Institute for Biomolecular Science, Department of Chemistry, University of Sheffield, UK). All titrations were performed in triplicate.
23. (a) Vermeulen, L. A.; Thompson, M. E. *Nature* **1992**, *358*, 656-658. (b) Ho, T.-F.; McIntosh, A. R.; Bolton, J. R. *Nature* **1980**, *286*, 254-256.
24. Malkin, J.; Zelichenok, A.; Krongauz, V.; Dvornikov, A. S.; Rentzepis, P. M. *J. Am. Chem. Soc.* **1994**, *116*, 1101-1105.
25. Bolm, C; Dinter, C. L.; Seger, A.; Höcker, H.; Brozio, J. *J. Org. Chem.* **1999**, *64*, 5730-5731.

26. Kalinowski, H.-O.; Berger, S.; Braun, S. *Carbon-13 NMR Spectroscopy* John Wiley and Sons Ltd.: New York, 1984.

Chapter 4 - A Multi-Addressable Phenoxynaphthacenequinone-Dithienylethene Hybrid Photochromic System

4.1 - Introduction

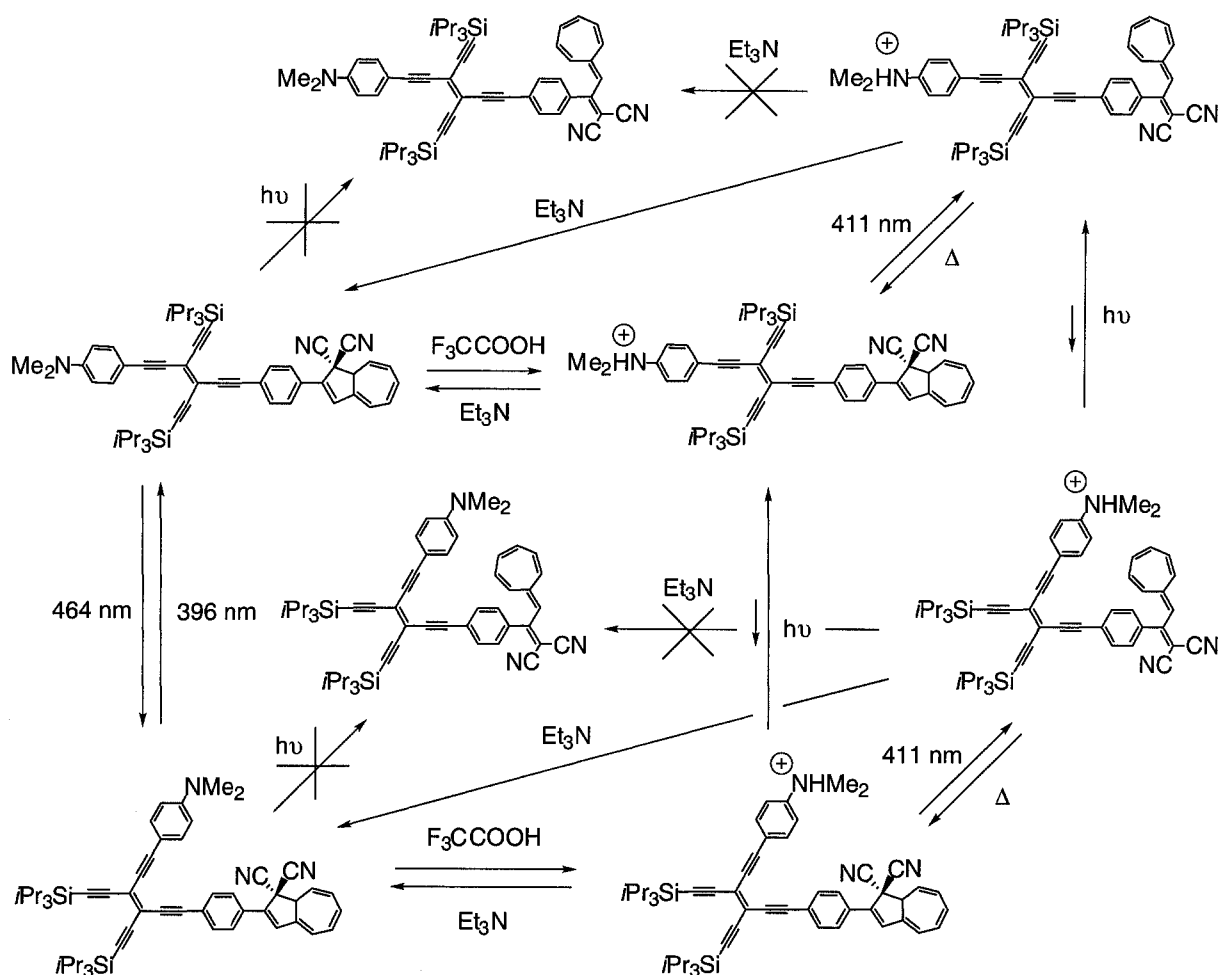
As stated throughout this thesis, photochromes are molecules that can interconvert between two or more stable states that display different absorption spectra upon irradiation with appropriate wavelengths of light. An important application of photochromic molecules is in molecular information storage systems, in which each isomer of the photochrome represents either “0” or “1” of a binary code. In order for a photochrome to be applied to such systems, it must possess high fatigue resistance and thermal irreversibility. This ensures the data can be written, read, and erased several times without decomposition of the medium. This also ensures that once the data is written, it will remain intact until the appropriate light stimulus is applied.

Key to the progress of the area of molecular information storage is the development of multi-addressable switching units, in which more than two pieces of information can be stored in the same molecule and, therefore, at the same storage site in the memory medium. In the recent, influential book “Molecular Switches” edited by Professor Ben L. Feringa, he states in his preface that the future of molecular switching technology involves “the construction of more complex systems which incorporate several switchable functions.”¹ As the number of

addressable units increases within a molecule, the amount of information it can contain in sequence increases exponentially. For example, in a binary system containing two molecules each with two stable states (0 and 1), there are four possible combinations (00, 01, 10, 11). In the case of two molecules possessing three possible states each (0, 1, and 2), there are now nine possibilities (00, 01, 02, 10, 11, 12, 20, 21, 22). For these reasons, it is desirable to investigate multi-addressable photochromic systems.

4.2 - Multi-Addressable Molecular Switches in the Literature

Diederich and coworkers have developed a multi-addressable chromophoric molecular switch which uses light and pH to access six states of the same molecule (Scheme 4.1).² This switch contains three key components: 1) a tetraethynylethene (TEE, 3,4-diethynylhex-3-ene-1,5-diyne) core, which can reversibly photoisomerize between its *cis* and *trans* forms; 2) a dihydroazulene (DHA) unit, which can photoisomerize to its vinylheptafulvene (VHF) form; 3) a proton sensitive *N,N*-dimethylanilino (DMA) group. The diagram of its transformations in Figure 4.1 is set up as a cube, in which the *cis-trans* isomerization of the TEE goes from bottom to top, the protonation/deprotonation of DMA goes from right to left, and the photoisomerization of DHA to VHF goes from front to back. Of the eight possible states, six can be addressed using three different switching processes.

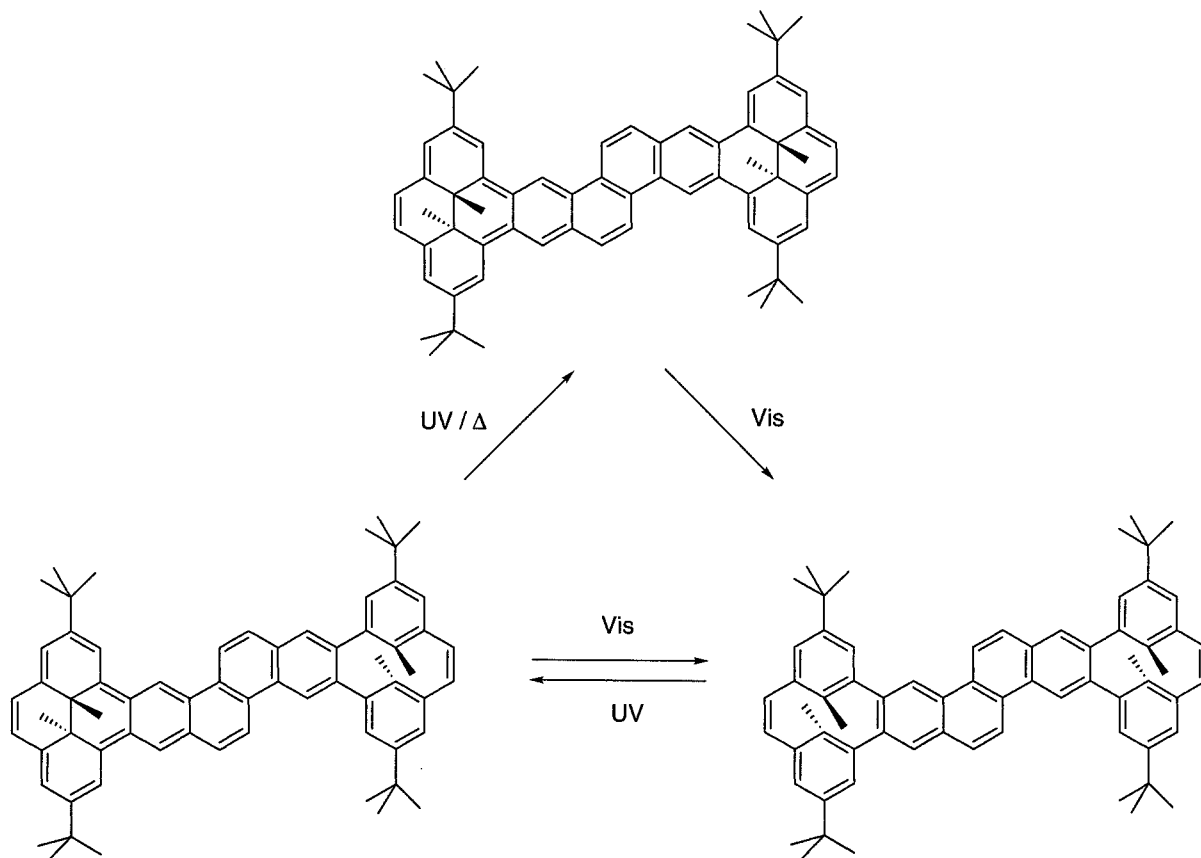


Diederich 1999

Scheme 4.1.

This system has two major problems in terms of device applications. The first is the use of thermally reversible switching units (TEE and DHA/VHF). Secondly, as discussed throughout this thesis, addition of chemical reagents such as acids and bases in a pH switch is not realistic for practical applications of these materials; more desirable is an all-photon-based

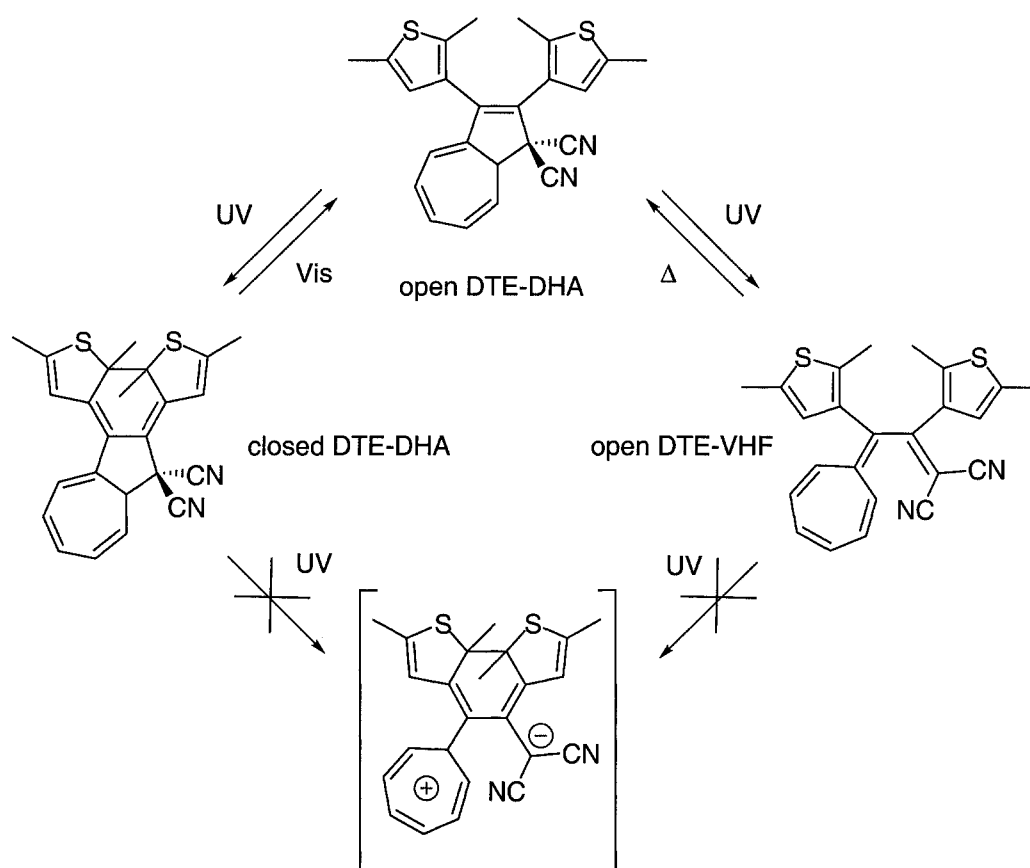
multi-addressable system in which more than two states of a molecule can be created simply by irradiation with more than two appropriate wavelengths of light.



Mitchell 1999

Scheme 4.2.

Mitchell and coworkers describe a novel three-way molecular switch based on a double dimethyldihydropyrene-metacyclophanediene photochrome (Scheme 4.2).³ In this case, three different states are accessible using light energy as the stimulus, however the difficulty in the synthesis of such photochromes as well as their inherent thermal reversibility make them less than desirable for application.



Daub 2001

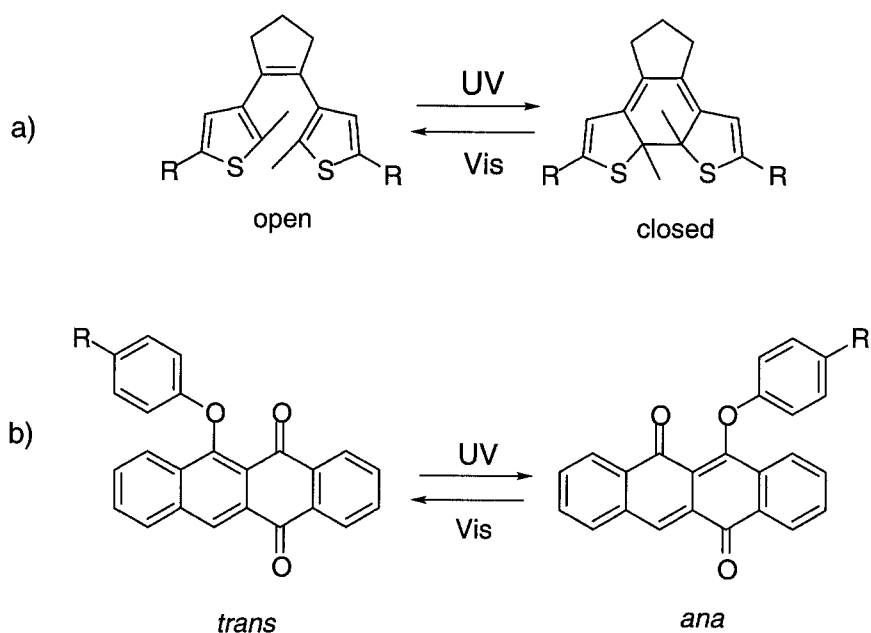
Scheme 4.3.

Daub and coworker have reported multi-addressable photochromism within a dithienylethene-dihydroazulene (DTE-DHA) hybrid in which three different states are accessible using light energy (Scheme 4.3).⁴ Irradiation of the half open DTE-DHA form of the hybrid (state 1) with UV light produces both the fully closed DTE-DHA and the fully open DTE-VHF forms (state 2). Since the DHA-to-VHF photoisomerization is thermally reversible, whereas the ring-opening/ring-closing DTE photochromism is not, continuous irradiation with

UV light eventually affords only the half closed DTE-DHA (state 3). The fourth possible state, shown in brackets in Scheme 4.3, is inaccessible, as each photochrome is not completely independently addressable.

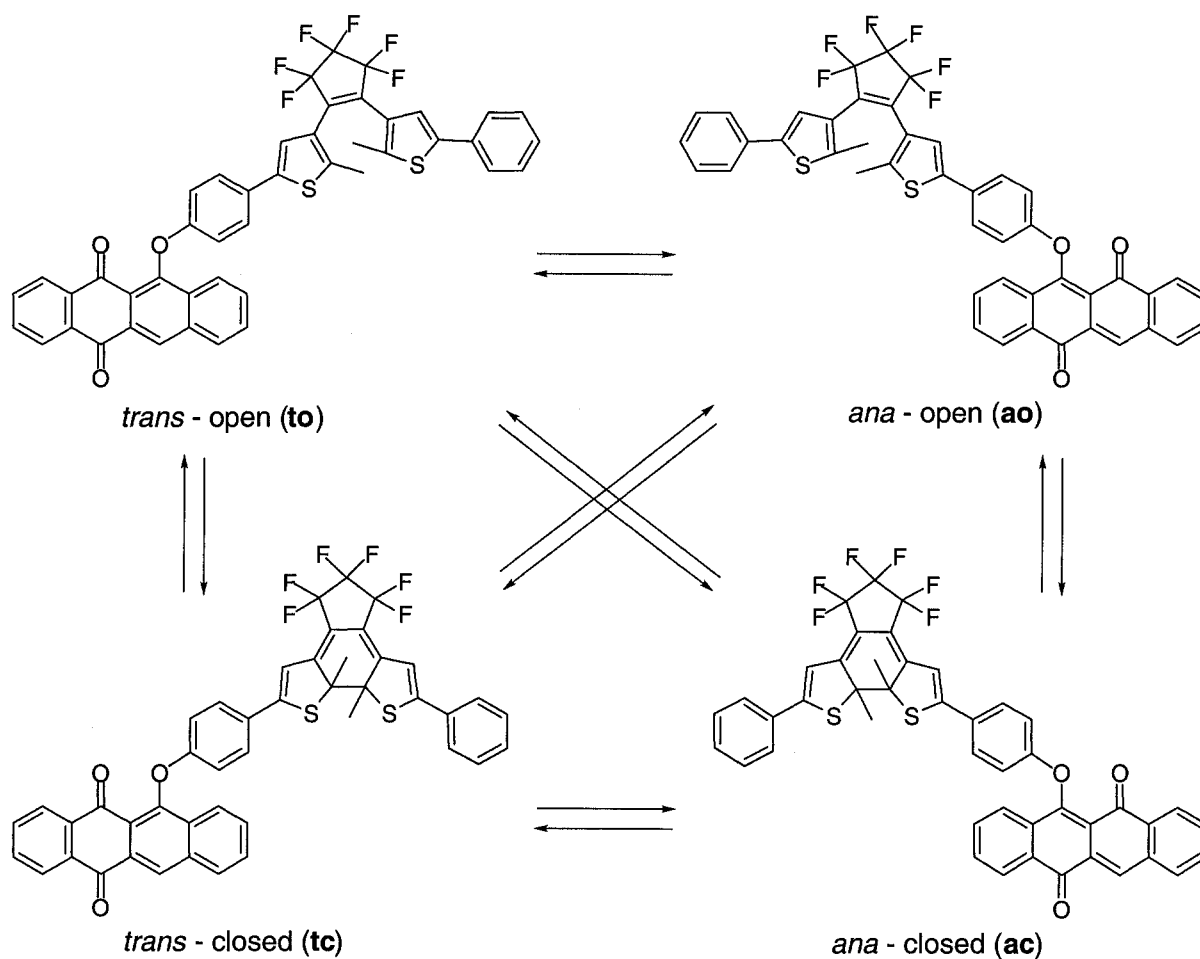
4.3 - A Phenoxynaphthacenequinone-Dithienylethene Hybrid

Dithienylethene (DTE) photochromes, discussed in detail in Chapter 2, interconvert between a colorless ring-open form (labeled simply as 'o' in this chapter) and a colored ring-closed form (labeled simply as 'c' in this chapter) as shown in Scheme 4.4a, and have been the most promising candidates for molecular read/write systems due to their desirable photochromic properties. Phenoxynaphthacenequinone (PNQ) photochromes, discussed in detail in Chapter 3, interconvert between their *trans*- (labeled simply as 't' in this chapter) and *ana*- (labeled simply as 'a' in this chapter) forms (Scheme 4.4b) and not only possess desirable photochromic activity, but also differ in the electron accepting ability between their two forms.



Scheme 4.4. Photochromism of a) dithienylethene and b) phenoxy-naphthacenequinone

My strategy in developing a multi-addressable photochromic system involves covalently tethering a PNQ photochrome to a DTE photochrome, as illustrated in Scheme 4.5. The absorption of DTE's closed form can be tailored by simply changing the pendant 'R' groups on the thiophene rings. Extending the linear conjugation pathway created upon photocyclization results in the absorption of the closed form to be red-shifted (higher wavelengths). This provides a handle for the design of a hybrid photochromic system in which the absorptions are independently addressable, allowing four distinct states within the same molecule (**to**, **ao**, **tc** and **ac**). Herein is reported the synthesis and characterization of the first multiaddressable PNQ-DTE hybrid photochromic system in which four states are accessible using light energy as the only stimulus.



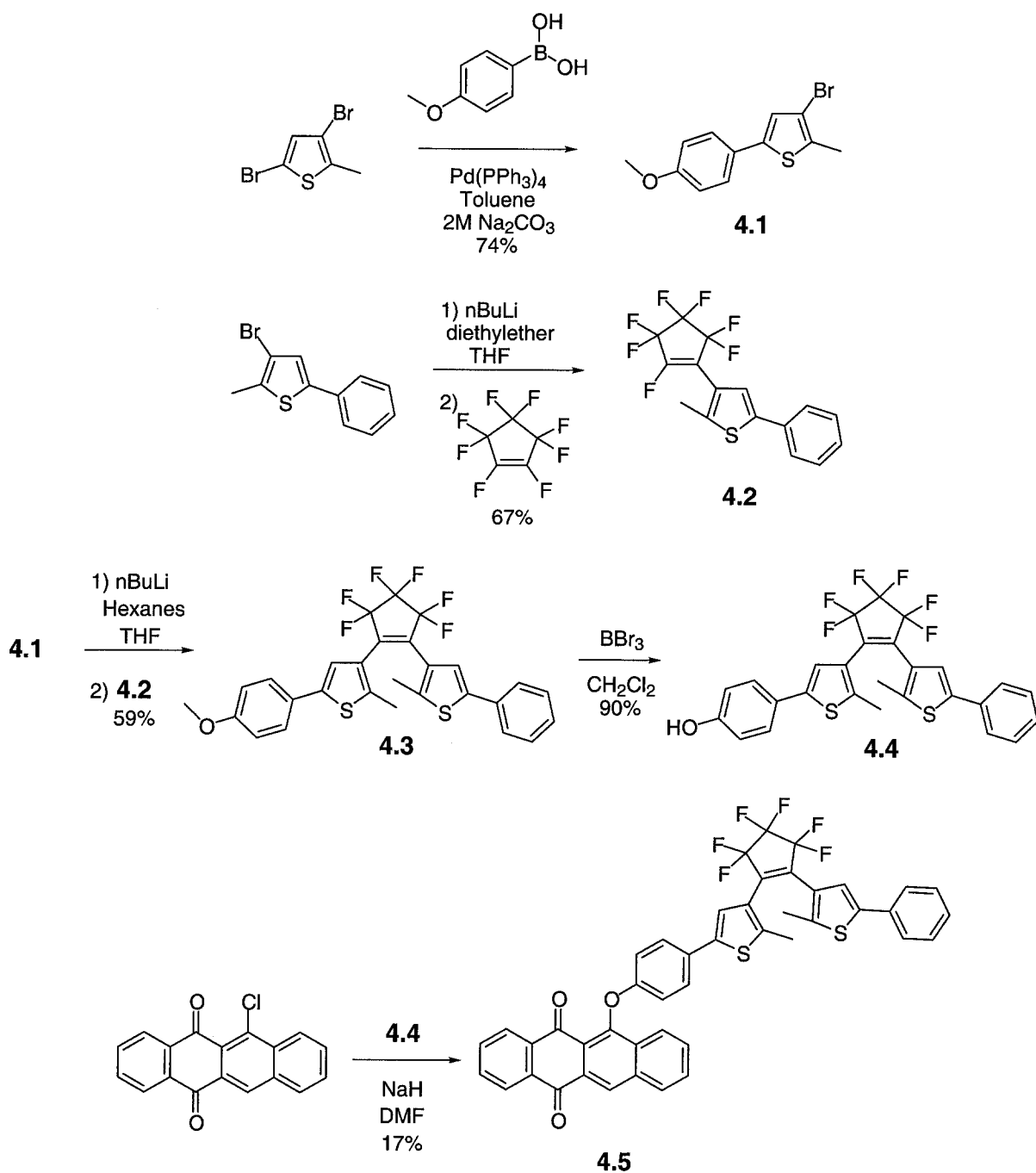
Scheme 4.5.

4.3.1. - Synthesis

The synthesis of the PNQ-DTE hybrid **4.5** was achieved by first synthesizing the DTE component, followed by coupling to the naphthacenequinone moiety (Scheme 4.6). The DTE component was synthesized starting with a Suzuki coupling between 3,5-dibromo-2-methylthiophene⁵ with 4-methoxyphenyl boronic acid, to afford the known 3-bromo-5-(4-

methoxyphenyl)-2-methyl-thiophene **4.1**⁶ in moderate yield. Lithiation of 3-bromo-2-methyl-5-phenylthiophene⁷ followed by quenching with octafluorocyclopentene produced **4.2** in moderate yield. This molecule shows the characteristic small ¹H-¹⁹F coupling (3 Hz) in the ¹H NMR spectrum and a small ¹³C-¹⁹F coupling (5 Hz) in the ¹³C NMR spectrum between the thiophene methyl group and the vinylic fluorine on the cyclopentene ring.⁸ Lithiation of **4.1** followed by addition of thiophene **4.2** afforded photochrome **4.3**, characterized by its change in color upon irradiation with UV light. Deprotection of the methoxyphenyl group of **4.3** is achieved using boron tribromide, affording photochrome **4.4** in quantitative yield. All precursors were characterized by ¹H and ¹³C NMR spectroscopy, mass spectrometry, infrared spectroscopy and melting point.

Reaction of the phenoxy-dithienylethene **4.4** with known 6-chloro-5,12-naphthacenequinone⁹ (**3.5** in Chapter 3), using NaH as the base, affords the hybrid double photochrome **4.5**, albeit in low yield. The product is characterized mainly by the presence of peaks from each component of the hybrid integrating to the appropriate value in the ¹H NMR spectrum.



Scheme 4.6

4.3.2 - UV-vis Absorption Spectroscopy of Control Molecules

Control photochromes PNQ **3.6** (see Chapter 3 for synthesis) and DTE **4.3** were used to assess the expected photochromic behaviour of hybrid **4.5**. Figure 4.1 shows the spectra of PNQ **3.6** in its *trans*- and *ana*-forms (**3.6t** and **3.6a**), and those of DTE **4.3** in both its ring-open and ring-closed forms (**4.3o** and **4.3c**). The arrows on the spectra denote the regions at which each form is transparent. From this data, it is clear that DTE **4.3c** can be irradiated at wavelengths above 550 nm without affecting the PNQ in either of its forms (**3.6t** or **3.6a**). Also, PNQ **3.6** can be selectively irradiated at wavelengths above 400 nm without affecting DTE **4.3o**. According to these spectra, it also appears that DTE **4.3c** has a transparent region between 400 and 450 nm, which may be exploited in the hybrid switch as a window to irradiate the *ana*-PNQ without affecting the closed form of the DTE component. The presence of these transparent regions are important in being able to independently address each form of each photochromic unit, therefore maximizing the number of possible states the hybrid can adopt.

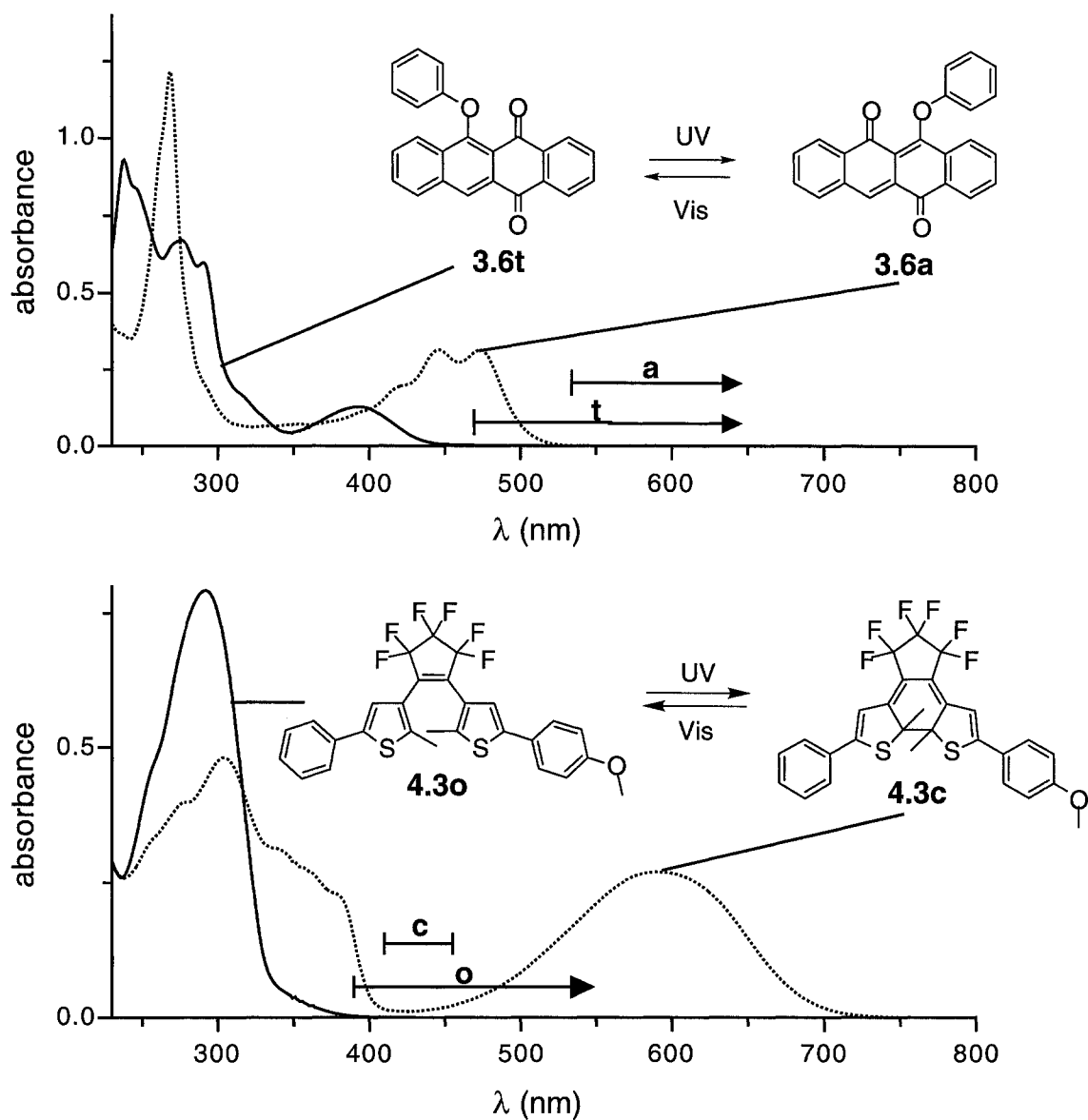


Figure 4.1. UV-vis absorption spectra of control photochromes **3.6** and **4.3**. Arrows indicate the transparent region of the spectrum for each form of each photochrome. Spectra were recorded using 2×10^{-5} M acetonitrile solutions. The spectrum of PNQ **3.6a** was obtained after irradiation of the **3.6t** solution with 365 nm light for 120 seconds. The spectrum of DTE **4.3c** was obtained after irradiation of the **4.3o** solution with 365 nm light for 60 seconds.

A solution of **3.6:4.3** in a 1:1 molar ratio was prepared at identical concentrations to the above UV-vis absorption study to see if each form of each photochrome can be independently addressed. The UV-vis absorption spectral changes are highlighted in Figure 4.2. Upon irradiation of the *trans*-open mixture (**to**) with 365 nm light, the absorbances corresponding to the *ana*-closed mixture (**ac**) appear with λ_{max} values at 445, 478 and 592 nm. Upon irradiation of **ac** with broad band light > 557 nm, the absorbance corresponding to the closed form of the DTE disappears, forming the *ana*-open mixture (**ao**). Irradiation of **ao** with broad band light > 434 nm results in the regeneration of the original spectrum corresponding to **to**. Irradiation of **ao** with 365 nm light regenerates the spectrum corresponding to **ac**. The **ac** mixture can also be irradiated with broad band light > 434 nm to return to the **to** mixture. All of these transformations are illustrated in Figure 4.2.

The only state that is inaccessible is the *trans*-closed mixture (**tc**). Upon irradiation at wavelengths throughout the UV region, both the isomerization of the *trans*- to *ana*-forms of the PNQ and the ring-open to ring-closed forms of the DTE occur. The seemingly transparent window of the closed form of the closed form of DTE **4.3c** between 400 and 450 nm, shown in Figure 4.1, is obviously not completely transparent. Irradiation of the **ac** mixture with wavelength within this window shows slow decrease of both the **a** and **c** absorptions. This suggests that it will also be difficult to access the **tc** state in the hybrid **4.5**.

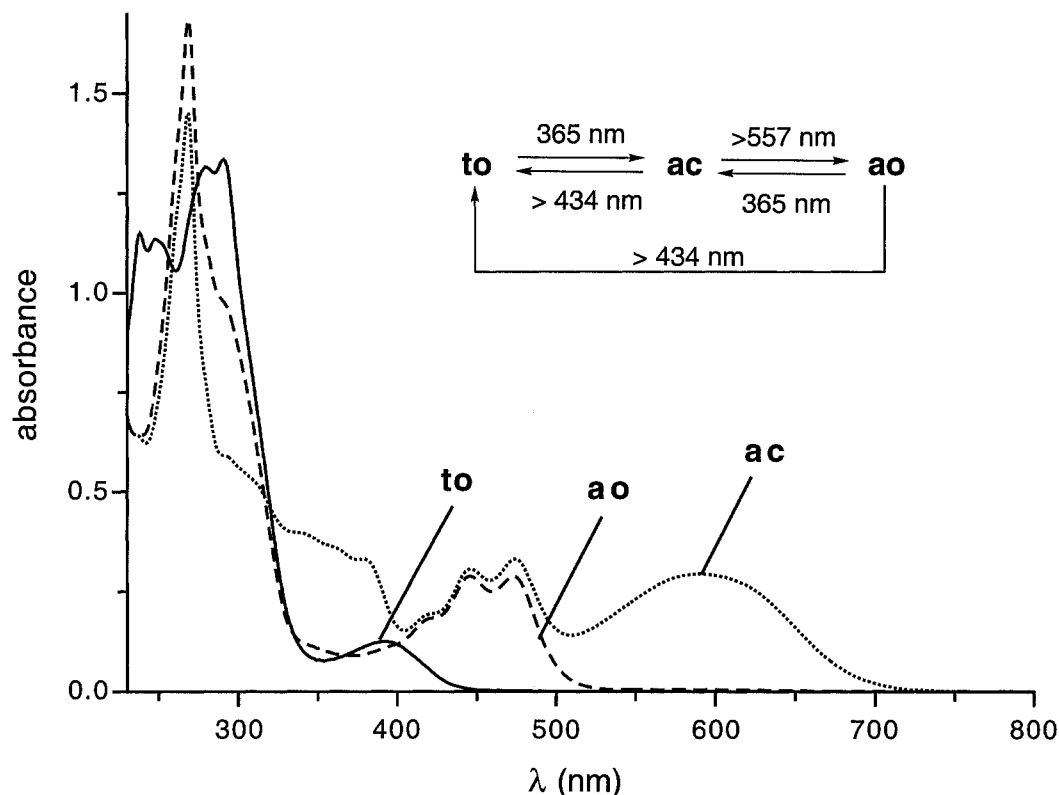


Figure 4.2. UV-vis absorption spectra of a 1:1 mixture of **3.6:4.3**, performed as a control experiment for hybrid **4.5**. The *trans*-open (**to**), *ana*-closed (**ac**), and *ana*-open (**ao**) mixtures are all accessible by irradiation with appropriate wavelengths of light. Spectra were obtained using 2×10^{-5} M acetonitrile solution. Irradiation times (λ) are **to** \rightarrow **ac**: 120 seconds (365 nm); **ac** \rightarrow **ao**: 60 seconds (>557 nm); **ao** \rightarrow **ac**: 60 seconds (365 nm); **ao** \rightarrow **to**: 300 seconds (>434 nm); **ac** \rightarrow **to**: 300 seconds (>434 nm).

4.3.3 – UV-vis Absorption of PNQ-DTE Hybrid 4.5

Before continuing, it is important to note that only the **to** form of the photochromic hybrid will be pure, as all other forms (**ac**, **ao**, and **tc**) are represented by photostationary states. Upon irradiation of the *trans*-PNQ with UV light, a photostationary state is reached

which contains mostly *ana*-form (typically 80-85%). Similarly, irradiation of the open form of DTE with UV light, a photostationary state is reached which contains mostly ring-closed form (typically >80%).

UV-vis spectroscopy studies were performed on the PNQ-DTE hybrid **4.5**. As illustrated in Figure 4.3, the spectrum of the hybrid **4.5** in its *trans*-open form (**4.5to**) overlaps well with the spectrum of the 1:1 mixture of **3.6t**:**4.3o**, with identical λ_{max} values at 282, 291, and 390 nm. The small change in intensity in the UV region implies a minor interaction between the ground states of the two chromophores. Whether this interaction affects its ability to function as a multiaddressable switch can only be tested by examining its photochromic behaviour.

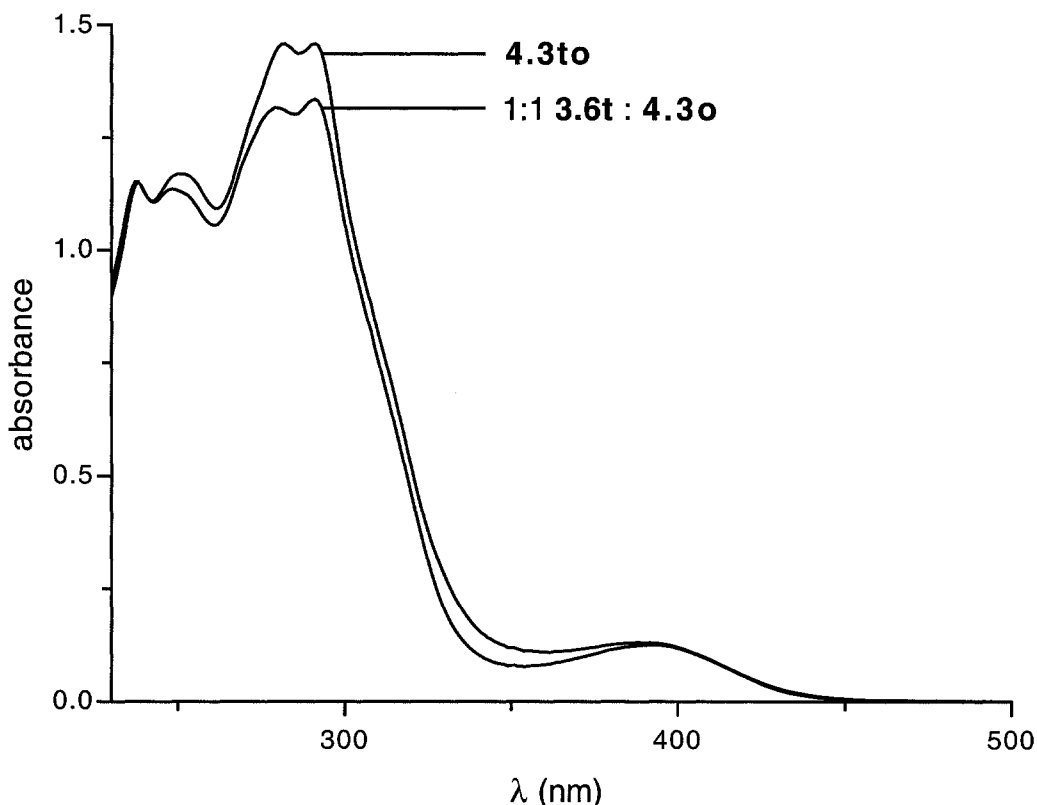


Figure 4.3. Overlapping the UV-vis absorption spectrum of PNQ-DTE hybrid **4.5** in its *trans*-open form (**4.5to**) with the spectrum of a 1:1 mixture of **3.6t:4.5o**. The λ_{\max} values of both spectra are 282, 291, and 390 nm. Spectra were measured using 2×10^{-5} M acetonitrile solutions.

The photochromic behaviour of the PNQ-DTE hybrid **4.5** differs from that of the 1:1 mixture of the controls **3.6:4.3** previously discussed. Upon irradiation of the *trans*/ring-open form of PNQ-DTE **4.5to** with 365 nm, the conversion to the ring-closed form **4.5ac** occurred much slower than in the 1:1 mixture of **3.6:4.3** (15 minutes compared to 2 minutes). The absorption of the ring-closed form of the DTE component in hybrid **4.5** is formed after 2 minutes of irradiation at 365 nm, however the isomerization from the *trans*- to *ana*-form of the PNQ is very slow within this hybrid system. This suggests the presence of an alternate decay

pathway of the excited state of the PNQ component of the hybrid that competes with the photoisomerization reaction, most likely energy and/or electron transfer.

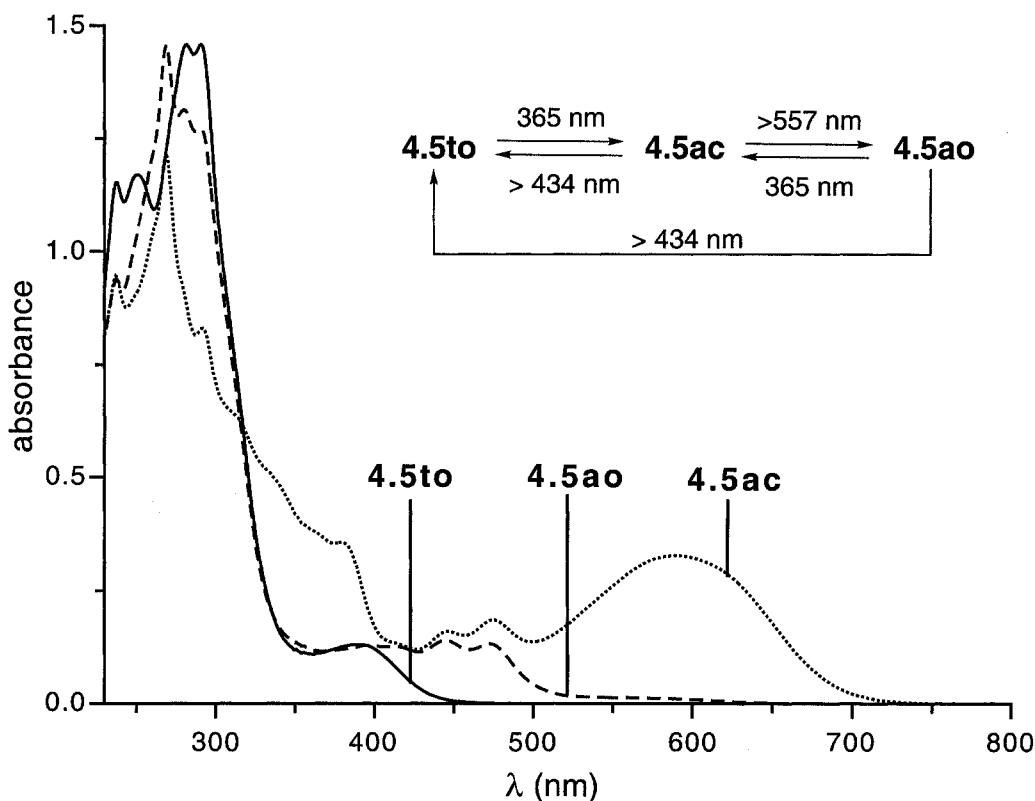


Figure 4.4. UV-vis absorption spectra of PNQ-DTE hybrid **4.5**. The *trans*-open (**to**), *ana*-closed (**ac**), and *ana*-open (**ao**) mixtures are produced by irradiation with appropriate wavelengths of light. Spectra were obtained using 2×10^{-5} M acetonitrile solution. Irradiation times are (λ) **to** \rightarrow **ac**: 900 seconds (365 nm); **ac** \rightarrow **ao**: 60 seconds (>557 nm); **ao** \rightarrow **ac**: 120 seconds (365 nm); **ao** \rightarrow **to**: 300 seconds (>434 nm); **ac** \rightarrow **to**: 300 seconds (>434 nm).

Aside from this interesting kinetic phenomenon, the *trans*/ring-open form of PNQ-DTE **4.5to** can be photoisomerized to the *ana*/ring-closed form **4.5ac** by irradiation with 365 nm light for 15 minutes. This *ana*/ring-closed form **4.5ac** behaves similarly to the 1:1 mixture of the controls **3.6a**:**4.3c** as irradiation with > 557 nm light for 60 seconds results in the

absorption spectrum corresponding to the ana/ring-open form **4.5ao**. Both the ana/ring-closed **4.5ac** and ana/ring-open **4.5ao** forms can be converted back to the trans/ring-open form **4.5to** by irradiating with > 434 nm light for 5 minutes. The ana/ring-open form **4.5ao** can also be isomerized back to the ana/ring-closed form **4.5ac** by irradiation with 365 nm light for 2 minutes.

This leaves only the elusive **4.5tc** state, in which the PNQ component is in the *trans*-form and the DTE component is in its closed form. After optimizing this system, I found that the control DTE **4.3o** photochemically ring closed to **4.3c** much more quickly when irradiated with 313 nm light (20 seconds compared to 120 seconds with 365 nm). This same increase in the rate of conversion of the ring-open to the ring-closed form of the DTE at 313 nm applies to the DTE component in the PNQ-DTE hybrid **4.5**. By exploiting the slow conversion of the *trans*- to *ana*-form of the PNQ component in hybrid **4.5**, and the fast conversion of the DTE component using 313 nm, the trans/ring-closed state **4.5tc** is achieved. Upon irradiation of the trans/ring-open form **4.5to** with 313 nm light for 20 seconds, the absorption spectrum showing the expected absorbance of the trans/ring-closed form **4.5tc** is observed. More specifically, the presence of the broad absorbance centered at 592 nm corresponding to the ring-closed form of the DTE component, and the absence of the absorbances at 445 and 478 nm corresponding to the *ana*-form of the PNQ component are observed. This completes the fourth state of this hybrid switch, as illustrated in Figure 4.5 and Scheme 4.7.

Upon irradiation of this *trans*/ring-closed form **4.5tc** with light > 557 nm, the ring-closed form of the DTE component was converted to the ring-open form. A small absorbance at 445 and 478 nm remains corresponding to a small amount of *ana*-form present. By comparing the intensity of this minor *ana*-form absorbance at 478 nm to that for the photostationary state of *ana*/ring-open **4.5ao**, it was found the amount of *ana*-form is about 14% of that in its photostationary state (unknown to date) within the hybrid. In this case, since the absorbance of the *ana*-form of the PNQ component in **4.5tc** is so small, it is easy to visualize the four different states by UV-vis absorption.

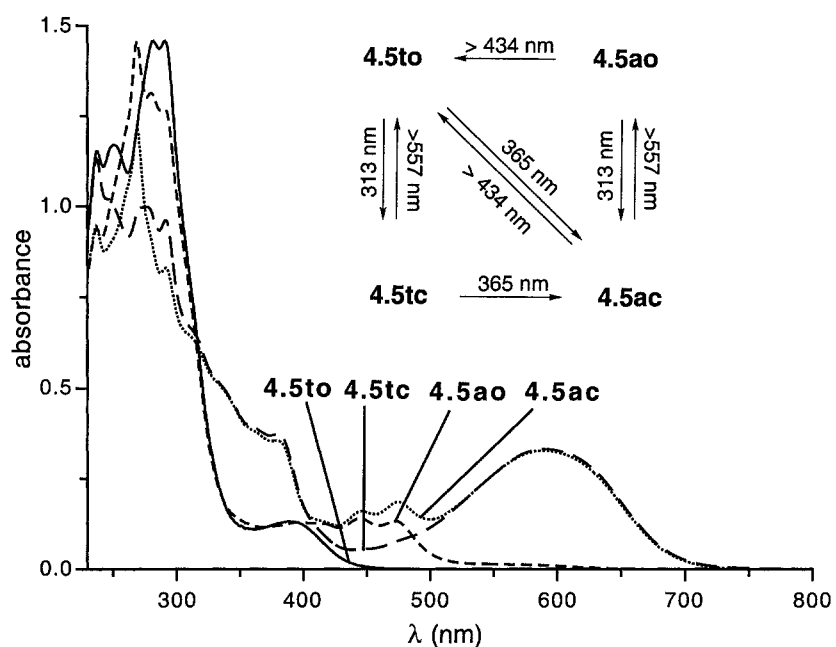
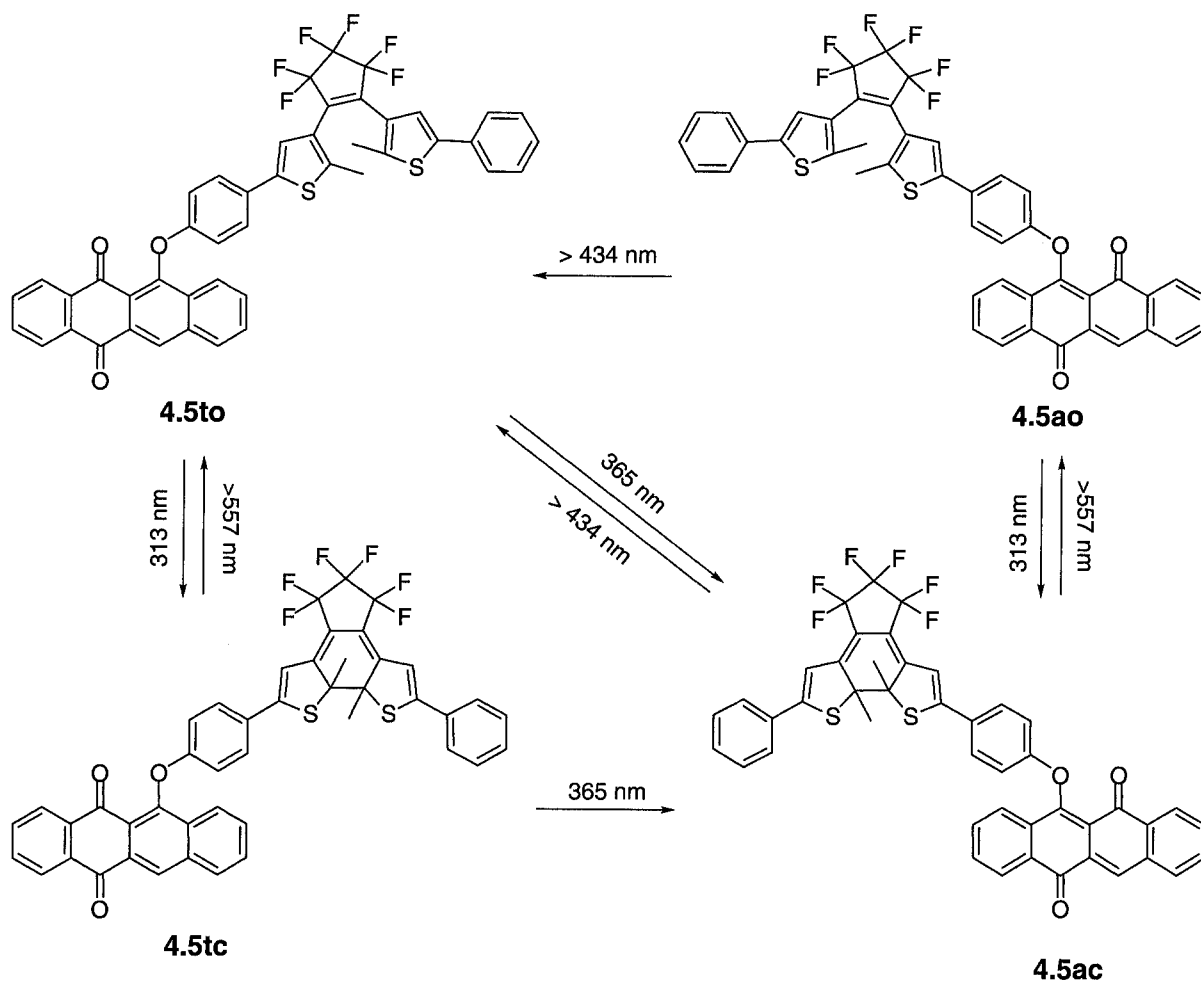


Figure 4.5. UV-vis absorption spectrum of hybrid **4.5**. The *trans*-open (**to**), *ana*-closed (**ac**), *ana*-open (**ao**) and *trans*-closed (**tc**) mixtures are shown by irradiation with appropriate wavelengths of light. Spectra were obtained using 2×10^{-5} M acetonitrile solution. Irradiation times (λ): **to** \rightarrow **ac**: 900 seconds (365 nm); **to** \rightarrow **tc**: 20 seconds (313 nm); **ac** \rightarrow **ao**: 60 seconds (>557 nm); **ao** \rightarrow **ac**: 20 seconds (313 nm); **ao** \rightarrow **to**: 300 seconds (>434 nm); **ac** \rightarrow **to**: 300 seconds (>434 nm).

4.4 – Summary



Scheme 4.7

This system represents the first quaternary photochromic switch: four different states are accessible with light input within the same molecule (Scheme 4.7). This hybrid should also be electrochemically active, as the PNQ moiety has been shown to possess different reduction potentials. These results represent preliminary studies on this hybrid system. In

order to fully understand this system, the photostationary states of each form must be resolved using ^1H NMR spectroscopy. Transient absorption studies would also be beneficial to study the slow interconversion rate between the *trans*- and *ana*-forms of the PNQ moiety within the hybrid **4.5**. There is perhaps an electron or energy transfer pathway between the PNQ and DTE components that competes with the photoisomerization pathway of the PNQ within the hybrid. Cyclic voltammetry studies should also be performed to see if each component within the hybrid is reduced/oxidized at the same potential as their corresponding control photochromes. This is a significant set of molecules for these reasons and studies on them will continue in our group.

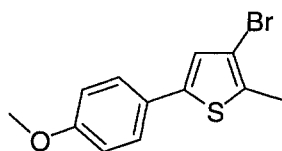
4.5 – Experimental

General: All solvents for synthesis were purchases from Caledon Laboratories Limited. THF and diethyl ether were distilled over sodium/benzophenone, hexane was distilled over potassium/benzophenone, and acetonitrile and CH_2Cl_2 were distilled over calcium hydride before use. All other solvents were used as received. Solvents for NMR analysis were purchased from Cambridge Isotope Laboratories and used as received. Column chromatography was performed using silica gel 60 (230-400 mesh) from Silicycle Inc. All other reagents and starting materials were purchased from Aldrich. 3,5-dibromo-2-methylthiophene,⁵ 3-bromo-2-methyl-5-phenylthiophene⁷ and 6-chloro-5,12-naphthacenequinone⁹ were prepared as described in the literature.

^1H NMR spectroscopy was performed on a Varian Inova-300 or Bruker AMX 400 instrument. ^{13}C NMR characterizations were performed on a Bruker 300 or Bruker AMX 400 instrument. Chemical shifts (δ) are reported in parts per million relative to tetramethylsilane using the residual solvent peak as a reference standard. Coupling constants (J) are reported in Hertz. The number of ^{13}C NMR resonances of several compounds do not equal the number of different carbons in the molecule. This is especially true for the compounds containing perfluorinated cyclopentene rings. This is due to the two and three bond ^{19}F - ^{13}C coupling, which causes splitting of the signal making it indistinguishable from the baseline noise. This problem may be circumvented by performing ^{19}F -decoupled ^{13}C NMR experiments. Also, consecutive

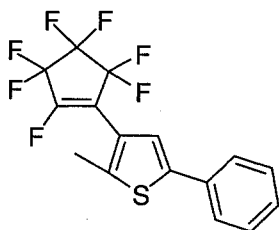
quaternary carbons show very weak signals due to longer relaxation times and poor NOE's to ^1H atoms. This problem may be circumvented by increasing the concentration of the sample and by increasing the acquisition time.¹⁰

FT-IR measurements were performed using a Nicolet Magna-IR 750 or a Nexus 670 instrument and values are reported in cm^{-1} . UV-vis measurements were performed using a Varian Cary 300 Bio spectrophotometer. UV irradiation was performed using a hand-held UV lamp operating at $350 \mu\text{W}/\text{cm}^2$ for 313 nm and 365 nm irradiation. Irradiation with visible light was performed using the light of a 150-W tungsten source that was passed through a 434 nm ($> 434 \text{ nm}$) or 557 nm ($> 557 \text{ nm}$) cutoff filter to eliminate higher energy light.



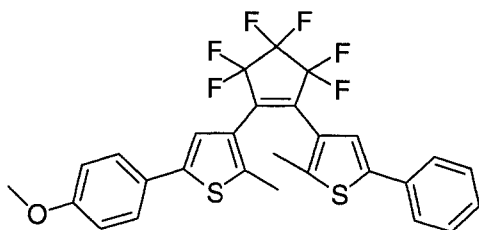
3-bromo-2-methyl-5-(4-methoxyphenyl)thiophene 4.1.⁶ This molecule has been characterized in the literature, however an alternate synthesis is reported herein. To a degassed mixture of toluene (30mL) and 2M Na_2CO_3 (aq) (15 mL) under Ar atmosphere was added 3,5-dibromo-2-methylthiophene⁵ (1.61g, 6.28 mmol). An ethanolic solution (3 mL) of 4-methoxyphenyl boronic acid (1.05g, 6.91 mmol) was subsequently added followed by $\text{Pd}(\text{PPh}_3)_4$ (0.25 g, 0.22 mmol). The mixture was heated to reflux for 40 h after which time the heating source was removed and the mixture was allowed to cool to room temperature. The layers were separated and the aqueous layer was extracted with diethyl ether (2 x 30 mL). The

organic layers were combined, washed with saturated NaHCO_3 (aq) (30 mL), dried over Na_2SO_4 , gravity filtered and the solvent was removed *in vacuo*. Purification by column chromatography using silica (9:1 hexanes: CH_2Cl_2) afforded 1.32 g (74%) of pure product as a white solid. Mp = 105-106 °C (lit. Mp = 106 °C). ^1H NMR (100 MHz, CDCl_3) δ 7.43 (d, $J=8.7$ Hz, 2H), 6.96 (s, 1H), 6.88 (d, $J=8.7$ Hz, 2H), 3.81 (s, 3H), 2.38 (s, 3H). Literature: (200 MHz, CDCl_3) δ 7.43 (d, $J=8.9$ Hz, 2H), 6.98 (s, 1H), 6.90 (d, $J=8.9$ Hz, 2H), 3.83 (s, 3H), 2.40 (s, 3H).



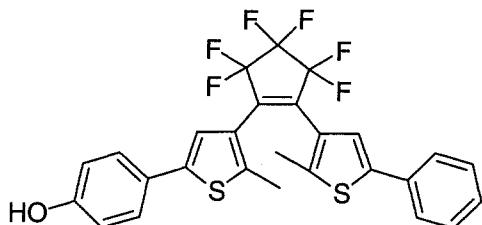
Phenylthienylperfluorocyclopentene 4.2. A vigorously stirred solution of 3-bromo-2-methyl-5-phenylthiophene⁷ (1.25 g, 4.7 mmol) in diethylether (20 mL) and THF (7 mL) cooled to -78°C was treated with *n*-butyllithium (1.98 mL of 2.5 M solution in hexanes, 4.9 mmol) dropwise under argon. After 15 min, octafluorocyclopentene (1.57 g, 1 mL, 7.41 mmol) was added via syringe. The reaction mixture was stirred at this temperature for 1 h, the cooling bath was removed and the mixture was allowed to warm to room temperature where it was stirred for a total of 16 h. The solvent was removed *in vacuo* and the residue mixture was partitioned between CH_2Cl_2 and H_2O . The organic layer was separated, washed with water and then brine, dried over Na_2SO_4 , filtered and evaporated *in vacuo*. Purification by column chromatography through silica (hexanes) afforded 1.22 g (67%) of the product as a white

solid. Mp = 35-37°C. ^1H NMR (400 MHz, CDCl_3) δ 7.55 (d, $J=7.2$ Hz, 2H), 7.40 (t, $J=7.2$ Hz, 2H), 7.32 (m, 1H), 7.25 (s, 1H), 2.48 (d, $J=3.2$ Hz, 3H) ^{13}C NMR (125 MHz, CD_2Cl_2) δ (9 of 14 signals were observed) 143.94, 143.09, 133.62, 129.50, 128.56, 126.11, 122.67, 120.86, 14.86 (d, $J=4.9$ Hz). FTIR (KBr-cast) 3066, 2929, 1696, 1602, 1502, 1471, 1446, 1386, 1360, 1330, 1278, 1200, 1151, 1120, 1074, 1028, 972, 894, 855, 835, 757, 689, 618, 556. EIMS (m/z): 366.03 (M+).



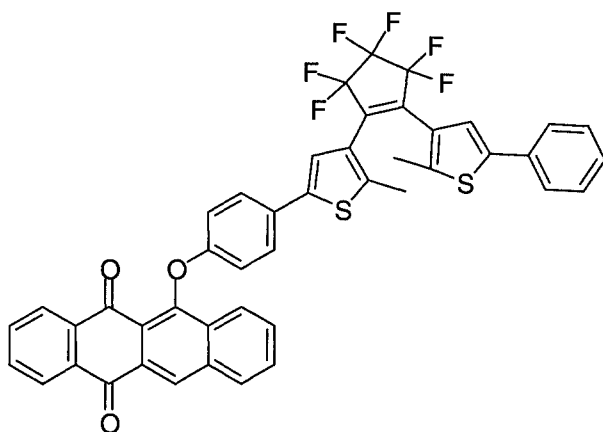
Methoxyphenyl-phenyl dithienylperfluorocyclopentene 4.3. A vigorously stirred solution of methoxyphenylthiophene **4.1** (500 mg, 1.76 mmol) in a mixture of diethylether (25 mL) and THF (15 mL) cooled to -78 °C was treated with *n*-butyllithium (0.70 mL of a 2.5 M solution in hexanes, 1.76 mmol) dropwise under argon. After stirring at this temperature for 10 min, a solution of cyclopentene **4.2** (647 mg, 1.76 mmol) was added. The reaction mixture was stirred at -78 °C for 1 h, the cooling bath was removed and the mixture allowed to warm to room temperature where it was stirred for 16 h. The solvent was removed *in vacuo* and the residue was partitioned between CH_2Cl_2 and H_2O . The organic layer was separated, washed with water and then brine, dried over Na_2SO_4 , filtered and evaporated *in vacuo*. Purification by column chromatography through silica (9:1 CH_2Cl_2 :hexanes) afforded 570 mg (59%) of the product as a pale green solid. Mp = 35-37°C. ^1H NMR (400 MHz, CDCl_3) δ 7.54 (d, $J=7.4$

Hz, 2H), 7.46 (d, $J=9.0$ Hz, 2H), 7.38 (t, $J=7.4$ Hz, 2H), 7.32-7.28 (m, 2H), 7.16 (s, 1H), 6.91 (d, $J=9.0$ Hz, 2H), 3.84 (s, 3H), 1.96 (s, 3H), 1.94 (s, 3H). ^{13}C NMR (125 MHz, CDCl_3) δ (18 of 24 signals were observed) 159.50, 142.16, 141.28, 140.28, 133.37, 129.00, 127.88, 126.93, 126.20, 125.89, 125.70, 125.61, 122.44, 121.26, 114.39, 55.40, 14.54, 14.48. FTIR (KBr-cast) 3064, 3026, 3004, 2957, 2935, 2914, 2836, 1612, 1577, 1555, 1512, 1474, 1443, 1336, 1271, 1193, 1116, 1055, 1029, 986, 956, 900, 822, 758, 689, 628, 564, 538. CIMS (m/z): 551 ($M+1$).



Hydroxyphenyl-phenyl dithienylperfluorocyclopentene 4.4. To an anhydrous CH_2Cl_2 solution (5 mL) of methoxyphenyl dithienylperfluorocyclopentene **4.3** (170 mg, 0.31 mmol) under N_2 atmosphere was added BBr_3 (0.2 mL, 2.1 mmol) via syringe. The solution immediately turned from clear to dark red. The mixture was stirred for 24 h, after which it was diluted to 100 mL and washed with water (3×50 mL). The organic layer was dried over MgSO_4 , filtered and the solvent was removed *in vacuo*. Purification by column chromatography using silica (2:1 CH_2Cl_2 :Hexanes) afforded 150 mg (90%) of pure product as a pale pink solid. Mp = 61-63°C. ^1H NMR (400 MHz, CDCl_3) δ 7.54 (d, $J=7.4$ Hz, 2H), 7.42 (d, $J=9.0$ Hz, 2H), 7.38 (t, $J=7.4$ Hz, 2H), 7.32-7.28 (m, 2H), 7.15 (s, 1H), 6.85 (d, $J=9.0$ Hz, 2H), 4.83 (s, 3H), 1.96 (s, 3H), 1.94 (s, 3H). ^{13}C NMR (125 MHz, CDCl_3) δ (18 of 23 signals

were observed) 155.42, 142.16, 142.01, 141.23, 140.32, 133.33, 128.97, 127.87, 127.15, 126.47, 125.86, 125.69, 125.58, 122.41, 121.31, 115.83, 14.52, 14.44. FTIR (KBr-cast) 3362, 3064, 3026, 2952, 2918, 2853, 1612, 1517, 1443, 1336, 1275, 1193, 1137, 1116, 1055, 986, 892, 818, 749, 684, 529. CIMS (m/z): 537 (M+1).



DTE-PNQ hybrid 4.5. A mixture of a phenoxy-phenyl dithienylperfluorocyclopentene **4.4** (276 mg, 0.51 mmol) and NaH (12 mg, 0.51 mmol) in dry DMF (3 mL) was treated with 6-chloro-5,12-naphthacenequinone⁹ (107 mg, 0.37 mmol) and heated at 110°C for 16 h. The heat source was removed, the reaction mixture was poured onto ice water and the crude product was collected by vacuum filtration. Purification by column chromatography through silica (9:1 Hexanes:ethyl acetate) afforded 17 mg (17%) of the pure product as a yellow solid. Mp = 178-180°C. ¹H NMR (400 MHz, CDCl₃) δ 8.90 (s, 1H), 8.37-8.35 (m, 1H), 8.26-8.22 (m, 2H), 8.17 (d, *J*=8.0 Hz, 1H), 7.79-7.74 (m, 3H), 7.68 (t, *J*=8.0 Hz, 1H), 7.53 (d, *J*=8.0 Hz, 2H), 7.45 (d, *J*=8.0 Hz, 2H), 7.37 (t, *J*=8.0 Hz, 2H), 7.31 (m, 1H), 7.27 (s, 1H), 7.14 (s, 1H), 6.90 (d, *J*=8.0 Hz, 2H), 1.93 (s, 3H), 1.92 (s, 3H). ¹³C NMR (125 MHz, CDCl₃) δ (37 of 41 signals

were observed) 181.22, 159.05, 152.30, 152.19, 151.98, 151.90, 142.20, 141.26, 140.63, 136.24, 136.10, 135.36, 134.40, 133.83, 133.52, 133.34, 131.54, 130.72, 130.41, 130.28, 130.10, 128.99, 127.88, 127.68, 127.61, 127.46, 127.24, 127.14, 125.85, 125.61, 124.77, 122.41, 121.71, 120.97, 115.42, 14.51, 14.48. FTIR (KBr-cast) 3069, 3030, 2952, 2922, 2853, 1680, 1577, 1508, 1474, 1430, 1396, 1344, 1275, 1232, 1172, 1137, 1107, 1051, 986, 896, 818, 758, 719. Anal. Calcd for $C_{45}H_{26}F_6O_3S_6$: C, 68.17; H, 3.30. Found: C, 67.85; H, 3.46.

4.6 – References

1. Feringa, B. L., Ed. *Molecular Switches*, Wiley-VCH: Weinheim, 2001; preface.
2. Gobbi, L.; Seiler, P.; Diederich, F. *Angew. Chem. Int. Ed.* **1999**, *38*, 674.
3. Mitchell, R. H.; Ward, T. R.; Wang, Y.; Dibble, P. W. *J. Am. Chem. Soc.* **1999**, *121*, 2601.
4. Mrozek, T.; Gorner, H.; Daub, J. *Chem. Eur. J.* **2001**, *7*, 1028.
5. Gilat, S. L.; Kawai, S. H.; Lehn, J.-M. *J. Chem. Soc. Chem. Commun.* **1993**, *18*, 1439-1442.
6. Gilat, S. L.; Kawai, S. H.; Lehn, J.-M. *Chem. Eur. J.* **1995**, *1*, 275.
7. Irie, M.; Lifka, T.; Kobatake, S.; Kato, N. *J. Am. Chem. Soc.* **2000**, *122*, 4871.
8. (a) Fernandez-Acebes, A.; Lehn, J.-M. *Chem. Eur. J.* **1999**, *5*, 3285. (b) Kawai, S. H.; Gilat, S. L.; Lehn, J.-M. *Eur. J. Org. Chem.* **1999**, 2359.
9. Buchholtz, F.; Zelichenok, A.; Krongauz, V. *Macromolecules* **1993**, *26*, 906-910.
10. Kalinowski, H.-O.; Berger, S.; Braun, S. *Carbon-13 NMR Spectroscopy* John Wiley and Sons Ltd.: New York, 1984.

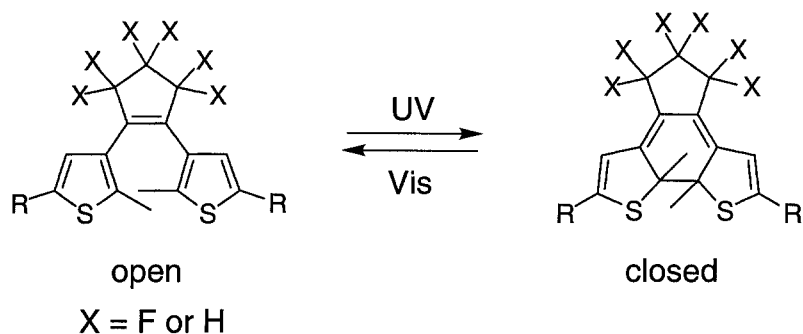
Chapter 5 – Conclusion

This thesis has addressed several concepts within the area of using photochromic molecules in the development of all-photon mode molecular devices. This is an extremely active area of research and is continuously attracting scientist from different disciplines. During my studies in this area I have had several opportunities to discuss my research with scientists from all over the world. From biochemists to physicists, I have found that some aspect of this type of research interests them, as its applications span many areas.

5.1 – Chapter 1: Introduction

In the first chapter, I gave an introduction to the basic concepts involved in photochromic molecules, particularly the properties necessary for applications of these molecules as molecular switches within molecular devices. A survey of various photochromes illustrated that the phenoxynaphthacenequinones (PNQ) and dithienylethene (DTE) are the most promising candidates due to their high fatigue resistance and thermal irreversibility. For this reason, this thesis has focussed on only these molecules.

5.2 – Chapter 2: Dithienylethenes (DTE)



Scheme 5.1

The second chapter of this thesis deals with the issue of immobilizing dithienylethene photochromes (Scheme 5.1) into a polymer matrix while still maintaining their photochromic activity. Practical handling of such materials requires them to be in a polymeric rather than a monomeric form. To this end, a series of DTE polymers were synthesized using Ring Opening Metathesis Polymerization (ROMP) (Figure 5.1). This polymerization technique was chosen due to its functional group compatibility, mild reaction conditions and its ability to generate well-ordered homopolymers.

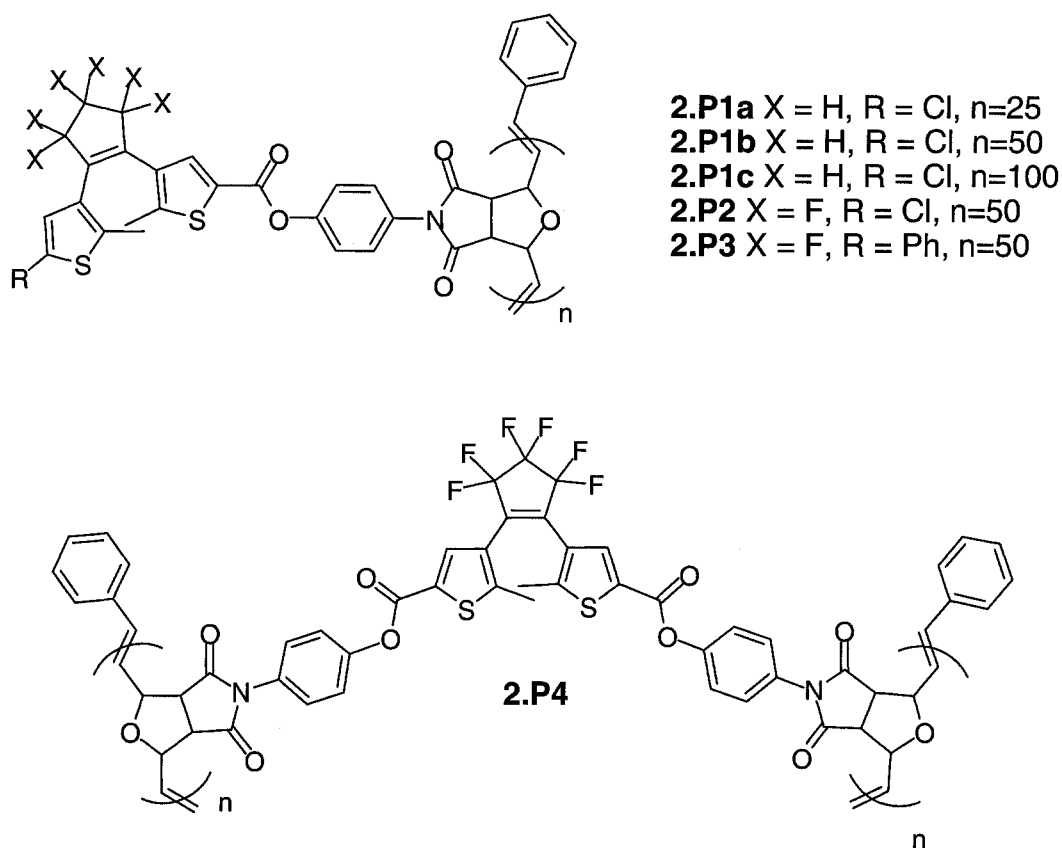


Figure 5.1. Photochromic homopolymers based on DTE.

The DTE polymers all showed identical photochromic behaviour to their corresponding monomers in solution, indicating that each photochrome is acting independently within the polymer matrix in solution. The polymers are easily cast as thin films using spin-coating methods. Solid-state photochromism is also observed in all of the DTE polymers. In order to complete the characterization of this class of photochromic polymer, it is important to quantify the conversion of the open to closed form of the DTE within the

polymer. It is important for device applications to maximize the conversion in the solid-state, which translates into maximizing the change between the two forms.

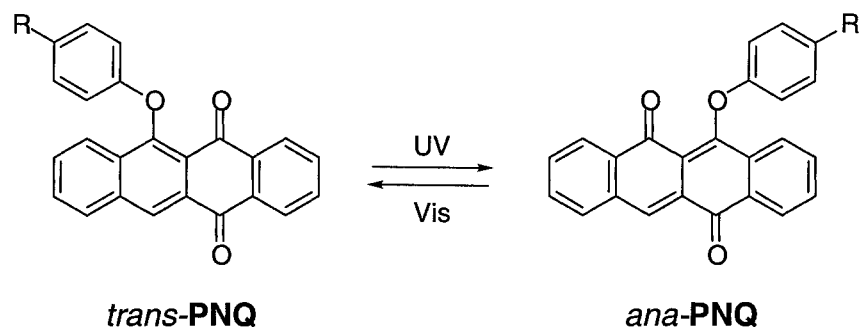
I ended Chapter 2 with a discussion about some preliminary results of how these DTE polymers can reversibly change their refractive index upon irradiation with appropriate wavelengths of light. Studies on these polymers are currently underway at McGill University by Dr. Christopher Barrett. In this respect, it is important to use the pendant functionality on the thiophene rings to explore its effects on the change in refractive index. By changing the pendant functionality on the thiophene rings, the linear conjugation pathway created upon cyclization can be tailored. The effect of this change should be studied as a function of refractive index change.

These results are very promising for the development of functional photochromic materials as this polymerization technique provides a means to polymerize photochromic systems without sacrificing their activity. This opens the door for more in depth studies of photochromic systems in the solid-state which show differences in properties other than just absorption, such as refractive index, emission, conductance and magnetic properties. This is key to the progression of the area of photochromic molecular devices. One of the main criticisms of this area is that most systems that are justified as potential molecular devices have only been investigated in solution. Using this universal polymerization method, these

potential molecular devices may be able to make the transition from a round bottom flask to a film, sheet or bead.

5.3 – Chapter 3: Phenoxynaphthacenequinone (PNQ)

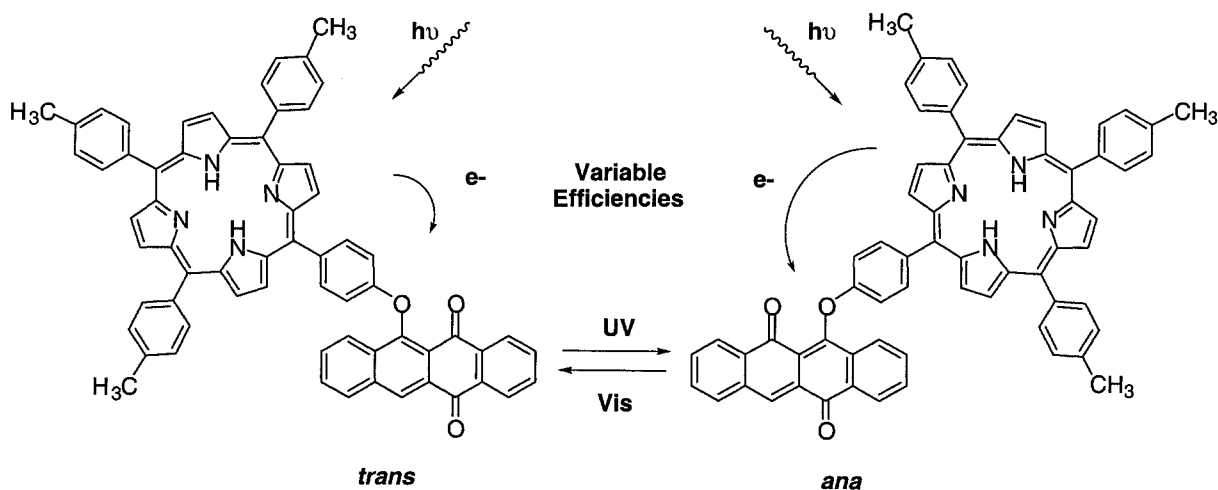
Chapter 3 begins with an introduction to photo-induced electron transfer (PET), one of the key steps in converting light energy to chemical energy in photosynthesis. PET from an electron donor to an electron acceptor results in a charge-separated state, consisting of the radical cation of the electron donor and the radical anion of the electron acceptor. The most common donor/acceptor diads use porphyrins as the electron donors and quinones as the electron acceptors. Regulation of PET can be exploited in molecular devices by regulating the formation of this charge-separated state.



Scheme 5.2.

Phenoxynaphthacenequinone (PNQ) interconverts between its *trans*- and *ana*-forms (Scheme 5.2). I have found that the difference in structure between the two forms is

accompanied by a change in reduction potential (electron accepting ability). The *ana*-form of PNQ is a better electron acceptor than the *trans*-form. This led me to synthesize a series of porphyrin – PNQ hybrids in which PET regulation is the goal: PET from the porphyrin to the *ana*-form should be favored over that to the *trans*-form (Scheme 5.3).



Scheme 5.3.

The first porphyrinic PNQ system studied is a covalently linked hybrid. The intimacy between the porphyrin and the PNQ photochrome shuts down the photochromic activity of the PNQ, making it useless in regulating PET. This problem is circumvented by synthesizing a hybrid system in which the two chromophores are associated through strong hydrogen bonds. In this system, the *on/off* nature of the complex allows for sufficient distance between the porphyrin and PNQ to allow for the photoisomerization of the PNQ photochrome. PET was assessed using luminescence spectroscopy: A decrease in emission of the porphyrin

corresponds to an increase in PET between the porphyrin and PNQ. These studies concluded that PET is regulated by toggling between the *trans*- and *ana*-forms of PNQ.

A porphyrinic-PNQ random copolymer was then described, in which PET is also regulated by photoisomerization of the PNQ moiety. This is interesting due to covalent attachment of the porphyrin to the PNQ, albeit a very long one. As stated throughout this thesis, applications of this technology require the system to function in the solid-state. It is therefore important to investigate the solid state properties of the porphyrinic PNQ copolymers.

Applications of this system include a non-destructive read-write system for molecular information storage, in which the read function is the emission of the porphyrin and the write function is the photoisomerization of PNQ. The excitation and emission wavelength of the porphyrin lie outside the absorption spectrum of both forms of the PNQ photochrome, therefore reading the information has no effect on the PNQ's photoisomerization. High emission of the porphyrin will indicate the *trans*-form is present, whereas low emission of the porphyrin will indicate the *ana*-form is present.

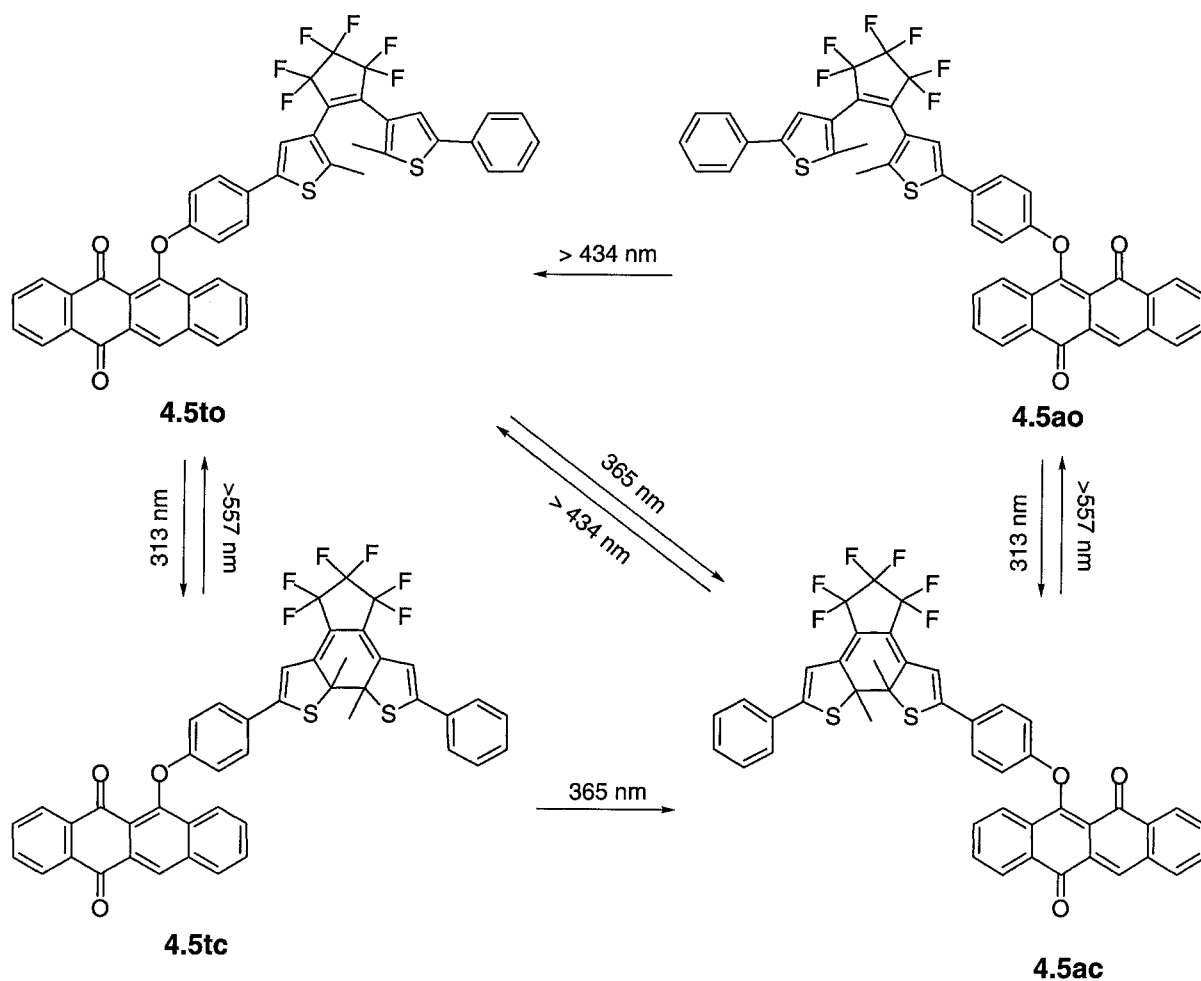
Another application of this system lies in its ability to reversibly produce a charge-separated state upon PET. Conducting polymers require a doping step in order to conduct electricity, which involves adding a chemical agent to either add an electron or extract an

electron. This creates a charge, which allows a current to flow through the material. Photochemical doping has precedent for being effective, where photoirradiation of the material in the presence of either an electron donor or acceptor allows PET, creating a charge-separated state. This induced charge similarly allows for current to flow through the material. Regulation of the formation of the charge-separated state within the porphyrin PNQ copolymer could provide a means to photo-regulate current through it, providing that the copolymer conducts electricity. This would provide a photo-regulated transistor, in which the irradiation of the porphyrin and applied current remain constant, and photoisomerization would regulate the flow of electrons through the material.

5.4 – Chapter 4: PNQ-DTE Hybrid

Chapter 4 focussed on the synthesis and characterization of a novel PNQ-DTE hybrid photochrome in which four state are accessible using light energy (Scheme 5.4). The development of multi-addressable molecular switches are important, as evidenced by the literature, due to their potential to change between several functions within the same molecule. The hybrid **4.5** was synthesized and was found to possess slightly different photochromic activity than its constituent components. More specifically, the photoisomerization between the *trans*- and *ana*-form of the PNQ component was much slower than expected. This phenomenon, coupled with the fast photoisomerization of the open to closed form of the DTE

component with 313 nm light, was exploited to generate the most elusive **4.5tc** state illustrated in Scheme 5.4.



Scheme 5.4.

As discussed in detail in Chapter 3, PNQ's are also electrochemically active. Switching between each form corresponds to a change in reduction potential. Recent result from our group have suggested electrochemical switching of certain dithienylethene derivatives.¹ As stated through this thesis, electrons and photons are the most desirable stimuli for the

development of molecular devices. By exploiting the photochromism and electrochromism/electrochemistry of these systems, more states will be accessible and gated photochromism may be observed for some of the forms. For instance, reduction of the PNQ moiety may shut down the photoisomerization of the DTE component, or vice versa with the oxidation/reduction of the DTE component.

Applications of this hybrid system mainly involve molecular information storage systems, as the amount of information within a material composed of this photochromic hybrid would far exceed simple mono-photochromic systems. Important in its application is figuring out how to read each state (detect which state is present) without using absorption methods, as irradiation with light destroys the information by causing a subsequent photoisomerization reaction. The fact that both of these components are electrochemically active offers promise, as the material could potentially be written/erased with light energy and read with electrochemistry. Future studies using this hybrid photochromic system will continue in our research group.

5.5 – Summary

I hope this thesis has educated the reader to the potential of photochromic molecules in the development of molecular devices. The main impetus for researchers in this area, in my opinion, should be to incorporate these systems into functional materials in order to show the

rest of the scientific community that their potential is real. Multi-disciplinary, collaborative efforts with synthetic chemists, materials chemists, physical chemists, physicists, and engineers is key in the progression of molecular devices. Research in this area, such as that presented in this thesis, bring the molecular machine one step closer from science fiction to great scientific achievement.

5.6 – References

1. Peters, A. P.; Branda, N. R. manuscript in preparation.